The Dynamic Interaction Between a Magnetically Levitated Vehicle and a Flexible Track

by Alan Lawton , B.Sc.

Thesis submitted to the University of Nottingham

for the degree of Doctor of Philosophy , May , 1988

The Dynamic Interaction Between a Magnetically Levitated Vehicle and a Flexible Track

CONTENTS

ACKNOWLEDGEMENTS

I express my appreciation and thanks for the help and assistance of my tutors , Dr Ed Williams and Dr Colin Fox of the Mechanical Engineering Department at Nottingham . They were rather brave in tackling what was , at the time , a completely new application with a completely unknown student . I hope that they are as pleased with our collaboration as I am .

I am similarly grateful to a number of other people within British Rail . Dr Maurice Pollard's enthusiasm and commitment to maglev initiated the whole project and encouraged me to register this work at Nottingham . Charles Frederick provided valuable guidance and support during the time that I have worked for him , despite the fact that maglev is , officially , no longer of interest to BR . Finally , my thanks to George Dodgson for his commitment and his concern when almost everything seemed to be going wrong .

SUMMARY

The only commercially operating magnetically levitated (maglev) transport system in the world is the link between Birmingham International Airport and the National Exhibition Centre . Comparative financial analysis for this route showed that the construction costs for both wheeled and maglev systems were similar and that the cost of the guideway accounted for over 70% of the total . In part this was because the guideway was elevated ; a likely requirement for any future urban system . A substantial reduction in installation costs for a system of this nature can only be achieved by the use of cheap , lightweight and flexible guideways .

The British Rail Research maglev vehicle was designed for use on a rigid guideway and it was known that excessive flexibility would make the suspension control system unstable . The aim of the study was to develop a maglev suspension control strategy that was insensitive to guideway flexibility .

Vibration measurements were carried out on the Birmingham guideway to establish its modal properties

. It was found to be sufficiently rigid to allow the existing controller to work without problems . Measurements were also made on the guideway of a Swiss cablecar transit system . This was felt to represent the extremes of both lightness and flexibility and established the range of guideway dynamics that were likely to be encountered .

For the initial experimental work , a section of the British Rail maglev test track was modified to incorporate three sections of flexible track . A personal computer was installed on board the vehicle and software was written to aid frequency response testing and dynamic system modelling . Tests were carried out to establish the dynamic parameters of the new sections of guideway .

The existing rigid guideway controller separated magnet control from suspension control . Guideway flexibility destroys this separation and induces additional feedback terms that degrade system stability .

Theoretical studies of an improved controller took advantage of the fact that that the suspension magnets act directly onto the guideway and affect the position of both vehicle and guideway . As the guideway is lightly damped it is only flexible over a narrow bandwidth and the new suspension controller is able to use vehicle inertia to react forces that control the guideway at its natural frequency . Theory suggested that this would restore the

separation of magnet and suspension control , even with a flexible guideway .

For a variety of reasons , experimental implementation of the new controller proved to be difficult . Suspension performance on the flexible portions of the guideway was never adequately demonstrated . The work did however enable a very accurate theoretical model of the system to be developed . This model contrasted with earlier predictions because , on rigid guideways , it predicted substantially smaller phase margins than the earlier models had suggested . It showed that the new controller had only modest benefits relative to the original rigid guideway suspension controller .

This led to the development of an improved controller , a "lumped" controller where magnet and suspension control are not separated . Modelling for a single degree of freedom vehicle on a single mode guideway showed that large improvements in suspension performance could be made .

Further modelling of a three degree of freedom vehicle and a five mode three degree of freedom flexible guideway used parameters that represent the production vehicles at Birmingham . This work defined limits for guideway flexibility and vehicle dynamic performance and showed that maglev guideways for production scale vehicles , with the "lumped" controller , can be very flexible indeed .

The major aim of the project was achieved . A suspension controller was developed that will allow a maglev vehicle to work on a guideway that is far lighter , more flexible and far cheaper than the guideway required for a conventional wheeled vehicle .

NOMENCLATURE

A	Magnet coil area
B	Magnet flux density
F	Magnet force
g	Magnet airgap (z_V-z_G)
G	Controller electrical gain
G_A	Gain in a current feedback loop
G_f	Gain in a magnet flux feedback loop
G_F	Magnet force characteristic (N/v)
G_g	Gain in a magnet gap feedback loop
G_V	Voltage gain of a magnet chopper
HP	High pass filter
I	Magnet current
j	$(-1)^{1/2}$
K_B	Linearised rate of change of magnet force with respect to flux density
K_F	Magnet force characteristic (N/v)
K_g	Linearised rate of change of magnet flux density with respect to magnet airgap (magnet negative stiffness)

K_I Linearised rate of change of magnet flux density with respect to current

K_{stat} Modal static stiffness

L_L Magnet leakage inductance , that inductance that is solely dependent on the magnet

L_M Magnet mutual inductance , that inductance that is dependent on the magnet and guideway together

LP Low pass filter

M_V Vehicle mass

N Number of magnet turns

PA Phase advance filter

R Magnet resistance

R_G Guideway receptance (m/N)

R_V Vehicle receptance (m/N)

s Laplace operator

T_1, T_2 Controller time constants

u_0 Magnetic space constant

w Frequency

w_n Natural frequency

z Proportion of critical damping

z_G Guideway displacement

z_V Vehicle displacement

CHAPTER 1 THE PROBLEM

1.1 INTRODUCTION

In the late 1960's , magnetically levitated (maglev) transport began to move from the domain of fantasy and science fiction towards commercial reality . The image of silver coloured vehicles that glided smoothly and rapidly between pollution and decay free cities (the cities were usually surrounded by a pink or orange bubble) proved irresistible to engineers and governments alike . By 1970 , many governments were sponsoring research into high speed , non-contacting ground transportation systems . A maglev system was under development in Germany with two more under development in Japan . In France and Britain , pneumatically levitated vehicles were developed , the British system being the Tracked Hovercraft . In France , traction power came from aircraft gas turbines and in Britain the traction power was from Linear Induction Motors (LIMs) .

The essential requirements for all these rival transport systems were the ability to design lightweight vehicle structures , a good understanding of dynamics , aerodynamics and control systems , the availability of sufficient instrument and electronics technology and lots of money . The rapidly developing aerospace , electronics and computing industries were able to provide the technological skills for high speed , non-contacting ground transport and , for a while , the governments of the developed world provided the money .

With one exception , all these projects are now abandoned . The German maglev project is the only significant development left of all the earlier schemes , although this is a massive project , described in Ref 1.1 . The Emsland test centre , built at a cost of several hundred million pounds , has a 31 kilometre test track to run a 400 km/h vehicle . This system has yet to find a commercial application .

The other projects were all cancelled for the same reasons . High speed , non-contacting ground transport is fabulously expensive ; it can be noisy , there are dangers associated with the high speeds and the problems of track junctions are largely unresolved . The dominant difficulty though is cost , but not particularly vehicle cost . The cost of developing the German vehicle will be less than the development cost of an equivalent size aeroplane .

The vital difference is in the cost of the infrastructure . High speed ground based transport systems require guideways , all of which are elaborate in comparison to railway track . However it is the comparison with the infrastructure costs of aeroplanes that has denied commercial credibility for high speed maglev and other non-contacting ground transport .

Such hard nosed accountancy is not always acceptable to the general public . The outcry in Britain over the Government's decision to cancel the Tracked Hovercraft project was widely believed to have motivated the decision to invest in an alternative system . At this time (1975) , British Rail Research had completed a study of a transport system for city centre movements in Sheffield , Ref 1.2 . The requirement was for a system based around small , light , low-speed vehicles that were capable of climbing steep gradients and turning through small radius curves . A comparison of wheeled and magnetically levitated vehicles was undertaken and the maglev option was approved .

The Department of Transport provided funding for British Rail Research to develop a maglev vehicle that would be capable of carrying 10 people at a maximum speed of 20 m/s . Although this application was very different to the Tracked Hovercraft , there was still a theme of "Government support for maglev " , which was politically attractive .

The vehicle was to be a rigid box that used the airgap between vehicle magnets and guideway as a suspension . Traction and Braking were to be provided by a LIM . The development work was successfully completed by 1978 when a partially commercial application was found for the technology . In 1976 , an American manufactured "people-mover" had been installed at Gatwick Airport to transport passengers within the airport boundaries . The British Railway Industry was incensed , but the choice of an American system had been dictated by the absence of appropriate and developed British technology .

In 1978 a large new terminal building was planned for Birmingham Airport . The terminal building was to be situated only half a mile away from British Rail's Birmingham International Station which is on the main London-Birmingham line . This station also serves the National Exhibition Centre . There was a requirement to transport people between the British Rail station , National Exhibition Centre and the new airport terminal building .

Cost comparisons between a conventional wheeled system and a maglev system were made and , as at Sheffield , gave a small advantage to the maglev system , see Fig 1.1 . The minimal maglev cost advantage was based largely on reduced maintenance because of a reduction in the number of moving parts . There was also a significant cost-benefit due to lower guideway contact stresses .

A development consortium of British companies was formed and the Department of Trade and Industry provided them with funding as aid for the development of new products . The consortium members were :-

West Midlands County Council

Brush Electrical Machines

Metro - Cammell

Balfour Beatty

GEC Transportation Projects

GEC General Signal

GEC Transmission and Distribution Projects

GEC Witton Kramer

British Rail Research acted as consultants to the members of the consortium .

Changes to the successful BR prototype vehicle were minimised in order to reduce the technical risk for this new project. However , substantial amounts of re-design work and some new development were still necessary . The commercial vehicle had to be twice as large as the prototype vehicle . This meant a substantial re-design of the vehicle structure and traction , braking and suspension system components . The commercial vehicle also required the development of an automatic driving and stopping system because the prototype had relied on an on-board , human driver .

A further problem arose because of a conflict between the nature of the maglev vehicle suspension and the geography of the guideway at Birmingham . The

prototype vehicle at Derby had been developed on a solid guideway and an assumption that was inherent in the development and function of the suspension controller was that the guideway would not move significantly in response to suspension forces . The guideway at Birmingham had to cross two roads and a large car park in it's 750 metre length and it was therefore specified to be elevated six metres above ground level . An elevated guideway that is not continuously supported must , in principle , be flexible and it will therefore move in response to vehicle suspension forces .

Considerable cost , time and effort had been expended on the development of the BR suspension controller for rigid guideways . The risk of developing this controller to accommodate flexible guideways was deemed unacceptable . Instead , the elevated guideway was specified to be made sufficiently rigid that the maglev vehicle , with its rigid guideway suspension controller , would function correctly . In Ref 1.3 , Williams explores the limited tolerance of the controller to guideway flexibility .

There are two different types of problem that are grouped under the general heading of vehicle-guideway dynamic interaction . There is a problem if a vehicle , with any type of suspension , travels along a flexible guideway that has a cyclic variation in its loaded profile . As the vehicle

travels over the guideway , a vehicle guideway force is induced that has the wavelength of the variation in loaded profile and as vehicle speed varies , the frequency of the induced force varies . A flexible guideway will have a series of resonant frequencies , any or all of which may be excited by a combination of constant pitch guideway features and a particular vehicle speed . If the vehicle is multi-body and includes suspension elements , this dynamic interaction is complicated although it is well described in the literature . Kortum's paper , Ref 1.4 , provides an excellent summary and bibliography for this subject . Guideways that have been built in the past have pitches , e.g. span lengths of 10 to 25 metres with fundamental natural frequencies in the range of 4 to 8 Hz . The minimum critical speeds for these guideways are therefore in the range 40 to 200 m/s .

The BR maglev system has a maximum speed of 20m/s and is not a candidate for this type of dynamic interaction between vehicle and flexible guideway .

The other type of problem is limited to vehicles with active suspensions or those passive systems such as railway lateral suspensions with the potential for instability . Such suspensions are affected by guideways which move relative to ground because this is a degree of freedom that is not usually considered by the suspension designer . If the vehicle suspension cannot rely upon the guideway to react

suspension forces at all frequencies then the suspension may become unstable , a maglev vehicle has the potential to become unstable at zero speed . This is the problem that affects the low speed British Rail maglev vehicle on flexible guideways and it is the problem that caused concern when building the Birmingham system and which was the dominant influence on the cost of the system . The solution to this problem can provide a real commercial advantage for maglev systems relative to any wheeled alternative .

Fig 1.1 shows that the largest proportion of overall capital expenditure at Birmingham is not the cost of the vehicles , it is the cost of the infrastructure and particularly the cost of the guideway . Low speed transport systems will generally find applications for short distance movements and this implies travel through congested urban areas . It is highly likely that guideways in urban areas will have to be elevated in order to minimise building costs and so they will be flexible .

A wheeled transport system will also require an elevated guideway to operate in urban areas . Wheeled vehicles are a mature technology and their existing requirement that any guideway resonance must be at a frequency well above vehicle suspension frequencies is unlikely to change .

Guideways that are not flexible will be heavy and expensive , guideways that are flexible will be

relatively light and cheap . The vehicle that can run on the most flexible guideway will be the most economical vehicle to use , almost regardless of vehicle cost . If a maglev vehicle suspension controller can be developed that can tolerate a guideway that is more flexible than the guideway required for wheeled vehicles then the maglev suspension is an asset .

A suspension controller which is tolerant of flexible guideways will , for the first time , provide a real commercial reason for using a maglev suspension . Maglev will no longer be desired for fantastic reasons , it will appeal to an accountant .

This thesis describes a programme of work aimed at the development of a suspension controller for a low speed maglev vehicle that is tolerant of flexible guideways .

1.2 THE BRITISH RAIL VEHICLE FOR RIGID GUIDEWAYS

1.2.1 A Description

This section describes the vehicle as it existed prior to the start of this project .

Fig 1.2 shows the vehicle on its guideway . The vehicle has eight magnet pairs which pull the vehicle upwards towards the levitation rails of the guideway

. The lift force is transmitted into the vehicle body via vertical struts , one at each corner . The magnets are mounted in pairs , cantilevered from the struts , and the two pairs at each corner are separated laterally by 10 mm . Vehicle traction and braking is from two LIMs below the vehicle . The LIMs face downards onto an aluminium-steel reaction plate on the top face of the guideway . Normal braking is provided by reversing the motor drive and emergency braking is by vehicle de-levitation onto Ferodo pads that bear onto the top face of the levitation rails .

On board electrical power was collected as a three phase supply from the trackside by means of a five wire sliding contact system .

1.2.2 The Vertical Suspension

Guideway roughness is the source of excitation to the maglev suspension and this excitation affects the suspension in a manner that is common to all suspensions . Any ground vehicle is required to follow the terrain and must therefore follow long wavelength guideway irregularities . Any vehicle must also provide a measure of passenger , or payload , comfort and therefore must not respond to short wavelength irregularities in the guideway . All suspensions are designed to act as low pass mechanical filters ; vehicle displacements should be

the low pass filter outputs from ground displacement inputs .

$$z_V = LP\ z_G \qquad \text{Eq 1.0}$$

where z_V and z_G are vertical displacements of the vehicle and guideway and LP is a low pass filter characteristic .

In principle , an active suspension may achieve this objective by measuring the deviation of the track from straight , filtering this measurement and ensuring that body displacements match the filtered measurement . In practice , this objective cannot be achieved directly , there is no measuring device that can perform the required measurement . Fig 1.3 shows a practical means by which the suspension characteristic of Eq 1.0 can be achieved .

Fig 1.4 shows the implementation of the ideal suspension , based on perfect track measurement .

To fulfil the suspension filter requirement of Fig 1.3 , two feedback signals are combined to produce one error signal as a magnet force demand . A measurement of magnet gap (vehicle-guideway relative displacement) is processed through a low pass filter . If this signal is maintained constant , the vehicle will follow low frequency , long wavelength track features . A measurement of the vehicle absolute displacement , processed through a high pass filter , is also used as a magnet force demand . If this signal is maintained constant then the vehicle will ignore high frequency , short wavelength track

features . The suspension will therefore adopt the characteristic of a low pass filter . It is implicit that the magnet force does not produce guideway displacements , that the guideway is not flexible and that magnet force is a function only of input demand .

If the control loop is broken at A then :-

$$o = PA * G_F * R_V [(HP + LP)i - LP\ z_G]$$

where R_V is the receptance of the vehicle inertia , PA is a first order phase advance filter and system gain , G_F is the magnet force characteristic and HP is a high pass filter characteristic .

If the filters are complementary , HP + LP = 1

$$HP = \frac{as + bs^2}{1 + as + bs^2}$$

$$LP = \frac{1}{1 + as + bs^2}$$

$$o = PA * G_F * R_V[i - LP\ z_G]$$

which is identical to the response of Fig 1.4 . Stability is assessed without regard to system inputs , z_G , therefore the OLR can be calculated by taking the ratio o/i and discarding the z_G term . It is apparent that the low pass filter characteristic does not affect stability .

$$OLR = o/i = PA * G_F * R_V$$

This is important in development work because the suspension can be commissioned , without running the vehicle , to provide adequate stability levels with any filter characteristic . Running tests can then be undertaken to optimise the suspension filters without affecting system stability .

The suspension characteristic of the system in Fig 1.3 is :-

$$z_V = \frac{LP\ z_G}{1 + 1/(PA * G_F * R_V)}$$

If the system gain is high , z_V = LP z_G and the required suspension characteristic is achieved .

On a vehicle with a passive suspension , the spring stiffness defines both the suspension frequency and the tare to laden suspension deflection . With this active suspension , the electronic filter defines the suspension frequency and the gain of the magnet control loop , G_F , with units of N/m , defines the tare to laden deflection of the suspension . Thus the filter may be set to 2 Hz for vibration isolation , but the suspension deflection for a given load change might correspond to a 6 Hz suspension frequency . This active suspension tends to have a constant height , regardless of load . This is an important requirement for a maglev vehicle where the current-force relationship becomes very inefficient at large magnet gaps .

1.2.3 Vertical Suspension in Three Degrees of Freedom

The vertical suspension provided by the electro-magnets must control the vehicle body in pitch , bounce and roll (the orthogonal parameters) . This is achieved by measuring vehicle-guideway relative displacement and vehicle absolute position at each corner , these measurements are used to compute the orthogonal displacements and error signals . These orthogonal variables are then combined to produce error signals for each corner , which drive current through each magnet pair . This technique effectively eliminates any combination of magnet forces that twist the vehicle body . Jayawant discusses this issue in Ref 1.5 .

1.2.4 Vehicle electro-magnets

The suspension magnets are in pairs , each of which form a U shape , magnetic flux runs through the levitation rail in a longitudinal direction . The magnets are designed to operate with a nominal 15mm airgap and a designed mean airgap flux density of 0.8 Tesla .

A variety of materials and construction methods are used in the existing vehicle magnet cores , ranging from high cost , low hysteresis laminations to low cost , solid mild steel . The two coils on each magnet have 750 turns of aluminium foil and are rated at 20 Amps . Each magnet dissipates 800 watts

and the stationary , levitated vehicle draws 8 amps from the mains supply .

The analysis techniques that were available for dynamic modelling were limited to the study of linear systems . Equations 1.1 and 1.2 describe the non-linear relationship between magnet force , F , flux density , B , airgap , g , and current , I .

$$F = \frac{B^2 * A}{2 * u_0} \qquad \text{Eq 1.1}$$

$$B = \frac{N * I\, u_0}{2 * g} \qquad \text{Eq 1.2}$$

N is the number of magnet turns , A is the coil area and u_0 is the magnetic space constant .

The magnet force-displacement-current relationship is modelled using three constants .

$K_B = dF/dB = 2*F/B$

$K_I = dB/dI = B/I$

$K_g = dB/dg = -B/g$

Experimental work by Redfern , Ref 1.6 , found that the theoretical values for K_B were accurate , but those of K_I and K_G were affected by magnet saturation and leakage and these experimentally determined values were only 50% of the theoretical values .

$K_B = 7500$ N/Tesla

$K_I = 0.025$ Tesla/A

$K_g = -26.5$ Tesla/m

The electrical impedance of the magnet was also found to be important and to consist of three separate elements . The magnet resistance , R , is a simple constant which is mildly temperature sensitive . The magnet inductance is split between mutual inductance and leakage inductance . The mutual inductance , L_M , is determined by the flux which links the guideway and the vehicle magnets . The leakage inductance , L_L , is determined by the flux which remains internal to the magnet and vehicle and which provides no useful magnet force . These values were also determined experimentally (Ref 1.6) and were found to be :-

$R = 2.7$ Ohms

$L_M = 0.34$ Henrys

$L_L = 0.29$ Henrys

The development of the BR vehicle involved the definition of an accurate magnet model , shown within the dotted boundary in Fig 1.5 . The most interesting component of this model is K_G , which is negative . K_G models the magnets ability to increase its attractive force as it approaches the guideway . K_G is a "negative spring " and the magnet and vehicle suspension controller have to overcome the de-stabilising behaviour associated with K_G .

Fig 1.5 shows the control elements that were added to provide a well behaved magnet with a flux output that was a linear function of input demand .

In principle the output flux density is determined by input demand , d ,and airgap , g = $z_V - z_G$:-

$$B = \frac{d}{G_F + \frac{sT_2 * (R + s(L_L + L_M))}{(1+sT_1) * G * K_I}} - \frac{g * K_G (R + sL_L)}{R + s(L_L + L_M) + G * G_F * K_I \frac{(1+sT_1)}{sT_2}}$$

T_2 is chosen to be small so that in the working frequency range of the suspension :-

$$B = d / G_F$$

Fig 1.6 shows a plot of the predicted flux response of the magnet controller . The response is flat with only small phase lags in the frequency range of 0 to 10 Hz .

1.2.5 The Lateral Suspension

There is a lateral offset between the magnet pairs at one corner , designed to produce vehicle steering forces . As the offset magnet pairs move relative to the levitation rails , so the angle of inclination of the vehicle guideway magnetic flux will change . A horizontal restoring force will always be produced , this is illustrated in Fig 1.7 . As flux density is proportional to vehicle weight , so the horizontal restoring force is proportional to vehicle weight and the vehicle has a lateral suspension natural frequency that is independent of payload . This behaviour can be modelled as a simple lateral spring for small vehicle movements . However these forces provide no damping in the suspension and this is unsatisfactory .

Lateral damping forces are provided in response to a contrived , absolute velocity signal that is an integrated measurement of vehicle lateral acceleration . This demand signal is used to transfer current between the offset magnet pairs at each corner . In this way , the total magnet current and hence total magnet vertical force is largely constant at each corner and is independent of lateral force . The front and rear of the vehicle are controlled by separate transducers and hence lateral and yaw damping is introduced . There is also an effect on the roll suspension because the line of action of the magnet lateral force is below the vehicle centre of gravity .

1.2.6 Vehicle Electronic Hardware

The development of this vehicle and it's suspension was intimately associated with the development of the hardware required for the suspension . Some of this hardware was not commercially available and some commercially available hardware was used in novel applications . Not all the vehicle electronic hardware is relevant to this work , but it is necessary to describe the components that influence and control the vehicle suspension .

A non-contacting , magnetically levitated vehicle needs a transducer to measure the distance

between vehicle and guideway ; that transducer must also be non-contacting . BR's vehicle measured the variation in capacitance with airgap between a 50mm * 100mm plate on the vehicle and the guideway . The ideal position for this plate would have been on the magnet face , looking up at the guideway . This would provide a measurement of the real magnet-guideway gap . The prospect of mechanical damage and the influence of contaminants on the perceived dielectric constant of the upward looking sensor meant that this option was unsatisfactory . Instead the plate was fixed to the vehicle underside and looked down onto the guideway .

The control system also required a measurement of vehicle absolute position . This is derived from accelerometers mounted on the vehicle corners . The chosen accelerometers were designed for use in an industrial environment and therefore had the necessary high resistance to impulsive loads . The accelerometer signals were processed by an electronic circuit which has a transfer function :-

$$\frac{4000s}{1 + 3.2s + 4.88s^2 + 4s^3}$$

This provides a double integration of the accelerometer signal , without the tendency to drift that is associated with simple integration .

Magnet flux density was measured by integrating the output of search coils that were embedded in the magnet pole faces . The coil output is proportional

to the rate of change of flux density , and is therefore incapable of sensing the steady state flux required to support the vehicle weight . The search coil output is processed by an electronic circuit which has a transfer function with the form :-

$$\frac{as}{1 + bs + as^2}$$

This combines an integrator with a high pass filter that has unity gain in the pass band . The coefficients a and b are chosen such that above 0.3 Hz , the circuit output is a signal that is proportional to magnet flux . This signal is combined with a measurement of magnet current that has been processed by a circuit which has a transfer function with the form :-

$$\frac{1 + bs}{1 + bs + as^2}$$

This low pass filter is the complement to the high pass filter that is perceived to affect the magnet flux signal . The output of this circuit is only significant below 0.5 Hz and in this frequency range the whole suspension will work effectively and magnet-guideway displacement will be constant . Magnet current is therefore proportional to magnet flux , in this frequency range . Magnet flux is measured , at all relevant frequencies , by a summation of the processed current and rate of change of flux density measurements .

The devices that provide power to the magnets were built entirely by British Rail and were "state of the art" in 1974 . The variable mark-space ratio ,

double sided , transistor choppers were designed to work from a 300 volt supply that came from rectified three phase mains . The current rating for each magnet was 20 amps continuous , 60 amps peak , and the chopping frequency was 1kHz . Parallel transistors were used because , in 1974 , there were no commercially available discrete transistors with an appropriate current rating .

1.3 PROJECT PLANS

This work was registered at Nottingham University in September 1983 , project plans were defined and BR's financial resources were allocated for the start of 1984 . In this first project year , it was planned to build an experimental guideway with variable flexibility . This guideway was to be completed by June 1984 and commissioned and tested by the end of 1984 . Tests of the Birmingham guideway were also planned for 1984 , in order to confirm that it had been built to specification and to provide data for future modelling work . The first year was also planned for the development of the computer software that was necessary for control system analysis and testing .

The second year was planned for the theoretical development of a controller that would be tolerant of flexible guideways , followed by manufacture ,

commissioning and performance testing of the controller .

The third year was planned for documentation of the work and , with the cooperation of West Midlands Passenger Transport Authority , testing on a production scale vehicle .

Unfortunately , it was not possible to follow these plans . In June 1984 , only six months after the project work had started , the Government's financial support was cancelled . This project had been funded directly from the Department of Transport , whilst the Department of Industry funded the companies developing the Birmingham system . A decision was made that any development of suspension controllers for flexible guideways should be provided by the companies that might make a profit from the application . In effect , the funding for the project was planned to disappear at the end of March 1985 , fifteen months after the project start . This meant that the project work had to be substantially re-organised and ultimately the work was affected quite significantly by this decision .

It was anticipated that the activity within the project that would most require BR's financial aid was the testing and commissioning of the suspension controller . This was the activity that was brought forward and pushed through whilst funding was still available . Unfortunately , the thinking time that

was available to devise a suitable controller then became rather limited .

1.4 OBJECTIVES

The main aim of this work was to gain an increased understanding of the maglev vehicle/guideway dynamic interaction problem and thereby enable the development of a controller for the BR maglev vehicle that will be tolerant of flexible guideways . The new controller must allow operation of the vehicle on guideways that are sufficiently light , flexible and hence cheap that maglev transport systems become cheaper than wheeled alternatives .

1.5 REFERENCES

1.1 Gottzein and Rogg . Status of High Speed Mag-lev Train Development in FRG . Paper for I.Mech.E Conference "Mag-lev Transport now and for the future " , 1984

1.2 Dobbs et al . Magnetically Levitated and Wheeled Minitram Comparison Study . Internal BR document TREDYN 3 , 1975

1.3 Williams . Interaction Between a Magnetically Levitated Vehicle and a Flexible Track . Internal BR document , IMDOS 85 1981

1.4 Kortum . Vehicle Responses on Flexible Track . Paper for I.Mech.E Conference "Mag-lev Transport now and for the future" , 1984

1.5 Jayawant . Electromagnetic Suspension and Levitation . IEE Procedings A , Vol 129 , Part A No.8 , November 1982

1.6 Redfern . A Detailed Investigation of the Suspension Magnet Dynamic Parameters . Internal BR document , 1976

CAPITAL COSTS FOR DIFFERENT TRANSPORT SYSTEMS FOR AN AIRPORT LINK

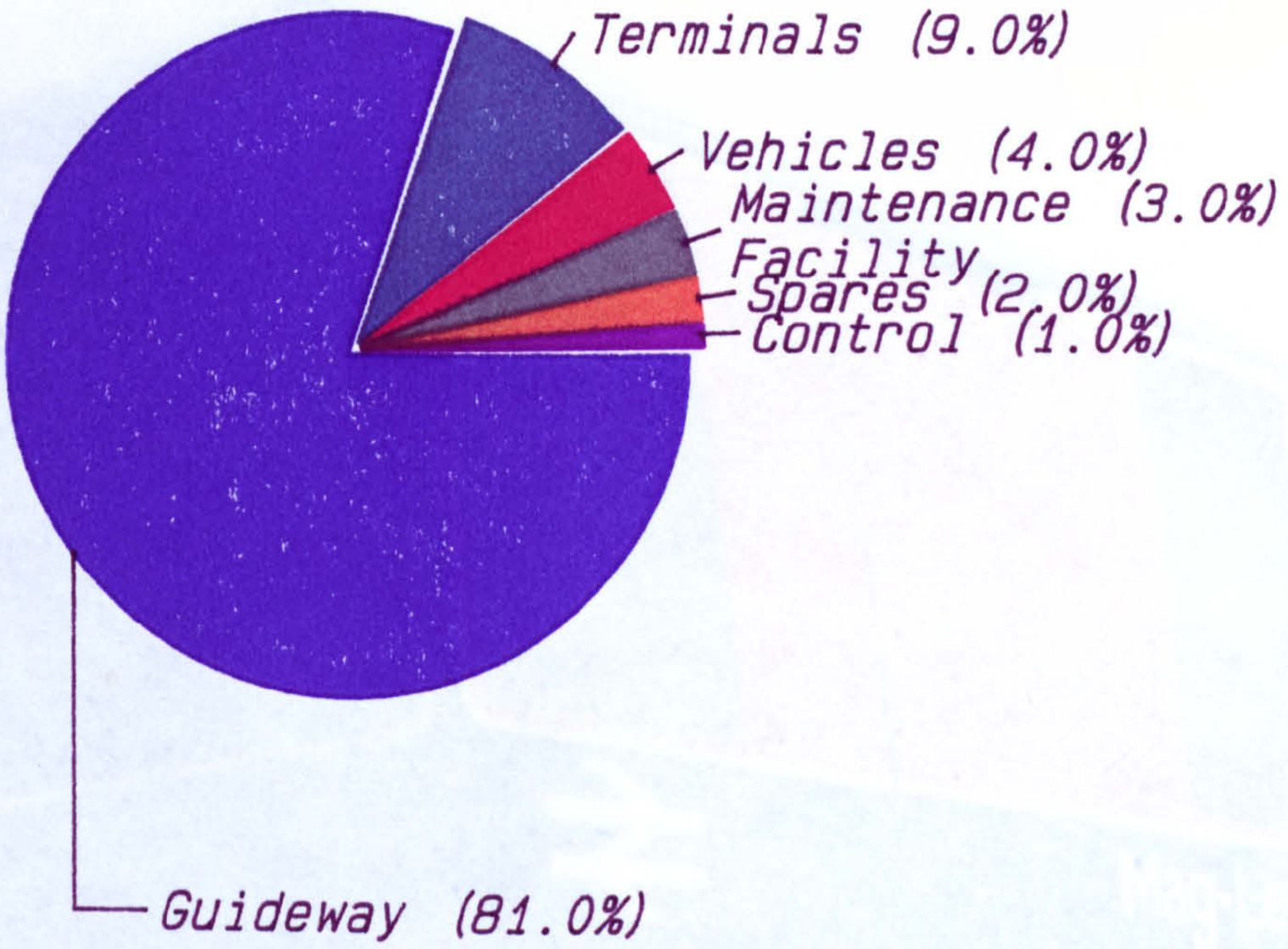

A CONVENTIONAL WHEELED VEHICLE

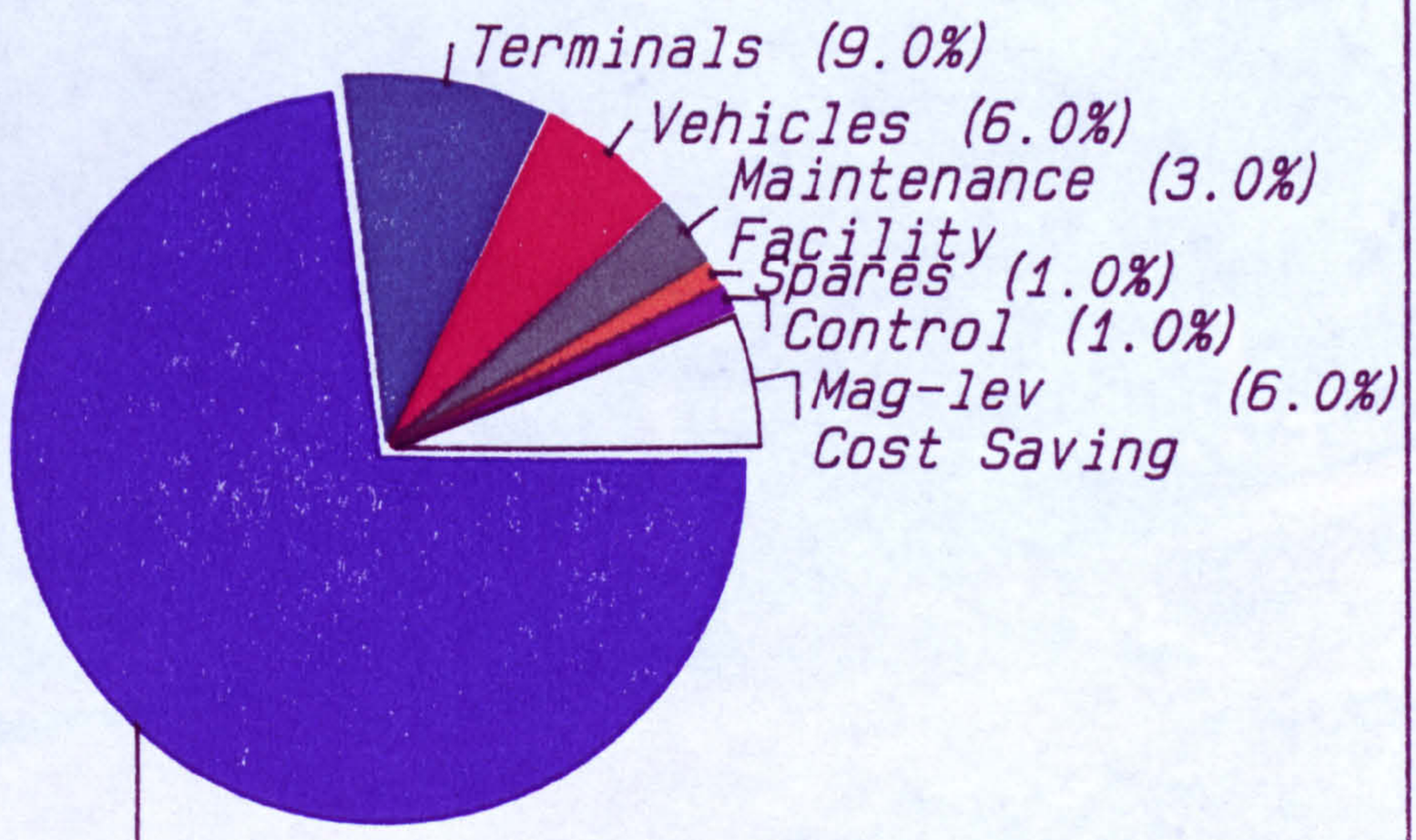

A CONVENTIONAL MAGLEV VEHICLE

FIG 1.1 COMPARATIVE COSTS

PPMLEV4

FIG. 1.2. THE BR. MAGLEV VEHICLE ON THE FLEXIBLE GUIDEWAY AT DERBY

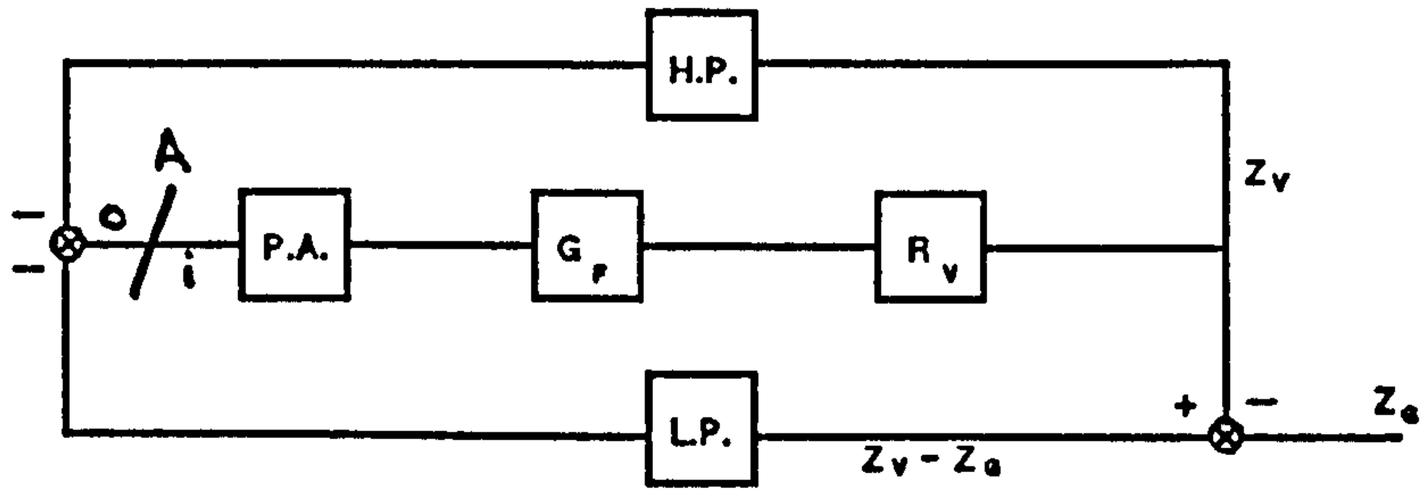

FIG.1.3 A SINGLE DEGREE OF FREEDOM VEHICLE CONTROLLER

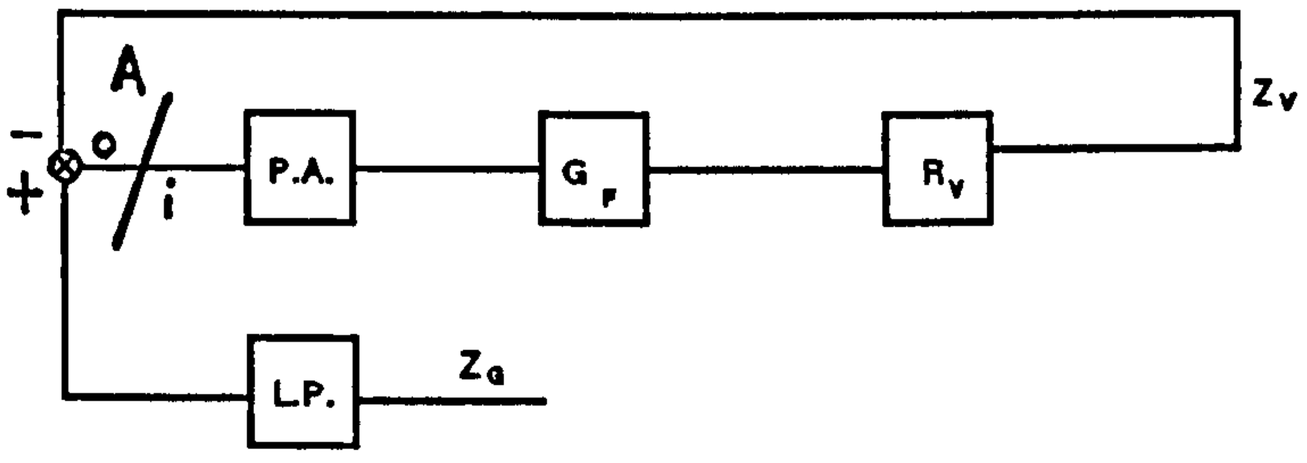

FIG.1.4 AN EQUIVALENT CONTROLLER TO FIG.1.3

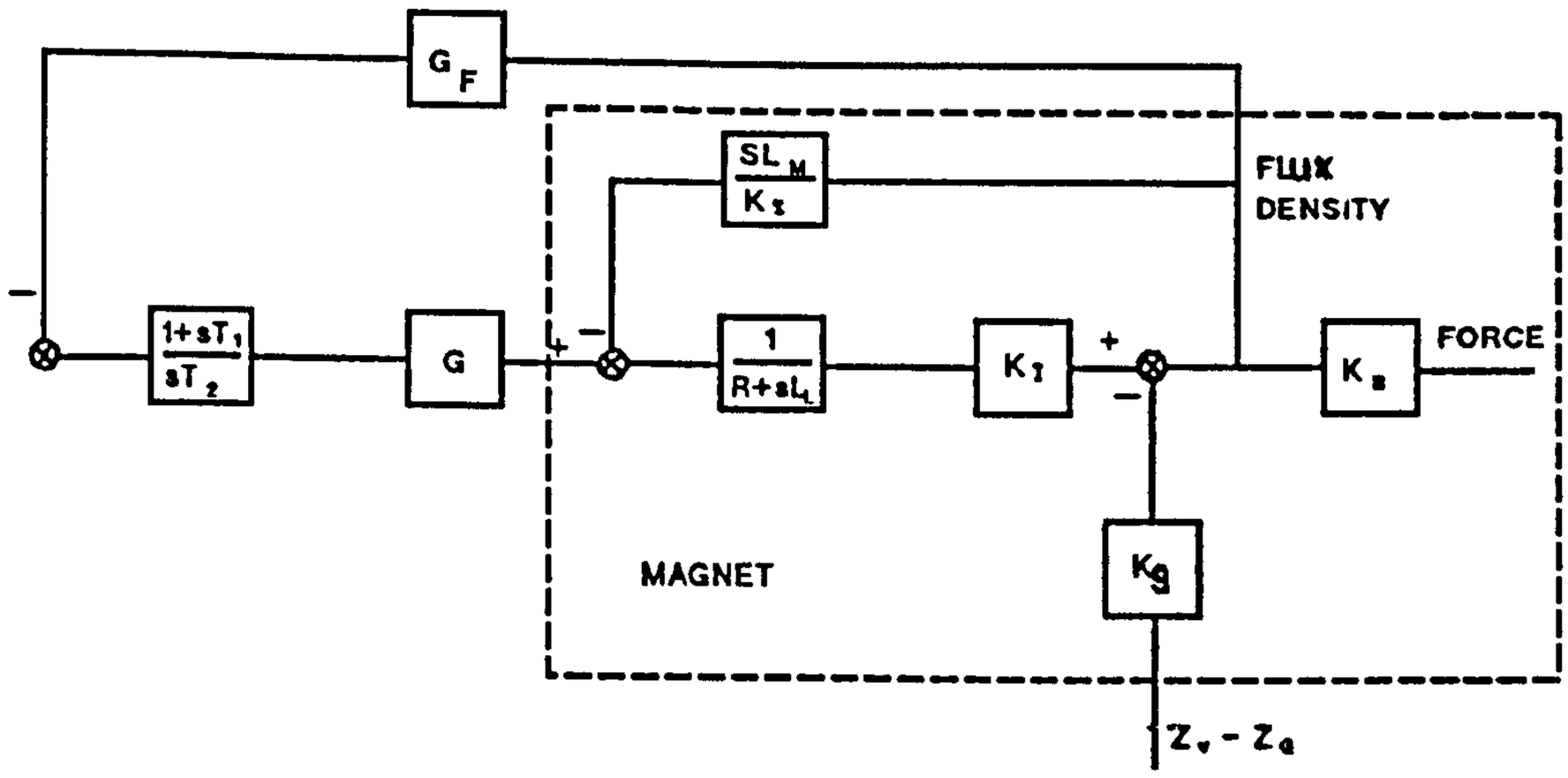

FIG.1.5 MODEL FOR THE MAGNET AND CONTROLLER

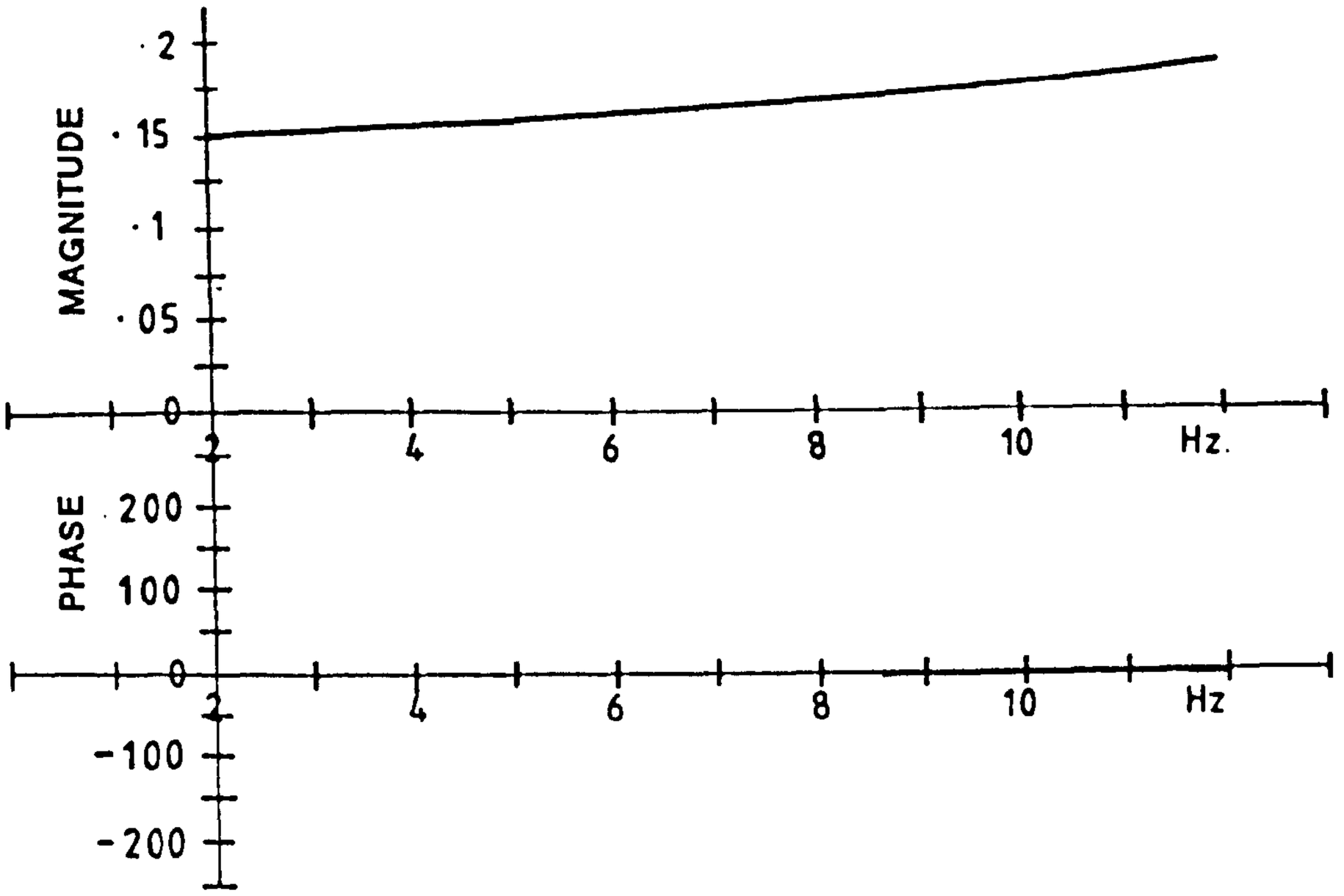

FIG.1.6 FLUX RESPONSE FOR THE CONTROLLER IN FIG. 1.5

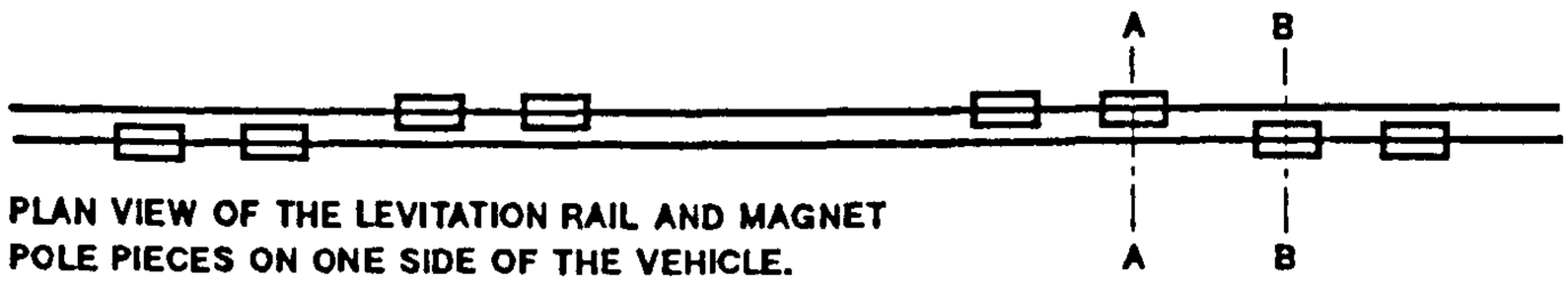

PLAN VIEW OF THE LEVITATION RAIL AND MAGNET POLE PIECES ON ONE SIDE OF THE VEHICLE.

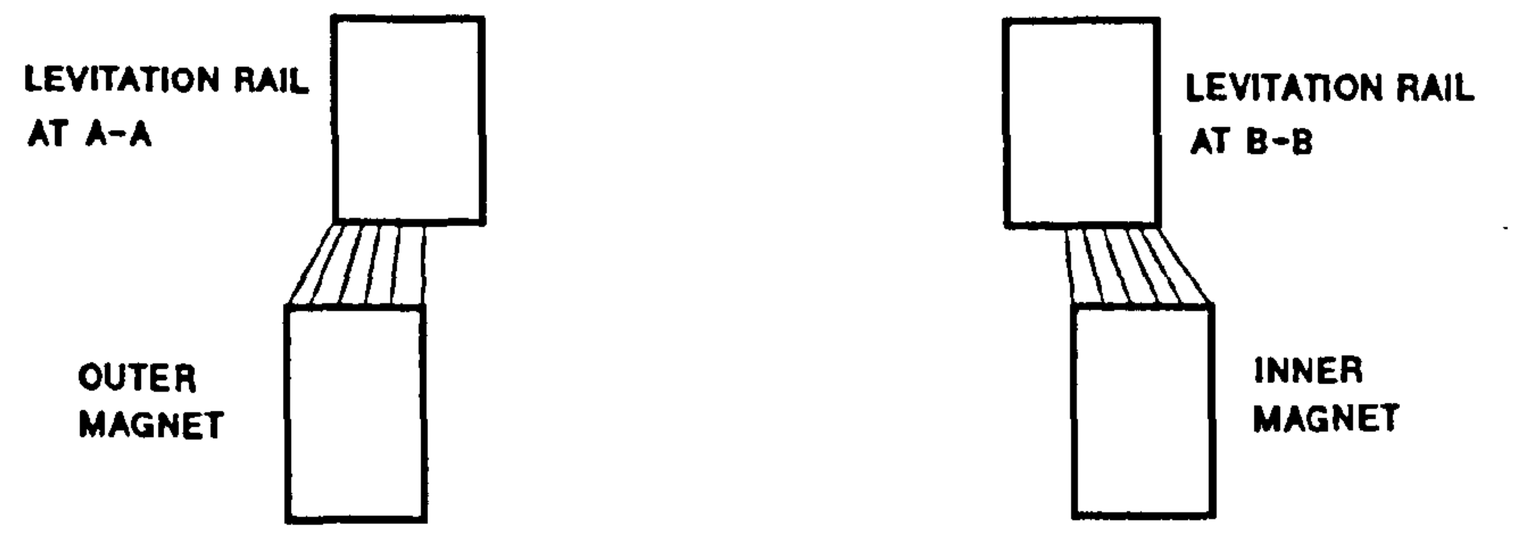

00737DG

FIG.1.7 LATERAL RESTORING FORCES AT A VEHICLE CORNER

CHAPTER 2 SOFTWARE FOR MODELLING AND MEASURING

2.1 INTRODUCTION

The software developed for use in this project followed experience of using an early desk-top computer in suspension development work during 1980 and 1981 . That computer , a Hewlett-Packard 85 (HP85) , was used during the development of several active suspensions for rail vehicles . The computer was used to communicate with a Hewlett-Packard 3582A spectrum analyser to capture , store and display frequency response measurements made by the spectrum analyser . The computer was also used to model active suspension systems , to allow direct comparison of theory and practice . This type of work was novel to British Rail because the size and portability of the HP85 allowed the computer to be taken to the test system . Test data was available immediately that tests had finished and equivalent theoretical data was available shortly after that . This was a great improvement over any previous test procedure , though

there were several problems , caused mainly by computer hardware limitations .

The computer was limited by memory size to models no larger than 12th order , limited by processor speed to require 100 seconds to calculate one frequency response value for a 12th order model and limited in output by a three inch display screen and printer width . The software for system modelling was also limited because it could only calculate frequency responses and not , unfortunately , eigenvalues and vectors .

This situation was improved considerably when a Hewlett-Packard 9816 (9816) was purchased for use on this project . The 9816 was one of the first 16 bit desktop machines available and it improved computational speed by a factor of 10 , memory size by a factor of 25 and display area by a factor of 10 . Unfortunately , software from the HP85 was not transferable to the new machine and new software had to be written . By the time that this project had finished , the author had written a suite of software that performed all the functions of the HP85 software , together with much improved facilities for graphical output , model editing , data storage and processing , eigenvalue calculation was also possible . A chart describing the functions of the software is shown as Fig 2.1 .

2.2 DATA CAPTURE AND PROCESSING

Applications of this software for frequency response measurements with the spectrum analyser are described in detail in Chapters 3,4 and 6 .

The 9816 computer was used to download data from the spectrum analyser via the IEEE interface and prepare it for storage on either 3.5 inch floppy discs or on a Winchester disc . With additional data from the operator , the 9816 would convert the measured frequency response and power spectra to engineering units before storage with complementary data such as channel sensitivity , number of ensemble averages , frequency range and the effect of any DC offset .

A particular problem in using the spectrum analyser occurs when the inputs need to be processed through analogue filters . Ideally the frequency response of each filter will be identical and the measured frequency response will then be undistorted , but in practice this will not be true . The 9816 data capture software has an option to use the analyser to measure the relative frequency response of the two filters , and retain this response in memory . The system then performs the frequency response measurement and divides that nominal frequency response by the relative filter frequency response . This arithmetic yields the

desired frequency response , undistorted by ill-matching analogue filters .

An extension to this software is used to measure the OLR of the maglev vehicle , the problems that are inherent with this measuring technique are discussed in chapter 6 . The OLR of the maglev vehicle is difficult to measure because the normal maglev vehicle suspension input , track displacement , is difficult to quantify and the maglev vehicle is unstable without closed loop control . OLR measurement is possible if a noise signal can be injected into a control system as shown in Fig 2.2 .

If the whole system is stable and if the input is i_1 , the frequency response measured between B and A is :-

$$-1 / H(jw)$$

If the input is i_2 , the frequency response measured between B and A is

$$G(jw)$$

The 9816 software controls the measurement of these two frequency responses after prompting the user to provide the correct input and calculates the OLR , G(jw)*H(jw) , by dividing one response into the other .

After storing the frequency response on disc , the 9816 is able to process frequency response data by addition , subtraction , multiplication or division by another frequency response , multiplication by a real constant , integration or

differentiation . Resultant frequency responses may be stored on disc or displayed on either screen or plotter .

A modal analysis programme was also available to process the frequency response data . This Fortran programme , written at the Royal Aircraft Establishment and described in Ref 2.1 and 2.2 , was adapted to run on the 9816 by J.R.Evans . Originally the programme had been written for a Hewlett-Packard 1000 (HP1000) computer but , after modification , took only twice as long to run on the 9816 as it did on the HP1000 , though the HP1000 had cost ten times more than the 9816 .

A final option for data processing is to calculate and display the confidence levels of a measured frequency response . The calculations are described by Bendatt and Piersoll in Ref 2.3 . Experience has shown that calculations for 90% confidence levels seem to give a better guide to measurement quality than the 95% figure used by Bendatt and Piersoll . Confidence levels of 95% were often large in comparison to the frequency response , even when that response "looked good" and was well matched by theoretical predictions .

2.3 DATA DISPLAY

The display software will provide alphanumeric output to the 9816 screen or any compatible printer . Graphical output of theoretical or experimental values is available on the 9816 screen , a variety of dot-matrix printers or any Hewlett-Packard pen plotter . Graphical output is either an X-Y plot of power spectral density (PSD) , frequency response or coherence against frequency or a Polar or Nichols plot of frequency response . Several different sets of data may be plotted on the same axes .

2.4 SYSTEM MODELLING

2.4.1 Which Modelling Method ?

Ever since 1965 , British Rail Research has invested heavily in a suite of programs for modelling the behaviour of linear railway vehicle suspensions . There is also software for non-linear modelling . In common with other vehicle modelling systems , there is a heavy emphasis on frequency domain work , rather than time domain . This is because the input to the rail vehicle , track displacement , is not easily described by a discrete series of data points , unless that series is extremely and expensively long . Track inputs are normally described by means of a spatial PSD , so that the vehicle-suspension

frequency response , if stable , may be used to calculate the PSDs of specific vehicle variables .

British Rail's main suite of programs was dedicated to modelling conventional passive railway suspensions as a set of second order differential equations . Although it was possible to form models of control systems within these programs , the author has found this an awkward and cumbersome task . In 1980 , British Rail Research began a project to develop active suspensions for rail vehicles . The project leader , R.M.Goodall , devised a system of modelling discrete linear systems that had the advantage of generality to include control , mechanical and electrical systems . System modelling was easy for the engineer and the form of the model led to algorithms which were easy to program . Unfortunately , system modelling was restricted to the calculation of frequency responses , at that time there was no means of calculating system eigenvalues .

Previous experience with Goodall's modelling method provided the incentive to choose this as the primary means of modelling in the maglev flexible guideway project .

2.4.2 The Modelling Method in Detail

The two degree of freedom mechanical system shown in Fig 2.3 can be described by the block

diagram shown in Fig 2.4 . In this diagram the blocks are rational functions (they have numerator and denominator) of s , the Laplace operator . This type of block circuit diagram can be used to describe electrical , electro-magnetic and analogue electronic systems as well as mechanical systems . If the order of the block numerator and denominator is limited to 2 , then a general block has the form :-

$$\frac{a + bs + cs^2}{d + es + fs^2}$$

and this provides the basis for a simple , quick and easily understood means of modelling linear , lumped parameter , dynamic systems .

The block diagram , Fig 2.4 , provides a means of forming the equations that define system behaviour . For instance , in the case of mechanical systems , the blocks define the relationships between physical variables such as force or displacement . Six variables are used in Fig 2.4 , indicated by the circled numbers . These are :-

x_1 Force on mass 2

x_2 Displacement of mass 2

x_3 Force in spring 2 and damper 2

x_4 Acceleration of mass 1

x_5 Displacement of mass 1

x_6 Velocity of mass 1

In general the equations can be written in matrix form that is analogous to the state equation :-

$$[X] = [A][X] + [B]x_i \qquad \text{Eq 2.1}$$

where :-

[X] is a vector of the n physical variables defined by the block diagram .

[A] is a sparse nxn rational polynomial matrix in the Laplace operator , s , defined by the block circuit diagram .

[B] is a rational polynomial vector in s , defined by the block circuit diagram from the way in which the scalar system input , x_i , affects the system .

The definition of [A] is simplified when it is realised that the column and row position of any element in [A] is given by the the numbers of the variables preceding and following the relevant block in a diagram such as Fig 2.4 . This type of block circuit diagram modelling was devised by Goodall and is described in Ref 2.4 .

The system matrix [A] for Fig 2.4 is :-

$$\begin{bmatrix} 0 & 0 & -1 & 0 & 0 & 0 \\ 1/m_2s^2 & 0 & 0 & 0 & 0 & 0 \\ 0 & k_2+c_2s & 0 & 0 & -k_2-c_2s & 0 \\ 0 & 0 & 1/m_1 & 0 & -k_1/m_1 & -c_1/m_1 \\ 0 & 0 & 0 & 0 & 0 & 1/s \\ 0 & 0 & 0 & 1/s & 0 & 0 \end{bmatrix}$$

which is 75% sparse . The vector [B] , shown for convenience as a row vector , is :-

$$[\ 1 \qquad 0 \qquad 0 \qquad 0 \qquad 0 \qquad 0\ ]$$

2.5 FREQUENCY RESPONSE CALCULATIONS

The original software for the HP85 performed frequency response calculations described by a manipulation of Equation 2.1 to the form :-

$$[X/x_i] = [I-A]^{-1}[B] \qquad \text{Eq 2.2}$$

where $[X/x_i]$ is a vector of transfer functions between the physical variables , defined in a block circuit diagram , and the scalar system input .

If s=jw is substituted into Equation 2.2 then both [I-A] and [B] reduce to complex matrices and [I-A] may be inverted . In the HP85 program , the nxn complex array and the n-element complex vector are converted to a 2nx2n real array and a 2n-element real vector to take advantage of the HP85 BASIC language extensions for matrix arithmetic . The HP85 solves Equation 2.2 for the real equivalent variables , by inverting [I-A] and post-multiplying by [B] , the complex frequency responses are then re-formed .

Early software for the 9816 used similar language extensions for real matrix arithmetic , but applied to a slight variant of the problem . An alternative form of the frequency response equation 2.2 is :-

$$[I-A][X/x_i] = [B] \qquad \text{Eq 2.3}$$

This is a familiar matrix equation , though for a system of linear equations with complex coefficients . These may be solved with the 9816 language extensions after suitable conversion from complex variables to real . These intermediate , real solutions must be reformed to the complex problem solutions .

This software was easy to write , though inefficient with the computers resources , and ran successfully until December 1984 . At that time the APT Tilt Development Group , which was using the authors software , began to complain that frequency response calculation was not fast enough . The 9816 was able to produce a frequency response vector for a 20th order system in 10 seconds ; but this meant 15 minutes to calculate a typical requirement for 100 frequency values . The APT group wished to work with 40th order systems , the calculation time was a function of n^3 and two hours of calculation for a set of frequency responses would not be acceptable . A software re-write was required .

The 9816 language extensions solved the linear equations by a Gaussian reduction with back substitution , using a sophisticated pivoting strategy to preserve numerical stability . No allowances were made for a sparse matrix and solutions for all variables were calculated , even though they may not have been required . The method worked on the 2nx2n equivalent real array and thus

required $8n^3$ real multiplications rather than n^3 complex multiplications .

The author's current 9816 software for frequency response calculations also uses Gaussian reduction and back substitution , but differs from the old method in four respects .

1 All arithmetic is complex , even though the BASIC language has no complex functions . This replaces $8n^3$ real multiplications with n^3 complex multiplications , each of which requires only four real multiplications and two additions . As there is no requirement for real to complex conversion , the computational workload is halved . Also , the complex array requires only half the storage capacity that the real array requires .

2 Frequency responses are calculated only for user selected variables . The matrix equation 2.3 is manipulated to position the variables of interest in the last rows and columns in order to limit the work done in the back substitution process .

3 Gaussian reduction works by converting any non-zero term below the diagonal of [I-A] to zero . However in this particular problem a high proportion of the elements of [I-A] are zero before calculations begin . The current software uses a Boolean array to match any non-zero terms in [I-A] with a logical false . Thus any step in

the Gaussian reduction is preceded by a logical IF to ensure that work is only done when it is required . The workload increase of IF statements is amply rewarded .

4 The current software uses no explicit pivoting strategy whatsoever . In general , a Gaussian reduction strategy will require the pivot element to be chosen with care to preserve numerical stability . However , as this particular problem always starts with unity along the diagonal of [I-A] , the system matrix is always sparse and double precision arithmetic is used exclusively , numerical instability has not been experienced by any of British Rail's engineers in the course of several hundred thousand calculations .

There is no guarantee that problems of numerical instability will not occur in the future , but comfort is taken from Wilkinson's comments in Ref 2.5 where he supports the idea that matrices from damped mechanical and electrical systems will be well conditioned and eigenvalues will be well separated .

The current software is six times faster than the original version for 20th order systems and , importantly , its computational speed depends more upon n^2 than the n^3 of the original software .

2.6 EIGENVALUE CALCULATIONS

2.6.1 Initial Attempts

The initial approach to this problem was to manipulate [I-A] to produce the system characteristic equation , which could then have been factorised to yield the system characteristic values . Barnett in Ref 2.6 and Kaillath in Ref 2.7 give proofs that convert a general rational polynomial matrix [R] to the Smith-McMillan form . This form is also a rational polynomial matrix , which is equivalent to [I-A] , and is diagonal .

Noting that the form of [A] may allow a singular matrix , the system characteristic equation may be formed from the multiple of the diagonal elements of the Smith-McMillan form of [A] . The diagonal elements have a particular form that comes from the algorithm used to compute them .

If d(s) is the monic (normalised by the highest order coefficient value) least common multiple of all the denominator elements of [R] .

then [N] = d(s)[R] where [N] is a non-rational polynomial matrix in s .

Gantmacher in Ref 2.8 describes three elementary operations that may be carried out on [N] .

1 Multiplication of any row or column by a non-zero constant .

2 Addition to any row or column of any other row or column multiplied by any polynomial .

3 Interchange of any two rows or columns .

These operations are all achieved by multiplication of [N] by another matrix which has a non-zero , constant determinant , thus preserving system characteristic values . The algorithm that Gantmacher describes , reduces [N] to its Smith form , [S] , where any of the diagonal elements will divide into all following diagonal elements , providing that [I-A] is non-singular . If [I-A] is singular then elements beyond the r^{th} , where r is the matrix rank , will be zero . Knowing that the characteristic equation of [N] has a factor $(d(s)^n)$, the non-zero diagonal elements will all contain at least the polynomial d(s) .

Dividing d(s) into the Smith form , [S] , of the non-rational matrix [N] and reducing the elements to the lowest terms will produce the Smith-McMillan canonical form of [I-A] . For this particular problem , assuming non-identical characteristic values , the system characteristic equation will be defined by the elements of the highest ordered , non-zero diagonal element of [S]/d(s) .

Protek , an independent software house , were commissioned to write a Pascal program for the 9816 to implement this algorithm . They were succesful , but only in part . For matrices smaller than , say , fourth order the program worked well and consistently

as it did for higher order systems made up of subsets of uncoupled low order systems . For genuine high order systems , in excess of tenth order , the program invariably failed to complete its calculations . The computer failed with errors of arithmetic underflow , overflow or limits to memory capacity .

Study of this behaviour led to the conclusion that the algorithm was prone to numerical instability and , sadly , the algorithm allows no opportunity to introduce an adequate pivoting strategy to avoid this problem .

Kaillath in Linear Systems , Ref 2.7 , cautions that the Smith and Smith-McMillan forms " will not generally be convenient for actual numerical computations " . It is unfortunate that the author had not read Kaillath's book before initiating this work .

2.6.2 The Successful Method

The eigenvalue problem was eventually solved by a completely different method that owes more to an engineering appreciation of the problem than it does to elegant mathematics . Note that each transfer function block in the matrix [A] has the form :-

$$\frac{a + bs + cs^2}{d + es + fs^2} \qquad \text{Eq 2.4}$$

and may be formed , analogue computer style , from the integrator circuit shown in Fig 2.5 .

The output from the integrator circuit is a combination of two integrator outputs plus , if c is non-zero , the input . The integrator equations for all the elements of [A] can , in principle , be calculated by this technique and the state matrix of the system can be formed . Techniques for calculation of eigenvalues from a state matrix are well established , and so the eigenvalue problem can be solved .

Several practical problems were discovered , the most immediately obvious was the value of 1/f in Fig 2.5 , for f=0 . The integrator realisation of the problem fails and a differentiation operation is implied . This is not valid in a state equation and the problem is insoluble unless the special case of f=0 and c=0 occurs . In this case the function :-

$$\frac{a + bs}{d + es} \qquad \text{Eq 2.5}$$

can be formed by the integrator network shown in Fig 2.6 .

This network has a similar problem to that in Fig 2.5 , in that the integrator network is not valid and differentiation is implied if e=0 , as with blocks 2,3 and 5,3 in Fig 2.4 . The transfer function block can then only be formed into state equations if b=0 and e=0 , when the whole block reduces to a real constant a/d .

The program that forms the state matrix works through three , consecutive processes .

1 The program checks through each block of [A] and tags each block as having either 0 , 1 or 2 integrators and then allocates the relevant state variable number(s) to that block . The program flags a warning if a differentiation is described within a block .

2 The program once again checks through each block of [A] and , for each block , defines the portion of the state equation that is defined within the block .

Consider the block shown in Fig 2.5 , the following state equation portions can be defined .

$$\dot{x}_2 = x_1 \qquad 2.4$$

$$\dot{x}_1 = - ex_1/f - dx_2/f \qquad 2.5$$

Note that equation 2.4 is complete and equation 2.5 is not , as it does not include the effects of the block input .

3 The program then looks for an element of [A] that provides an input to incomplete state equations , a block in the block circuit diagram that is an input to another block . The output of the block in Fig 2.5 , which will be the input to another block is :-

$$\text{output} = x_1(b-ce/f)+x_2(a-cd/f)+\text{input}*c/f \qquad \text{Eq } 2.6$$

Equation 2.6 raises the further practical problem that an input block may well have its own input blocks , which may also have input blocks and so on . This problem is solved by a

recursive routine that searches for inputs to a particular block , fills in the appropriate terms in the state equation and either returns if c=0 or calls itself again . This routine also checks that it is not working in a loop of the control circuit that contains no integrators as this would lead to the routine calling itself indefinitely .

Steps 2 and 3 of the algorithm are illustrated as flowcharts in Figs 2.7 and 2.8 .

Once the state matrix has been formed , eigenvalues are calculated by reduction of the asymmetric state matrix to Hessenburg form , followed by the QR solution . These transforms have not yet been modified to work with a matching Boolean array , as was done with frequency response calculations , in order to reduce the amount of computational effort for a sparse matrix .

2.7 CONCLUSIONS

The software described in this chapter has been used extensively and successfully by a British Rail's engineers with a variety of skill and knowledge . All users have been able to use the software with minimal tuition and without any documentation at all . This demonstrates an agreeable simplicity of use , absent

in other linear system modelling packages that the author has experienced .

This system modelling program suite is well suited for use by inexperienced users . The software allows model development to be recorded along with response calculations . This is highly appropriate in industry where analysis costs are minimised by allowing experienced engineers to supervise the work of others . These attributes may well have a value in an educational environment .

The 9816 software has proved to be extremely popular and successful . It is in use on six other computers at British Rail and three of those computers were bought specifically to run this software .

2.8 REFERENCES

2.1 Gaukroger , Skingle and Heron . "Numerical Analysis of Vector Response Loci " . Journal of Sound and Vibration 1973 29(3) .

2.2 Copley . "Analysis of Subcritical Response Measurements from Aircraft Flutter Tests " . Shock and Vibration Bulletin , Part 3 , May 1981 .

2.3 Bendatt and Piersoll . " Random Data : Analysis and Measurement Procedures " . Wiley Interscience 1971 .

2.4 Goodall . "Calculation of the Frequency Responses of Complex Control Systems Directly from the Physical Parameters ." Trans. Inst. Measurement and Control , vol2 , no 3 . 2.5

2.5 Wilkinson . " The Algebraic Eigenvalue Problem " . Clarendon Press , Oxford , 1965 .

2.6 Barnett . " Introduction to Mathematical Control Theory " . Clarendon Press , Oxford , 1975 .

2.7 Kaillath . " Linear Systems " . Prentice-Hall Information and System Sciences Series , 1980 .

2.8 Gantmacher . " Theory of Matrices , Vol 1 " . Chelsea Publishing Company New York , 1959 .

FIRST MENU

A Measure Frequency Responses
B Display Frequency Responses or PSDs
C Calculate Frequency Responses
D Manipulate Frequency Responses or PSDs

OPTION A MENU A1 for MEASUREMENT

A Measure from a HP3582A Spectrum Analyser
B Measure from a Solartron TFA

Return to First Menu

OPTION B MENU B1 for DISPLAY

A Load Data from Disc Storage
B Use Last Calculated Data

MENU B2 for Choice of Display Device

A Plot Graphs on the VDU
B Plot Graphs on a Choice of Pen Plotters
C Print Data to a Choice of Printers

MENU B3 for Choice of Display Format

A Numeric Printout
B Niccols Chart
C Frequency Plot of PSD , Frequency Response or Coherence
D Polar Plot

MENU B4 What Next ?

A Re-plot Current Data
B Plot New Data Over the Current Data
C Plot New Data
D Calculate Confidence Levels for Current Frequency Response Data

Return to First Menu

OPTION C MENU C1 for CALCULATIONS of Frequency Response

A Load an Old Model from Disc
B Load an Old Model from Disc , Edit and re-store onto Disc
C Create a New Model and Store onto Disc

MENU C2 for Choice of Calculation Type

A Eigenvalues
B Frequency Responses

MENU C3 What Next ?

A Store Frequency Responses on disc	GOTO Menu C3
B Display Frequency Responses	GOTO Menu B2
C More Calculations with the Current Model	GOTO Menu C2
D Work with a New Model	GOTO Menu C1

Return to First Menu

OPTION D MENU D1 for MANIPULATION of Frequency Responses

A List "Set-up" Parameters for Experimental Data
B Perform Block Mode Arithmetic on Frequency Response Data
C Calculate PSDs of Frequency Responses from Design Spectral Data

Load Data from Disc

Perform Manipulation

MENU D2 What Next ?

A Display the Manipulated Data	GOTO Menu B2
B Store Data onto Disc	
C Manipulate New Data	GOTO Menu D1

Return to First Menu

FIG 2.1 SOFTWARE FUNCTIONS

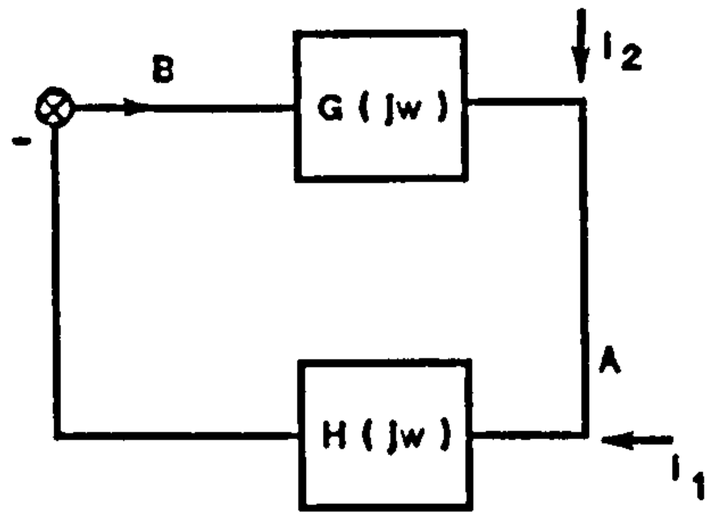

FIG.2.2 OLR MEASUREMENT OF A CLOSED LOOP SYSTEM.

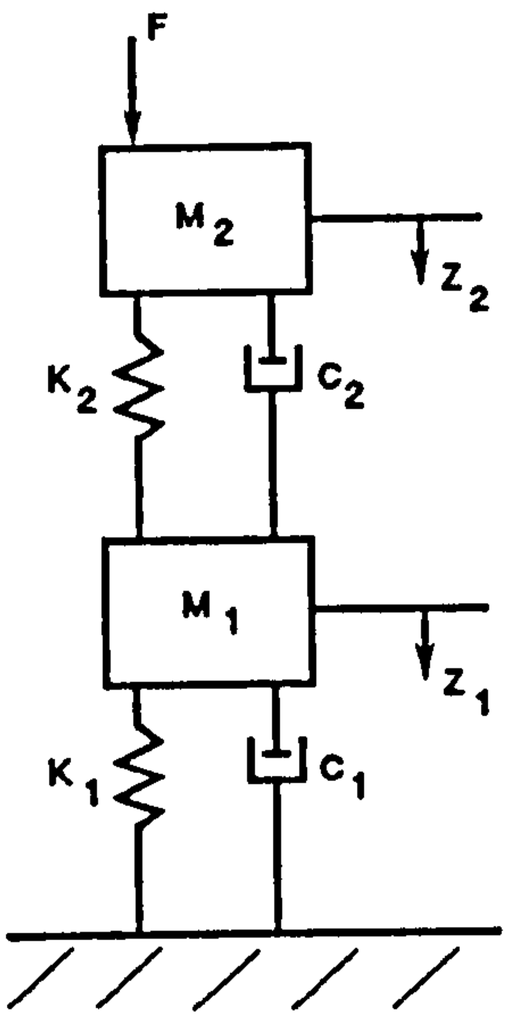

FIG.2.3 A TWO DEGREE OF FREEDOM MECHANICAL SYSTEM.

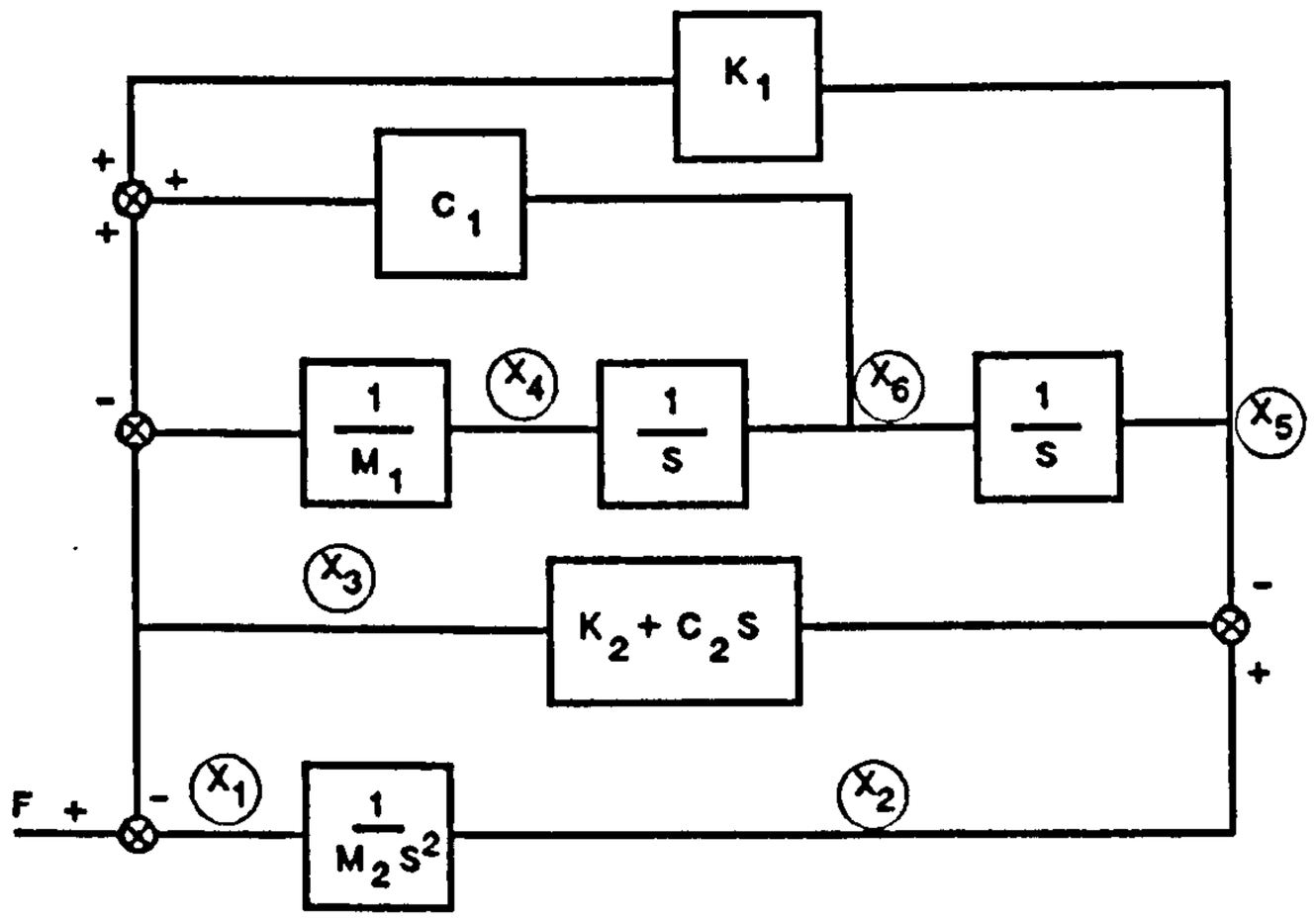

FIG.2.4 A BLOCK DIAGRAM FOR THE SYSTEM IN FIG. 2.3.

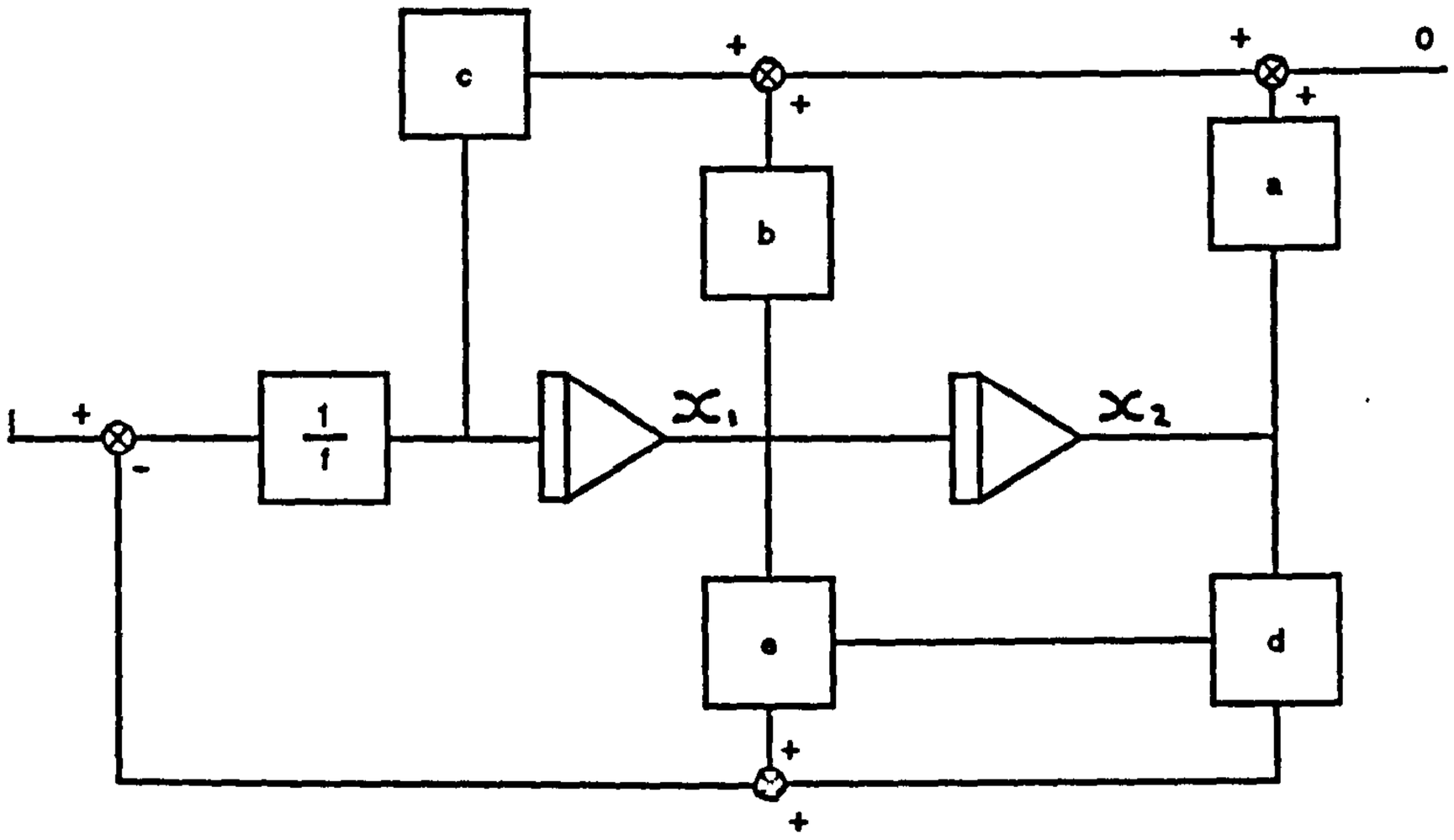

FIG.2.5 INTEGRATOR EQUIVALENT TO EQUATION 2.4

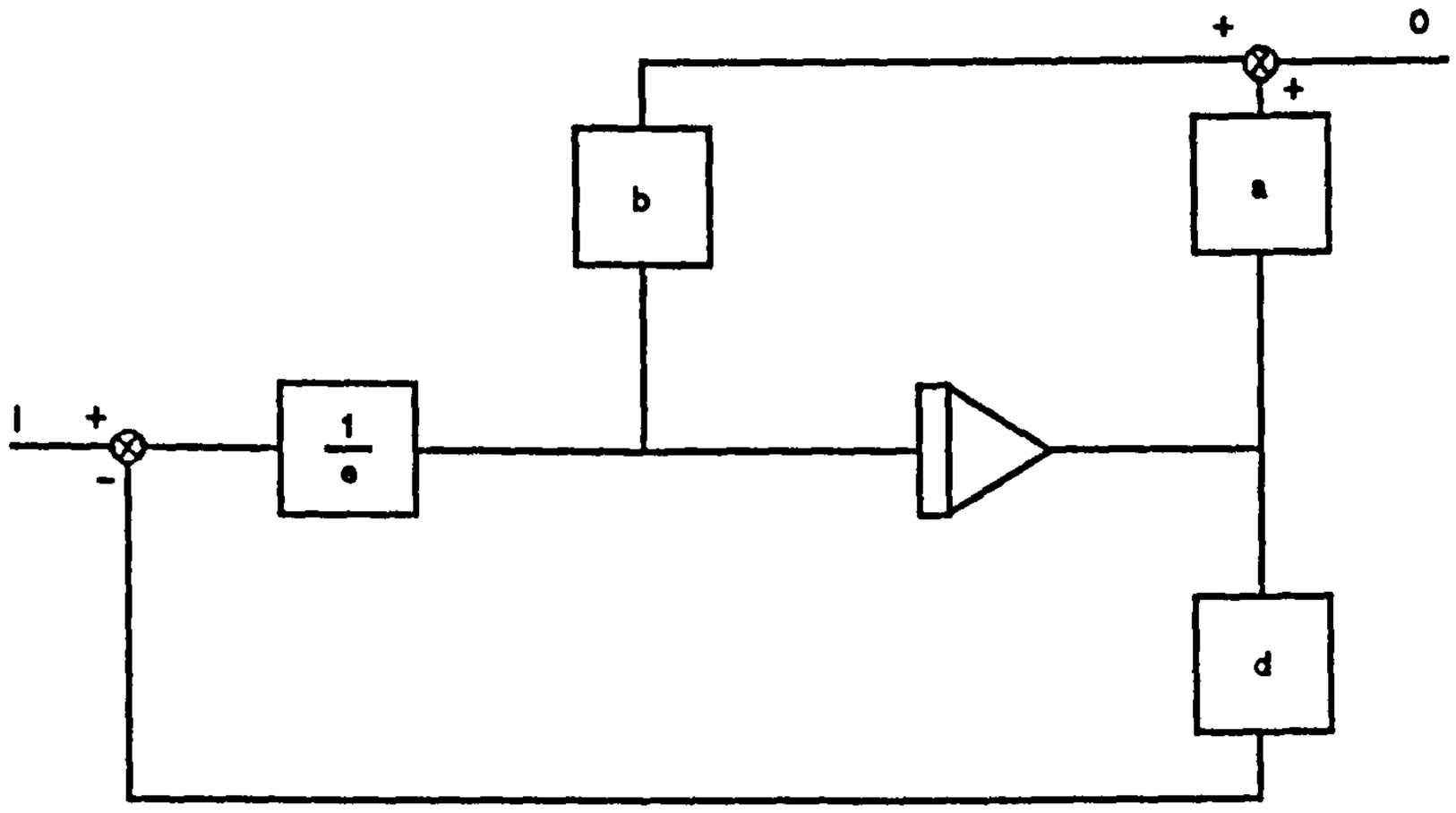

FIG.2.6 INTEGRATOR EQUIVALENT TO EQUATION 2.5

00739DG

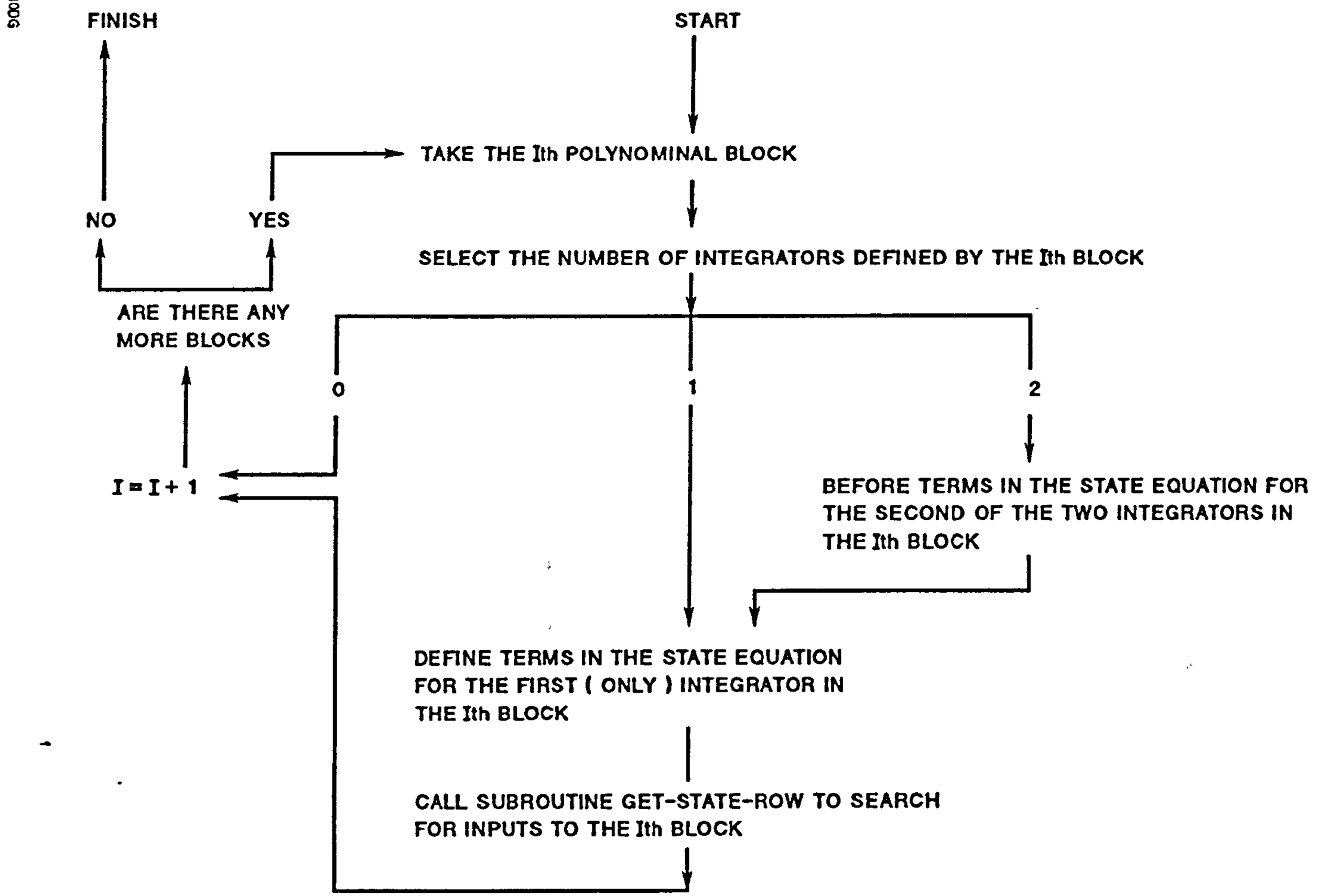

FIG.2.7 MAIN ROUTINE IN DERIVATION OF STATE MATRIX

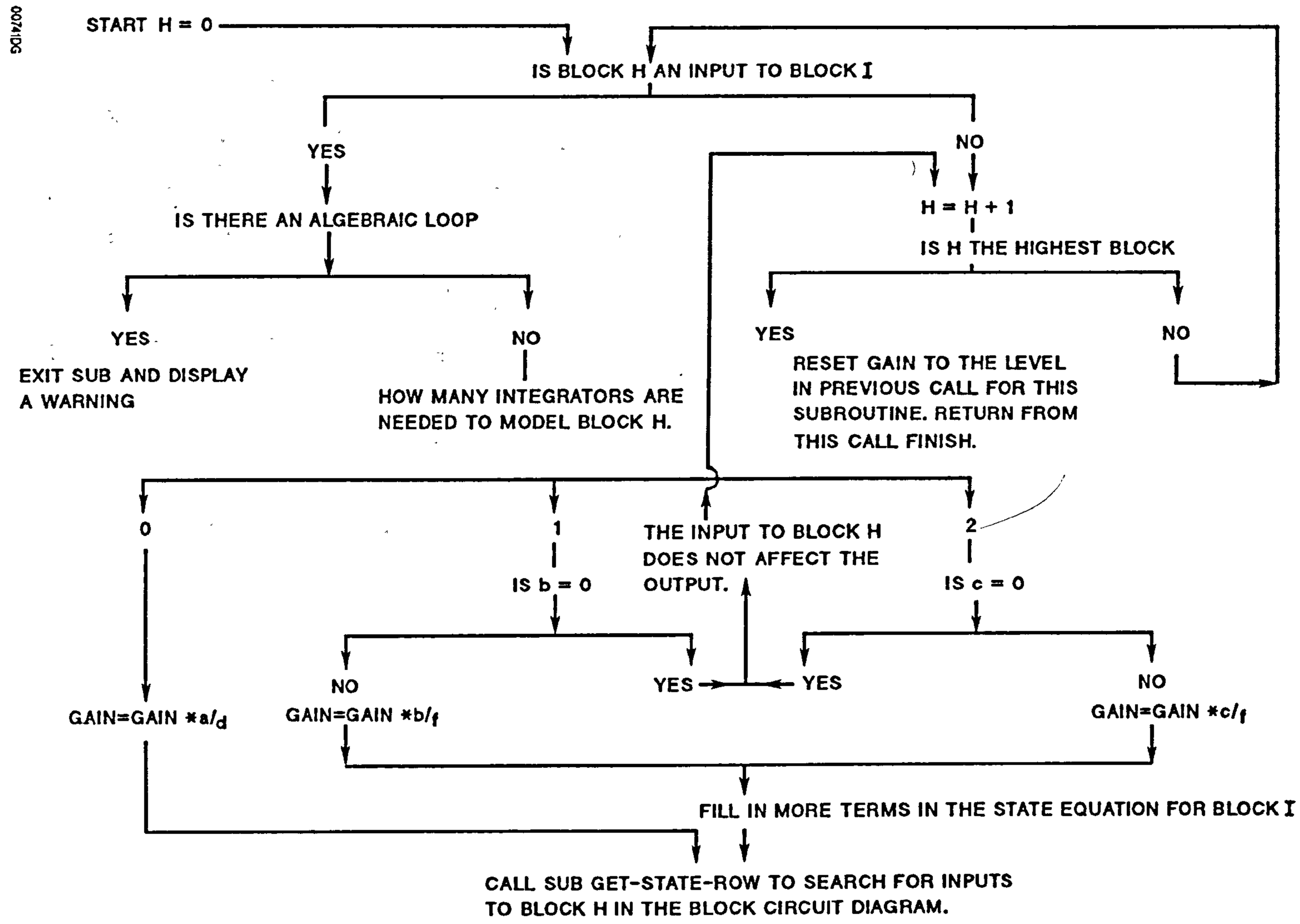

FIG.2.8 RECURSIVE ROUTINE TO DEFINE INPUTS TO POLYNOMINAL BLOCKS

CHAPTER 3 TESTS ON EXISTING GUIDEWAYS

3.1 INTRODUCTION

The aim of this project was to develop a suspension controller for a maglev vehicle on a flexible guideway in order to make maglev systems cheaper to build . There were two contemporary guideways that were relevant to this aim , the maglev guideway at Birmingham and an unusual guideway at Zurich .

The guideway at Birmingham was designed to be rigid . It was necessary to test this guideway to determine whether it had been built to specification . It was essential to decide if the rigid guideway suspension controller would work satisfactorily , before vehicle commissioning work commenced . This could only be done if the guideway dynamics were well understood .

The other contemporary guideway that was of interest was an opposite to the guideway at Birmingham . This guideway was built by a Swiss

cablecar manufacturer and it was very flexible . This guideway , at Zurich , would clearly present a number of magnetic and dynamic problems if it was to be used with a maglev vehicle . However this guideway was potentially so cheap that some investigation of its dynamic characteristic was required .

3.2 THE AEROBUS GUIDEWAY

In March 1983 the author visited Dietlikon near Zurich in response to a request for information from the company , Gerhard Muller A G . Herr Muller holds patents on a novel and very intriguing form of railway , a combination of cable car and monorail , called Aerobus . Photographs of the vehicle and guideway appear as Figs 3.1 and 3.2 . The cable support towers (span lengths) may be up to 500 m apart and therefore an Aerobus railway can be installed very cheaply . One prototype system had been installed temporarily at Mannheim during the 1970s , but only recently had commercial development restarted . Herr Muller wished to know if it would be possible to fit a maglev suspension to Aerobus . The program of work which this thesis describes had commenced only two months before Herr Muller's enquiries . The overhead cable of Aerobus seemed to be the most flexible guideway a maglev vehicle could

encounter and so Herr Muller's enquiry was well timed and well received .

A visit to Zurich was undertaken to provide a meeting for technical discussion to determine , broadly , if an Aerobus maglev suspension was commercially or technically feasible . The visit was also to provide an opportunity to test a standard Aerobus vehicle and its overhead cable guideway to determine operating parameters such as speed , ride quality and characteristic vibrations .

The physical parameters of the guideway are listed in Table 3.1 .

3.3 A DESCRIPTION OF AEROBUS

The guideway consists of a lower cable from which the vehicle is suspended and an upper catenary cable . The catenary cable is formed from a pair of close coiled , 45 mm diameter , stainless steel cables . The contact cable is formed from two pairs of such cables that are held apart by vertically aligned leaf springs . Each of the two contact cable pairs are bridged by a top face of aluminium to provide a flat surface on which the vehicle wheels run . This aluminium is expensive , but vital , as it is used to keep the wheel contact stresses out of the tensioned cables . The main cables have an unlimited

life , but the aluminium must be replaced biennially .

The contact cable is hung in a "hogged" profile so that as the constant weight of a vehicle moves along a span , the contact cable is pulled down for the vehicle to follow a true horizontal path . It seems likely that this feature will be most useful when the vehicle negotiates a transition . Since it is impossible for a tensioned cable to guide a vehicle through curves , direction changes are formed by fastening a curved steel beam to the contact wire . The hogging of the contact wire is then used to ensure that the vehicle enters the transition (rigid steel beam) at the correct angle of attack . The practical limitation to this rather nice scheme is that any variation in vehicle weight will affect the accuracy of the angle of attack into the transition . An Aerobus vehicle (particularly a maglev Aerobus) must be designed to maximise the laden to tare weight ratio and this minimises the benefits of a contact wire that can only be hogged to match a specific vehicle weight .

The test vehicle that the author examined was one of the prototype vehicles from Mannheim . The structure is lightweight GRP with perspex windows and is made up of nine separate sections . The section joints are articulated vertically and laterally using soft rubber shear pads at roof and floor levels . Each section of the vehicle has a roof mounted

electric motor which drives a pair of flanged wheels via six separate V-belts . The wheel treads are cylindrical and have a 1 mm covering of rubber . Aerobus also has a pair of lateral guidance wheels .

The vehicle vertical suspension is in the rubber tread of the wheels and in some small , permanently inflated Firestone airsprings fitted between the body and the wheels . This suspension provides a lightly damped bounce frequency in the region of 5 Hz .

3.4 TEST RESULTS

The test track available for Aerobus was only 900 m long , it ran through a working quarry which caused a speed restriction of 25 mph because of undermining of the cable towers . The test track was straight , with a central hill , and had four spans of cable with lengths of 120 m , 340 m , 320 m and 140 m . Vertical gradients and transitions were severe , see Fig 3.2 , and braking distances were estimated conservatively . As a consequence , vehicle speed was never allowed to be constant for more than 20 to 30 seconds in one run . Subjectively , the ride was perfectly acceptable for the short distances involved but significant noise and vibration was observed as the vehicle passed through span transitions .

Tests were carried out on the overhead guideway by placing an accelerometer on the 340m span contact cable centre about 50 m from the mast between the 120m and the 340 m span . Signals from the accelerometer were recorded on analogue tape as the Aerobus travelled along the test track towards the 120m span . Peak accelerations of around 3 g were recorded as Aerobus passed the transducer .

On one test run the signal gain was deliberately set high . At passing time there was massive signal distortion and clipping but after the vehicle had passed the test span and stopped at the end of the site there was a good record of the decaying contact cable oscillations . A PSD of this signal is shown as Fig 3.3 , although the signal was non-stationary and the validity of the PSD was thus limited , it gives an indication of the natural frequencies of the cable system .

Fig 3.3 shows sets of peaks in the spectrum , there are four peaks to each set , with centre frequencies of 0.9 Hz , 2.7 Hz , 4.5 Hz , 6 Hz , 8 Hz and 10 Hz . The 6 Hz and 8 Hz sets have much lower amplitudes than the other sets . Analysis of the dynamic behaviour of railway overhead electrified lines has revealed a similar phenomenon . An explanation for this behaviour is that there are four coupled spans in the system , and for any mode shape within a span , an n-span coupled system will have n

associated natural frequencies associated with each harmonic .

The transducer was situated approximately one seventh of the way along one span , at this position the transducer would have been close to a node for the seventh harmonic , assuming that there was a true seventh harmonic . This is a possible explanation of the low amplitude response for the 6 Hz and 8 Hz sets . The 0.9 Hz set is likely to be the first harmonic , the 2.7 Hz the third harmonic , 4.5 Hz the fifth harmonic , 6 Hz the seventh , 8 Hz the ninth and 10 Hz the eleventh . If this hypothesis is correct , Aerobus did not excite the even harmonics of the cable system .

3.5 THE BIRMINGHAM GUIDEWAY

During 1983 the world's first commercially operating magnetically levitated railway was commissioned . Vehicles run between British Rail's Birmingham International Station and West Midland County Council's new terminal at Birmingham Airport . The guideway for the maglev vehicles is elevated and consists of a series of bridgelike structures , as a consequence it is likely to be more flexible than a guideway at ground level .

West Midland County Council gave permission for this guideway to be dynamically tested during March

1983 as the maglev vehicles were not yet commissioned and running on the guideway . Tests were arranged for March because once the Birmingham vehicles were available there would have been no other opportunity for guideway tests .

Fig 3.4 is a simple sketch of the guideway structure and Fig 3.5 is a mid-span cross-section which shows the vehicle levitation rails . Photographs of the guideway appear as Figs 3.6 and 3.7 . Dynamic tests on a structure of this size posed the problem of how the structure should be excited . The supported guideway mass was around 80 tonnes and it was expexcted that the first bending frequency might be as high as 10 Hz . Conventional test techniques would not provide enough energy for adequate excitation of this large structure .

Orthodox excitation by hydraulic actuator was not feasible . The guideway elevation above ground and lack of a rigid reaction base were obvious difficulties , compounded by the absence of a hydraulic power supply and only a 4 kvA electrical power supply . As an alternative , an impulse hammer would have to weigh around 1 tonne to produce a significant displacement in the guideway .

A quite simple means of excitation was employed using a large mass which was suspended below the guideway by rope slings . This mass was released , almost instantaneously , and the acceleration responses of the guideway and the applied force

change signals were processed to yield guideway frequency responses . These responses were analysed to determine natural frequencies and damping levels for the Birmingham guideway .

3.6 TEST METHODOLOGY

The mass suspended below the guideway was a builders waste disposal skip which , when full of ballast , weighed between 7 and 7.5 tonnes , depending on recent rainfall . The mass was suspended from the guideway via a hand pumped hydraulic actuator (which was used to lift the mass a few millimetres off the ground) , a load cell and a 16mm high tensile steel bolt . This bolt supported the weight of the mass and was severed to provide a very "square" step force input to the guideway . The force was applied to the vehicle levitation rails . This gave an effective loading point on one track centreline . Photographs of the test set-up appear as Fig 3.8 .

Accelerometers were mounted on the longitudinal centreline of both guideway tracks in one span , together with selected sites on the main Tee structures at each end of the test span . Accelerometer sites at the track centreline were selected to try and simplify the measured responses of the guideway by minimising the asymmetric (roll)

responses and maximising the symmetric (bounce) responses . It was assumed that the concrete tees would be rigid and that the track roll responses would only exist in the steelwork at frequencies in excess of 30 Hz .

Two separate sets of tests were performed , firstly with the force applied two thirds of the way along the span , secondly with the force applied half way along the span . It was intended that these tests would excite the first five harmonics of the simple span system . Each test was repeated three times and the measurements were averaged in the frequency domain , figs 3.9 to 3.13 show typical frequency responses .

3.7 ANALYSIS METHOD

The acceleration and force signals were initially recorded on an analogue tape recorder and then replayed from the tape recorder and analysed in a Hewlet-Packard 3582A spectrum analyser . Because the transform length of the analyser is limited , the frequency range of interest , 0 to 30 Hz , was analysed in 10 Hz sections . All three tests for any one combination of accelerometer site and input force were analysed and averaged in the frequency domain . The measured frequency responses were downloaded from

the analyser to a Hewlett-Packard computer for digital storage .

In effect , the analyser was used to select a narrow band signal from the broad band time responses played back from the tape recorder . The analyser input gain had to be selected to avoid clipping the broad band responses and hence the narrow band signals had a very low amplitude and poor digital resolution . The frequency responses of such signals had a very low coherence . This difficulty was overcome by analogue bandpass filtering the tape recorder signal . The input gain of the analyser could then be set to accommodate the low amplitude , narrow band signal . The analogue band pass filters also had the advantage of turning a step response into something that resembled an impulse response . The "impulse" response required no pre-FFT windowing and hence no windowing distortion occured .

The digitally recorded frequency responses were loaded into the Suspension Unit's Hewlett-Packard 1045-F computer for modal analysis . Modal analysis was carried out with the aid of the PAPA9 computer program obtained from the Royal Aircraft Establishment at Farnborough, described in Ref 3.1 and 3.2 .

3.8 DISCUSSION OF RESULTS

The quality of the measured frequency responses is generally very good , coherence for each set of three tests is only below 0.95 for responses at the span ends where the acceleration signal amplitudes were low . The responses , shown in Figs 3.9 to 3.13 , are extremely complex . Only a simplified modal analysis , which ignored low amplitude modes , was attempted . This was acceptable because it was still possible to synthesize the measured frequency responses to an acceptable degree of accuracy .

The main aim of this work was to determine a description of the guideway dynamic stiffness . The modal analysis parameters provide the basis of such a description and also an estimate of the quality of this information . The PAPA9 program synthesizes a frequency response from the estimated modal parameters and subtracts this from the measured response . After normalising this difference with respect to the measured response , the program calculates the mean of each value over the entire frequency range of the analysis . This mean value is defined as the Frequency Response Error (FRE) :-

$$FRE = 100/N \left(\frac{|FR_M(i) - FR_S(i)|}{|FR_M(i)|}\right)^{1/2}$$

where $FR_M(i)$ is the ith of N measured frequency response values in a set of N values . FR_S is a frequency response value that has been synthesized from the PAPA9 modal parameters .

Despite the fact that only seven modes from a set of twelve were used in the analysis , FRE was small . FRE varied between 7% and 18% with a mean of 12.5% over all measured responses . An error level as low as this provides substantial justification for the simplified modal analysis that was used .

Table 3.2 shows values for natural frequency and damping from the modal analysis of up to 24 measurements in the frequency range 5 to 15 Hz . The mode shape data is plotted in Figs 3.14 to 3.20 .

After testing was finished , the author discovered that the structure of the guideway was less symmetric than originally thought . The inner of the two main longitudinal beams that make up one track was designed to be 20% stiffer than the outer beam . This meant that despite the apparent symmetry of loading on one track , the two main beams responded with some asymmetry . Further , the transducers were not mounted on the track neutral axis and were sensitive to roll of the single track .

Testing revealed a very strong span to span coupling along the guideway which , in hindsight , was only to be expected . Because of the very high vertical stiffness of the bridge bearings , the Tee structure will couple the ends of one span directly to the adjacent one . Dynamically , all 700 m of this guideway act as one structure .

The two effects of single track asymmetry and span to span coupling are likely explanations of the large numbers of low amplitude modes found when analysing the frequency responses .

These tests are described in greater detail in Ref 3.3 .

3.9 DESIGN CALCULATIONS

Detailed analysis has been performed for seven modes . The author's confidence in the estimates for the natural frequency of the first four modes was enhanced by a simple analysis of the main longitudinal beams .

Each end of these beams is supported by a rubber shear pad bridge bearing with a vertical stiffness designed to be more than 500 MN/m . Logically , the vertical stiffness of the arm of the Tee support is unlikely to be significantly less than this . The author wrote a computer program to calculate the mid-span receptance of a spring supported beam . This showed that if the spring stiffness is greater than 100 MN/m , a beam of this type behaves substantially as though it were pinned at each end .

West Midland County Council provided data for the structural properties of the two beam types , which combined with the knowledge that the test span length was 15.35 m and the length of the adjacent

road bridge span was 17.01 m allowed the calculation of four fundamental beam bending frequencies . This data appears in Table 3.3 .

The four calculated frequencies are :-

6.92 Hz , 7.50 Hz , 8.43 Hz and 9.27 Hz

The first four measured frequencies are :-

6.23 Hz , 7.16 Hz , 8.56 Hz and 9.53 Hz

Further , all the experimentally determined mode shapes were fundamental in nature .

Damping levels in five of the seven experimentally determined modes vary between 2.0% and 2.6% . The other two modes show damping of 3.3% and 4% .

3.10 CONCLUSIONS

At Birmingham , the natural frequencies , damping and mode shapes of an unusual structure were determined by a novel and economical test method . A guideway with a 6 Hz natural frequency , 2% damping and a supported mass of 40 tonnes is within the stability range defined by Williams in Ref 3.4 . The commissioning of the Birmingham vehicles was allowed to proceed in the knowledge that guideway flexibility would not affect the performance of the vehicle suspensions .

Computer software and experimental techniques for dynamic testing were developed and proven for

future work . Guideway dynamic parameters were obtained that would allow modelling of the coupled vehicle-guideway system .

At Zurich the tests have provided an insight into the dynamic behaviour of a tensioned guideway , that will be neccesary for future modelling work . The behaviour of the tensioned guideway related to BR's experience of the dynamics of overhead electrified lines .

3.11 REFERENCES

3.1 Gaukroger , Skingle and Heron . Numerical Analysis of Vector Response Loci . Journal of Sound and Vibration . 1973 29(3)

3.2 Copley . Analysis of Subcritical Response Measurements from Aircraft Flutter Tests Shock and Vibration Bulletin part 3 May 1981

3.3 Lawton . Dynamic Tests on the Guideway for Maglev Vehicles at Birmingham International Airport . Internal BR Report TMDOS 143 , August 1984

3.4 Williams . Interaction Between a Maglev Vehicle and a Flexible Track . Internal BR Report IMDOS 85 1981

TABLE 3.1 AEROBUS GUIDEWAY PARAMETERS

Cable mass per unit length	
Catenary	2 * 11.5 kg.m
Contact	4 * 11.5 kg/m
Cable Tension	
Catenary	1.3 MN
Contact	2.6 MN
Cable Bending Stiffness	Unknown
Vehicle mass	Variable with a 1:2 tare to laden ratio
Wheel Load	A maximum of 1/160 of cable tension .

TABLE 3.2 MODAL ANALYSIS RESULTS FOR BIRMINGHAM

Natural frequency Hz	Damping % of critical
6.23 (.04)	2.0 (0.7)
7.16 (.09)	4.0 (1.2)
8.56 (.06)	3.3 (0.7)
9.35 (.11)	2.1 (1.2)
11.1 (.1)	2.3 (0.9)
12.4 (.1)	2.3 (0.8)
13.4 (.1)	2.0 (0.8)

The figures in brackets are the 90% Confidence levels calculated during the modal analysis .

TABLE 3.3 BIRMINGHAM GUIDEWAY PARAMETERS

Beam second moment of area ,	Inner	0.06 m^4
	Outer	0.05 m^4
Beam mass		1240 kg/m
Concrete Modulus		4×10^{10} N/m^2
Beam Length		15.35 & 17.01 m

FIG 3.1 THE AEROBUS VEHICLE

FIG 3.2 THE AEROBUS GUIDEWAY

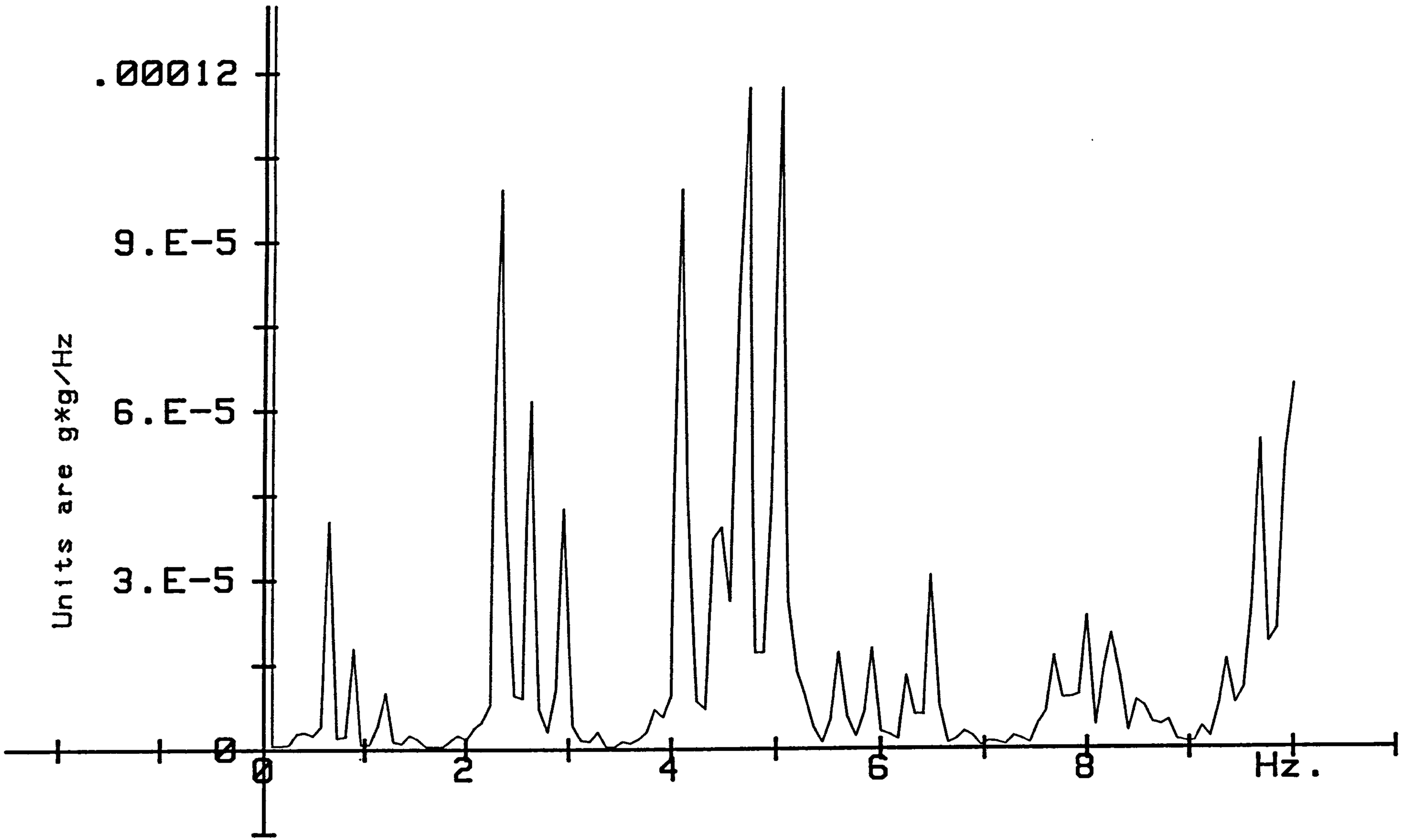

FIG 3.3 GUIDEWAY SPECTRUM

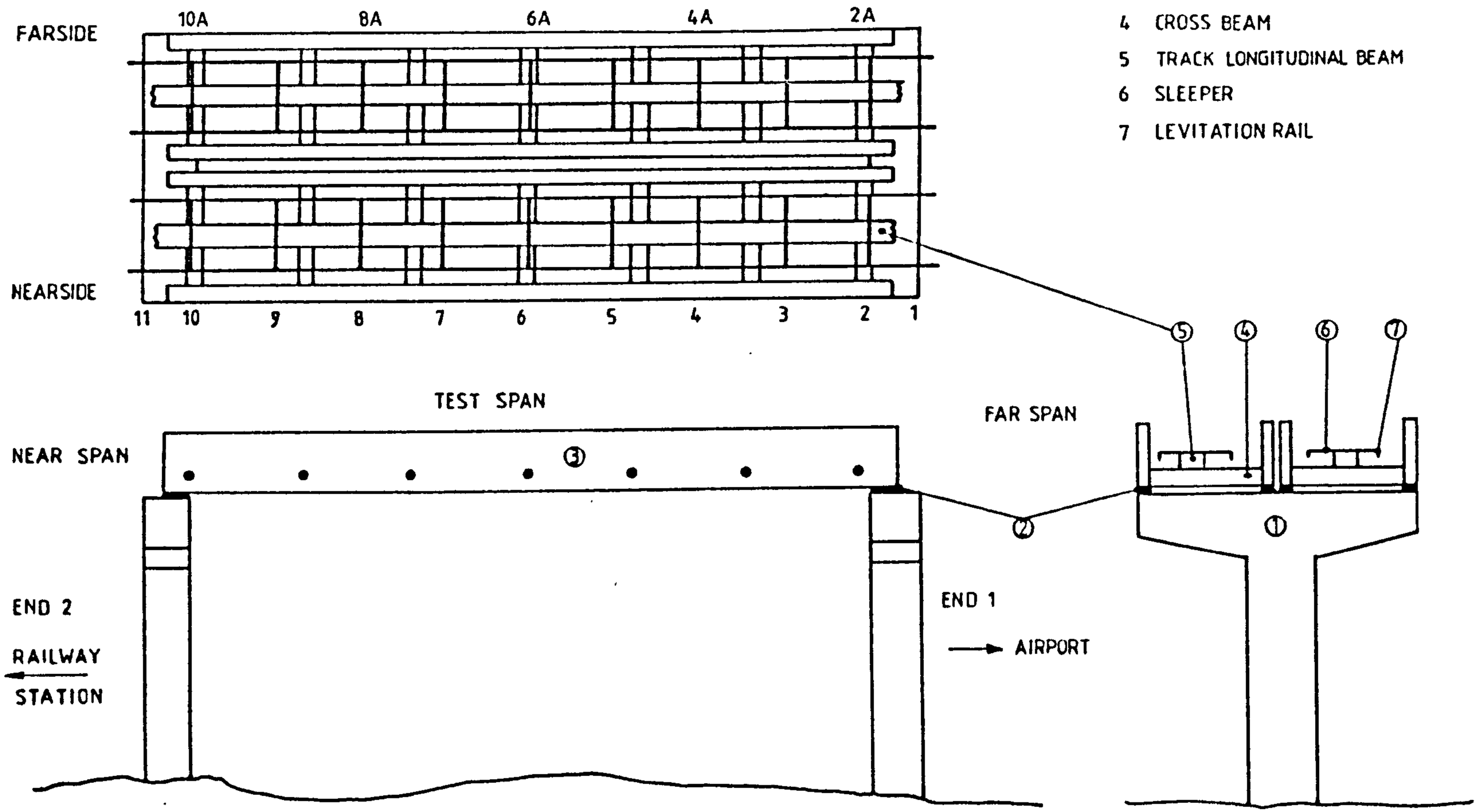

FIG. 3.4 GUIDEWAY STRUCTURE

1. TEE SUPPORT.
2. BRIDGE BEARING PADS.
3. MAIN LONGITUDINAL BEAM.
4. CROSS BEAM.
5. TRACK LONGITUDINAL BEAM.
6. SLEEPER.
7. LEVITATION RAIL.
8. L.I.M. RAIL.

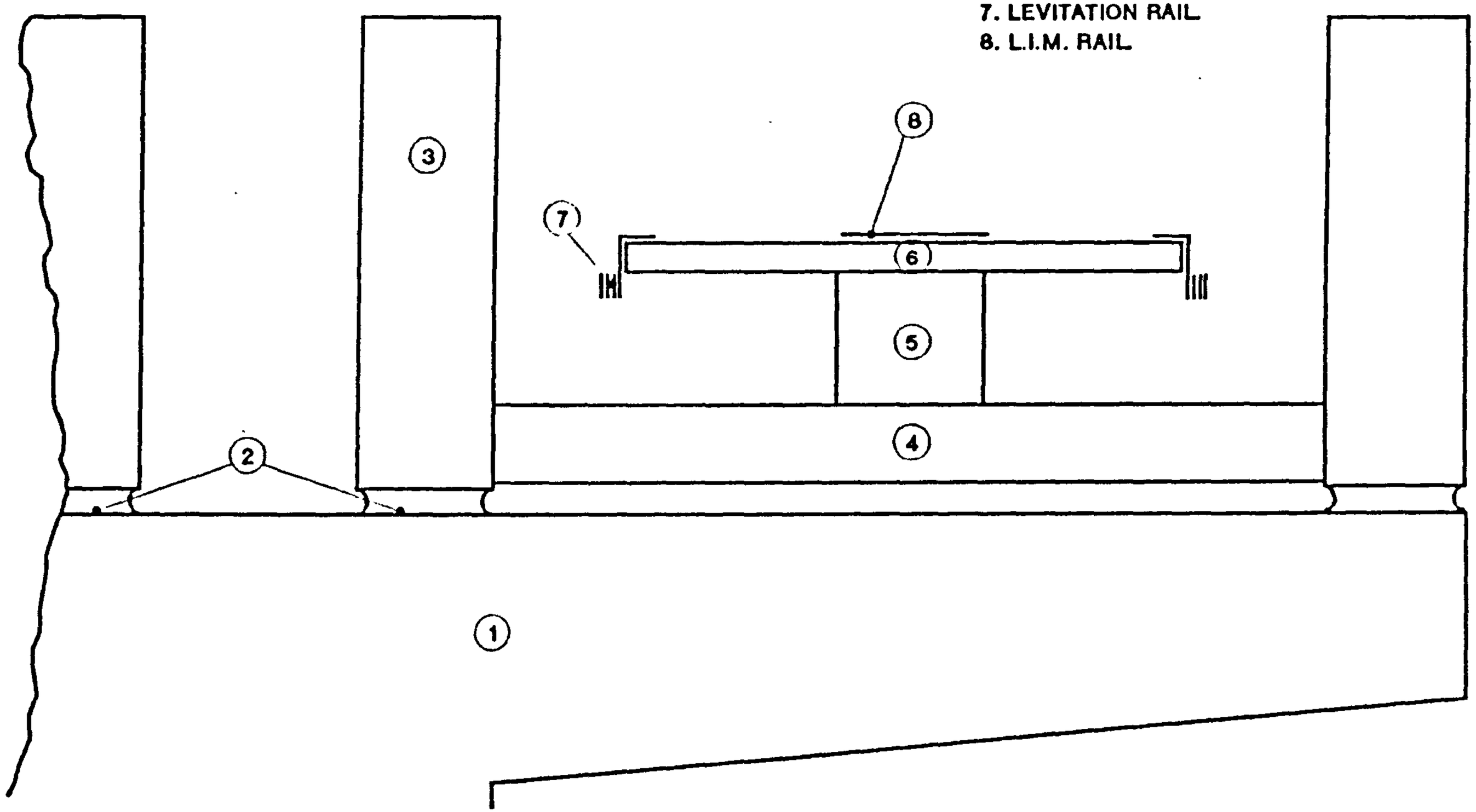

FIG. 3.5. GUIDEWAY SECTIONAL VIEW

FIG. 3.6 THE TEST SITE

FIG. 3.7 THE MAGLEV GUIDEWAY AT BIRMINGHAM

FIG. 3.8 TEST EQUIPMENT

Figs 3.9 to 3.13 have identical but unquantified sensitivity .

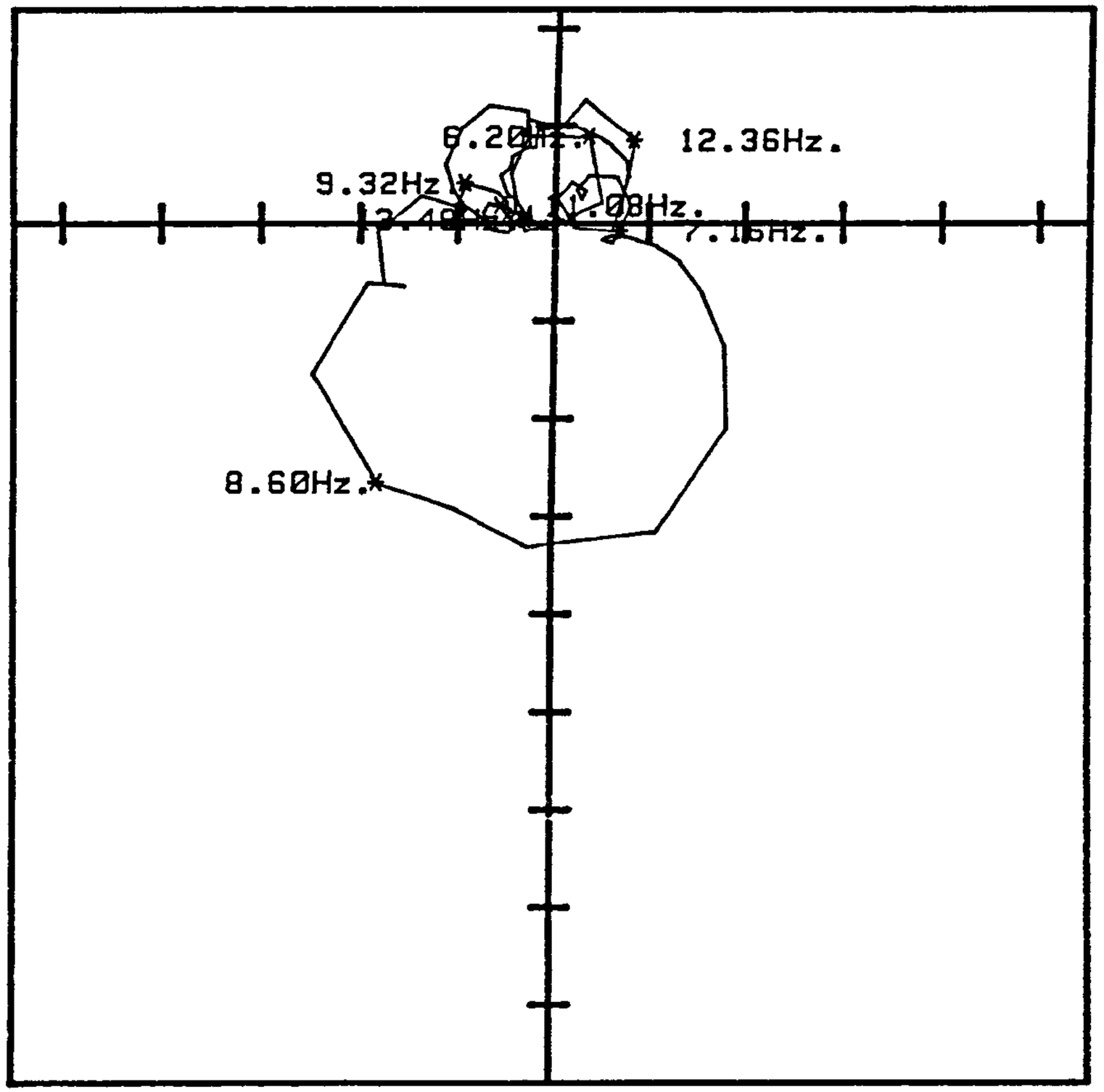

FIG 3.10 MAIN BEAM END

Figs 3.9 to 3.13 have identical but unquantified sensitivity .

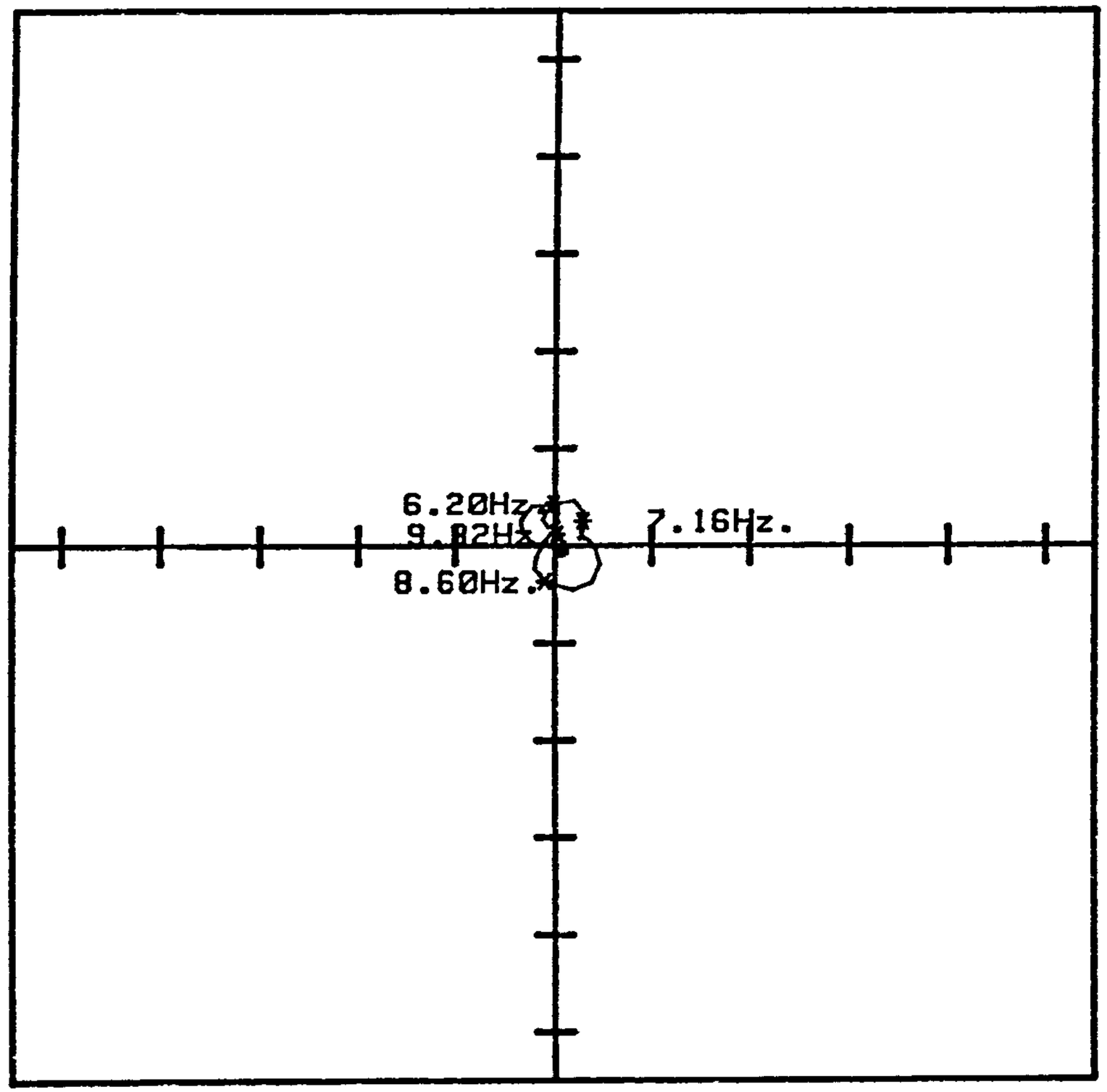

FIG 3.9 TEE STRUCTURE

Figs 3.9 to 3.13 have identical but unquantified sensitivity .

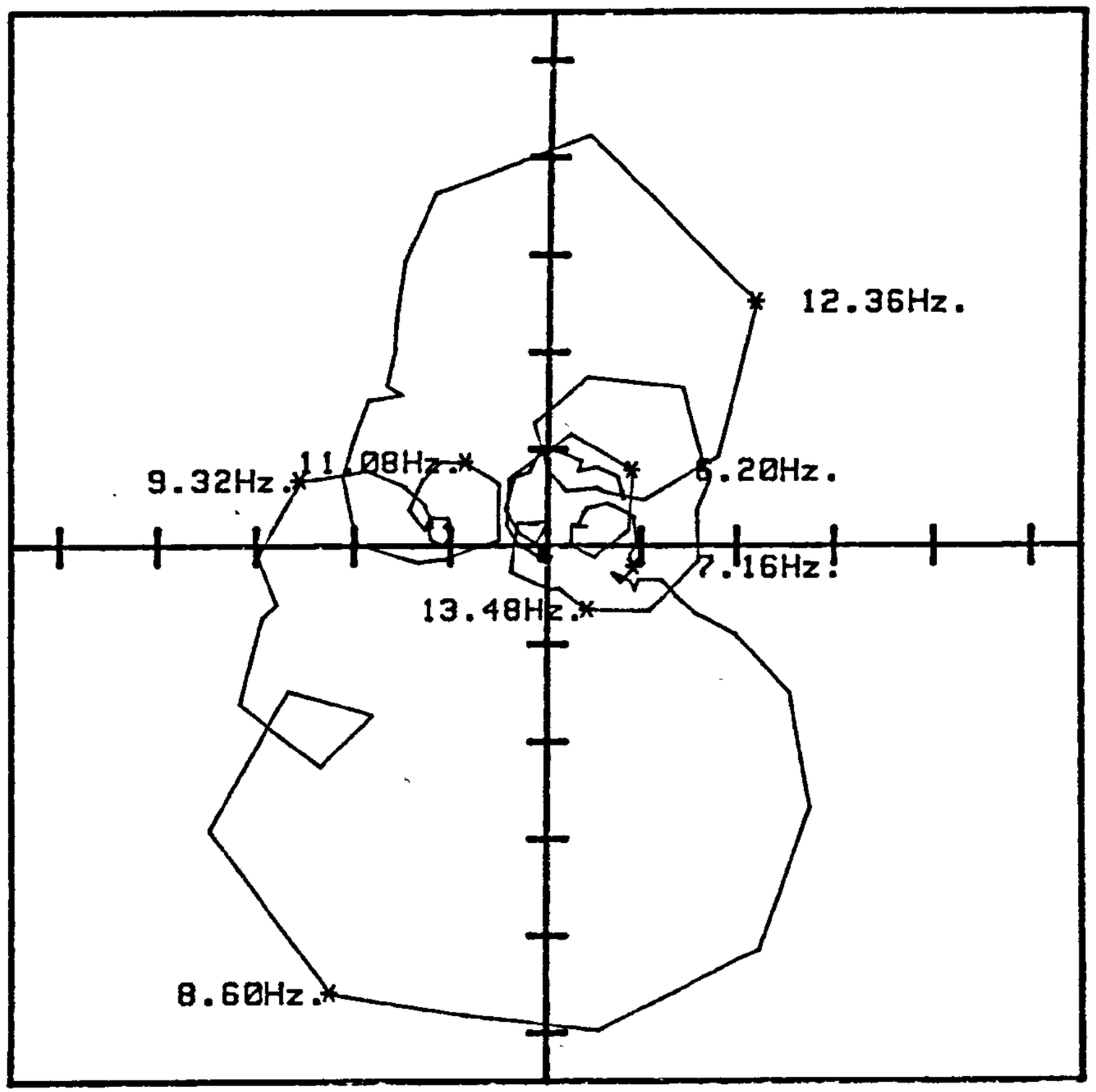

FIG 3.12 MID-SPAN

Figs 3.9 to 3.13 have identical but unquantified sensitivity .

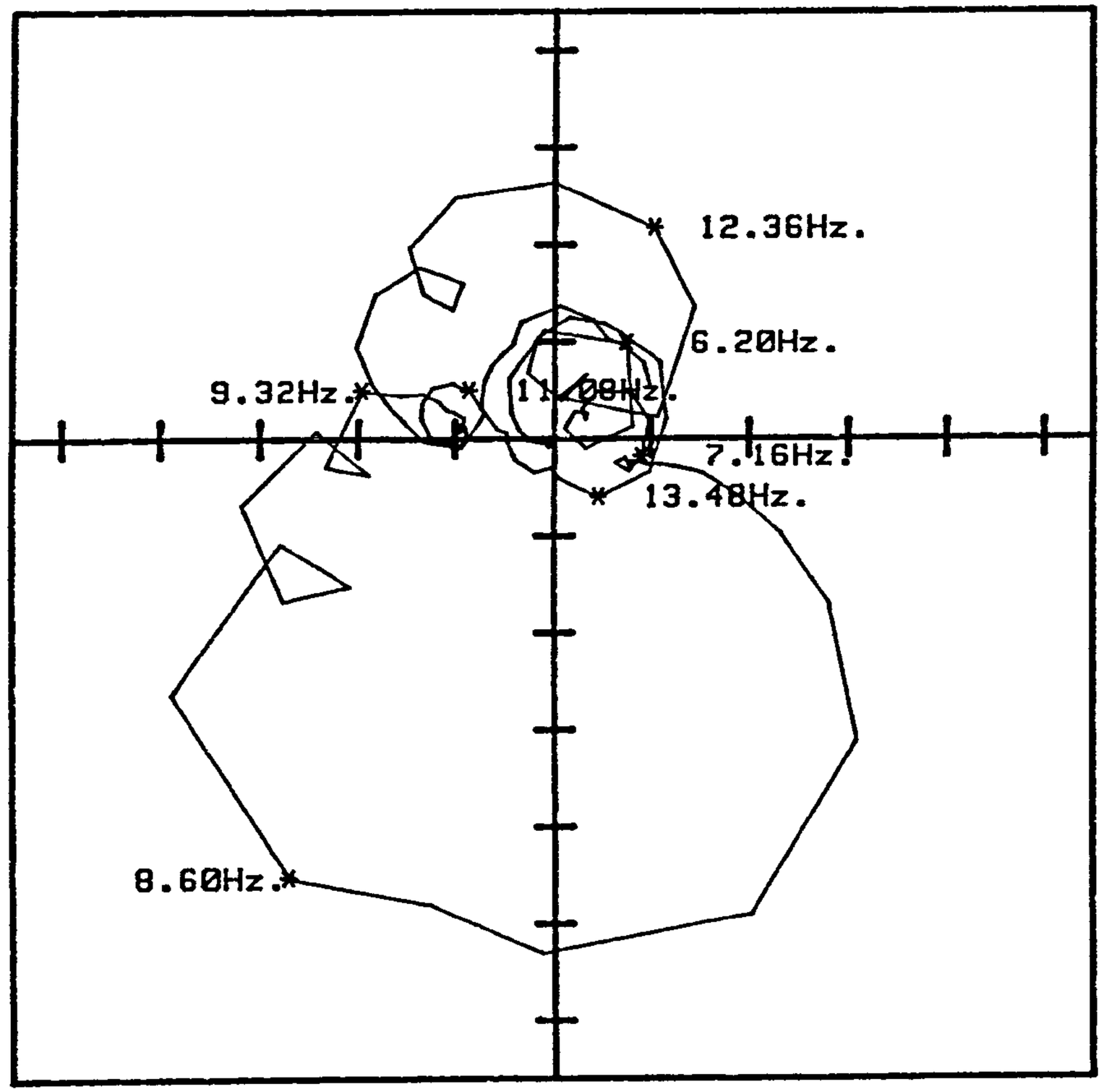

FIG 3.11 QUARTER SPAN

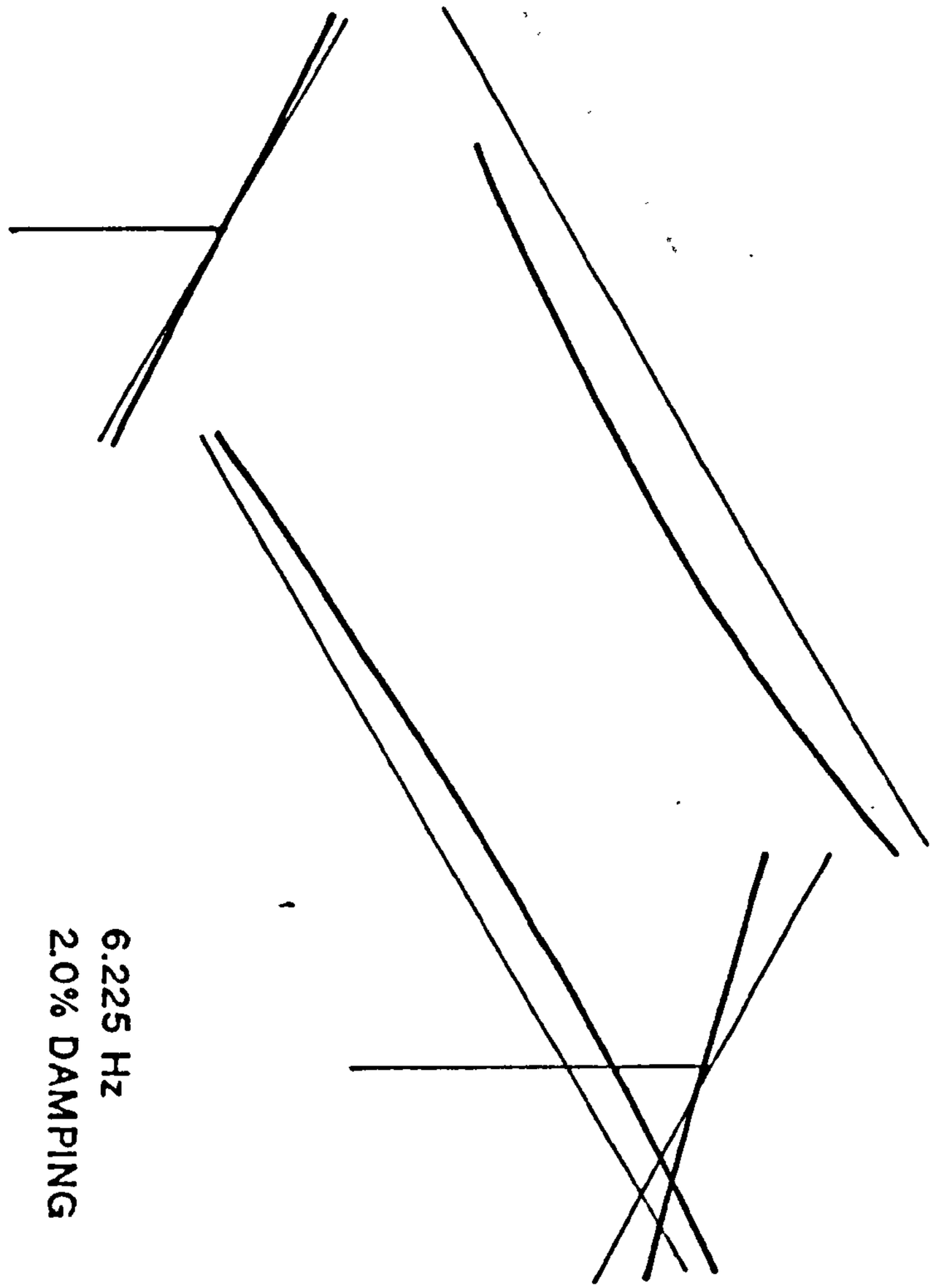

6.225 Hz
2.0% DAMPING

FIG. 3.14 MODESHAPE 1

Figs 3.9 to 3.13 have identical but unquantified sensitivity .

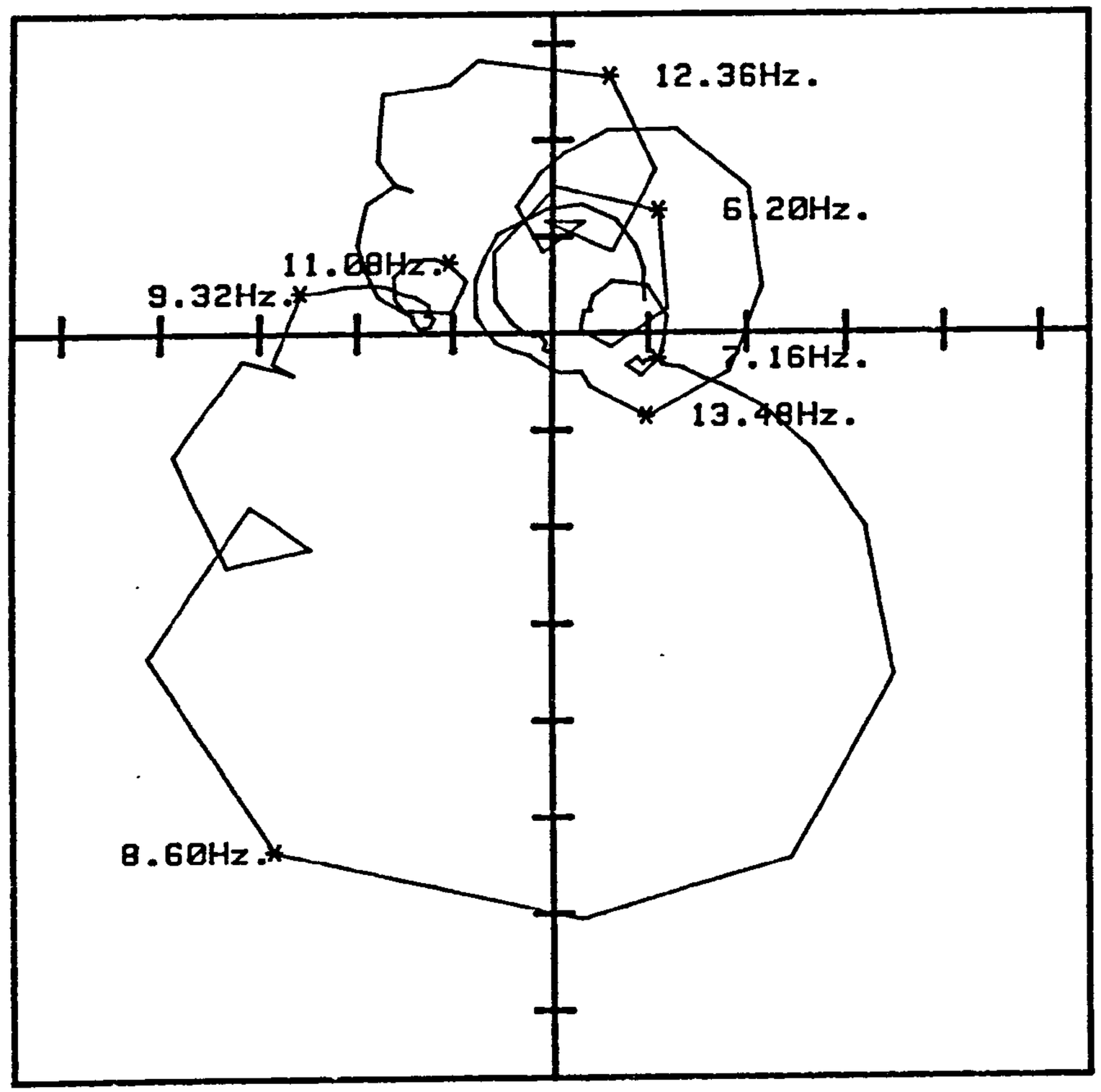

FIG 3.13 THREEQUARTER SPAN

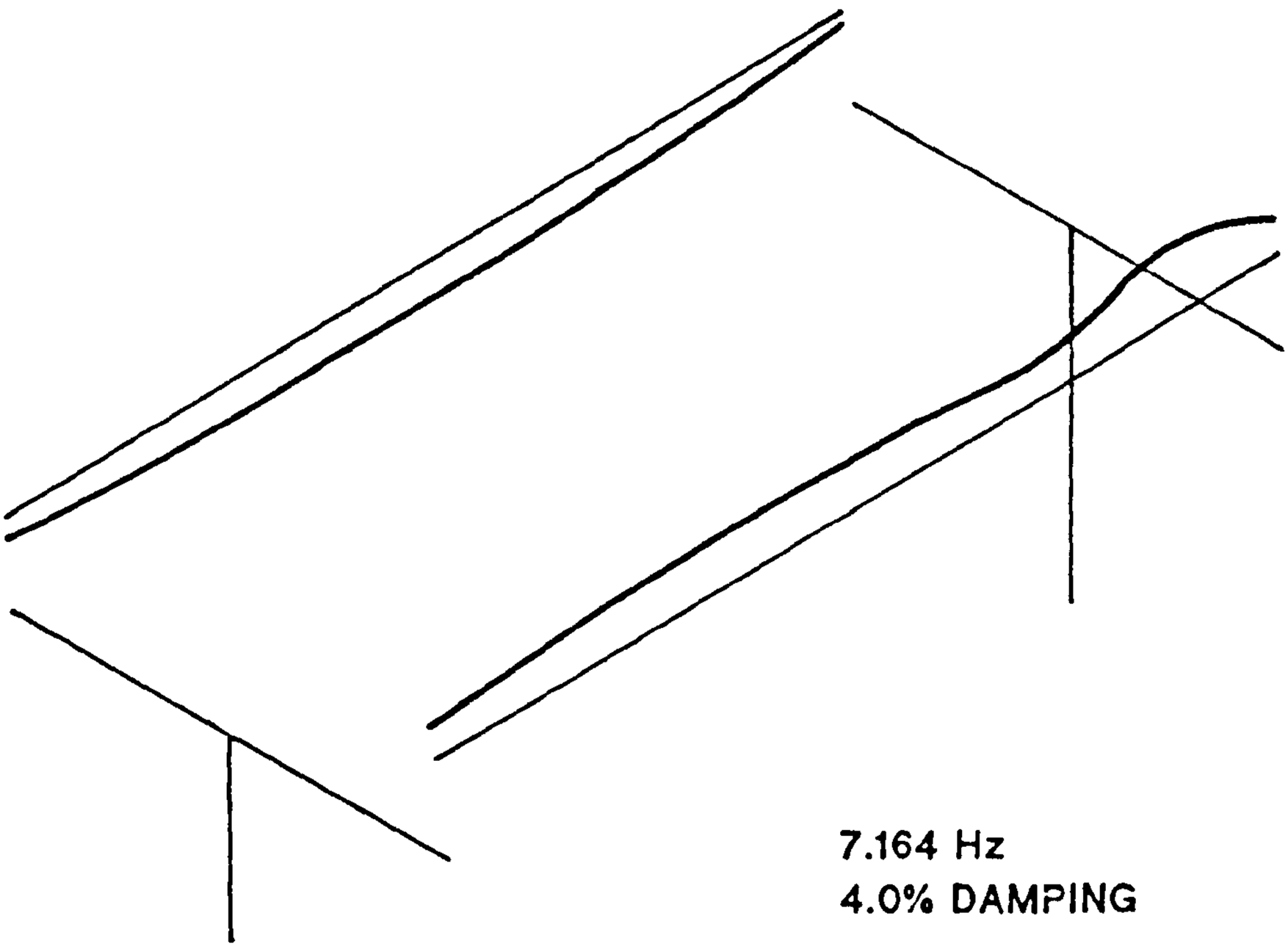

7.164 Hz
4.0% DAMPING

FIG. 3.15 MODESHAPE 2

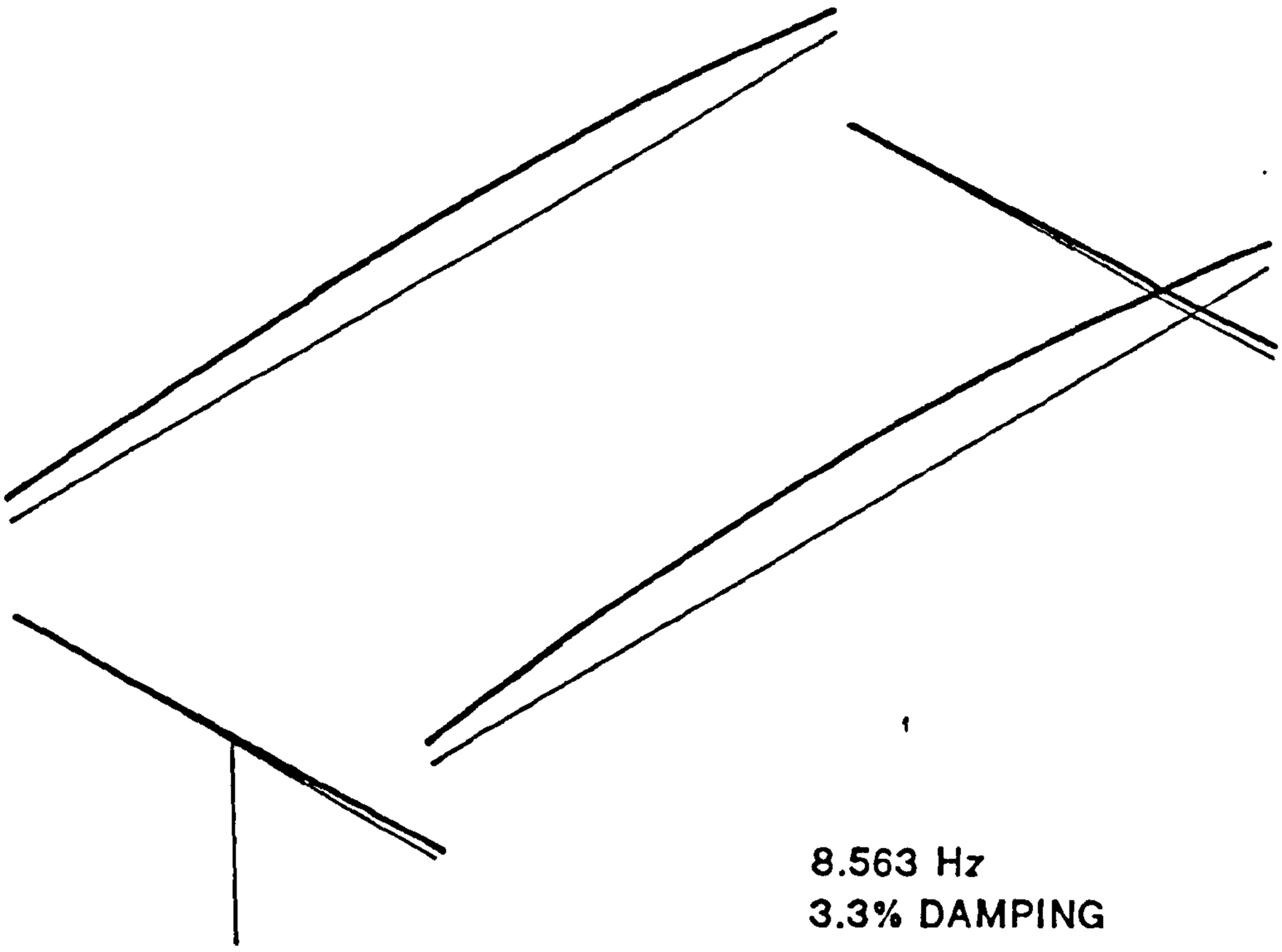

8.563 Hz
3.3% DAMPING

FIG. 3.16 MODESHAPE 3

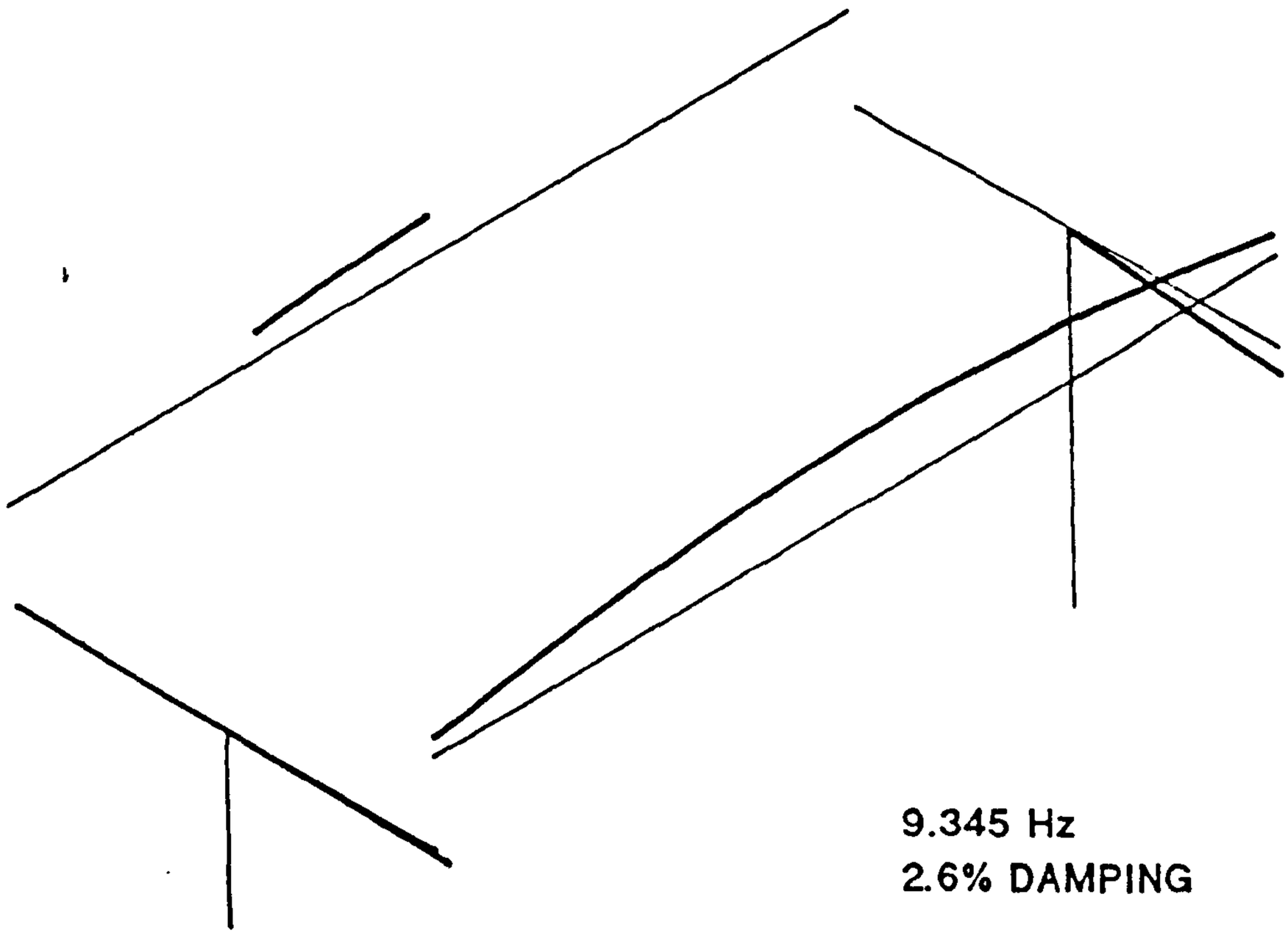

9.345 Hz
2.6% DAMPING

FIG. 3.17. MODESHAPE 4

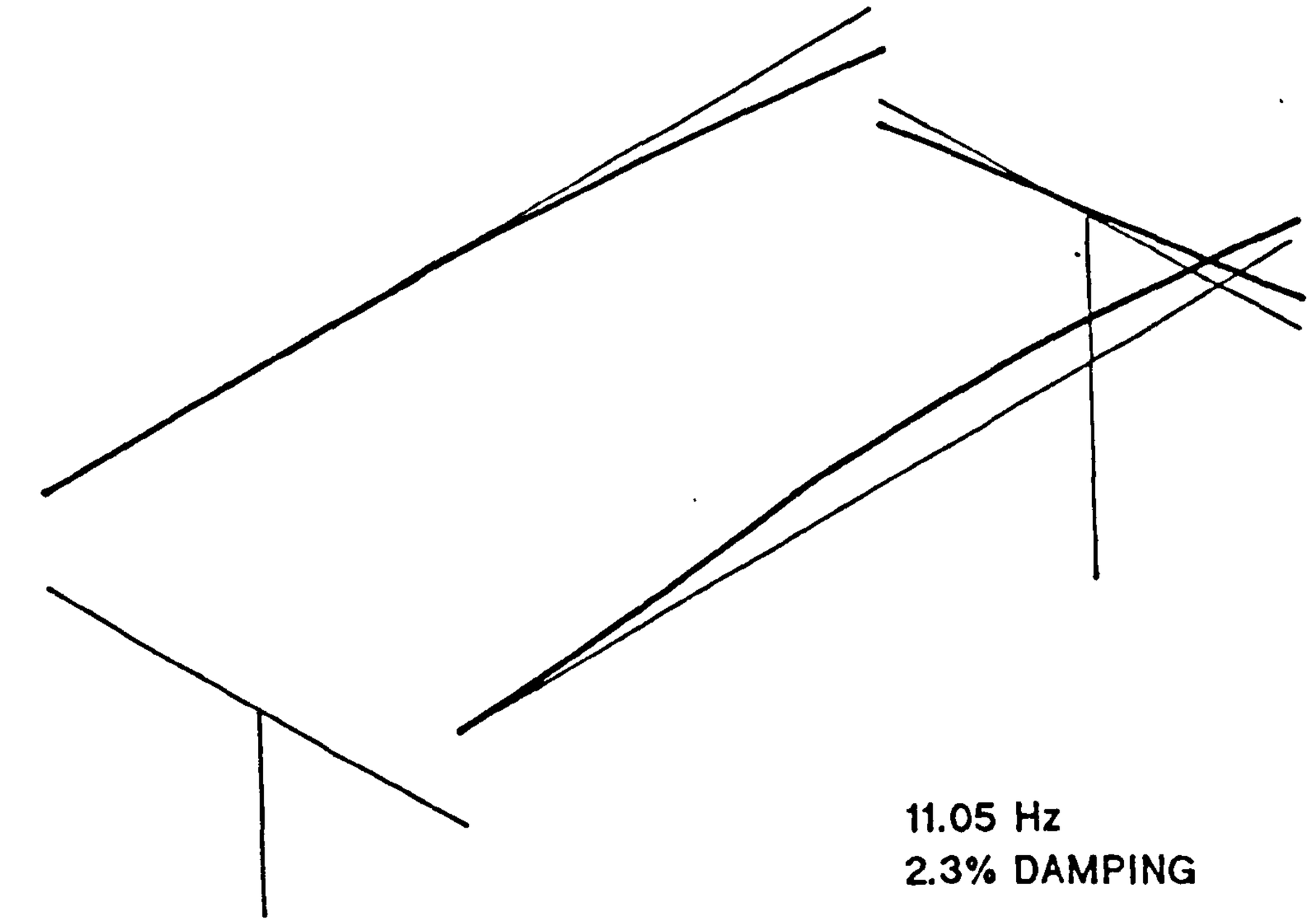

11.05 Hz
2.3% DAMPING

FIG. 3.18 MODESHAPE 5

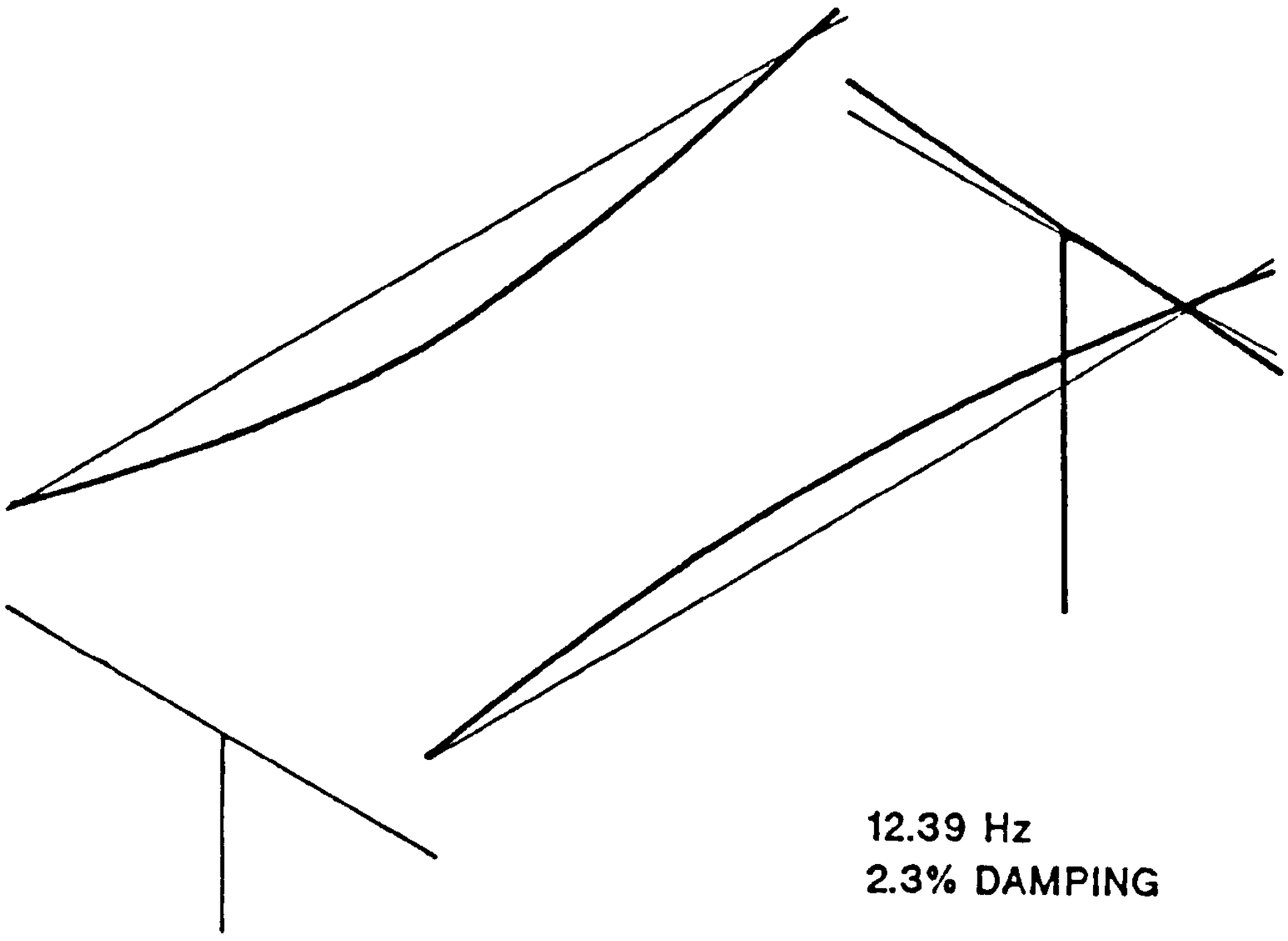

12.39 Hz
2.3% DAMPING

FIG. 3.19 MODESHAPE 6

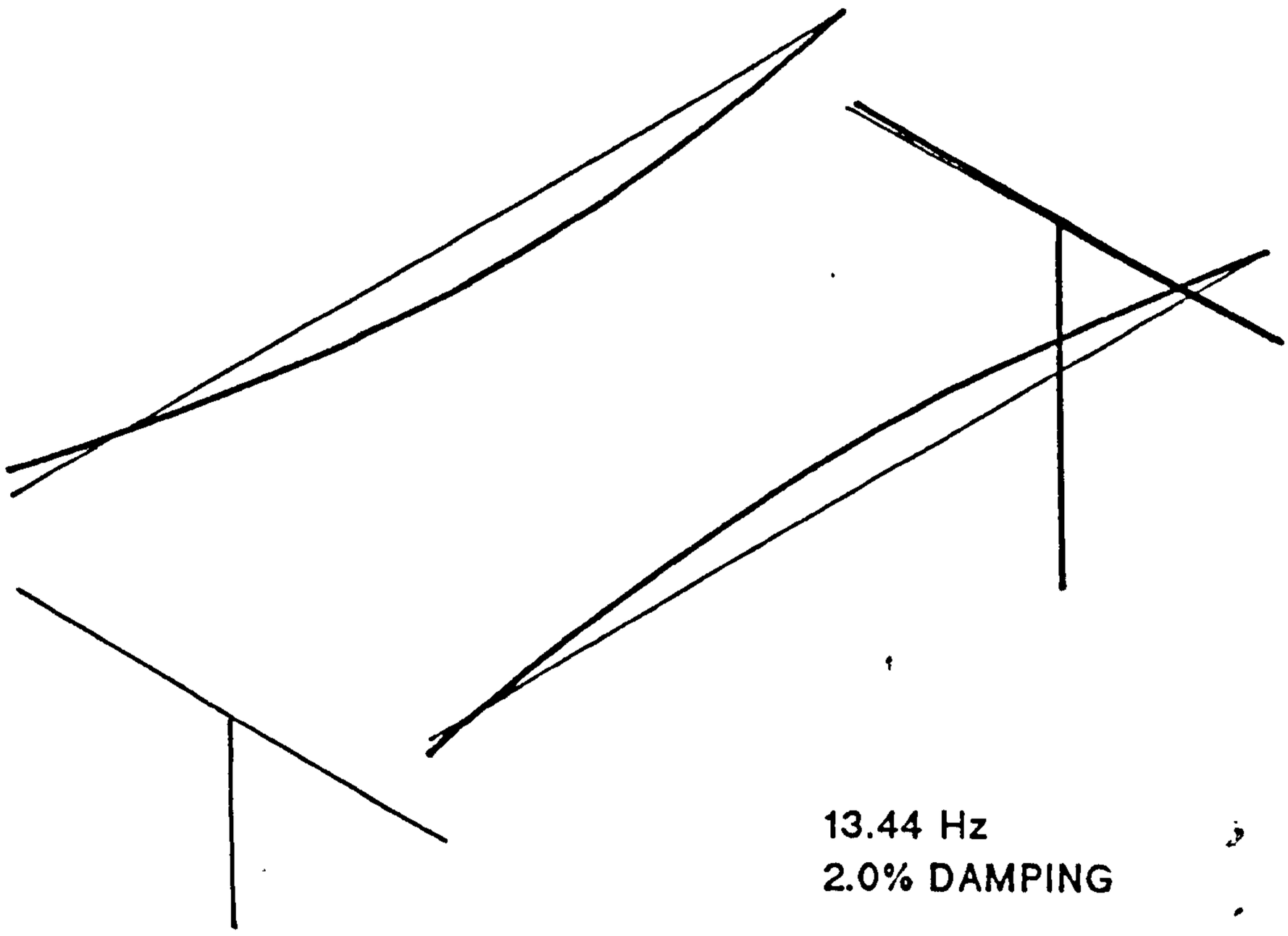

13.44 Hz
2.0% DAMPING

FIG. 3.20 MODESHAPE 7

CHAPTER 4 A GUIDEWAY FOR EXPERIMENTS

4.1 INTRODUCTION

The experimental work for this project required the use of a flexible guideway to support the BR vehicle . Because the existing Derby guideway had been built to be rigid , a new , flexible guideway was required . The new guideway had to be designed , built and commissioned before the experimental work could start . The flexible guideway had to be cheap to build in comparison to the guideway at Birmingham , but had to retain compatibility with the BR vehicle .

In order to predict the performance of a new vehicle suspension controller , it was essential to know the force-displacement frequency response of the guideway - as perceived by the vehicle magnets . This knowledge could not be obtained from a theoretical analysis of guideway dynamics . Modal damping , which was known to be an important factor , could not be predicted with the required degree of accuracy and

had to be measured . Dynamic tests of the new guideway were required .

This chapter describes the design and dynamic testing of the experimental , flexible guideway . The dynamic tests are described in more detail in Ref 4.1 .

4.2 GUIDEWAY DESIGN

Design of the experimental flexible guideway was the first activity for this project . The time lags involved in purchasing , manufacturing and construction were anticipated to be about six months . It was therefore essential to complete the guideway design as quickly as possible . This would allow guideway testing to occur late in the first year of the project . Design work commenced in January 1983 , an order for manufacture was placed with a local contractor in April and the guideway was commissioned to allow dynamic testing in November 1983 .

A disadvantage of attempting guideway design as the first project activity was the difficulty of specifying the required guideway dynamic properties . Williams in Ref 4.2 uses guideway modal inertia to assess guideway flexibility . This idea is difficult to relate to a guideway design process which will inevitably centre around the study of deflection under load , ie stiffness . Guideway flexibility in

this study is defined by natural frequency and static stiffness . This concept is much easier to relate to contemporary civil engineering design techniques than an assessment of modal inertia .

The lowest natural frequency of the Birmingham guideway was thought to be around 6 Hz . The specification for the flexible guideway design was to provide a range of natural frequencies around 6 Hz with as wide a range of guideway stiffnesses as possible . The flexible guideway had to be incorporated within a 40 metre length of the existing rigid concrete guideway at Derby . The existing horizontal curve was demolished and a straight length of flexible guideway was installed , this is shown in Fig 4.1 . Span length was similar to the Birmingham system at 15 m . The flexible guideway had to have a similar cross-section to the existing guideway , in order to provide continuity for the levitation rail , power supply , LIM rail and loading gauge between the new and old guideways .

The guideway was designed as a "bridge" , similar in style to the Birmingham guideway . At Derby there was no need to raise the guideway 6 m above the ground , a more modest 70 mm was planned . This gave space to fit a bridge bearing at each corner of each span to allow for thermal expansion of the guideway and to provide a dynamic decoupling of adjacent spans .

The guideway was designed as a bolted steel assembly , steel was preferred to concrete because of the authors negligible knowledge of concrete design . However , other advantages of steel were the ease of site delivery and the ease with which the structure might be modified in the future . A configuration of easily available steel sections was chosen for the structure , shown in Fig 4.2 .

The main longitudinal members were chosen to be a pair of the largest universal beams which , whilst still allowing space for slepers ,would fit within the track gauge . The sleepers were universal column sections which were required to couple the levitation rails to the main beams in order for the whole structure to act as a compound beam in vertical bending . The levitation rail assembly was laminated . The laminations were defined by the largest section that would not saturate magnetically , and which would keep eddy current losses to acceptable limits at the maximum vehicle speed .

The steel section chosen for the main longitudinal beams was not readily available in lengths greater than 14 m , but this was only one metre shorter than the spans of the Birmingham guideway and was therefore acceptable .

The natural frequency of the guideway is affected by the stiffness of the bridge bearings . There is a minimum acceptable stiffness of 8MN/m per bearing because this limits the step perceived by a

vehicle as it moves between spans to 3mm . This has a marginally acceptable influence on vehicle ride .

The weight of a 14 m span was calculated at 4.5 tonnes , less than 5% of the weight of one span of the Birmingham guideway . A similar cross-section was used in two shorter spans with lengths of 12 and 10 m . The lowest bending frequencies of these three spans were calculated to be 6.0 Hz , 7.9 Hz and 10.5 Hz , this was acceptable . The calculation method is described in Appendix A4 .

The structure was stressed to the specification for the Birmingham guideway , which was required to support the vehicle , without failure , if the vehicle were to fall symmetrically through the maximum allowable suspension gap onto the guideway . The impact forces that follow such an event are limited by the effects of guideway and bridge bearing flexibility . The forces are a maximum close to the end of a guideway span where guideway flexibility is a minimum . The sleepers that link the levitation rails and the main beams must accept stresses from both the direct vertical bending load and the longitudinal bending load required to couple the components of the structure into a compound beam .

Stress calculations were by hand and it was assumed that there would be a linear distribution of shear stress through the structure . This allowed the derivation of an analytical expression for the peak longitudinal bending force in any sleeper , for any

chosen combination of sleeper size and spacing . Peak longitudinal stresses were calculated to be 330 MN/m^2 at sleepers 0.75 m and 1.75 m from the span end . Vertical bending stress in the sleepers was calculated for the combination of peak dynamic force and static weight to be 68 MN/m^2 . Peak predicted stress was therefore 400 MN/m^2 .

The peak bending stress in the main beam was calculated to be 180 MN/m^2 for a similar event .

Table 4.1 defines the structural elements in the guideway . Appendix A4 provides more detail about the method that was used for calculating the guideway stresses .

4.3 GUIDEWAY COSTS

The three spans of the experimental guideway , with a total length of 36 metres , were delivered in a fully assembled state apart from the power supply rails . The cost was £8,500 or £250 per metre with a 6% allowance for the missing components . The equivalent track at Birmingham cost £809 per metre , excluding costs for the walkway and guideway support structure , Ref 4.3 .

4.4 GUIDEWAY TESTING

Tests to determine guideway dynamic properties were conducted almost exclusively on the 14 metre span with 8MN/m bridge bearing pads . This was the most flexible combination , the one which was expected to cause the greatest problems for the vehicle suspension . This guideway , like the guideway at Birmingham , was excited by impulse but the impulse came from a 4 kg hammer rather than a 7,000 kg dead weight . Like Birmingham , there was no convenient hydraulic supply to drive a shaker and no reaction point for the shaker . It was anticipated that the 4,500 kg guideway would be lightly damped and hence that impulse excitation would be adequate .

Hammer force was applied vertically to the top of the levitation rail at a sleeper end . Guideway vertical acceleration adjacent to the impact point or at the distant end of the sleeper was measured together with hammer force . This provided data for the guideway bounce and roll dynamic properties , as perceived by the mag-lev vehicle . The location of the accelerometers is shown in Fig 4.3 . The hammer force spectrum was tuned to be flat in the range 0 to 40 Hz by applying the hammer to the guideway via a rubber pad . A PSD of hammer force is shown in Fig 4.4 , this measurement was taken without the use of the rubber pad . It is clearly necessary to use the rubber pad and narrow band analogue filters to improve measurement quality .

The measurements were captured and processed by a Hewlett-Packard 3582 spectrum analyser to produce the inertance (acceleration/force) frequency response . Each test was repeated 32 times with frequency domain averaging . The averaged measurements were transferred to a Hewlett-packard 9816 computer , converted to receptance (displacement/force) frequency response and stored on disc .

The software described in Chapter 2 was used to calculate and plot the 90% confidence levels for these frequency responses . Fig 4.5 to 4.12 show the upper and lower 90% confidence levels of the measured frequency responses in green and not the frequency responses themselves . The confidence levels are very closely spaced and usually only one line is apparent , therefore random errors in the measurement are very small .

These frequency responses were analysed using the PAPA9 modal analysis software referred to in Chapter 2 , which can provide estimates of natural frequency , damping and modeshape of a structure . These properties were then used to define model parameters for the frequency response calculation software . The calculated frequency responses are plotted in red over the equivalent measured responses in Figs 4.5 to 4.12 .

4.5 TEST RESULTS

Figs 4.5 to 4.12 show that agreement between the measured and synthesized frequency responses are almost always better than 10% of the peak response . This is occasionally masked by the coarseness of the frequency increments for the synthesized response and is particularly true of the lightly damped second mode .

Because there is no correlation between succesive tests it is not possible to define modeshapes , however the data from individual tests has been used to propose "modeshapes" that are plausible . "Modeshapes" of the seven principal vertical modes are shown in Fig 4.13 . The "modeshapes" that will affect vehicle bounce are formed as the individual main beams bend in phase . The "modeshapes" that will affect vehicle roll are formed as the main beams bend 180 degrees out of phase . The "modes" are :-

Natural frequency Hz	Damping % of Critical	Modeshape Description
5.00	2.1	Fundamental anti-phase bending
5.94	1.0	Fundamental in-phase bending
12.4	2.0	Second anti-phase bending
18.8	1.9	Second in-phase bending
21.5	3	Third anti-phase bending
31.1	3	Whole structure torsion
32.8	4	Third in-phase bending

The static stiffness values are :-

Natural Frequency in Hz	Static Stiffness (MN/m)							
	Site 0	0R	1	2	-2	3	3R	5
5.00	1.3	-1.1	1.5	3.1	2.3	5.5	-5.8	58
5.94	3.2	3.6	3.6	7.4	7.7	18	20	**
12.39	**	**	21	9.2	8.2	10	-8.7	38
18.77	**	**	70	50	31	53	35	532
21.5	41	-33	631	106	97	22	-29	21
31.1	**	**	57	**	518	908	?	27
32.8	135	108	**	183	205	83	?	83

** means that the stiffness was too high to measure

? means that no data was recorded .

Each estimate of natural frequency and damping is a mean of up to eight individual estimates .

Fig 4.14 and 4.15 show the upper and lower confidence levels for the mid-span direct inertance of the 12 and 10 metre spans .

4.6 CONCLUSIONS

The flexible guideway has been commissioned , tested and modelled . The 14m span has a natural frequency of 5.94 Hz in simple bending , this compares with the design estimate of 6.04 Hz . Similar figures for the 12 m span are 7.9 Hz calculated and 8.0 Hz measured and for the 10 m span

are 10.5 Hz calculated and 11.0 Hz measured . The 14 m span has a guideway torsional mode that will affect vehicle roll . This mode has a natural frequency of 5 Hz , a lower frequency than the first vertical bending frequency . The guideway structure behaves as it was designed to behave and its dynamic behaviour has been accurately modelled . This guideway will be cheap to build in production quantities .

4.7 REFERENCES

4.1 Lawton . Structural Resonance Testing : A Study of the Mag-lev Flexible Guideway . Internal BR Document TMDOS 151 . September 1985

4.2 Williams . Interaction Between a Magnetically Levitated Vehicle and a Flexible Track . Internal BR document IMDOS 85 . 1981

4.3 John Harber , Surveyor at WMCC , private communication with author , May 1985 .

TABLE 4.1 STRUCTURE OF THE MAG LEV FLEXIBLE GUIDEWAY

Main Beams	406*178*67 Universal Beam to BS 4 Pt 1 , Beam separation is 400 mm I_{XX} = 24392 cm^4 I_{YY} = 1365 cm^4
Beam Diaphragms	381*102*55 Rolled Steel Channel to BS 4 part 2 , Diaphragm spacing is 0.1,1.75,3,5 and 7 m from each beam end .
Sleepers	152*152*37 Universal Columns to BS 4 part 3 Sleepers spaced as the diaphragms
Levitation rails	200*50*10 unequal angle cut from 200*100*10 unequal angle to BS 4848 and 90*6 rolled steel flat and 90*10 rolled steel flat
LIM Rail Support	254*89*36 Rolled Steel Channel to part 5
LIM Plate	260*5 to BS 1470 NS4H6 part 6

The part numbers are defined in Fig 4.2 .

APPENDIX A4 DESIGN CALCULATIONS

Guideway Natural Frequency

A symmetric beam that is restrained at both ends by a spring can be modelled as an asymmetric half beam that slides on normal rollers at one end with a spring restraint at the other end . Such a model is used to calculate receptances and is described in Ref A4.1 .

Ref A4.1 , Table 2 , System 1 defines a system receptance , C_{22} , which is calculated from two sub-system receptances , A_{22} and B_{22} .

$$C_{22} = \frac{B_{22} * A_{22}}{B_{22} + A_{22}} -$$

C_{22} becomes the receptance of beam spring system at the spring end of the half-beam when :-

A_{22} is the inverse of spring stiffness .

B_{22} is the receptance of a free-sliding beam at the free end . Table 7-1C in Ref A4.1 gives this receptance as a function of the beam properties .

A small computer programme was written that calculated the system receptance over a particular frequency range . As there is no damping within this calculation , the system receptance changes sign around a natural frequency . The system natural frequency can therefore be calculated to an accuracy

that is limited only by the computer architecture and the operators patience .

Guideway Stresses

The worst case for guideway stress occurs during a vehicle emergency de-levitation onto the guideway . It is assumed that , at worst , the vehicle might fall through the full suspension travel to land symmetrically onto the guideway . All configurations of guideway and bridge bearing pads must be able to absorb the kinetic energy of the vehicle following de-levitation , without structural failure .

Sleepers

A vertical load onto the sleepers will produce vertical and longitudinal bending . The longitudinal load comes from the need to transmit shear stress between the main beams and the reaction rails so that the whole structure behaves as a compound beam .

The shear stress at any point along the compound beam is proportional to the shear force at that point . Therefore if within the pitch of a given sleeper the shear force varies , the sleeper load is a summation of the load variation within that pitch . The worst case for any sleeper is when a step change in the shear force diagram just includes the the entire pitch of a particular sleeper . In practice this occurs when one magnet pair is mid-way between two sleepers .

On the assumption that :-

1 The shear stress at the top face of the main beam web can be calculated as if the sleepers were continuous along the beam . The multiple of this stress and the area of the main beam flange per sleeper pitch gives the shear force that is taken by the discrete sleepers .

2 Vehicle delevitation forces vary linearly along the span because of the effect of guideway flexibility . This is approximately true , impact force , P , will vary from 115 kN to 200 kN , for the least flexible combination of 10 m span and 40MN/m bearing .

The exact relationship is :-

$$P = \left\{ \frac{U}{\left(x^2(l - x)^2/(6*l*E*I) + 2/k_{pad} \right)} \right\}^{1/2}$$

U is vehicle kinetic energy at impact , k_{pad} is bridge bearing stiffness .

This is approximated by :-

$$P = 200 - 17x \text{ kN}$$

For a force , P , applied a distance , x , from one end of a beam of length l , the largest Shear Force is :-

$$S = P * (l - x)/l$$

For the 10 m span:-

$$S_{max} = 1.7*x^2 - 37x + 200$$

The maximum shear stress can be calculated from :-

$$T_{max} = S_{max} \int ydA/(I*b)$$

For the complete compound beam , $\int ydA = .00142$ m^3 and therefore :-

$$T_{max} = 84.5 * (1.7\ x^2 - 37\ x + 200)$$

Recalling assumption 1 , the maximum longitudinal sleeper forces will be T_{max}*pitch*main beam flange width :-

$$L_{max} = 0.75p(1.7x^2 - 37x + 200)$$

The longitudinal bending stresses are a function of this load , sleeper cross-section and length and can be calculated for a range of parameters .

Clearly , impact forces are a maximum at the span ends because guideway flexibility is a minimum at the span ends . Therefore shear stresses are high at the span ends and sleepers must be closely spaced to transmit the high shear loading . For sleepers that are spaced 0.1 , 0.75 , 1.75 , 3.0 and 5.0 m from the span ends , the longitudinal bending stresses have a maximum value of 330 MN/m^2 for the sleepers 0.75 and 1.75 m from the span ends .

The vertical load from a delevitation incident is 50 kN per sleeper , 10 kN of which is the static vehicle weight . This produces a peak vertical bending stress of 68 MN/m^2 . The peak combined stress is then 400 MN/n^2 , the sleepers would yield but not fail .

Main Beams

The worst case is for vehicle de-levitation in the centre of the longest span , with the stiffest

bridge bearings . Impact force is 90kN and peak bending stress , with an allowance for vehicle static weight is 180 MN/m^2 . The main beams would neither yield nor fail in the event of a worst case vehicle de-levitation .

References

A4.1 Bishop and Johnson . The Mechanics of Vibration . Cambridge University Press , 1960

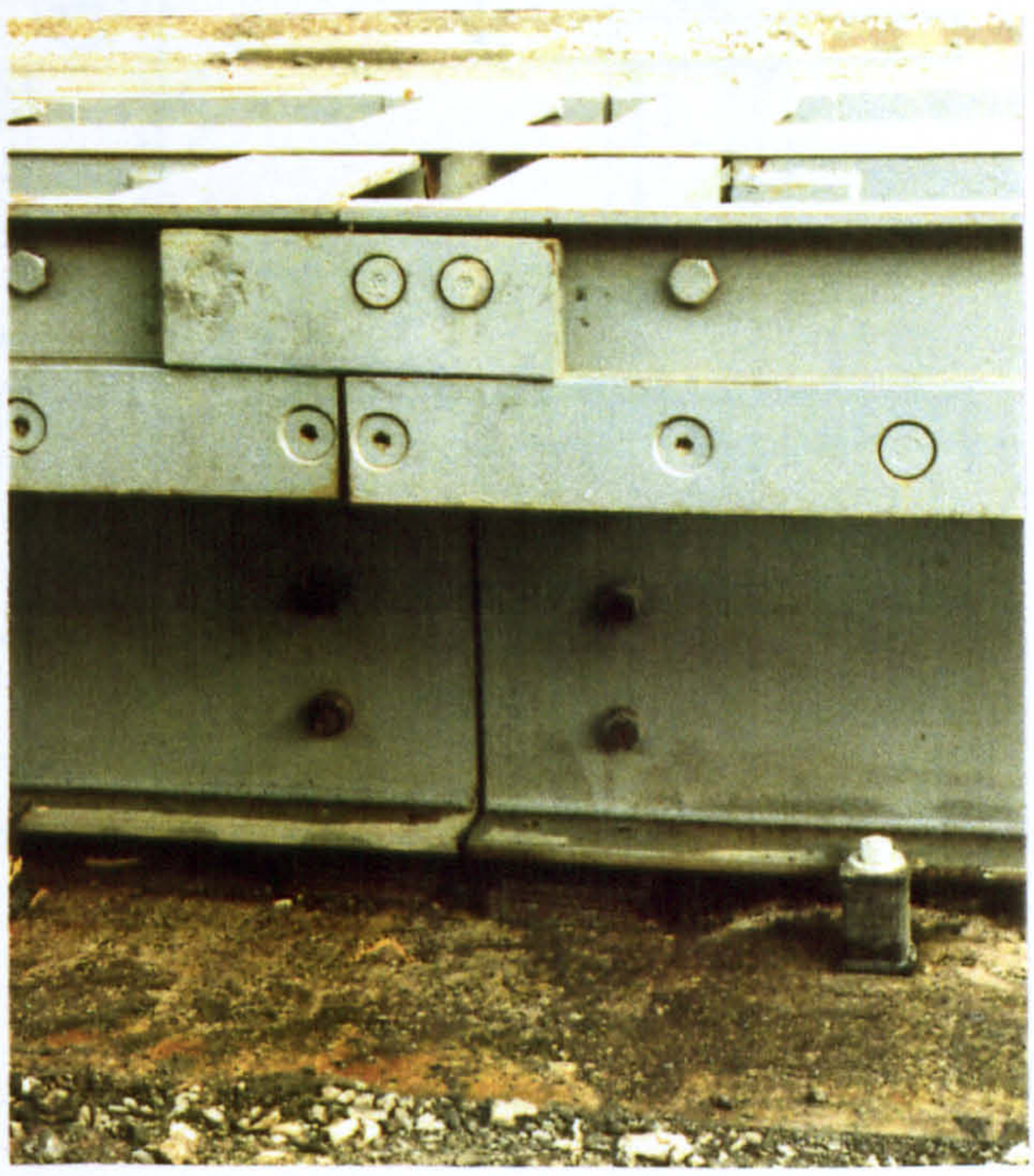

FIG. 4.1. THE FLEXIBLE GUIDEWAY AT DERBY

THIRD ANGLE PROJECTION

1APD-ALFT-04

AMENDMENTS

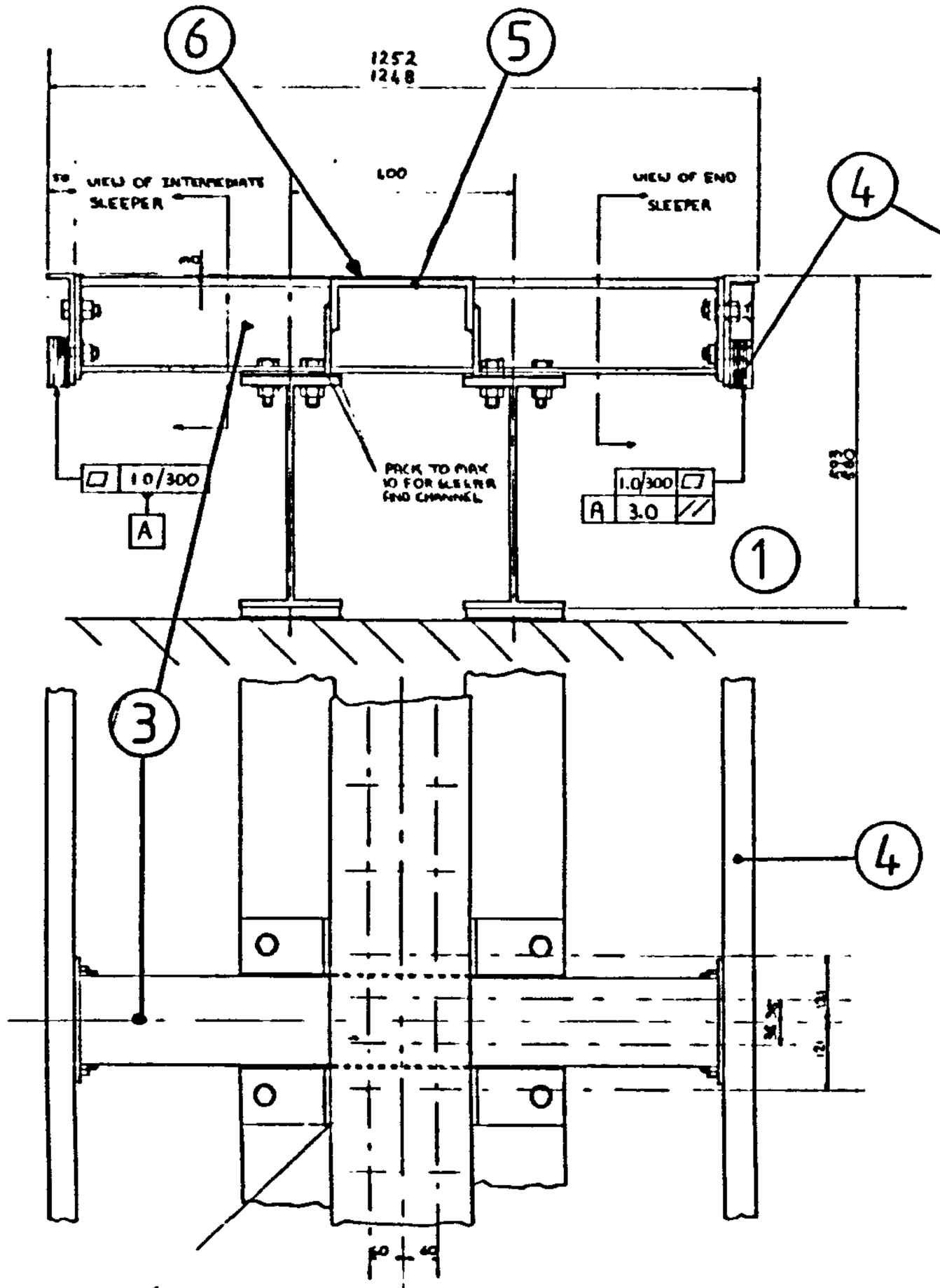

After every drill hole 65dia on a CSK for 6.6 dia CSK Pop Rivets fit for aluminium every 150

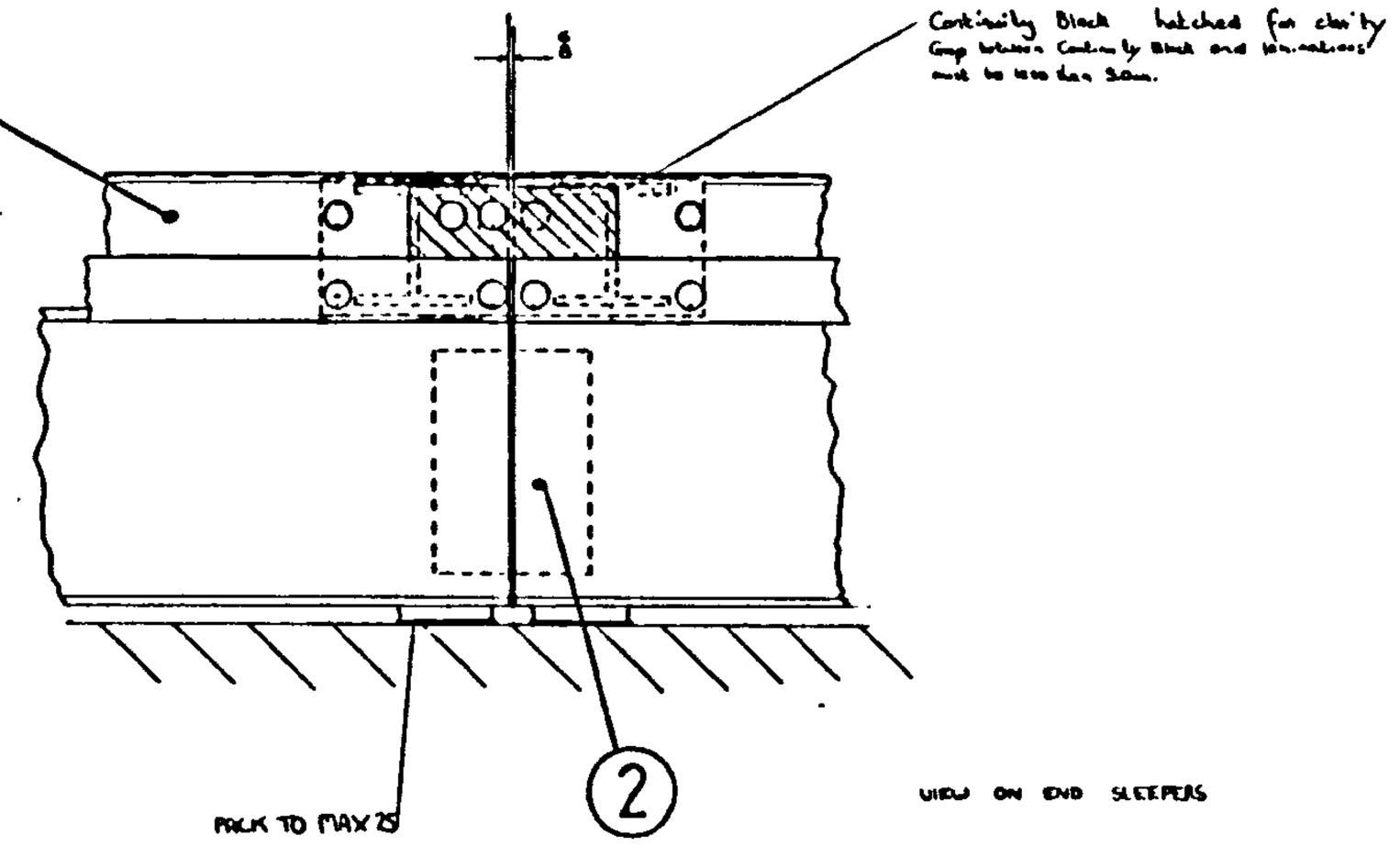

FIG 4.2

UNLESS OTHERWISE SPECIFIED

BRITISH RAILWAYS RESEARCH AND DEVELOPMENT DIVISION
VEHICLES GROUP

ASSEMBLY DETAILS

SCALE:- 1:5

1APD-ALFT-04

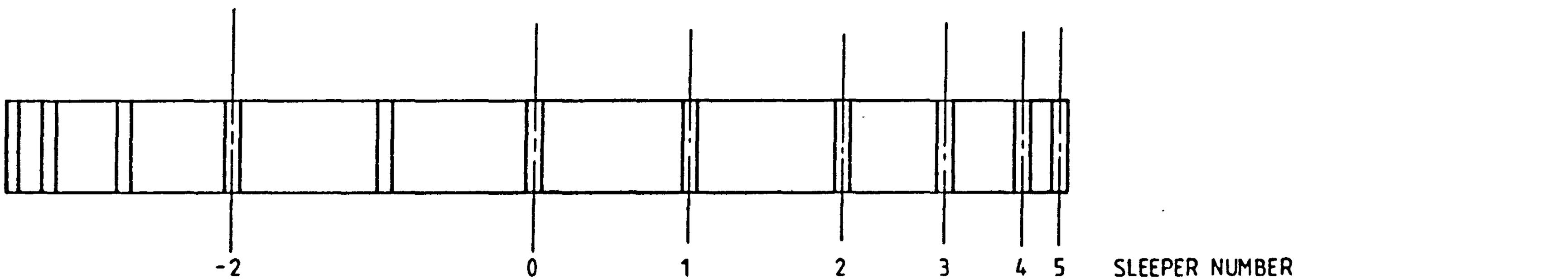

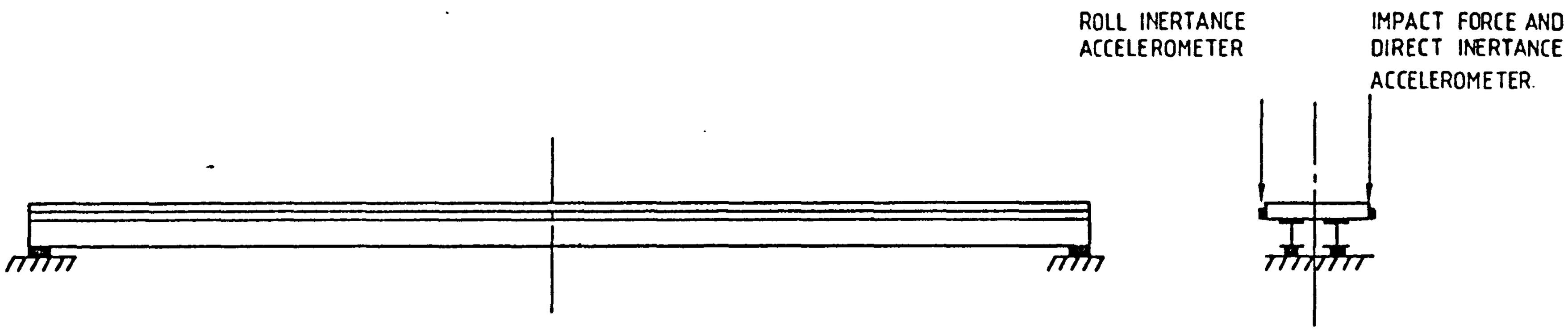

FIG. 4.3. TRANSDUCER LOCATION ON THE 14m SPAN

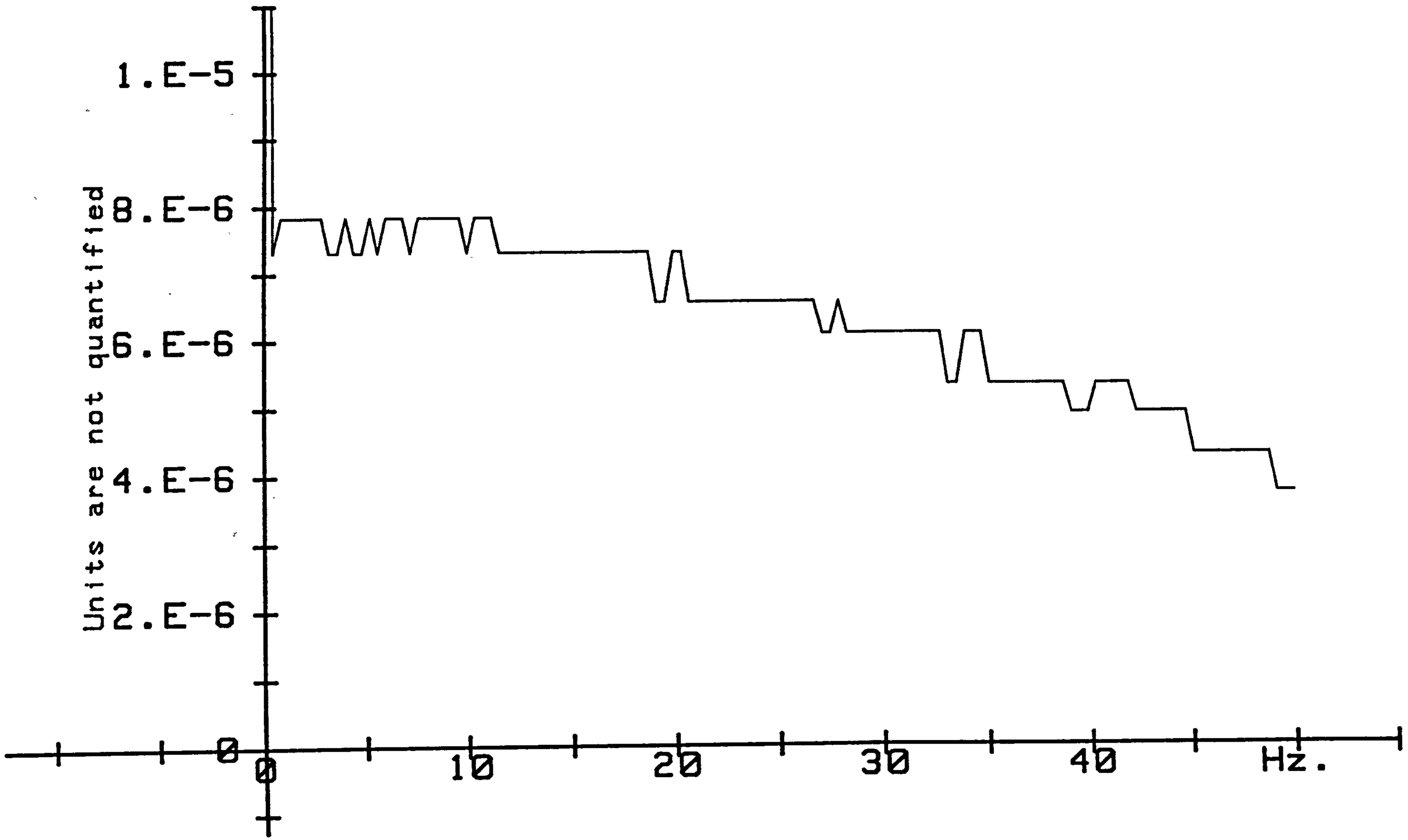

FIG 4.4 FORCE SPECTRUM

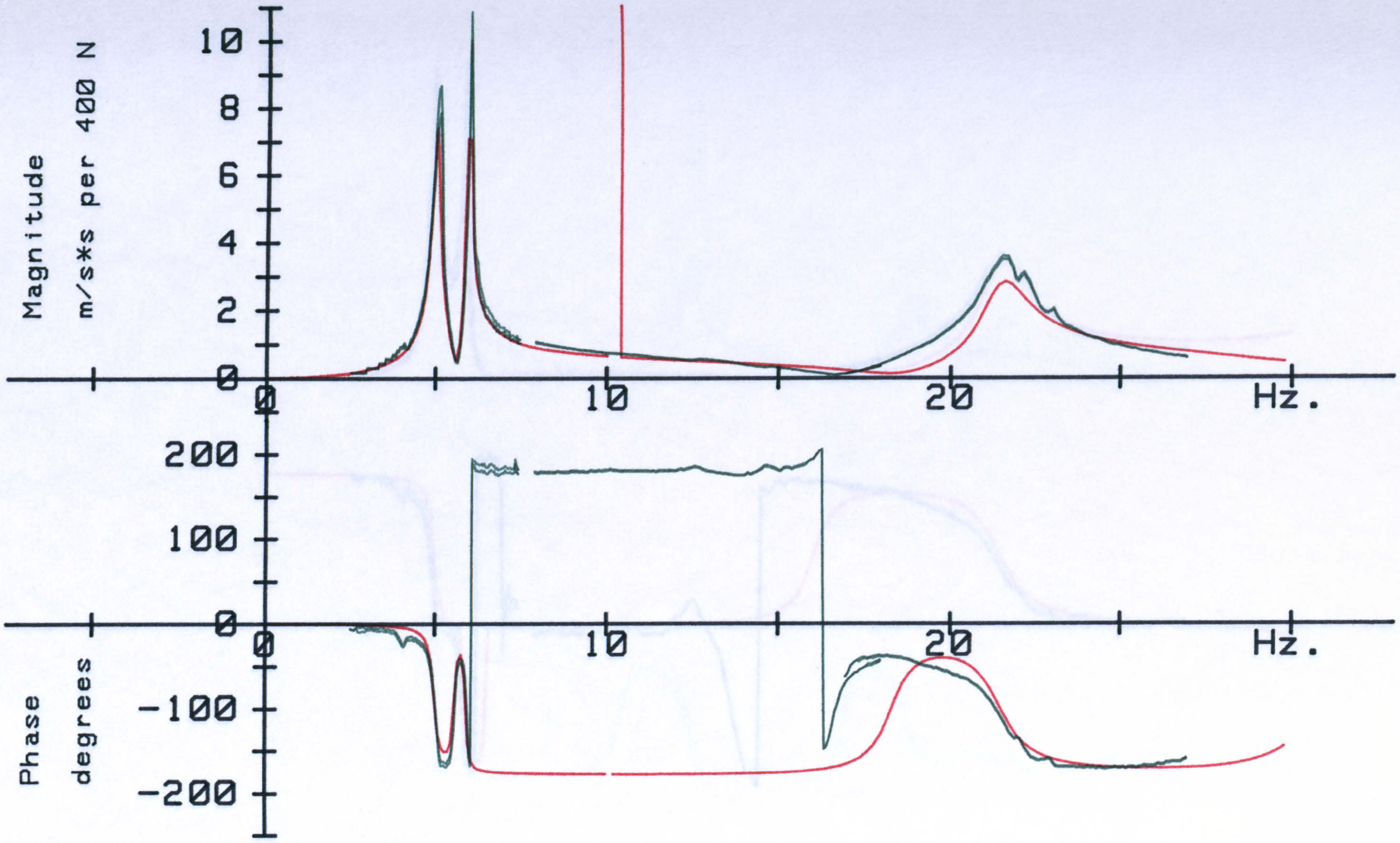

FIG 4.5 SLEEPER 0 B

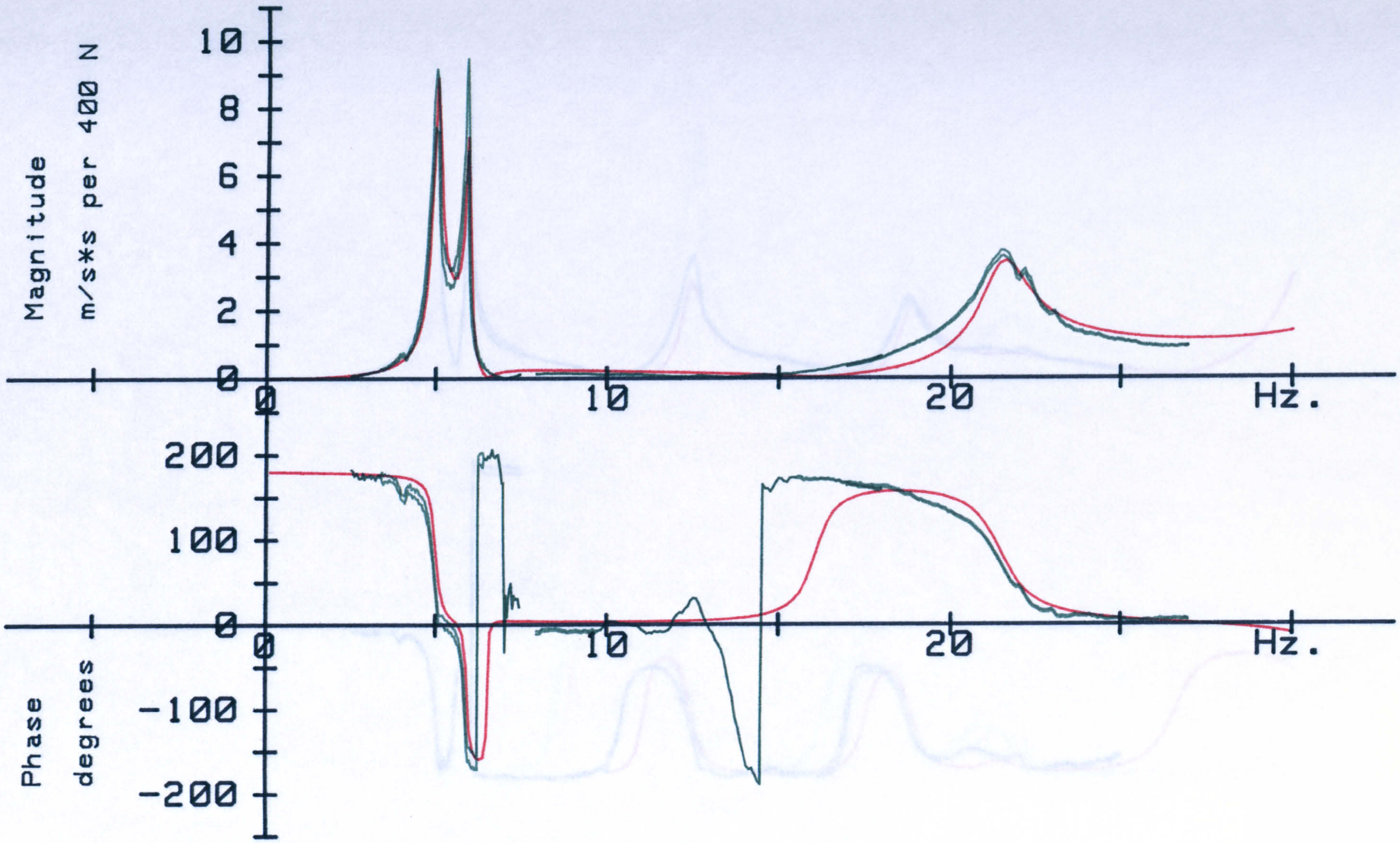

FIG 4.6 SLEEPER 0 R

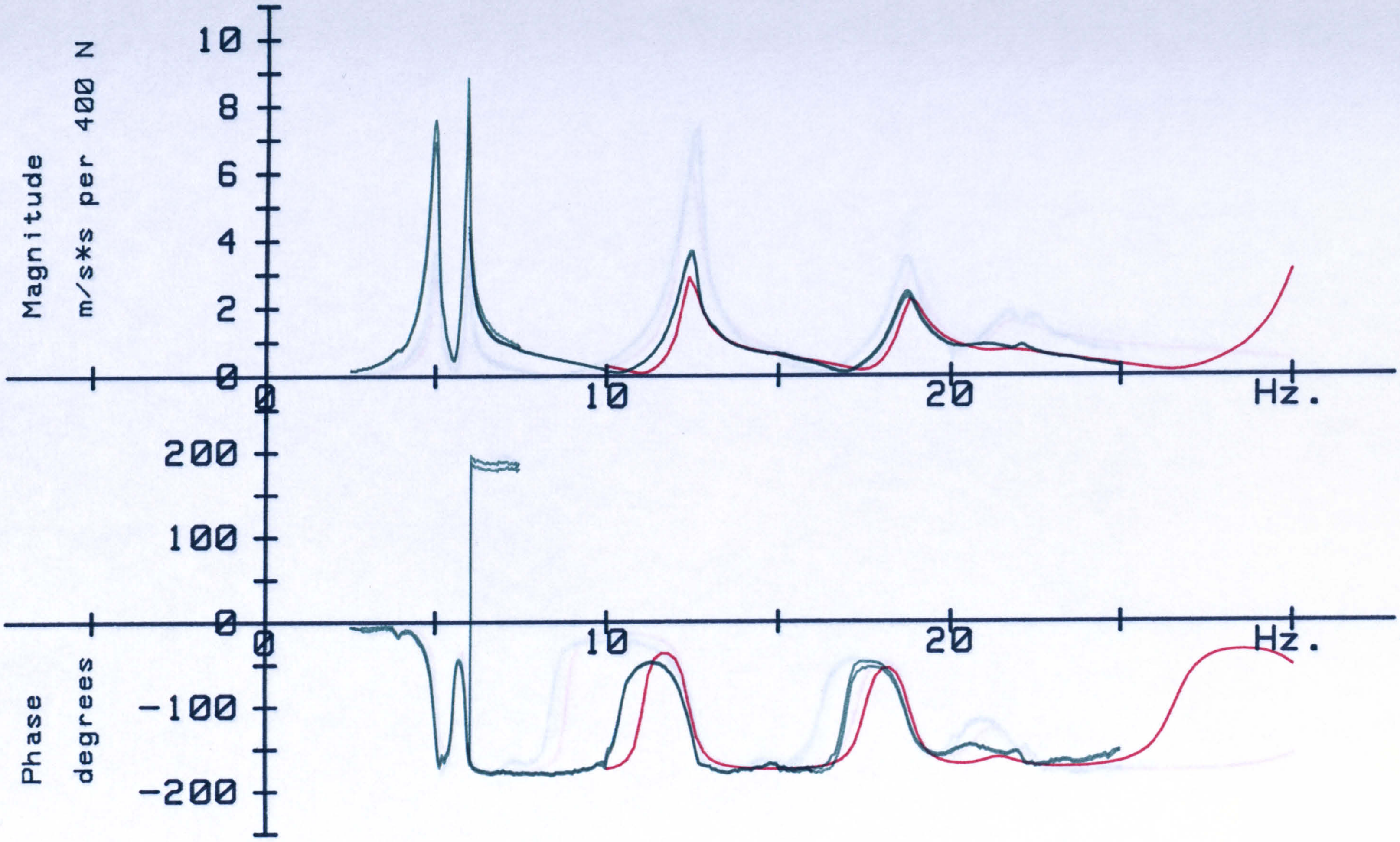

FIG 4.7 SLEEPER 1 B

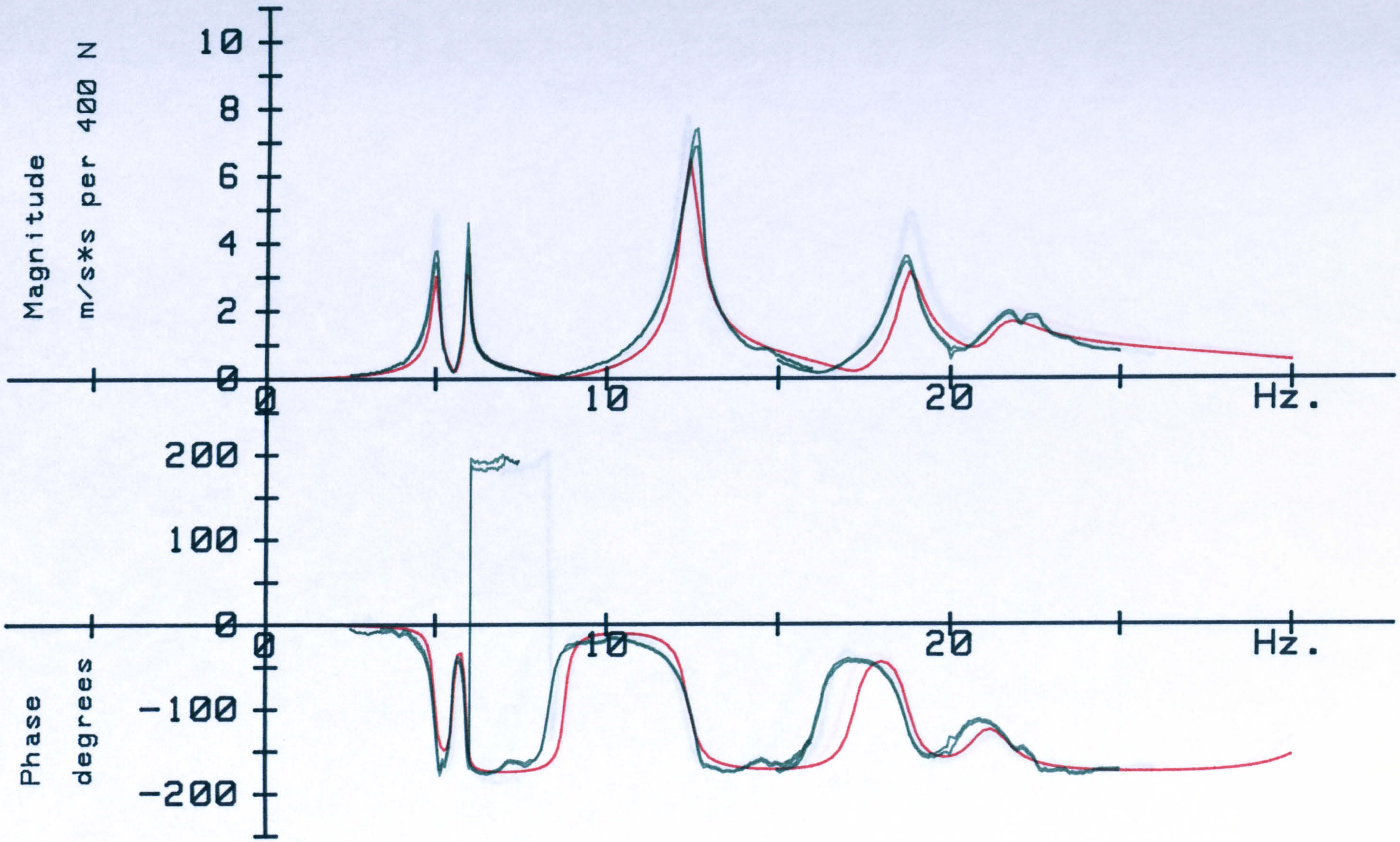

FIG 4.8 SLEEPER 2 B

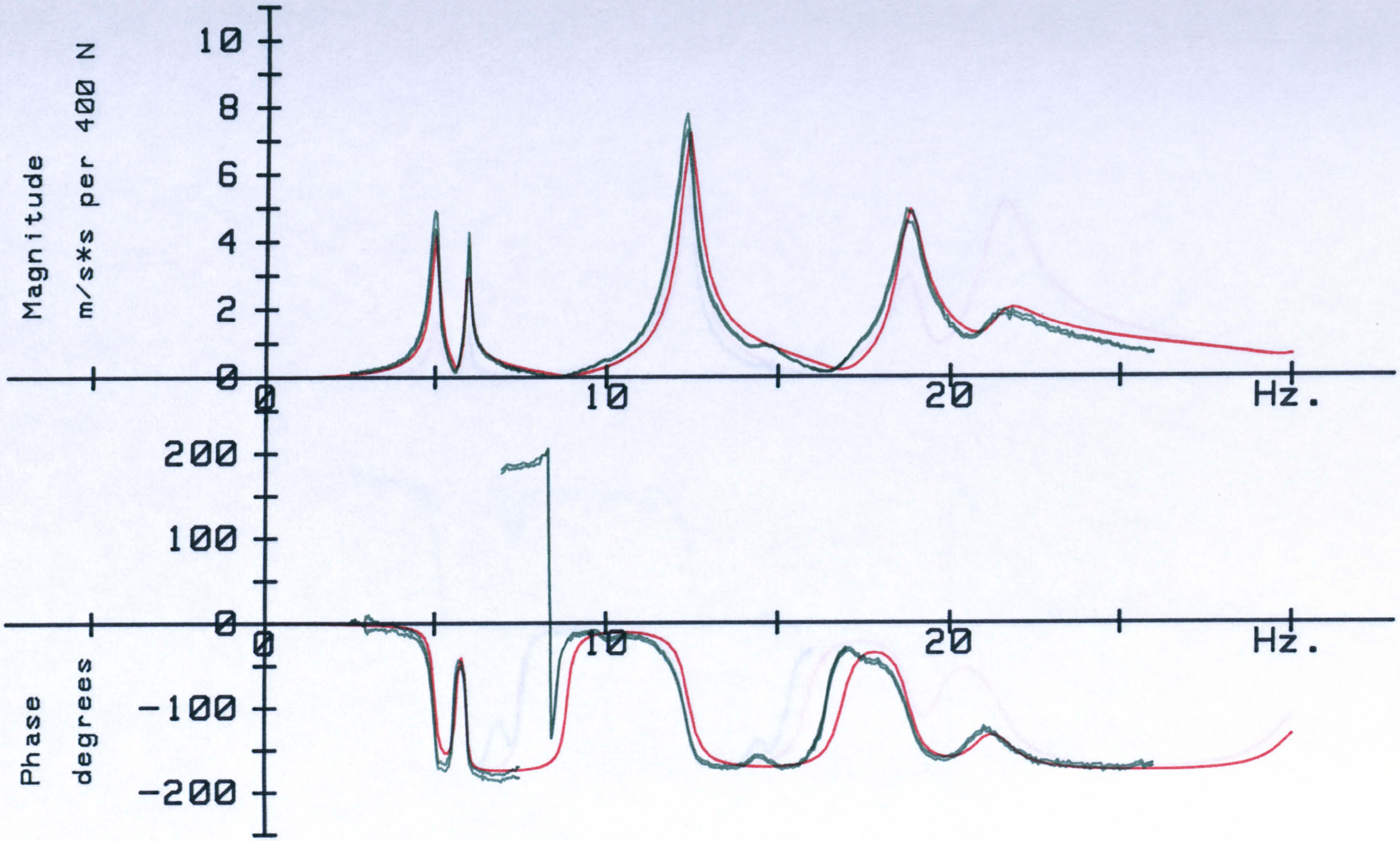

FIG 4.9 SLEEPER -2 B

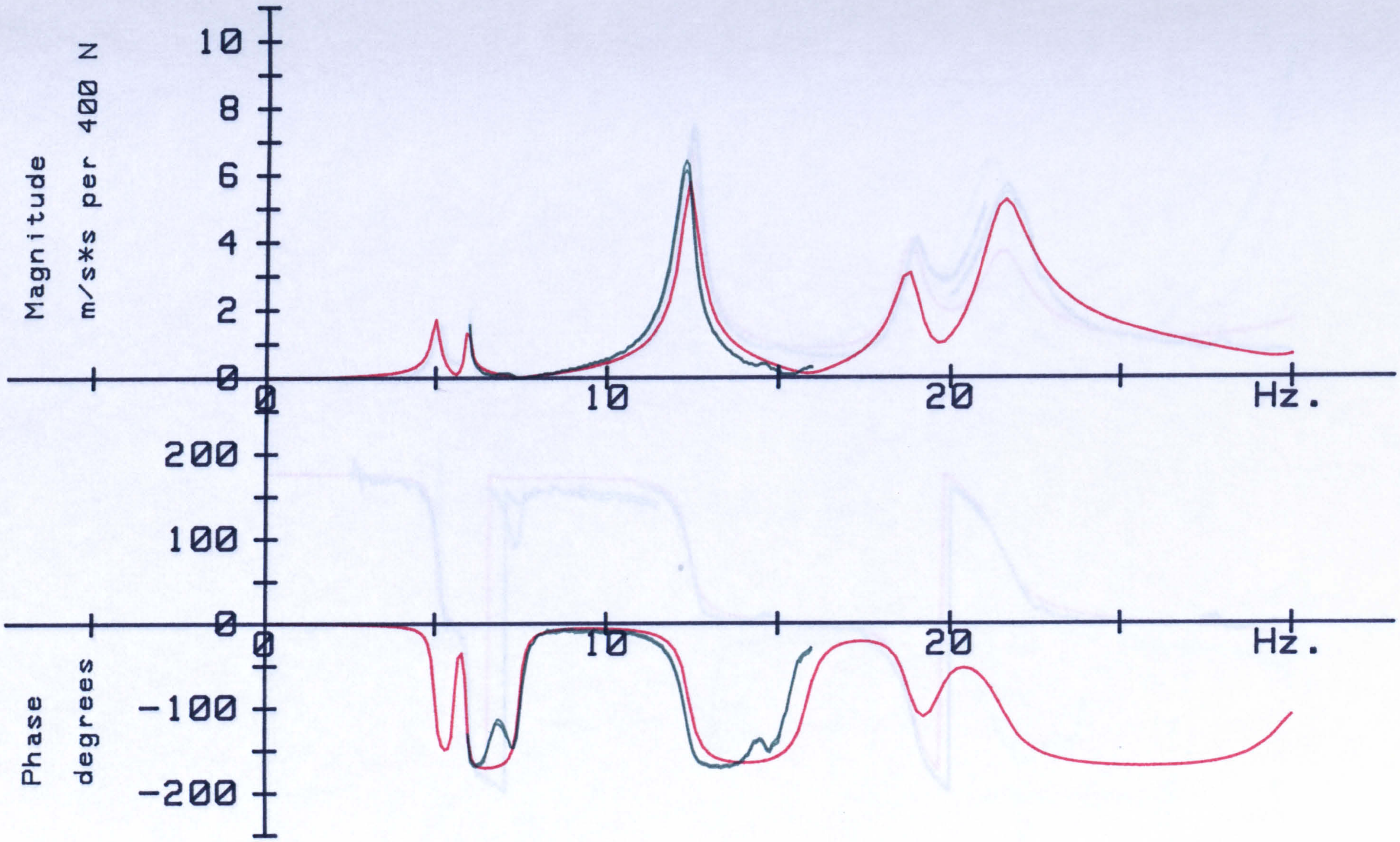

FIG 4.10 SLEEPER 3 B

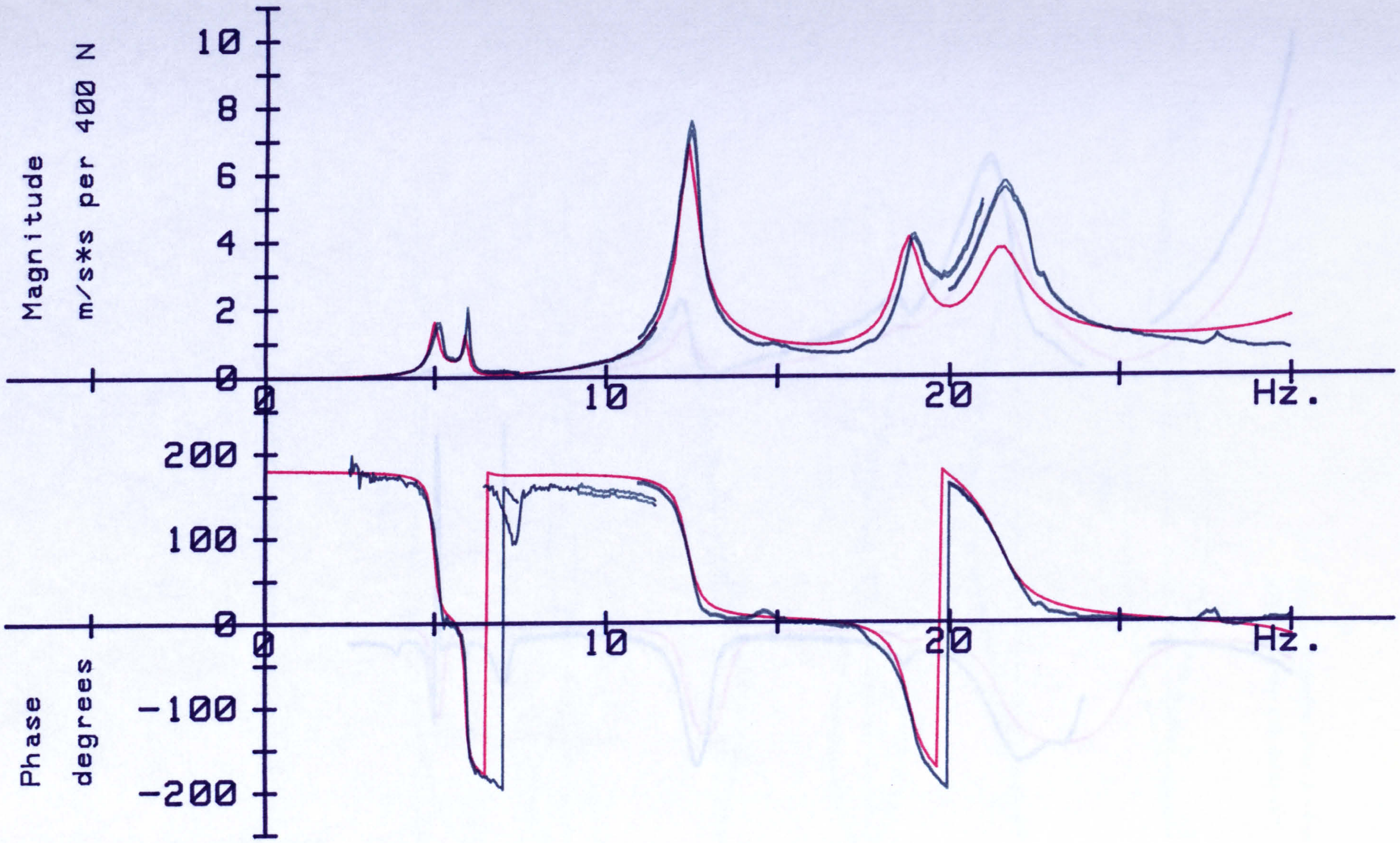

FIG 4.11 SLEEPER 3 R

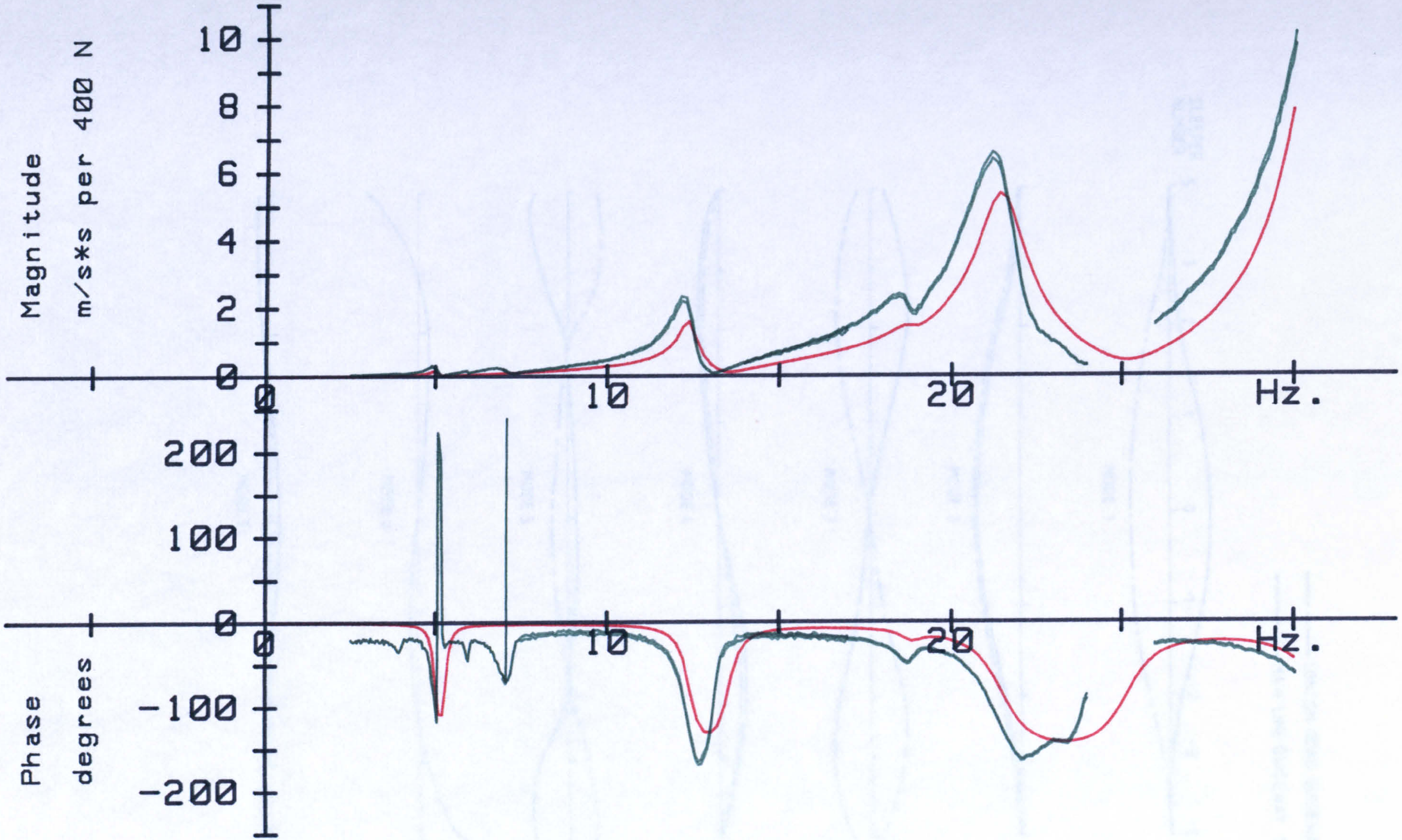

FIG 4.12 SLEEPER 5 B

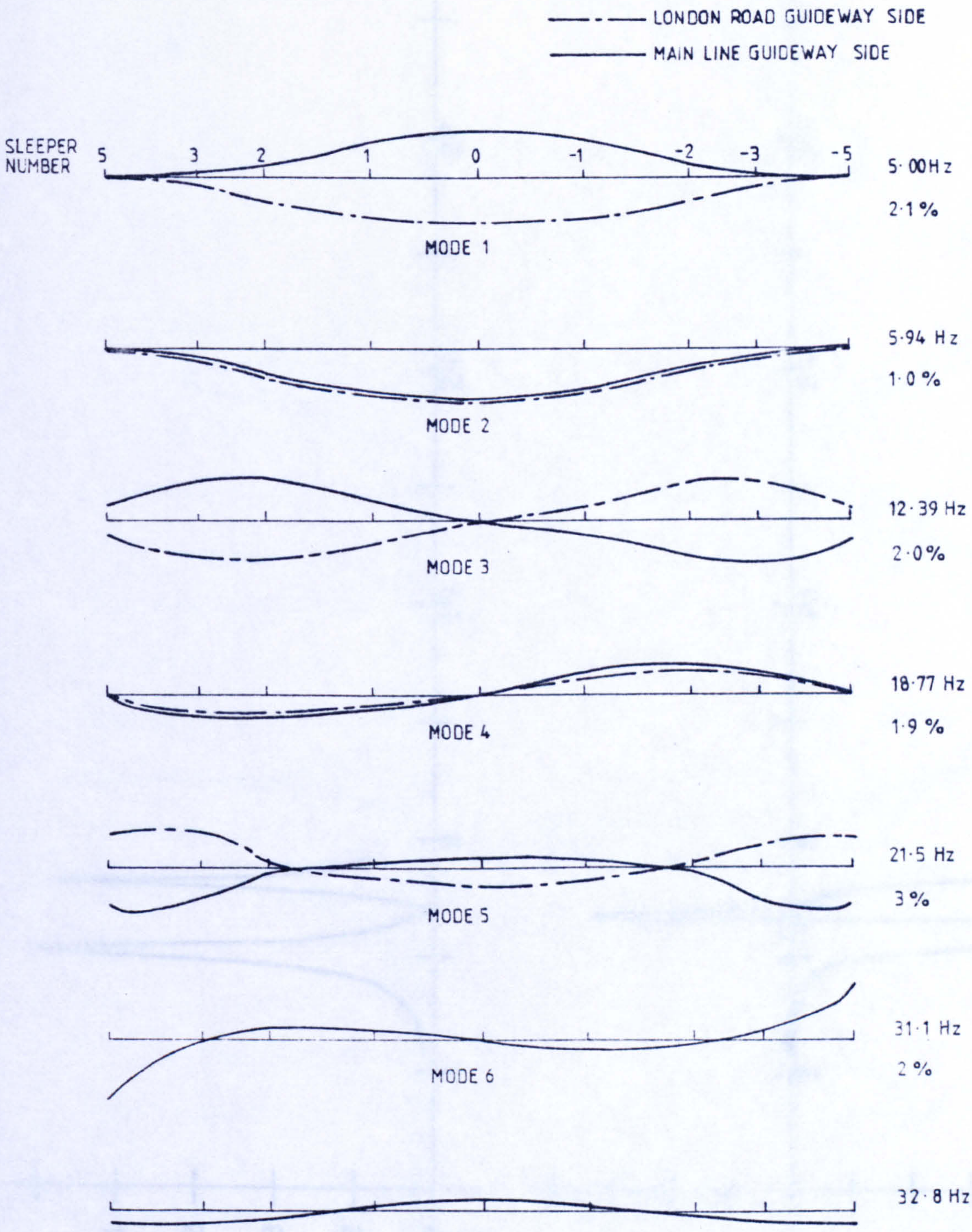
LONDON ROAD GUIDEWAY SIDE
MAIN LINE GUIDEWAY SIDE
SLEEPER NUMBER
5
3
2
1
0
-1
-2
-3
-5
5·00 Hz
2·1 %
MODE 1
5·94 Hz
1·0 %
MODE 2
12·39 Hz
2·0 %
MODE 3
18·77 Hz
1·9 %
MODE 4
21·5 Hz
3 %
MODE 5
31·1 Hz
2 %
MODE 6
32·8 Hz
4 %
MODE 7

FIG. 4.13.

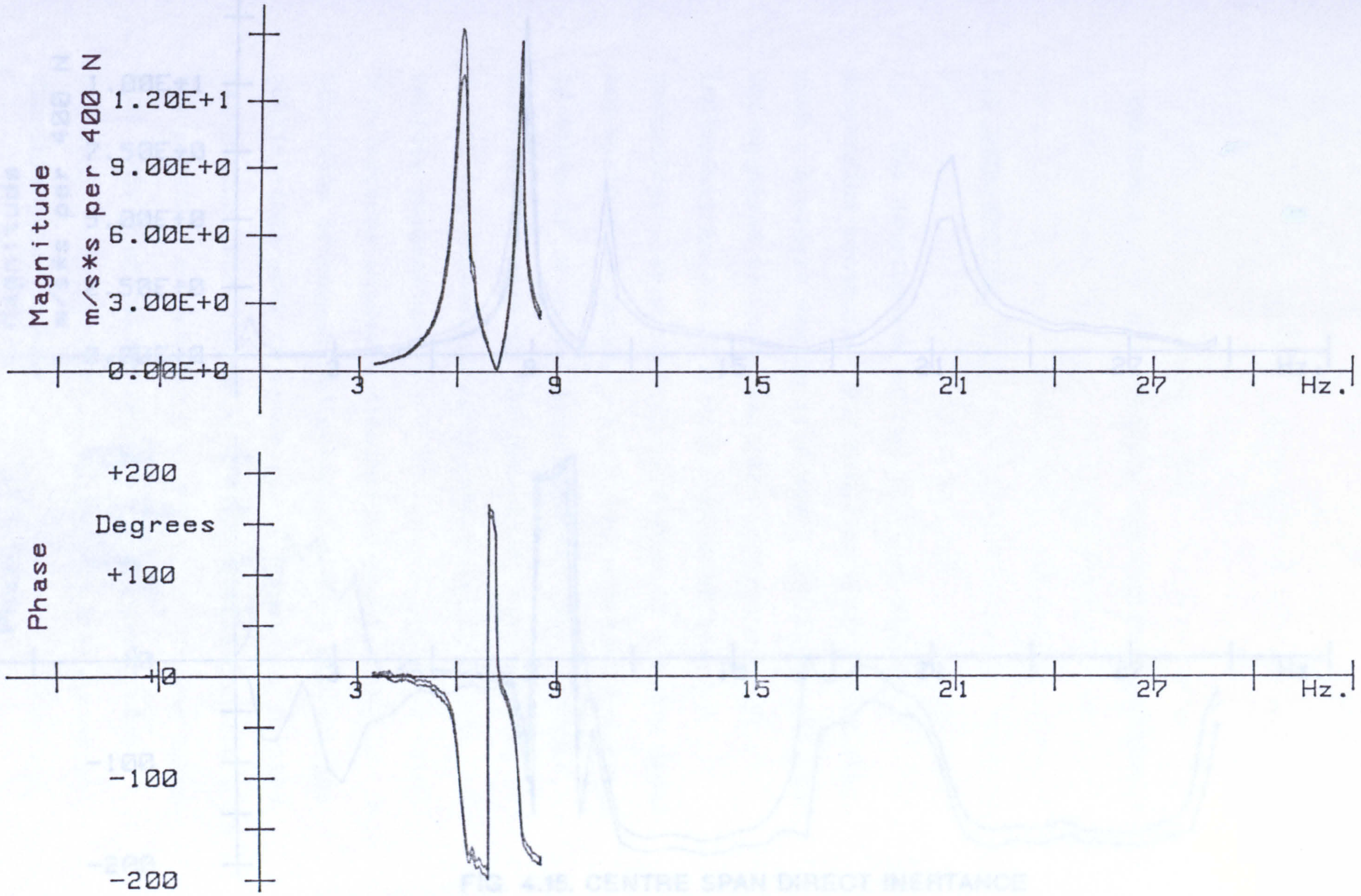

FIG. 4.14. CENTRE SPAN DIRECT INERTANCE
TRANSFER FUNCTION GAIN AND PHASE

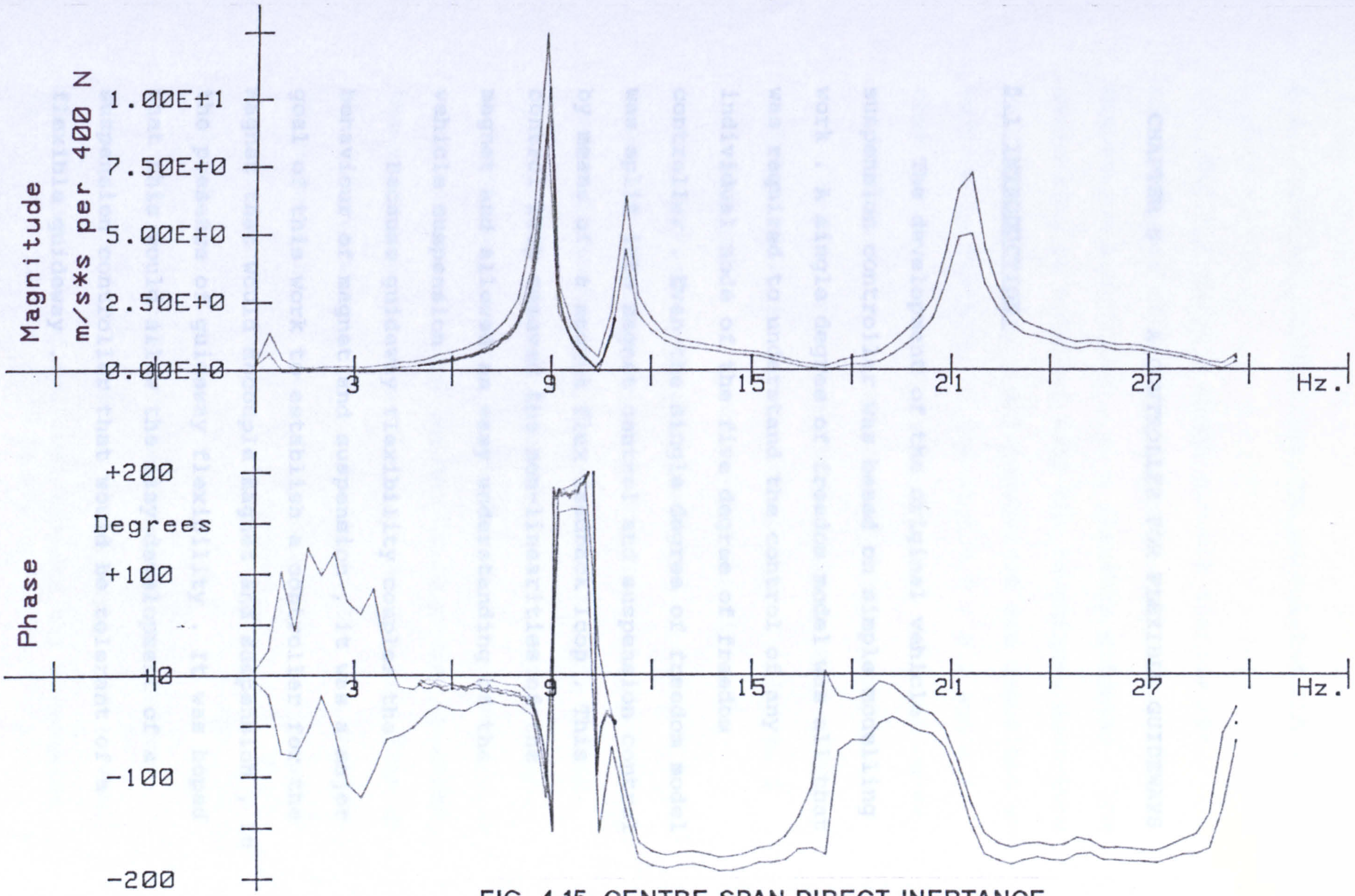

FIG. 4.15. CENTRE SPAN DIRECT INERTANCE TRANSFER FUNCTION GAIN AND PHASE

CHAPTER 5 A CONTROLLER FOR FLEXIBLE GUIDEWAYS

5.1 INTRODUCTION

The development of the original vehicle suspension controller was based on simple modelling work . A single degree of freedom model was all that was required to understand the control of any individual mode of the five degree of freedom controller . Even the single degree of freedom model was split into magnet control and suspension control by means of a magnet flux feedback loop . This control loop removed the non-linearities of the magnet and allowed an easy understanding of the vehicle suspension .

Because guideway flexibility couples the behaviour of magnet and suspension , it was a major goal of this work to establish a controller for the magnet that would decouple magnet and suspension , in the presence of guideway flexibility . It was hoped that this would allow the easy development of a suspension controller that would be tolerant of a flexible guideway .

5.2 THE ORIGINAL CONTROLLER ON A FLEXIBLE GUIDEWAY

5.2.1 Guideway Flexibility and Calculated OLR's

Fig 5.1 shows a block circuit diagram for a single degree of freedom vehicle , with the original suspension controller , on a flexible guideway . The suspension is modelled with the techniques described in Chapter 2 , the model parameters are described and defined in Table 5.1 . The Figs 5.2 , 5.3 and 5.4 show various OLR's for this system , with the outer feedback loop broken at Point A , shown in Fig 5.1 .

Fig 5.2 shows three OLR's , each for a guideway that has a single natural frequency at 2 (red), 6 (orange) and 12 Hz (green) respectively . The frequency responses were calculated at 0.1 Hz intervals and this limits the clarity of the graphplots within the bandwidth of lightly damped resonances . Clearly , the natural frequency that most severely reduces stability and phase margins is between the 6 Hz case and the 12 Hz cases , because these frequencies straddle the limiting bandwidth of the vehicle suspension controller . The OLR gain is close to unity at these frequencies and the phase changes from guideway flexibility will cause instability .

Fig 5.3 shows how the variation of guideway damping from 0.5% (red) to 1% (orange) , 2% (green) and 4% (purple) of critical affects the suspension

OLR . Clearly , the highest level of guideway damping gives the greatest suspension stability .

Fig 5.4 shows how the variation of guideway static stiffness from 3 (red) to 10 (orange) , 30 (green) and 100 MN/m (purple) affects the suspension OLR . Clearly , the highest value of guideway static stiffness gives the greatest suspension stability .

5.2.2 Magnet Control

Control of magnet force by flux feedback is discussed in Chapter 1 in the context of separate control loops for magnet flux (force) and vehicle displacement . This separation of the two loops is not absolute .

The feedforward frequency response of the magnet flux control loop , shown in Fig 5.1 , is affected by the receptance of both the vehicle and the guideway , R_V and R_G . If the guideway is not flexible , R_G is zero and the contribution of K_B , K_g and R_V to the feedforward frequency response of the magnet loop is :-

$$\frac{1}{1 - K_g * K_B / (M_V * w^2)}$$

This function may be evaluated in the knowledge that K_g is always negative , and although there is no phase change with frequency , the amplitude is frequency dependent and particularly so at low frequencies . At low frequencies , current control of the magnet loop is used to control magnet force , as

described in Chapter 1 . Experience has proved that this system is quite satisfactory .

At a frequency of 3 Hz , the gain of this factor is 0.5 , rising to 0.94 at 12 Hz . In the frequency range where flux feedback is dominant , this simple feedback gives a good force generator to drive an inertial vehicle mass , provided that the force is reacted from a rigid foundation . The magnet and suspension control loops are effectively decoupled by the original controller .

If there is some significant guideway flexibility , $|R_G| > 0$, then the contribution of R_V , R_G , K_g and K_B to the feedforward frequency response of the magnet control loop is :-

$$\frac{1}{1 + K_g * K_B * \left(\frac{1}{(M_V * w^2} - \frac{1/K_{stat}}{1 + 2zjw/w_n - w^2/w_n^2)}\right)}$$

It can be seen from this function that the behaviour of the magnet is affected by the vehicle and the guideway , the magnet and suspension control loops have been coupled together by guideway flexibility . The guideway receptance term has the potential to introduce large phase changes and substantial gain reductions in the forward gain of the magnet control loop . This can degrade the stability of the suspension .

Guideway flexibility produces a coupling of the loops that control the magnet flux (force) and vehicle displacement . Significant guideway

flexibility can affect the ability of the control system to provide a force generator that will drive an inertial vehicle mass .

An analytical expression for the OLR of the magnet control loop shown in Fig 5.1 is :-

$$OLR = \frac{G_V * K_I * G_f * (1 + sT_1)/sT_2}{(R + s(L_L + L_M) + K_g * K_B (R_V + R_G) * (R + sL_L)}$$

If the OLR is equal to -1 , the magnet control loop is at the point of instability . In this situation it is possible to separate out the receptance of the vehicle and guideway from the components of the magnet and the control system .

$$R_V + R_G = \frac{-1}{K_{gB}} \left(\frac{(1 + s(T_1 - R*T_3) + s^2*T_3(L_L + L_M))}{sR*T_3 + s^2*T_3*L_M} \right) \quad \text{Eq 1}$$

where $K_{gB} = K_g * K_B$ and $T_3 = T_2/(G_V*K_I*G_f)$

The right hand side (rhs) of Eq 1 is a complex function that has an infinite magnitude and a 90 degree lag at zero frequency . At infinite frequency , the function has a real positive value (K_{gB} is negative) . A typical function for the rhs of Eq 1 is shown in Fig 5.5 for three consecutive frequency ranges .

If there is no guideway flexibility , R_G is zero and the rhs of Eq 1 cannot equate to the real negative value of R_V . If there is no guideway

flexibility , the magnet control loop will always be stable .

The complex function for R_G , assuming just a single degree of freedom , approximates to a circle that may intersect the function for the rhs of Eq 1 . It is always possible to define parameters for R_G that will satisfy Eq 1 . Therefore it is always possible for guideway flexibility to destabilise this magnet controller .

5.3 AN ALTERNATIVE MAGNET CONTROLLER

The original controller is destabilised because gap changes due to movement of a flexible guideway induce uncontrolled force changes via the magnet negative stiffness . This effect is ameliorated by the magnet controller shown in Fig 5.6 . Table 5.2 shows the parameters changed from those used in the model of Fig 5.1 . Flux feedback is replaced by feedback signals for both current and gap . The gap signal produces a magnet current that produces a magnet flux change which compensates for the flux change from the magnet negative stiffness . The magnet flux response can be calculated from Fig 5.6 as :-

$$\frac{K_I}{[R+s(L_L+L_M)]*sT_2+K_B(R_V+R_G)[(R+sL_L)*K_g sT_2+G_A K_g+K_I G_g]+G_A}$$

If the integrator term , $(1+sT_1)/sT_2$, is set to a high rate ($T_2 << T_1$) then the magnet current will follow magnet gap feedback with great accuracy . The above expression then reduces to :-

$$\frac{K_I}{K_B * (R_V + R_G) * (G_A * K_g + K_I * G_g) + G_A}$$

K_g is always negative and therefore G_g can be set so that :-

$G_g = G_A * K_g/K_I$ and therefore the flux response to demand input is :-

$$K_I/G_A$$

The relationship between demand input and magnet flux becomes a real constant that is independent of any gap change caused by guideway flexibility . This controller has a characteristic that is neutral with regard to guideway flexibility . The use of a magnet controller of this nature allows a simple examination of the behaviour of the outer vehicle suspension loop because this controller decouples the two control loops even in the presence of guideway flexibility . However , the value of the feedback term G_g must be set accurately . Fig 5.7 shows the effect of variation in G_g from the "correct" value . The model in Fig 5.6 was excited by an input to the phase advance filter , responses were calculated for magnet current and magnet demand . Fig 5.7 shows the magnet flux response to demand input with G_g set 40% low (red) , 40% high [green) and at the "correct" value (orange) .

5.4 SUSPENSION CONTROL WITH GUIDEWAY FLEXIBILITY

5.4.1 Analysis

The provision of a magnet controller with a response that is independent of guideway or vehicle receptance allows the block circuit diagram of Fig 5.6 to be reduced to that shown in Fig 5.8 . The OLR for this system is :-

$$OLR = K_F*(R_V + LP*R_G)*G.PA$$

where K_F is the magnet force-demand characteristic

LP is the low pass suspension filter characteristic

PA is the phase advance filter

G is system gain

The influence of guideway flexibility is significant when the product of guideway receptance and suspension filter characteristic is greater than the vehicle receptance . In this situation , the OLR approximates to :-

$$OLR = K_F*LP*R_G*G.PA \qquad \text{Eq 2}$$

If it is assumed that the guideway natural frequency is greater than the suspension filter frequency , that filter will produce a 180 degree lag at the guideway natural frequency . The guideway receptance will produce a further 90 degree lag and the system wil be unstable if the gain is close to unity .

Equation 2 shows that there are two components of the OLR which can be manipulated to modify OLR and to improve stability . The low pass suspension filter may be changed to be more effective at the guideway natural frequency . This can be done by use of a multi-pole filter , but the increased lag from such a filter would produce it's own stability problems . The filter frequency may be reduced ; this will help stability but has implications for the performance of the vehicle suspension . This is discussed in the next section .

The filter phase response would be improved if the lag was no greater than 90 degrees , this can be achieved by adding a first order numerator term to the existing filter characteristic . This extra term in the filter adds some relative velocity damping to the suspension between vehicle and guideway . Intuitively this seems to be a good thing .

In the past , BR have used a simple electronic filter to produce phase advance in a variety of active suspension controllers . The filter has a transfer function :-

$$\frac{1 + sT_1}{1 + sT_2}$$

The degree of phase advance varies as a function of the high frequency gain , T_1/T_2 . As this gain increases above 5 , the increase in phase advance becomes less significant . In practice the high

frequency gain has been limited to approximately 5 for a phase advance of 42 degrees .

It is possible to use a more complex filter to provide more phase advance than with the first order system . A second order filter with the transfer function :-

$$\frac{1 + as + bs^2}{1 + cs + ds^2}$$

can produce a phase advance of 100 degrees for a high frequency gain of 5 . The increased phase advance of this more complex filter may be as high as 60 degrees albeit over a narrower frequency range than the first order filter . This narrower frequency range will still be much wider than the bandwidth of a guideway resonant frequency . This is expected to be very important to the stability of the vehicle suspension .

5.4.2 Modelling Results

The model in Fig 5.8 is used to predict OLRs for the BR vehicle at mid-span on the most flexible part of the guideway . The suspension filter frequency is varied from 4 Hz (red) , 2 Hz (orange) , 1 Hz (green) to 0.5 Hz (purple) and the OLRs are plotted in Fig 5.9 . The lowest frequency filter has the most beneficial effect on suspension stability , as predicted from the analysis in the preceding section . Chapter 1 showed that the electronic filter defines

the vehicle suspension characteristic , this limits the frequency that may be selected for a real vehicle suspension . The suspension was originally designed for 2 Hz , reduction of this frequency will increase the suspension travel - this is true for all vehicles . This can only be tolerated if a lightweight guideway could be assembled to higher tolerances than the existing guideways that were manufactured in situ , not in a manufacturing workshop . It is likely that this will be true , but the author feels that suspension travel will still limit the filter frequency to 1 Hz at its lowest .

Fig 5.10 shows five OLRs for the model in Fig 5.8 , with a 1 Hz suspension filter , with changes to the first order numerator term in the filter . This term is varied to add 0 (red) , 3 (orange) , 7 (green) , 20 (purple) and 70% (blue) of critical damping to the filter numerator . The effect of increased damping is to produce increased phase advance and to limit the filter attenuation of the resonant loop . A value of 20% of critical damping in the numerator produces a stable system whilst restricting the size of the resonant loop .

Fig 5.11 shows two OLRs for the model in Fig 5.8 with first (orange) and second order (red) phase advance filters . The latter produces a significant improvement in system stability .

5.5 CONCLUSIONS

A magnet controller has been proposed that has a neutral flux response characteristic that is unaffected by guideway flexibility . This controller decouples the magnet behaviour from the suspension behaviour and it becomes possible to develop an understanding of the controller parameters that affect guideway flexibility .

Simple modelling work shows that :-

A low suspension frequency is good for stability

A phase advance filter with lots of phase advance at guideway resonant frequencies is good for stability .

A suspension filter with a first order numerator set to optimise phase advance without increased high frequency gain is good for stability .

These proposals for a suspension controller were implemented on the BR experimental maglev vehicle at Derby .

TABLES

Each row of these tables defines an element of a control circuit diagram . The first two numbers define the particular block within the diagram (see the relevant Figure) , the following six numbers

define the behaviour of that block . As described in Chapter 2 , each block is a rational polynomial with third order numerator and denominator . Thus the last six numbers define the numerator and denominator respectively .

TABLE 5.1 Components of the model in Fig 5.1

1,2	1,.0052,0,0,.00033,0
2,3	30,0,0,1,0,0
3,4	1,0,0,2.67,.292,0
4,5	.025,0,0,1,0,0
5,1	-6.7,0,0,1,0,0
5,3	0,-.338,0,.025,0,0
5,6	60000,0,0,1,0,0
6,7	1,0,0,0,0,4500
6,8	Guideway Flexibility in m/N
7,9	1,0,0,1,0,0
7,11	0,.113,.0063,1,.113,.0063
8,9	1,0,0,1,0,0
9,5	26.5,0,0,1,0,0
9,10	1,0,0,1,.113,.0063
10,12	1,0,0,1,0,0
11,12	1,0,0,1,0,0
12,13	333,45.6,0,1,.0114,0
13,1	-1,0,0,1,0,0

TABLE 5.2 The Model in Fig 5.6 from Fig 5.1

```
5,1 delete
4,1 -.2,0,0,1,0,0
9,1 -212,0,0,1,0,0
```

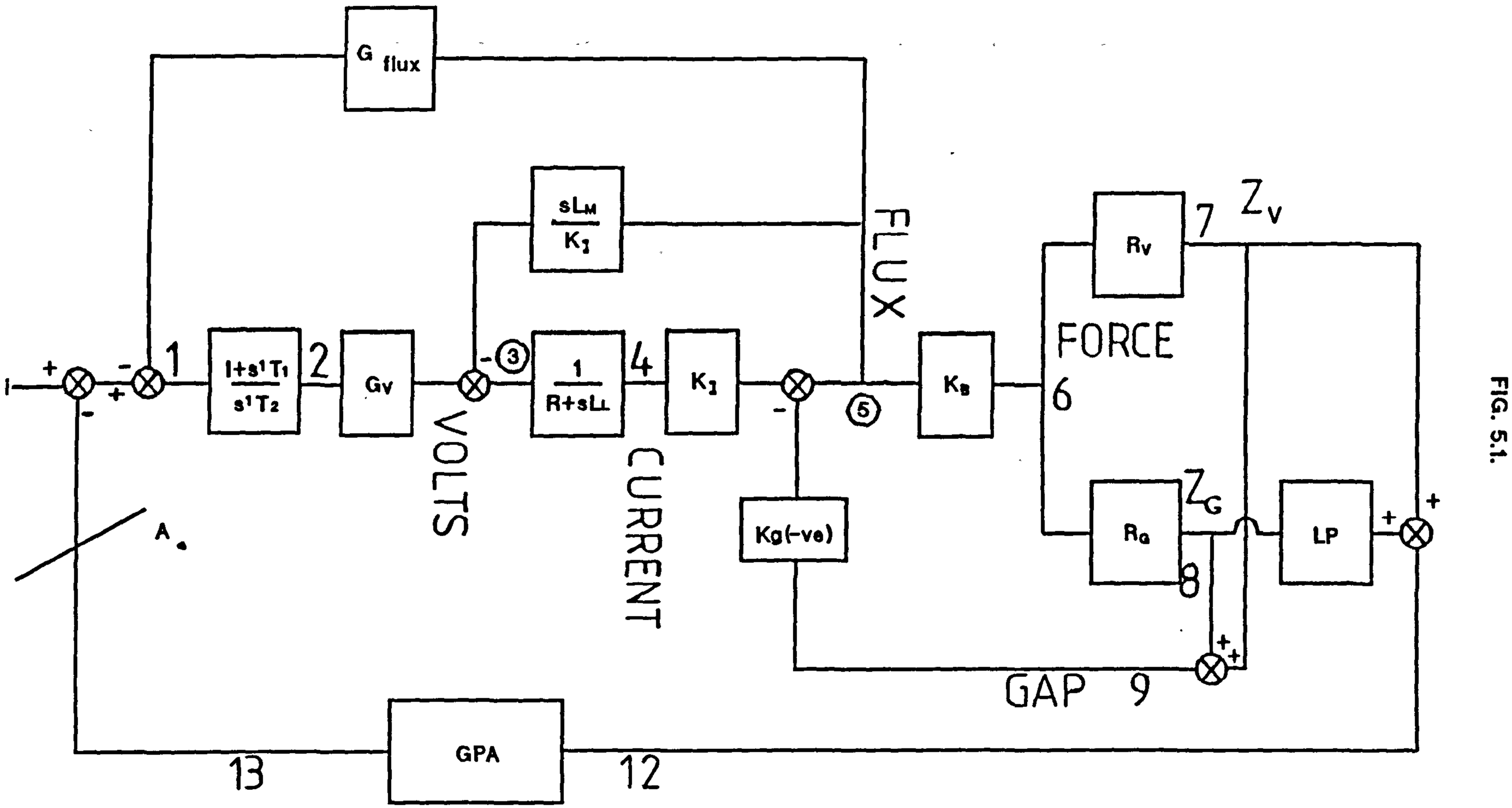

FIG. 5.1. THE ORIGINAL CONTROLLER

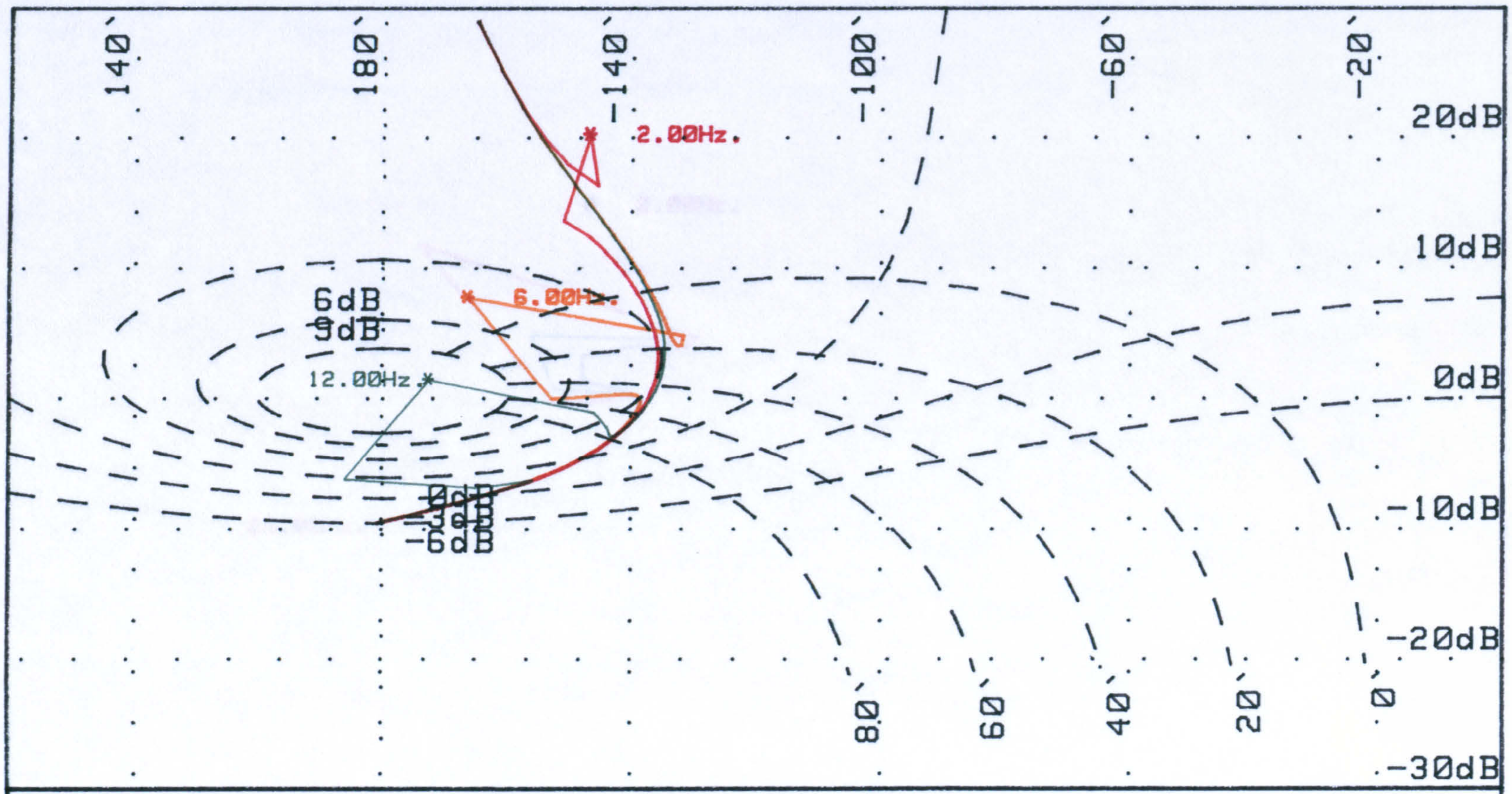

FIG 5.2 GUIDEWAY FREQUENCY

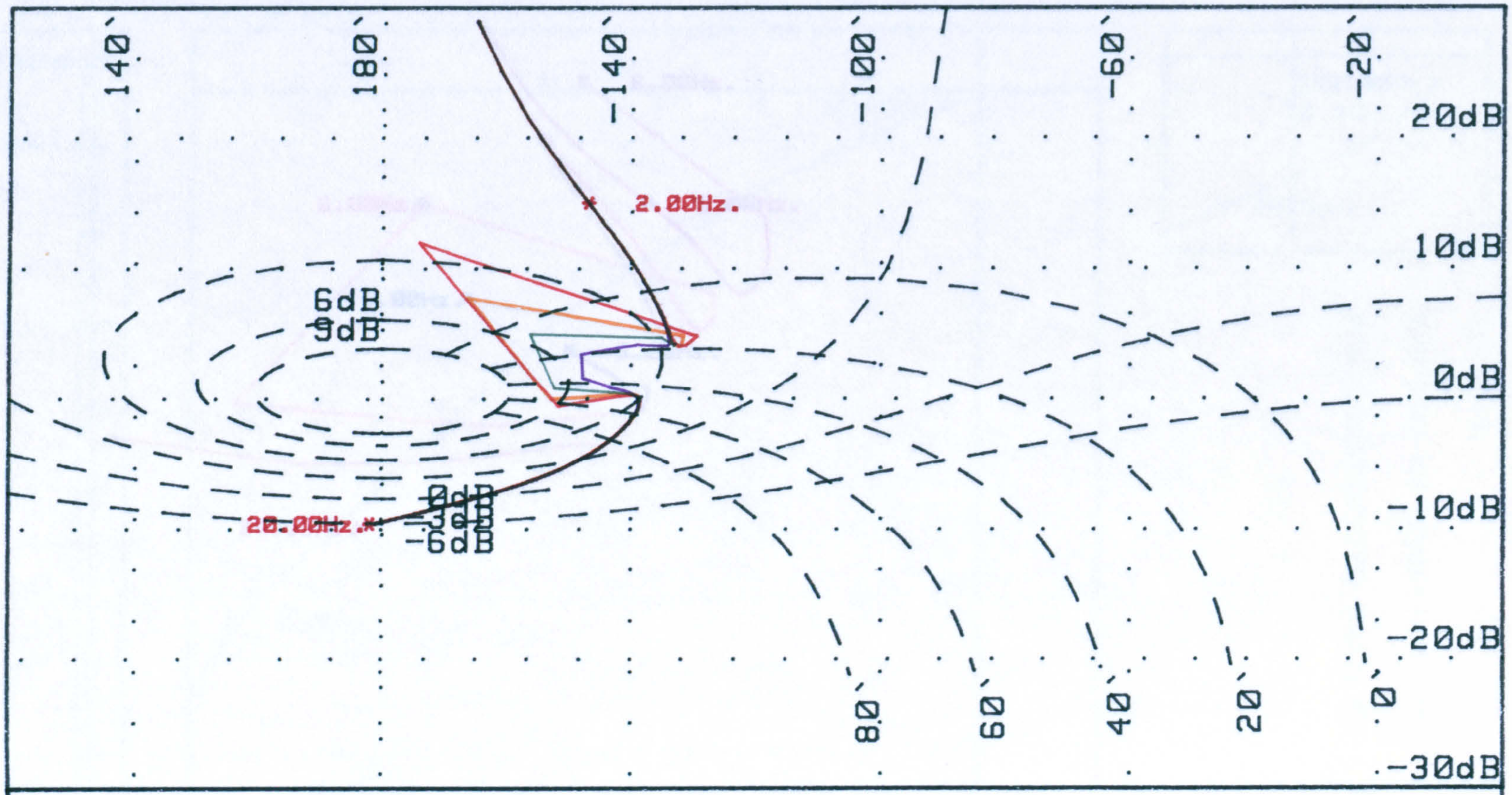

FIG 5.3 GUIDEWAY DAMPING

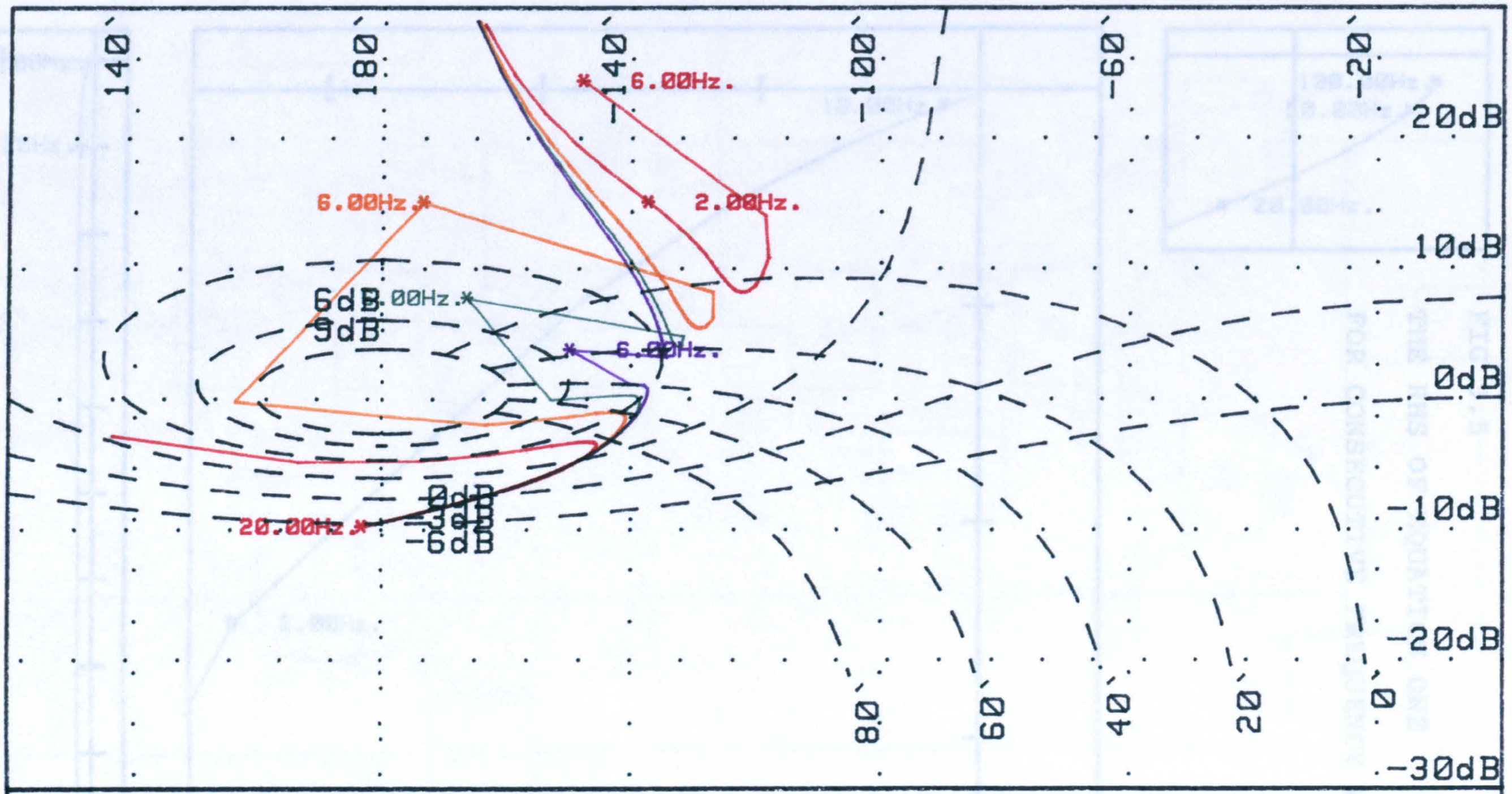

FIG 5.4 GUIDEWAY FLEXIBILITY

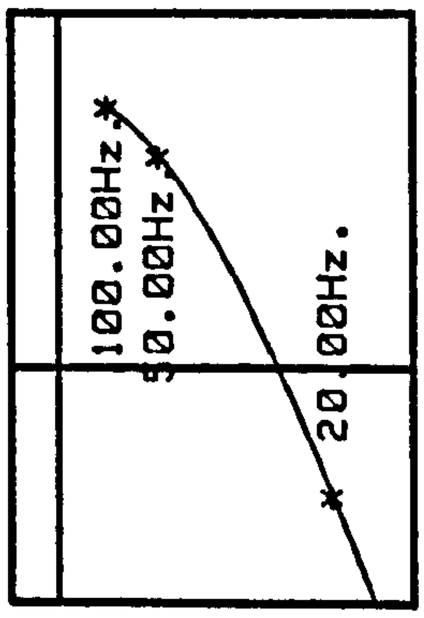

FIG 5.5

THE RHS OF EQUATION ONE

FOR CONSECUTIVE FREQUENCY RANGES

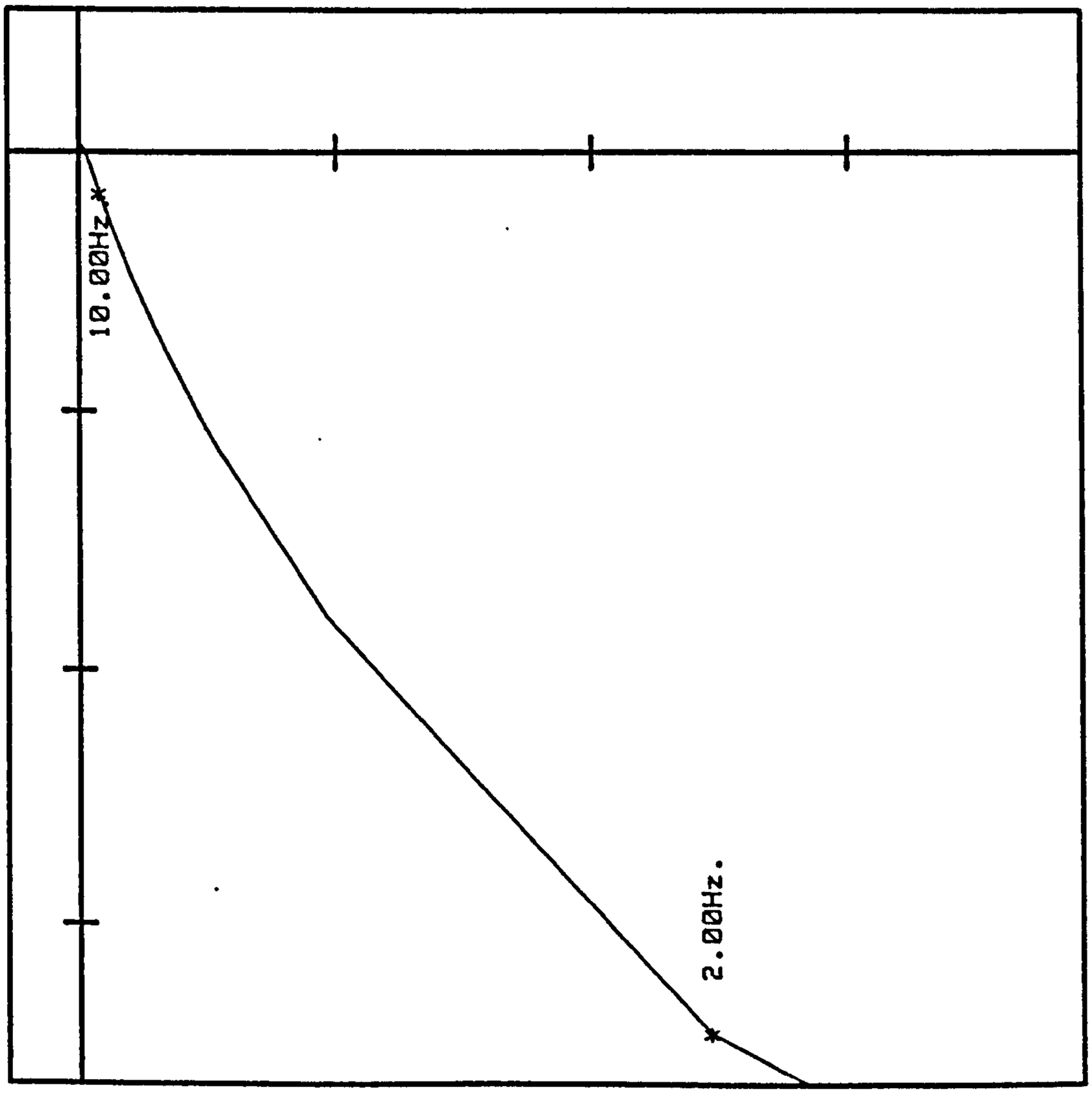

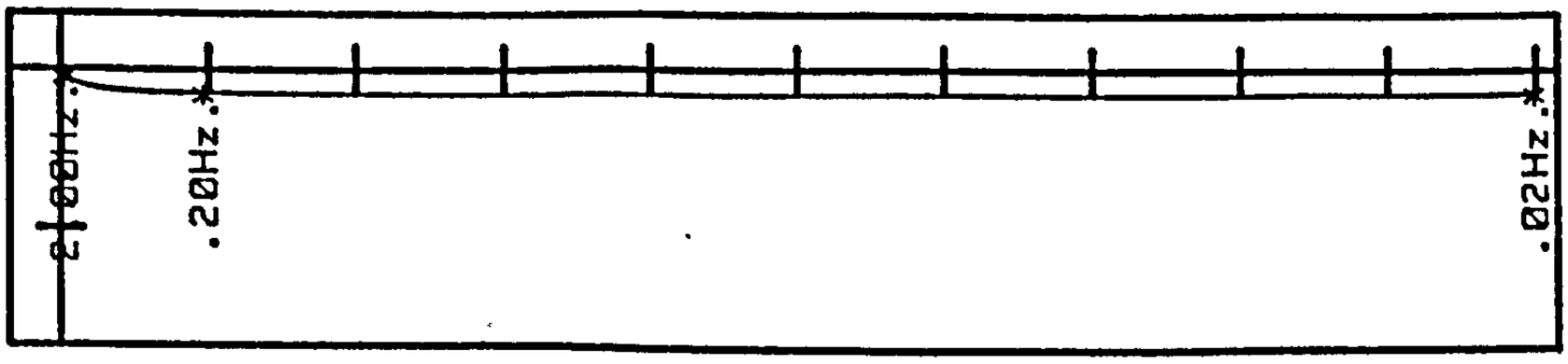

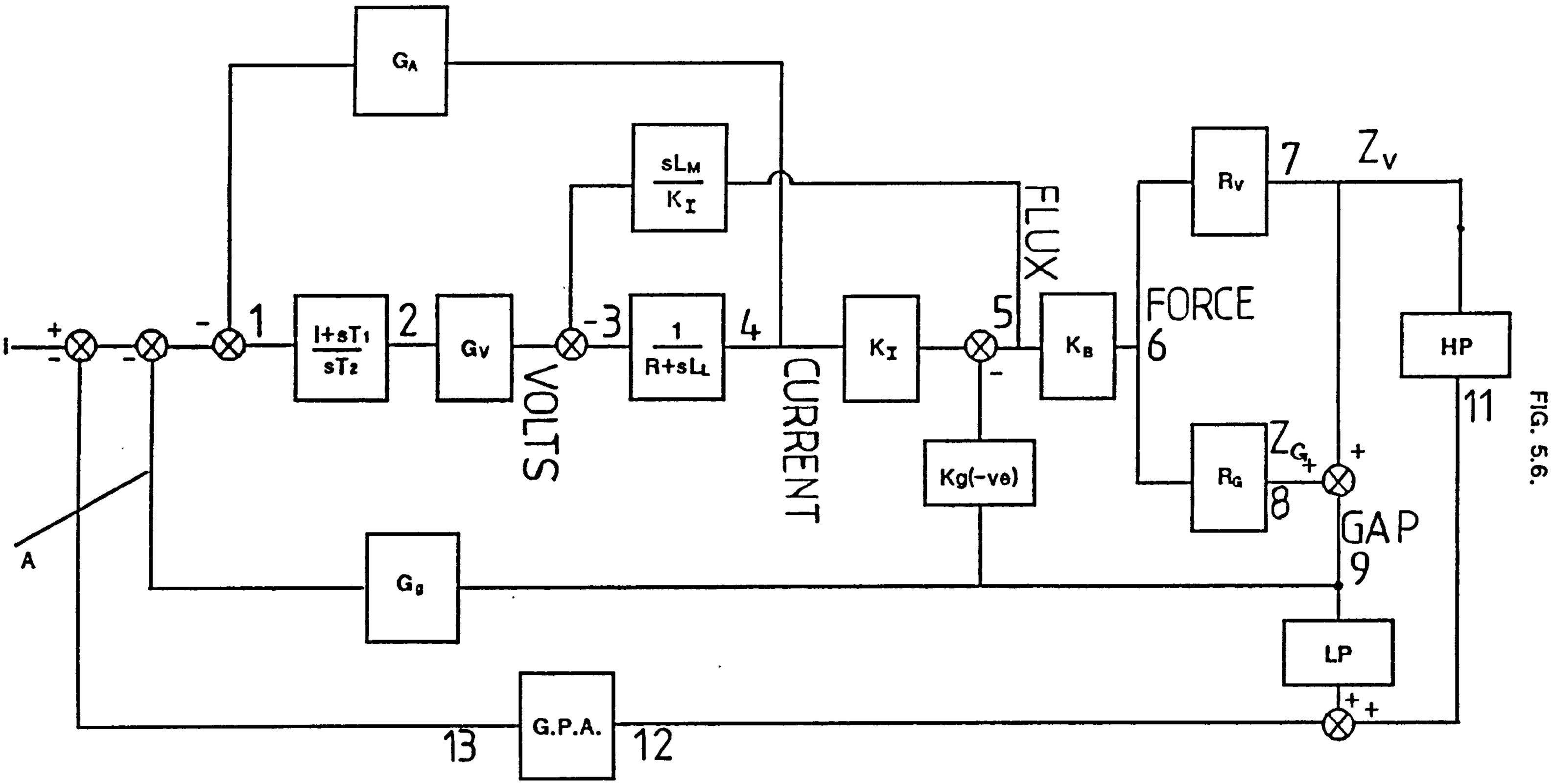

FIG. 5.6.

FIG. 5.6. THE NEUTRAL CONTROLLER

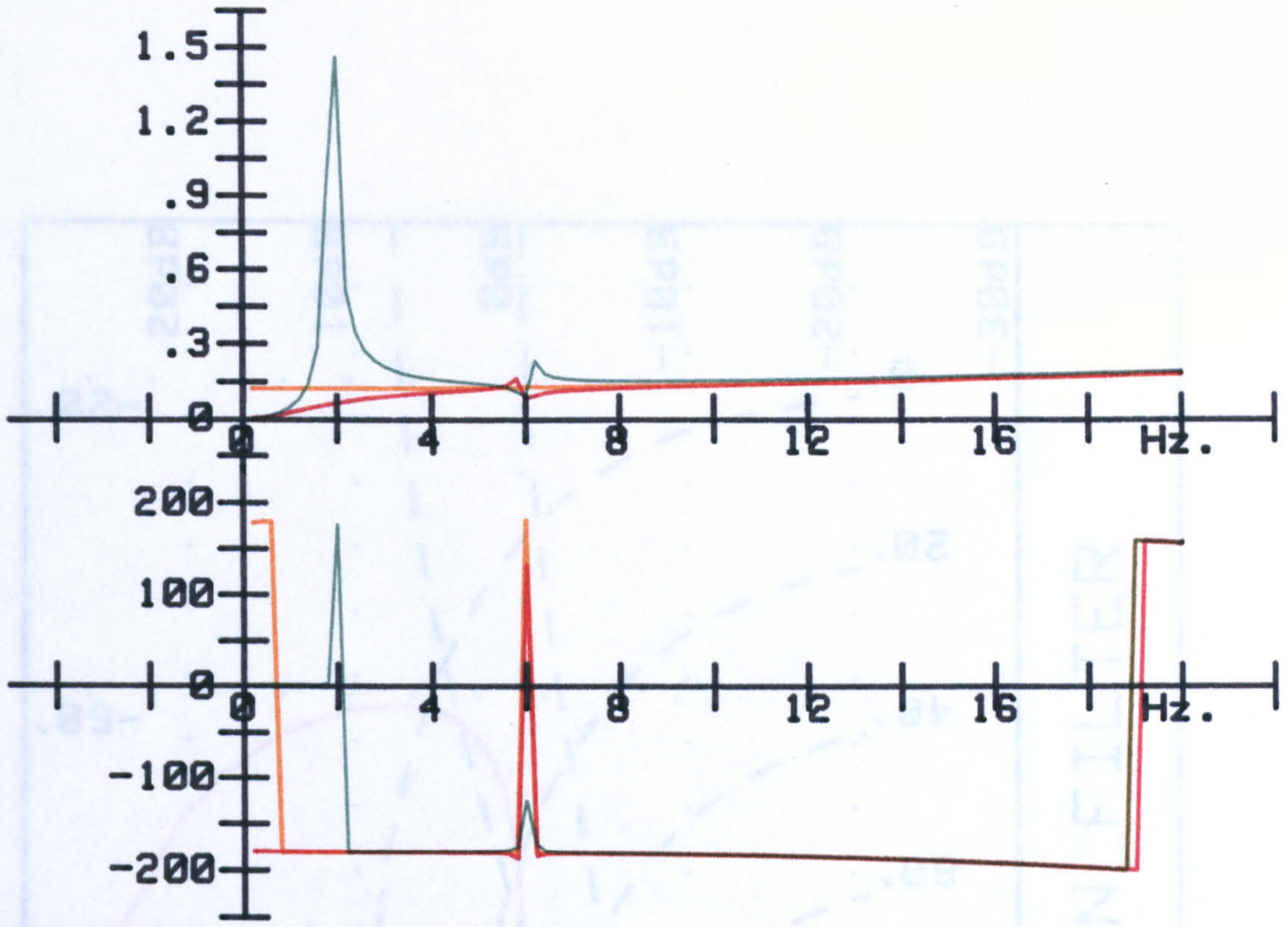

FIG 5.7 GAP FEEDBACK CHANGES

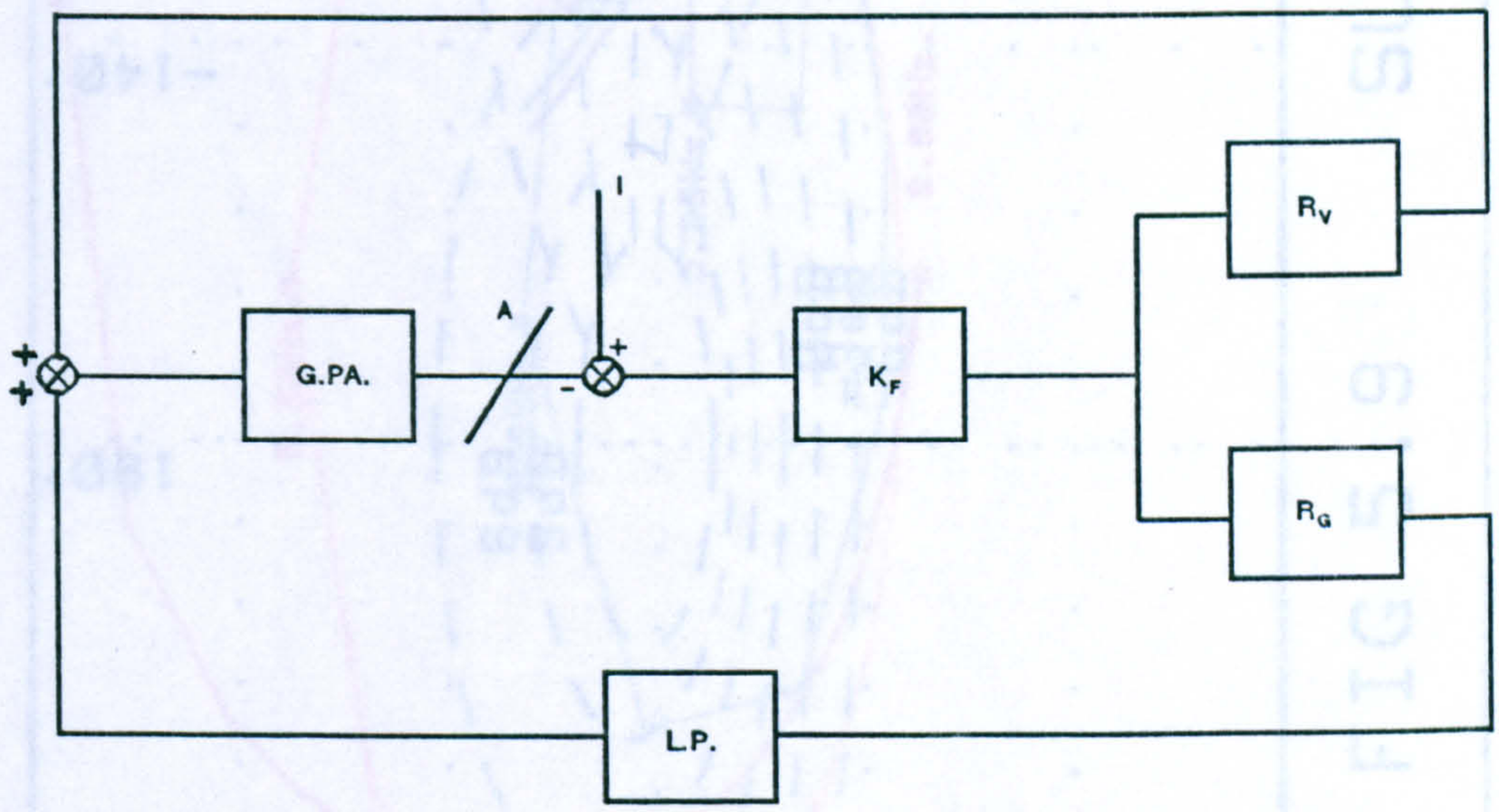

FIG. 5.8. A SIMPLIFIED MODEL OF THE NEUTRAL CONTROLLER

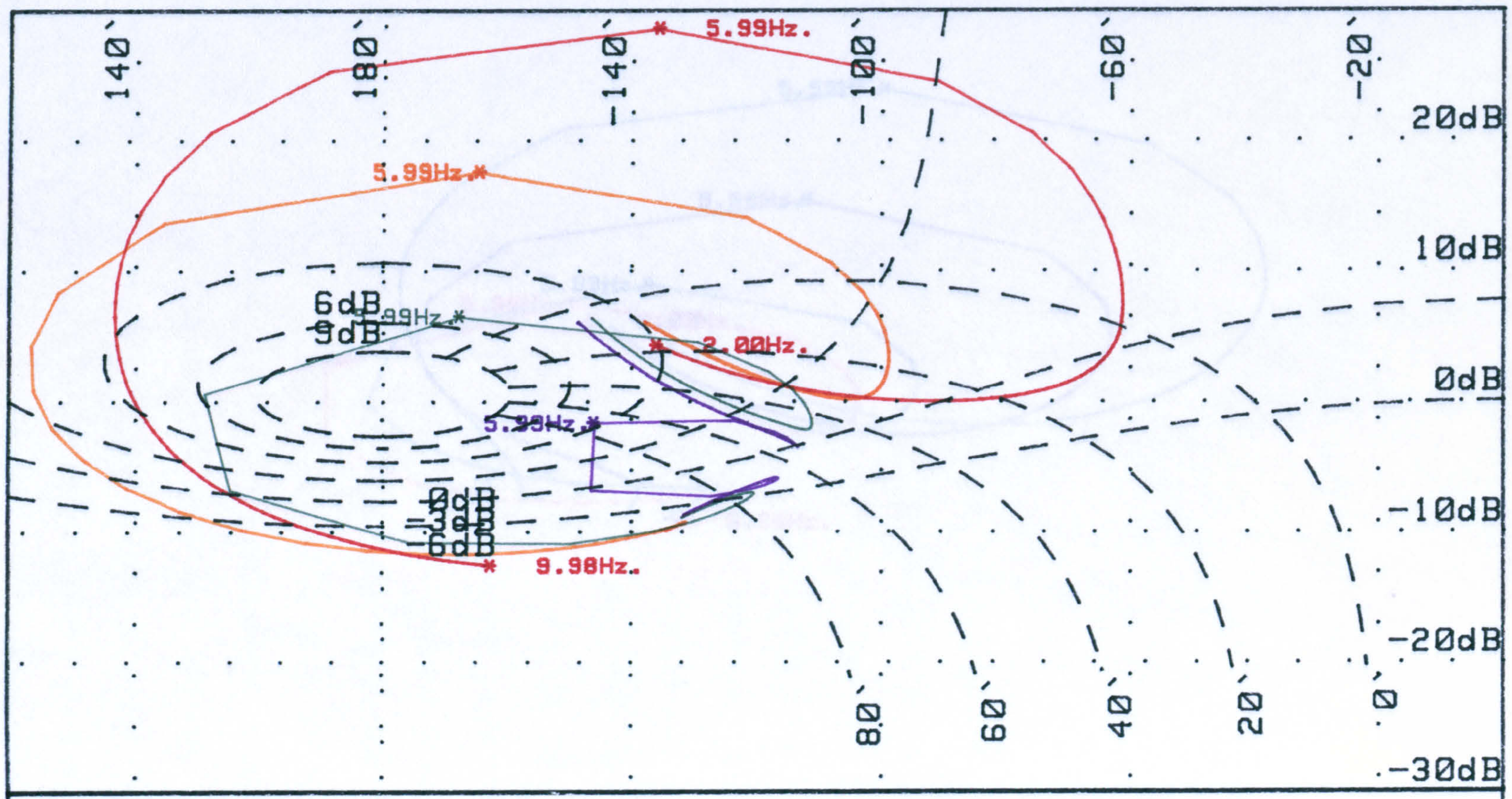

FIG 5.9 SUSPENSION FILTER

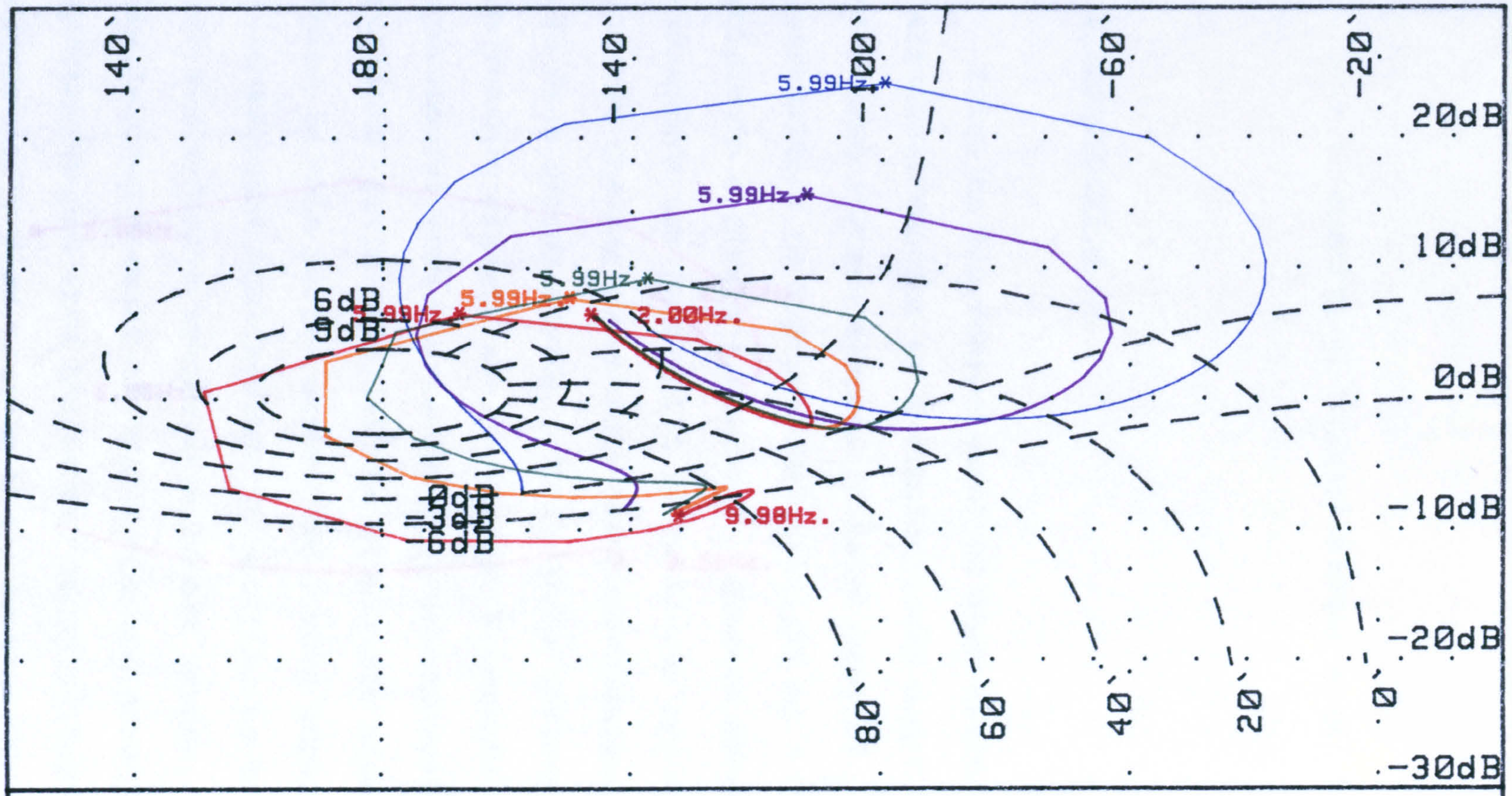

FIG 5.10 NUMERATOR CHANGES

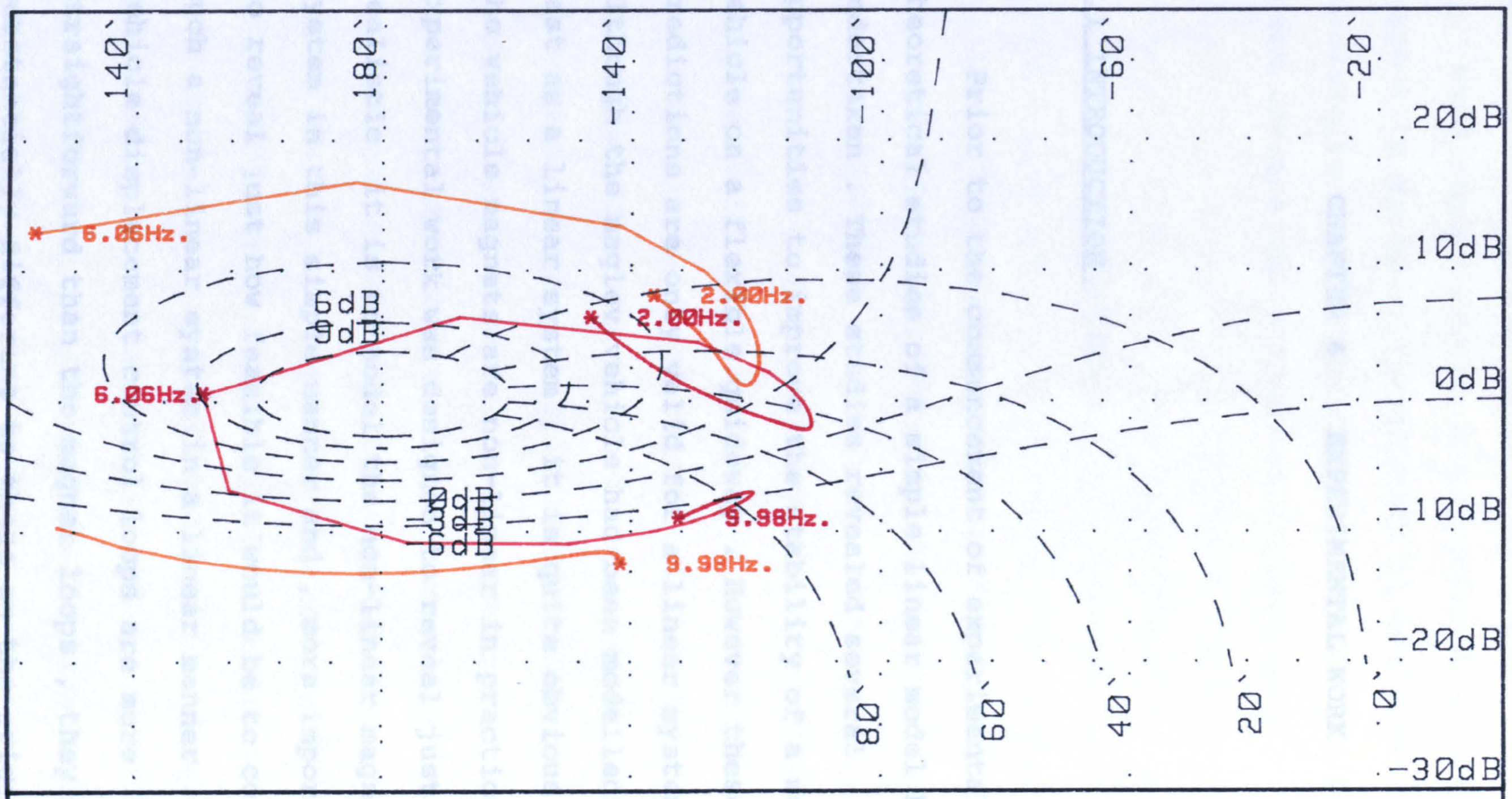

FIG 5.11 PHASE ADVANCE FILTERS

CHAPTER 6 EXPERIMENTAL WORK

6.1 INTRODUCTION

Prior to the commencement of experimental work , theoretical studies of a simple linear model had been undertaken . These studies revealed several opportunities to improve the stability of a maglev vehicle on a flexible guideway . However these predictions are only valid for a linear system and , although the maglev vehicle had been modelled in the past as a linear system , it is quite obvious that the vehicle magnets are non-linear in practice . The experimental work was designed to reveal just how realistic it is to model the non-linear magnet system in this simple manner and , more importantly , to reveal just how feasible it would be to control such a non-linear system in a linear manner . The vehicle displacement control loops are more straightforward than the magnet loops , they are not substantially different to those on the original vehicle control scheme . The major difficulty

anticipated for the experimental work was that of making the non-linear magnet loops work as well in practice as they were predicted to do in theory .

Once magnet behaviour was controlled with respect to guideway flexibility it would become possible to examine the benefits of changes to the phase advance and suspension filters .

6.2 LABORATORY TESTING

An underlying assumption in the working of the proposed magnet controller is that the magnet current is controlled in a manner that reflects the instantaneous magnet-guideway gap . In this way the magnet will be able to produce a controlled magnetic flux level that is independent of magnet gap , regardless of whether or not the guideway is behaving in a flexible manner . This control strategy has been discussed in Chapter 5 . In order to build a magnet controller of this nature it is crucially important to have very accurate control of magnet current . Magnet current was used as a feedback variable in the original controller , described in Chapter 1 , but this feedback was only effective at low frequencies . The existing magnet current transducer , a DC current transformer was not appropriate for high frequency control . A more suitable transducer was found , a Hall effect device manufactured by HEME Ltd. , of

Skelmersdale , Lancashire . This low cost , £70 , transducer produces a high level signal that is proportional to current and requires only a single sided 15 volt supply . Three of these transducers were compared with a reference transducer by measuring the transfer function between the HEME transducer and a reference transducer whilst the same magnet current flowed through each transducer . The reference transducer was a resistive shunt and isolation amplifier . The transfer functions are shown in Fig 6.01 , all three are very similar , all are flat to within 10% and all show phase lags of approximately 5 degrees at 80 Hz , relative to the reference transducer . One of the original inner loop control boards was modified , indeed simplified , by removing the DCCT rectifier circuits and the flux feedback circuits and by changing the low pass filtered current feedback to a constant gain . Measurements of the transfer function between magnet current and chopper demand voltage were made and the results for two choppers are shown in Fig 6.02 . The responses are flat , with phase lags of 0.4 degrees per Hz in the 0 to 10 Hz frequency range .

All the original chopper units were modified to incorporate the HEME current transducers and five new magnet loop control boards were built . A circuit diagram for these boards is shown as Fig 6.03 . Once modified , each chopper unit with its own drive board was tested and fitted to the vehicle .

6.3 VEHICLE COMMISSIONING November 1984 to February 1985

The maglev vehicle had been maintained in regular use throughout its life , earlier in 1984 a large guideway extension , incorporating a switch , had been installed to work with the vehicle . The vehicle was also in frequent use to provide "joy rides" for visitors to the Research Division . Modifications to the vehicle suspension control system for flexible guideway working commenced in October 1984 . Work began in the knowledge that the vehicle was proven , well developed and would therefore provide a sound basis for the new project work .

The vehicle was positioned on the rigid part of the guideway and the maglev suspension was reduced to its simplest working form . The pitch and roll control loops were broken , leaving only the bounce loop to control the vehicle position and the magnet controllers at any one end of the vehicle were switched off . The disabled end of the vehicle was supported at its nominal ride height and the vehicle was free to levitate at just one end . Because the pitch radius of gyration is similar to the magnet semi-spacing , the vehicle was able to behave as if it were levitating in bounce . The disabled vehicle end gave support in roll .

When the first two Heme controlled chopper units were fitted to the vehicle , levitation tests commenced with the aim of optimising gains for gap feedback in the magnet control loops . At this stage , early November , the practical problems of working with an experimental vehicle that was almost a decade old became apparent .

Maglev vehicle work is not conducive to conventional control system development techniques . Normal practice in commissioning a control system would involve testing and assessing system components individually , followed by system assembly and measurement of the OLR . The system would then be developed to provide a satisfactory OLR before closing the loop . None of this is possible with a maglev vehicle . It is not possible to test the magnet characteristics without levitating the vehicle to the correct magnet gap and the vehicle will not levitate unless the whole system is stable . In fact , unless the whole vehicle suspension is working fairly well , development is extremely difficult .

6.3.1 The Problems

Initially , there were a variety of problems that affected the vehicle :-

Lateral Instability This was the major problem , though the instability was only marginal . Once the vehicle had levitated , lateral oscillations of the

vehicle body at 1 Hz would develop over a period of twenty or more cycles to an amplitude of 25mm , a point where the operator would de-levitate the vehicle . This problem was made more difficult by the fact that with vehicle end 1/4 levitated the behaviour was a good deal less stable than with end 2/3 levitated .

Magnet Strut Bending This was a high frequency instability caused by a lateral bending resonance of the magnet mass on the stainless steel support strut at 20.1 Hz . This phenomenon is described in Ref 6.1 although the original control system required no special components to assist the suspension against the strut bending . With the new magnet controllers and the bounce loop operating at the same gain as the original control system , strut bending instability was a substantial problem .

Gap Transducer Drift As autumn turned into winter the weather became colder and damper and the gap transducer signals , which control ride height , needed to be zeroed more and more frequently . These capacitive transducers were designed and manufactured in house by British Rail Research and were known to be susceptible to damp ingress to the transducer head . In late-November one of the gap transducer signals was capable of drifting by over seven volts in a two hour period , indicating a 10mm vehicle movement . Two of the other three transducers were little better .

Random Vibration A low level random vibration was occasionally felt through the vehicle floor and was detectable on all the displacement and acceleration transducers .

Chopper Failures The magnet chopper units were designed in 1974 . There are few areas of modern technology that have advanced as fast as that of power semi-conductors and consequently the reliability of those 1974 choppers in 1984 was poor . The Mean Time Between Failures , MTBF , of the chopper units was around 10 working days .

6.3.2 The Solutions

By the end of February all but one of these problems had been solved and the vehicle was behaving in a relatively consistent manner . All suspension control loops were functioning , all magnets were working with their new controllers and the vehicle would levitate over the rigid guideway . The static vehicle ride was not good and the suspension would collapse if the vehicle was driven along the guideway , stability margins were obviously small , but this was a marked improvement . The solution to and explanation of the various problems were coupled together .

Lateral Instability A clue to the explanation of this behaviour was that lateral instability occurred only when two Heme controlled chopper units provided

the vehicle lift current . If one or both of the lifting choppers was an original , then there was no difficulty with lateral instability . The problem was caused by the loss of direct flux control in the new magnet controllers . Lateral guidance of the vehicle in its original form required that any lateral movement of the vehicle should be opposed by force changes due to changes in the angle of inclination of the magnetic flux . This is described in Chapter 1 . It is implicit that the magnitude of magnet flux does not depend upon lateral movements of the vehicle relative to the guideway . The original chopper control utilised flux feedback to help ensure that this was true . The Heme controlled choppers have no element of direct flux control and attempt only an indirect control of flux in response to vertical changes in the magnet gap . Lateral movement did have an effect on the magnetic circuit reluctance and produced force changes that opposed those of the lateral suspension .

Observation of the degree of lateral instability present suggested that only modest optimisation of the lateral guidance was needed to provide a workable vehicle . However , too much testing time had already been lost and a radical solution , certain of success was implemented . Additional control loops were added to the lateral suspension to provide independent displacement

feedback for each vehicle end . The lateral instability disappeared .

The problem of different behaviour at the two vehicle ends was resolved when it was discovered that the two coils which make up one of the U shaped magnets in corner 2 had , at least since Redfern's re-commissioning in 1981 , been connected to drive flux in opposing directions . This completely ruined the desired magnetic characteristics of one corner of the vehicle , destroying the suspension symmetry of the vehicle .

Magnet Strut Bending As with the lateral instability this phenomenon was greatly exacerbated by the loss of direct flux control . The problem was contained by the inclusion of a notch filter at 20.1 Hz with 5% damping in the main displacement control loop .

Gap Transducer Drift New gap transducer heads were manufactured with long trailing signal leads to eliminate local connectors . The old transducer heads were physically damaged and were contaminated by grease and dirt . They were replaced . The signal conditioning circuit boards were cleaned and varnished to avoid damp ingress .

Random Vibration The cause of this problem was the coils in magnet 1A shorting to ground when the magnet became hot and thus varying the number of effective Ampere turns in the magnet . The coils were replaced .

Chopper Failures There seemed to be no solution to this problem , which had become a major source of concern . An average chopper failure meant the destruction of five of the twenty power transistors within the chopper unit . The power transistors from the 1974 design were no longer manufactured and were unobtainable . At the end of February there were only twelve of these transistors left and these were from cannibalised equipment . An alternative contemporary equivalent transistor was urgently sought out .

6.4 MAGNET CONTROLLER DEVELOPMENT March 6th to March 14th

6.4.1 Current Response Measurements

Measurements of the frequency response between magnet current and demand voltage for a static vehicle are shown red in Fig 6.04 . Theoretical calculations from the model shown in Fig 5.6 with links for magnet negative stiffness and magnet gap feedback removed are shown blue . The calculations model a static vehicle , in its nominal position on the guideway and there is good agreement between the prediction and the measurement . This demonstrates that the magnet control loop is accurately modelled . Values of magnet resistance , leakage inductance and

mutual inductance are known for the magnet at nominal current and ride height .

A measurement of the current response for the magnets at corner 3 , with the vehicle levitated , are shown in red in Fig 6.05 . Modelling these measurements was not successful until more experimental work had been done .

6.4.2 Open Loop Response Measurements

A bounce OLR measured on March 11th appears in red on Fig 6.06 , this shows that phase margins are only 20 degrees . The gain seems oddly discontinuous below 3 Hz but is more consistent at frequencies above 6 Hz .

A pitch OLR recorded on March 14th , shown in Fig 6.07 , indicates slightly better phase margins than the equivalent bounce response although on a rigid guideway these responses should be identical . This difference is due to the inclusion of a notch filter in the bounce loop to control the magnet strut resonance . The response below 3 Hz is similar to Fig 6.06 because of its discontinuous nature .

A roll OLR was measured on March 13th and is shown in Fig 6.08 . The roll-lateral coupling effect , described by Redfern in Ref 6.2 , is seen as a peak in the magnitude response at around 3 Hz . The response below 3Hz is similar to the bounce and pitch responses because of its discontinuous nature .

An OLR was calculated from the model shown in Fig 5.6 and is shown in blue on Fig 6.06 . There is little agreement between this and any of the measured OLR characteristics at frequencies below 4 Hz . Major differences between theory and experiment are that at low frequency the measured results show a very low gain and at frequencies above 3 Hz have a significantly larger phase lags than the model predicts . The phase lag increases at higher frequencies .

6.4.3 Magnet Flux Measurements

Magnet flux was measured with a proprietary transducer manufactured by F.W. Bell in the USA . This transducer is a Hall effect device which measures the mean flux level with a small , 2mm x 2mm . , probe that was supported from ground and positioned within a magnet field . The test procedure was to perform flux response measurements on one corner in 4 which had its lateral demand signal removed . The first magnet flux response was measured on March 14th and is shown as Fig 6.09 . This measurement provided some explanation of the rather unsatisfactory match between prediction and measurement of the OLRs . The gain of this flux response falls away below 5 Hz , as does the measured OLR . Above 5 Hz when the gain is flat there is a phase lag of about 2 degrees per Hz ,

the ideal flux characteristic is flat with no phase lag at any frequency .

6.4.4 Flux Control Optimisation 15th March-April 1st

On March 19th , chopper unit 4 failed and only vehicle end 2/3 was able to levitate although the lateral demand signal was removed from corners 2 and 3 . The vehicle was stable laterally at end 2/3 with no lateral displacement feedback , relying only on the magnet lateral stiffness for a centring force . This produced a great improvement in the flux response measurements . Fig 6.10 shows two measurements of the flux response of magnet 3B with variation in magnet gap feedback which are similar to the modelled results in Fig 5.7 . Each plot has a flat (orange) characteristic which is the desired , neutral magnet characteristic . The red plot in Fig 6.10 relates to the green plot in Fig 5.7 , which has 40% too much gap feedback .The red plot in Fig 6.10 is inverted for experimental convenience .

On March 20th , further testwork continued with the aim of optimising the flux response for magnets 3A and 3B , but chopper 3A failed to a single sided condition and had to be replaced .

Chopper unit 3 was repaired and replaced on March 21st . Optimisation of the flux response at vehicle end 2/3 continued . Four sets of data were measured and recorded with levitation of vehicle end

2/3 , shown as Fig 6.11 , with flat responses for magnets 2A,2B,3A,3B . Gain levels were around 0.15 Tesla/volt , feedback gains were believed to be 2A-167 v/m , 2B-200 v/m , 3A-278 v/m , 3B-333 v/m . Chopper unit 4 was re-fitted to the vehicle on the afternoon of March 21st , allowing the whole vehicle to levitate for measurement of the flux response of magnet 2B . This was little changed from the response measured when just the vehicle end was levitated .

Frustratingly , chopper unit 3 failed on March 22nd . Attention shifted to optimisation of the magnets at corners 1 and 4 . Optimisation work on magnets 1A,1B,4A,4B continued slowly until March 29th when the lateral demand signal was removed from both corner 1 and corner 4 . By that time , control of the vertical suspension had improved to the level whereby the lateral stiffness of the magnets was all that was required to maintain lateral stability .

March 30th and 31st were days devoted to the repetitive testing of the magnets at end 1/4 . Each magnet was tuned , in turn , to optimum flatness of reponse because the whole vehicle movements coupled the response of one magnet into the others . The magnet controllers were also "tuned" to compensate for the differences in magnetic gain of the different magnets , magnet 4A was particularly poor in this respect , almost 40% less than the other magnets at end 1/4 . By March 31st the four magnets 1A,1B,4A,4B had been optimised to give the responses shown in Fig

6.12 with gap feedback gains of 1A-244 v/m , 1B-200 v/m , 4A-250 v/m , 4B-170 v/m . It was apparent that all the responses shown in Figs 6.11 and 6.12 were sufficiently flat to allow the vehicle to move onto the flexible guideway as soon as a full set of choppers were available .

April fools day was hard . Chopper unit 4 blew up , as did its replacement , then the replacement for the replacement also failed .

6.4.5 A Summary of Flux Control Optimisation

All eight magnets had required a considerable amount of careful work to optimise the controllers in order to provide the required responses . All the initial magnet flux responses were similar to Fig 6.09 in that the response below 3 Hz was discontinuous and had substantial phase lags . This factor seemed to provide ample justification for the low gain at low frequencies in the OLRs measured earlier .

Improvements to the flux response of the magnets were difficult to make , largely because of the coupling of vertical and lateral vehicle dynamics in the physical magnet flux distribution . Initially , neither the vertical nor the lateral vehicle suspension control was good and , as a consequence of this , attempts to measure magnet flux changes as a result of excitation to the vertical suspension were

confused by flux changes originating in poor control of the lateral suspension . Improvements to the magnet vertical flux control were only achieved slowly until such time as the quality of that control reached a level where the lateral suspension was stable , relying only on the lateral stiffness of the vertical suspension magnets . Once this happy state was achieved , accurate measurements of the vertical magnet characteristics became possible and magnet controller optimisation advanced more rapidly .

All the magnets produced a similar performance level with the exception of those with solid mild steel pole pieces at corner 4 . A phase lag exists between magnet current and magnet flux for any electro-magnet , this is due to the hysterisis of the magnet material . The phase lag for the magnets at corner 4 is twice as large as the phase lag at the other corners because the pole pieces are not made of a laminated , high quality magnetic material , but of solid mild steel .

Table 6.1 shows parameter changes from the model of Fig 5.6 which define a changed model . This model includes phase lag terms in the representation of the current transducer , the magnet current/flux characteristic and the power amplifier gain . In order to duplicate the way that experimental results were taken , guideway flexibility is removed from the model and the system input is summed into the phase advance filter . Frequency responses were calculated

between the analogue of current or flux and the suspension loop demand voltage .

The calculated current response is plotted blue in Fig 6.05 to compare with experimental results . Agreement in the 4 Hz to 15 Hz range is good . At higher frequencies the comparison deteriorates , but these frequencies are less important for suspension behaviour . The differences at low frequency are disturbing , although the coherence responses for the measurement in Fig 6.05 , shown as Fig 6.13 , offer some explanation . The coherence below 3 Hz falls to 0.1 , it is possible that the theoretical prediction is correct and the experimental results are misleading . At the time , it was not known why the coherence response was so low .

A predicted flux response is shown blue with four measured responses in Fig 6.12 . Agreement is good , but for phase errors of around 10 degrees , which are significant for considerations of stability . On the basis of current and flux prediction , the system is modelled accurately . The magnet controller works well enough to support the vehicle vertically and laterally and seems to work in a predictable manner .

The model defined from Table 6.1 produces the OLR shown green in Fig 6.06 . Phase margins are 15 degrees lower and more realistic than those predicted by the model shown in Fig 5.6 . The calculated responses now look a little more like the measured

responses shown in Figs 6.06 to 6.08 . At frequencies below 3 Hz , the predicted response is continuous and well behaved , unlike the measured responses and the predicted phase margins are highly optimistic .

6.4.6 Chopper Failures

During this period of 17 days , the vehicle was able to attempt a full lift of all four corners on only 2 days . Shortage of working choppers limited work to lifting just one vehicle end for 10 of the 12 working days , this was not due to any lack of financial or man-power commitment from British Rail . Intensive practice had reduced the time taken to strip , repair , rebuild and test a blown chopper unit to less than 12 hours . During this 15 day test period , around ten chopper repairs were carried out . The MTBF had plummeted to less than one working day , though this figure masks a marked difference in performance between two chopper types .

By March 15th there were none of the original chopper power transistors left , though a near equivalent contemporary transistor had been identified and stocks of these were purchased . Any choppers that failed in this test period were rebuilt using the new transistors and it quickly became apparent that the chopper units with the new power transistors had a very short life expectation . Some of these repaired units failed in seconds on the

vehicle , despite having been commissioned under power in the laboratory . As a contrast , the choppers in the vehicle that relied on the older power transistors kept working to at least the previous 10 day MTBF criterion . The immediate suspicion was that the new transistors were not sufficiently similar to the old ones .

All vehicle work with these choppers ceased on April 1st . When chopper unit 4 failed , a fully tested replacement was fitted in less than 30 minutes , this also failed the instant that it was switched on . So did a second replacement unit . Each of three chopper units had failed in seconds with no apparent cause , and certainly no apparent remedy . There was no evidence of a mismatch between the old and new transistor types and by definition it had become impossible to maintain the test programme with these chopper units .

6.5 A REDUCED PROJECT

April 1st 1985 was intended to be an important date for the Maglev Flexible Guideway Project . It should have been the date on which all experimental activity ceased , the end of a successful project . Indeed , during March , discussions with the Curator of the National Railway Museum had led to proposals of a date in July to hand over the maglev vehicle , a

portion of the guideway , the guideway switch and any available "memorabilia" . In practice , by April 1st 1985 , little worthwhile experimental data had been gained and the vehicle was not yet fully commissioned . British Rail R&D management were enthusiastic to improve this situation and a limited ammount of work was authorised for the financial year 1985-1986 . The first task was to replace the existing and unworkable maglev vehicle choppers , an essential requirement for commissioning the vehicle suspension .

During 1984 another project in the Suspension Unit had made use of maglev technology to drive a railway vehicle active suspension . The choppers for this system had been purchased by means of a development contract with Marconi , who had insisted on a minimum order of 10 choppers and six of these choppers were surplus to the project requirements . The Marconi choppers were not exact replacements for the existing choppers , although they had a similar specification . The Marconi choppers were rated at 300 volts and 50 amps , the original choppers were rated at 300 volts and 60 amps .

The major difference between the two types of chopper was that the Marconi unit was designed to be driven by a DC supply that , at switch on , would increase its voltage from 0 to 300 volts slowly . The original choppers were driven by a crude regulated three phase power supply that would cause great difficulties for the Marconi choppers . The original

choppers contained a substantial choke to limit the rate of change of voltage at switch on , these chokes were stripped from the original choppers and installed in series with the Marconi choppers . It was considered that the Marconi choppers would then be in a similar electrical environment to the original choppers .

Unfortunately there was one unavoidable disadvantage associated with the use of the Marconi choppers , there were only six choppers available and eight would be required to levitate the whole vehicle . Installation of the Marconi choppers allowed only one end of the vehicle to levitate and it was accepted that moving vehicle tests would be impossible . There was no alternative .

6.6 STARTING ALL OVER AGAIN March 30th to May 28th

6.6.1 More Flux Measurements

The period of May 2nd to May 8th was a repeat of the flux response measurement-gap feedback gain change cycle that had been carried out with the original vehicle choppers . During this time , great difficulty was experienced in optimising magnet responses to the quality of those previously recorded in Fig 6.11 . An example of this is shown in Figs 6.14 and 6.15 . Fig 6.14 shows optimised flux

responses for the four magnets measured sequentially at the end of work on May 7th . Fig 6.15 shows what should have been identical responses measured at the start of work on May 8th , they are quite different . A major difficulty had become apparent in that a single magnet controller could be optimised in isolation but when tested again , that optimisation would have disappeared .

A hypothesis for this behaviour follows from the relative size of the flux field and the Hall Effect flux probe . Despite the 25 mm width of the magnet pole faces , the flux field has a high intensity over a width of approximately 7 mm . There was some difficulty in positioning the 2 mm wide flux probe within the high intensity flux region so that it remained there as the vehicle moved under test . It seemed likely that the magnet loop optimisation involved some linearisation of the movement of the whole dynamic flux field around the static flux probe . Repositioning the flux probe for further tests provided a different linearisation and hence required a different optimisation .

In order to optimise the linear controllers for the non-linear magnets it was a requirement to obtain measurements of a system response that was a function of the effective vehicle-guideway flux for all magnets . Measurement of point flux levels within individual magnet flux fields was not adequate .

6.6.2 An Alternative To Flux Measurement

The inability to optimise the magnet controllers by point flux density measurement was a very serious problem because it had been expected that this would be the most direct means of commissioning the vehicle magnet controllers . The alternative strategy adopted was to assume that all the magnet characteristics were similar . All the individual magnet feedback gains could then be optimised together by observation of the vehicle OLR .

Measurement of the OLR , as described in Chapter 2 , is an awkward procedure . An OLR is measured as a multiple of two system responses, in practice one response is that of the phase advance filter . The phase advance filter response is unaffected by optimisation of the magnet control loop , hence optimisation of the magnet control loop was based on a simpler measurement of one system response , a Quasi-Open Loop Response (QOLR) .

Optimisation work on May 11th involved measurements of QOLR . Fig 6.16 shows the effect of changing gap feedback gain from 222 (green) to 148 (orange) to 121 (red) v/m , where the value of 148 v/m produced the highest gain response , though at frequencies below 1 Hz all three responses are poor quality . The measured responses show an unexpected peak at 2 Hz , which is matched by Coherence measurements of around 99% . These measurements are

in general agreement with Fig 5.7 , but were measured on a rigid guideway .

An OLR for the frequency range 0-25 Hz was measured and appears as Fig 6.17 . This emphasized the low frequency characteristics of a well defined , unexplained 2 Hz peak and a poor quality , low gain measurement below 1 Hz . Fig 6.17 also highlights the potential high frequency problem of the vehicle structural dynamic behaviour coupling with the control system . There are two structural modes apparent at 20.1 Hz and 23.0 Hz , both of these are vibrations of the magnets on their slender support struts .

On May 16th a gap transducer sensitivity check showed that both gap transducers were out of calibration . After re-calibration , further measurements of QOLR produced an assesment of optimal gap feedback of 121 v/m , shown red in Fig 6.18 . The high frequency structural modes were reduced by the notch filters until they no longer affected stability at these displacement loop gains .

A theoretical calculation of QOLR is shown blue in Fig 6.18 , this has no peak at 2 Hz and agreement at low frequencies is poor . Phase lags are now predicted with great accuracy . The model which produces these calculations is shown in Fig 6.19 . The changes from the model in Fig 5.6 are detailed in Table 6.2 . Important changes from the form of the model in Fig 5.6 are the representation of the magnet

structural vibrations , the compensating notch filters and accurate modelling of the absolute position filter . The model form has been changed to use just a low pass filter and not the high pass-low pass combination . This was discussed in Chapter 1 .

6.6.3 On The Flexible Guideway , at last

The vehicle was moved onto the flexible guideway , for the first time in nine months work , on May 20th . The vehicle was positioned with the working magnets just on the flexible guideway , the non-working end of the vehicle remained on the rigid guideway . The condition of the gap transducers had deteriorated and they were beginning to reproduce the problems of earlier in the year . On May 22nd it was apparent that the vehicle was levitating at a reduced ride height . The gap transducers were recalibrated and transducer sensitivity was reset to 1.3mm/volt , +/- 0.05mm/volt .

Further measurements of the QOLR allowed optimisation of the magnet gap feedback to 156 v/m . The optimal result is plotted onto Fig 6.18 in orange . A comparison with the previous optimisation shows that the transducer recalibration had improved the system , the gain at low frequencies was increased by approximately 3 dB . This improved performance is shown in Fig 6.20 , an OLR measured with an outer loop gain of 25k volts/m . Fig 6.20 still shows the

problems of the unexplained peak at 2 Hz and loss of gain at frequencies below 1 Hz , this problem is associated with measurements of low coherence below 1 Hz . A small loop in the OLR characteristic appears at 6 Hz , the frequency of the first symmetric guideway bending frequency . A notch filter was used to supress the structural modes at 20.1 and 23.0 Hz .

Work on May 24th was directed at discovering the source of the measured , unpredicted , 2 Hz peak in all the OLRs and QOLRs measured so far . Measurements were taken to compare the performance of the absolute position and gap transducers , a frequency response was measured to compare the absolute position signal with the gap signal . Below 0.6 Hz the absolute position filters do not calculate absolute position accurately , but above this frequency the frequency response between the two gap measurements should be a constant , unless the guideway moves . The sensitivity of the control signals should have produced a value for the ratio of gap signal divided into absolute position signal of 0.05 . The measurement was approximately 0.03 , the known control signal sensitivities were wrong and had , apparently , been set that way when the vehicle was commissioned in 1981 . The frequency response measurement is shown as Fig 6.21 .

On May 29th , a series of three QOLRs were measured with outer loop gains of 15k (red) , 30k (orange) and 45k v/m (green) . The measured frequency

responses are shown in Fig 6.22 and the coherences in Fig 6.23 , the 2 Hz peak is no longer present in these measurements . At frequencies above 1.5 Hz the measured gain changes with the outer loop gain , as it should . At lower frequencies , the measured gain appears to fall with increased outer loop gain . Fig 6.23 clearly shows that the low frequency coherence is higher with lower gains , this was surprising . Fig 6.24 shows PSDs of the two channels involved in these measurements . It is clear that in the frequency range to 1.5 Hz , an increase in gain is accompanied by a substantial reduction in signal power .

The technique that has been used for measurements of OLR and QOLR were discussed in Chapter 2 . Fig 6.25 describes the test technique where , in practice , G(w) is the frequency response of the bounce suspension excluding the phase advance filter . H(w) is the frequency response of the phase advance filter .

If the whole system is stable and :-

either $i_1 >> i_2$ then the frequency response B/A is 1/H(w)

or $i_2 >> i_1$ then the frequency response B/A is -G(w)

hence two measurements with the noise source applied firstly as i_1 and then i_2 allows calculation of OLR , with the vehicle working as a closed loop system .

Unfortunately for this test technique , the function of the vehicle suspension is to prevent disturbance of the suspended load , the maglev suspension opposes the effect of the test signal , thus denying the criterion that $i_2 >> i_1$, particularly at low frequencies . This means that OLR is not measured accurately and the measurement may tend to unity . It may be expected that when the system is close to instability , system noise will become large , $i_1 = i_2$ and OLR measurements will tend to unity .

It is likely that misleading measurements , produced by high gains in the low frequency range , have been a substantial contribution to the difficulties of optimising the magnet control loops .

6.6.4 Magnet Control - A Summary

It had not proved possible to use magnet flux measurement as a means of optimising the magnet controllers . This was due to problems of repeatability of flux measurement and , in hindsight , of uncontrolled variation in gap transducer sensitivity . Measurements of QOLR were used for succesful magnet optimisation , although good results were dependent upon consistency from the gap transducers . Indeed the success of the magnet controller is dependent upon consistency from the gap transducers .

Initially the QOLR measurements were in general agreement with predictions at frequencies above 3 Hz . Below 1 Hz the QOLR was smaller than predicted and between 1 Hz and 3 Hz it was larger than predicted . A longstanding error in transducer gain was discovered , subsequent correction gave better agreement between measured and predicted OLR at frequencies above 1 Hz . It is believed that below this frequency the action of the suspension is to prevent the successful measurement of the suspension characteristic and that the suspension model is accurate .

Fig 6.22 has a theoretical QOLR plotted in blue , at frequencies where accurate measurement is possible , agreement in phase is to within 3 degrees . Fig 6.26 shows measured and predicted OLRs and the level of agreement is again to within 3 degrees in the frequency range which allows accurate measurements .

The magnet controllers were developed to work in accordance with the theoretical description in Chapter 5 , but for the inherent phase lags within system components .

Subjectively the magnet controllers provide good lateral stiffness and stability although ride testing would be required to prove the adequacy of the lateral suspension . Any problems could be overcome , as was done initially with this work , by the provision of lateral gap transducers .

The vehicle model has been extended from the original theoretical study in Chapter 5 . Changes from the model in Fig 5.6 include the representation of magnet lags , magnet strut resonances and the notch filters required to compensate for the magnet strut resonances . These changes to the model account for a reduction in the predicted phase margin of approximately 40 degrees .

6.7 DISPLACEMENT LOOP DEVELOPMENT

6.7.1 Experiments

The outer loop suspension filter was modified as discussed in Chapter 5 . The low pass filter first order numerator term was varied and a set of measurements of OLR were taken with the relative damping coefficient set at 0.7%(red) , 7%(orange) , 12%(green) , 28%(purple) and 70%(blue) . A first order phase advance filter was used and the measurements are shown in Fig 6.27 . As with the simple theoretical model , it is not a simple task to select the optimum response . The 7%(blue) response produced the smallest resonant loop without producing changes at other frequencies .

Fig 6.28 shows the changes to the OLR caused by replacing the first order phase advance filter(red) by a second order filter(orange) that provides 65

degrees of phase advance . The coherence at 6 Hz for the quadratic filter measurement is low and measurement quality is poor (the OLT tends to unity) . It is clear that the extra phase advance was effective , and provided 20 degrees more phase advance in the OLR . Unfortunately the high frequency gain decreases much more slowly with the quadratic phase advance . This allows the gain increase of the second guideway mode at 18 Hz to destabilise the suspension .

The vehicle was repositioned so that the lift magnets were 1.0 metre onto the flexible guideway . On June 4th and 5th , the main loop filter frequency was changed to 1.66 Hz and OLRs were measured for a variety of phase advance characteristics . These measurements are plotted in Fig 6.29 .

Phase advance of filter (degrees)	Plot colour
41	red
65	green
80	orange
100	purple

Neither the most heavily damped nor the most lightly damped phase advance characteristic produces the best OLR . The largest phase advance (purple) has a healthy phase margin of 17 degrees , but gain falls off very slowly above 6 Hz . The smallest phase advance (red) has a negative phase margin but high frequency gain falls away at a desirable rate .

On June 6th , the last day available for test work , a series of OLRs were measured with outer loop filter frequencies of 1.33 Hz(orange) , 1.66 Hz (green)and 2.0 Hz(red) . These OLRs appear in Fig 6.30 . It can be seen that , as predicted in chapter 5 , the size of the resonant loop on the OLR characteristic is directly related to the filter frequency and a low filter frequency is an advantage for system stability . It was not possible to test with a 1.0 Hz filter because the system was not stable , this was believed to be due to coupling between the complementary filter characteristic and the absolute position filter characteristic .

6.7.2 A Summary of Displacement Loop Development

The modifications to the displacement loop controller worked much as predicted in Chapter 5 . However , practical problems limited the scope of the work . Most notable was the increased phase lag of the experimental system in comparison to the predictions of Chapter 5 . Fig 6.06 compares measurement in red with the prediction in blue , at 10 Hz there is a phase difference of 40 degrees . This phase difference has two equal components , inner loop hysterisis and the effect of magnet strut resonance and the compensating notch filters .

These effects meant that experimental work on the flexible guideway was always undertaken with the

system only marginally stable . This made it difficult to measure accurate OLRs , as discussed in 6.6.3 . As a consequence of this , the effect of filter numerator changes is difficult to assess , although there does seem to be a benefit with a small first order numerator term .

The effect of increased phase advance was discussed in Chapter 5 . The experimental work shows that increased phase advance can be generated and does aid stability with regard to the first guideway flexible mode . The price of increased phase advance is an increase in high frequency gain . Because of the very small phase margin of this particular vehicle , an increased high frequency gain allows higher frequency guideway modes to destabilise the suspension .

The use of a second order phase advance filter with modest phase advance (50 degrees) is best for this vehicle . It provides more phase advance than the first order filter (40 degrees) with a lower gain at high frequency . This is unlikely to be the best compromise in other vehicles that might well have higher phase margins .

6.8 CONCLUSIONS

The experimental work had some success , notably the demonstration that the magnet control technique

works sufficiently well for a vehicle suspension . Unfortunately the experimental difficulties with this particular vehicle in combination with the reduced timescale for experimental work meant that success was rather limited . The experimental work did reach a stage where the original ideas had been tested , problems were discovered , analysed and understood . The original project plan had allowances for this , there would have been both time and cash to attempt to correct the problems and , perhaps , to demonstrate a vehicle working on the flexible guideway . Sadly , government policy towards funding work of this nature changed rather quickly .

It would have been desirable to replace the gap transducers , provide a full set of choppers , fit low hysterisis magnet cores and redesign a stiffer magnet strut . Instead the vehicle was made to work under a very limited set of circumstances . An accurate vehicle model was determined , all the problems were understood and performance predictions for future vehicles can be made , with some confidence .

6.9 REFERENCES

6.1 Goodall . BR Magnetically Suspended Vehicle - A Description of the Design , Commissioning and Testing . TREDYN 8 March 1977 .

6.2 Redfern . Re-commissioning of the Maglev Test Vehicle . IMDOS 119 . Feb 83

TABLES

Each row of these tables defines an element of a control circuit diagram . The first two numbers define the particular block within the diagram (see the relevant Figure) , the following six numbers define the behaviour of that block . As described in Chapter 2 , each block is a rational polynomial with third order numerator and denominator . Thus the last six numbers define the numerator and denominator respectively .

TABLE 6.1

Changes to the model in Fig 5.6 to represent magnet lags .

2,3 30,0,0,1,1E-3,0	Power Amplifier
4,1 -.2,0,0,1,2e-4,0	Current Transducer
4,5 .025,0,0,1,6E-3,0	Magnet Hysterisis
5,3 0,-.338,-2E-3,.025,0,0	Magnet Hysterisis and Mutual Inductance

TABLE 6.2

Further changes to the model in Fig 5.6 to form the model in Fig 6.19

NB the HP-LP suspension filter in Fig 5.6 is changed to the LP form only .

```
        7,15    1,3.1E-4,0,1,3.1E-4,6.27E-5    Magnet
Strut Resonance
        15,18   1,1.38E-4,0,1,1.38E-4,4.79E-5 Magnet
Strut Resonance
        10,11   0,.201,0,1,.171,.107           Absolute
Position Filter Part 1
        11,12   1,0,0,1,1.88,0                 Absolute
Position Filter Part 2
        12,16   1,0,6.27E-5,1,1.58E-3,6.27E-5 Notch
Filter
        16,17   1,0,4.79E-5,1,6.92E-4,4.79E-5 Notch
Filter
```

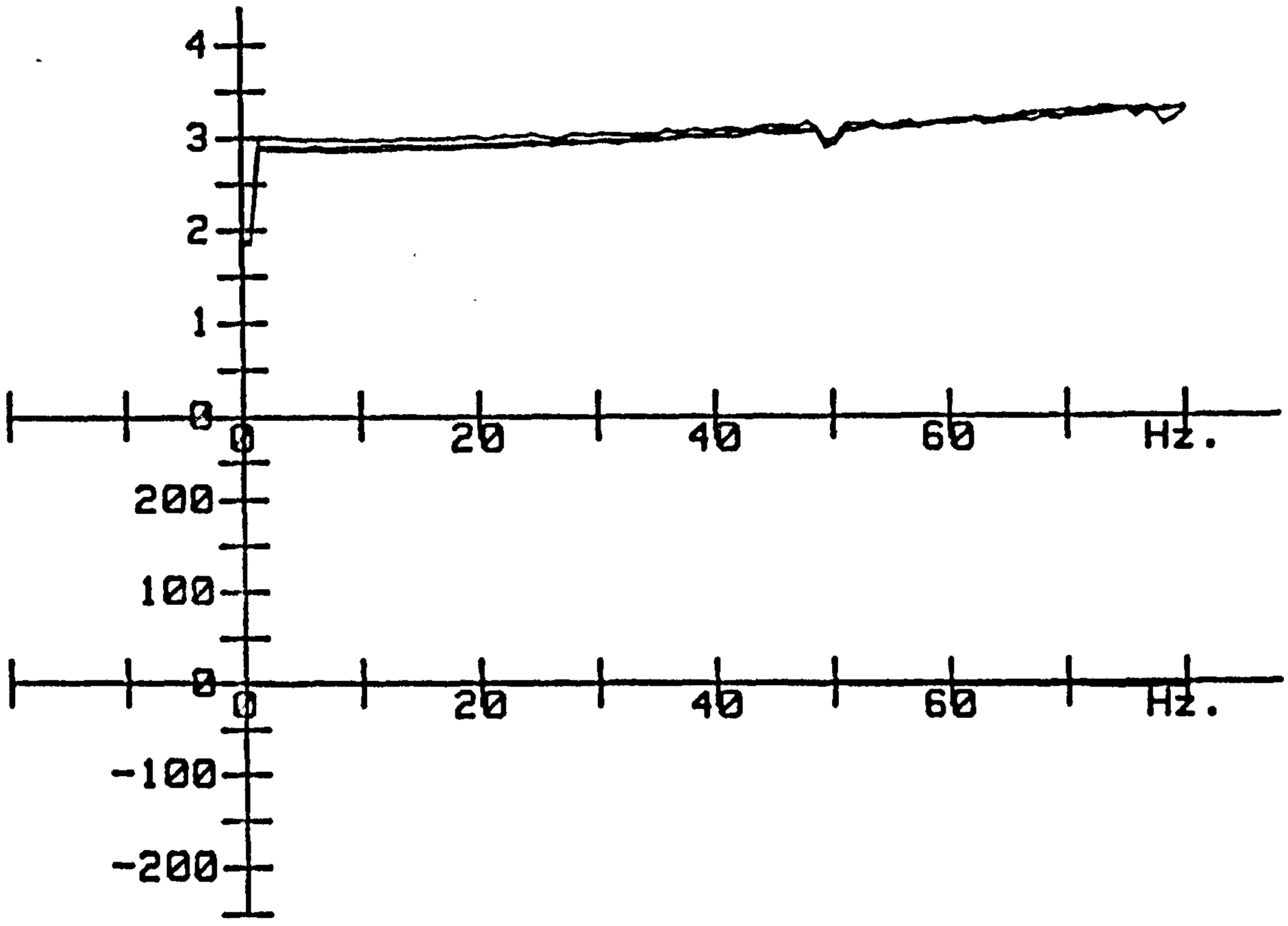

FIG 6.01 HEME RESPONSES

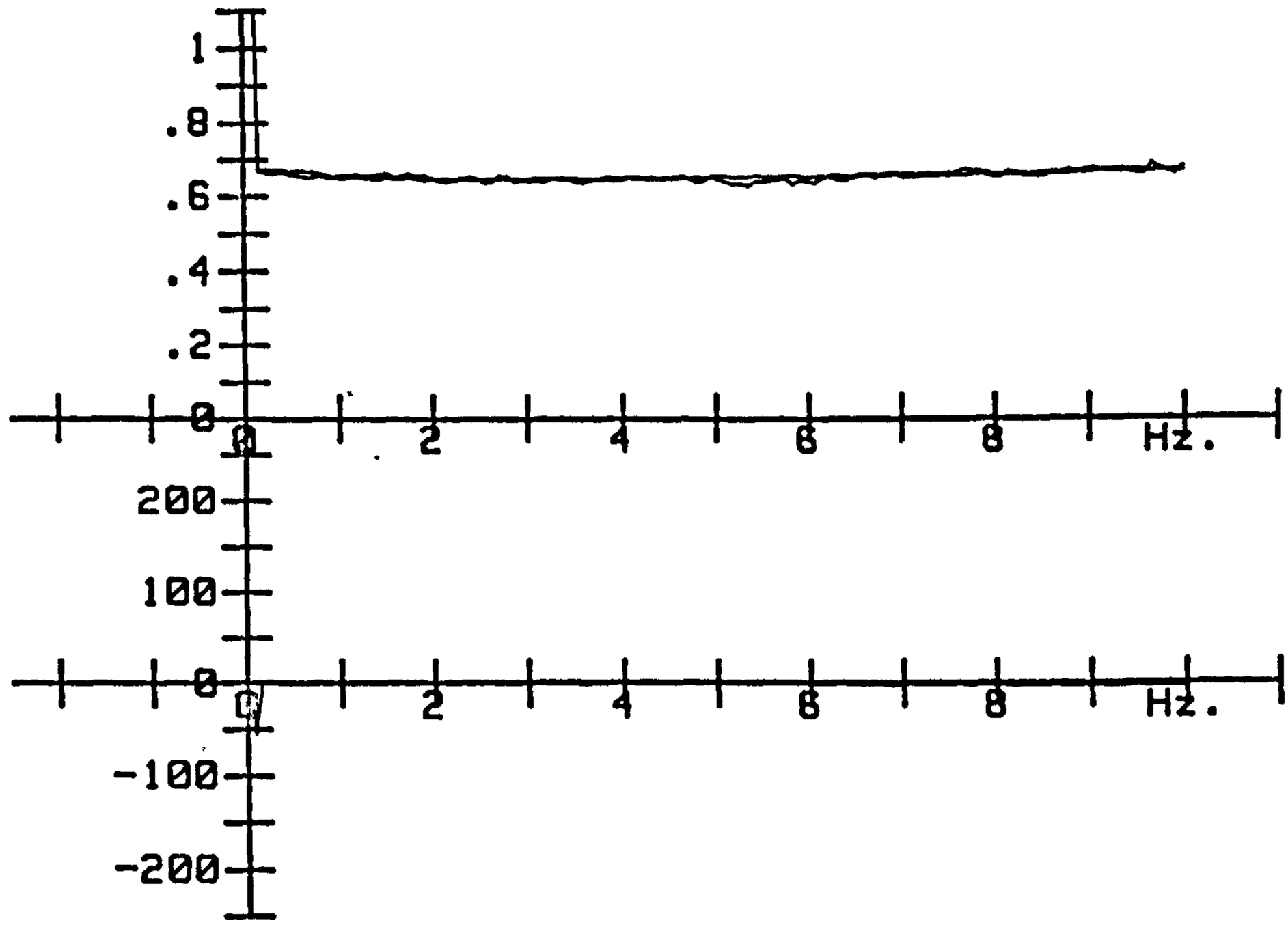

FIG 6.02 CHOPPER CURRENTS

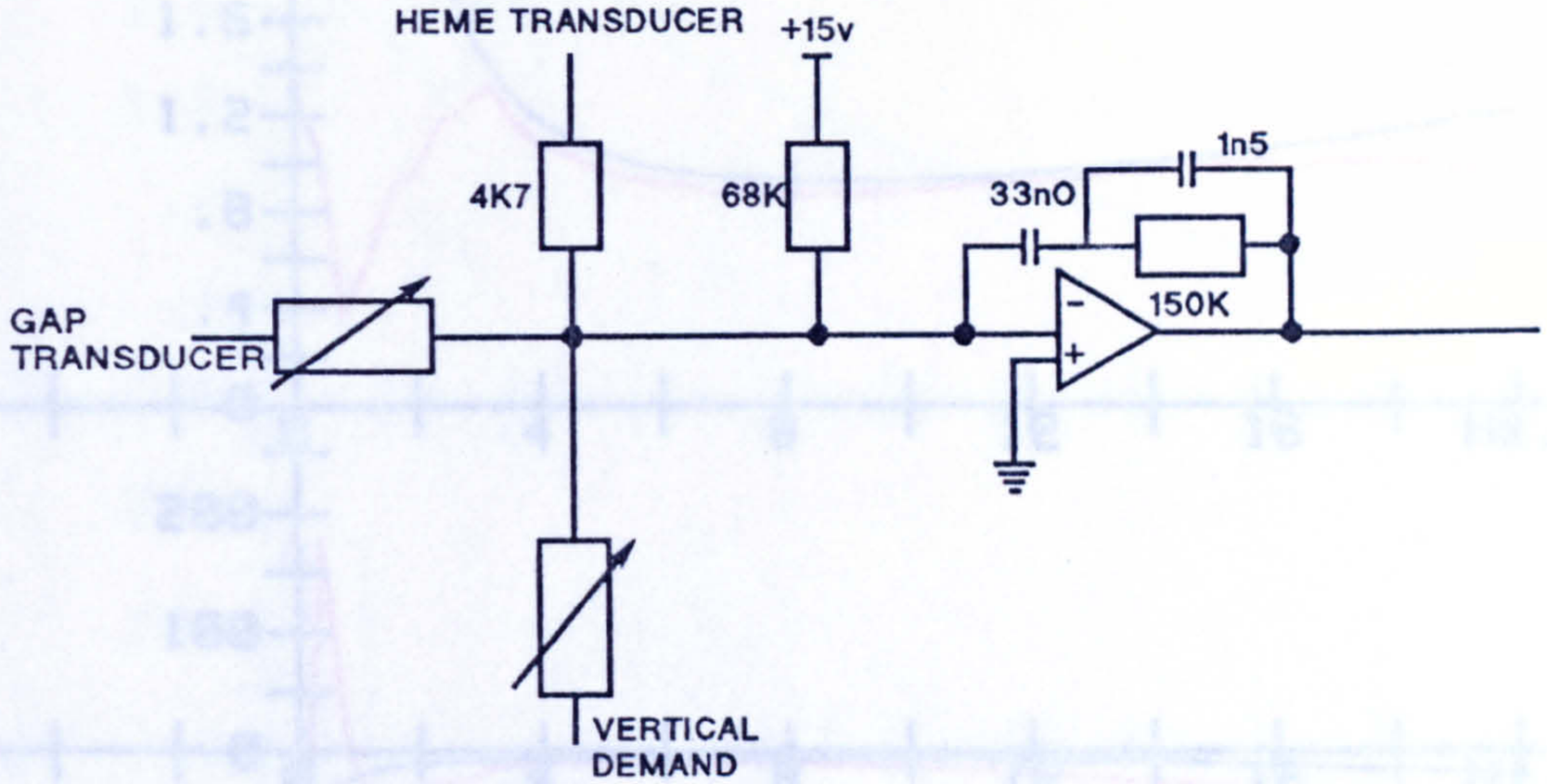

FIG. 6.03. CIRCUIT DIAGRAM FOR A MAGNET CONTROL BOARD

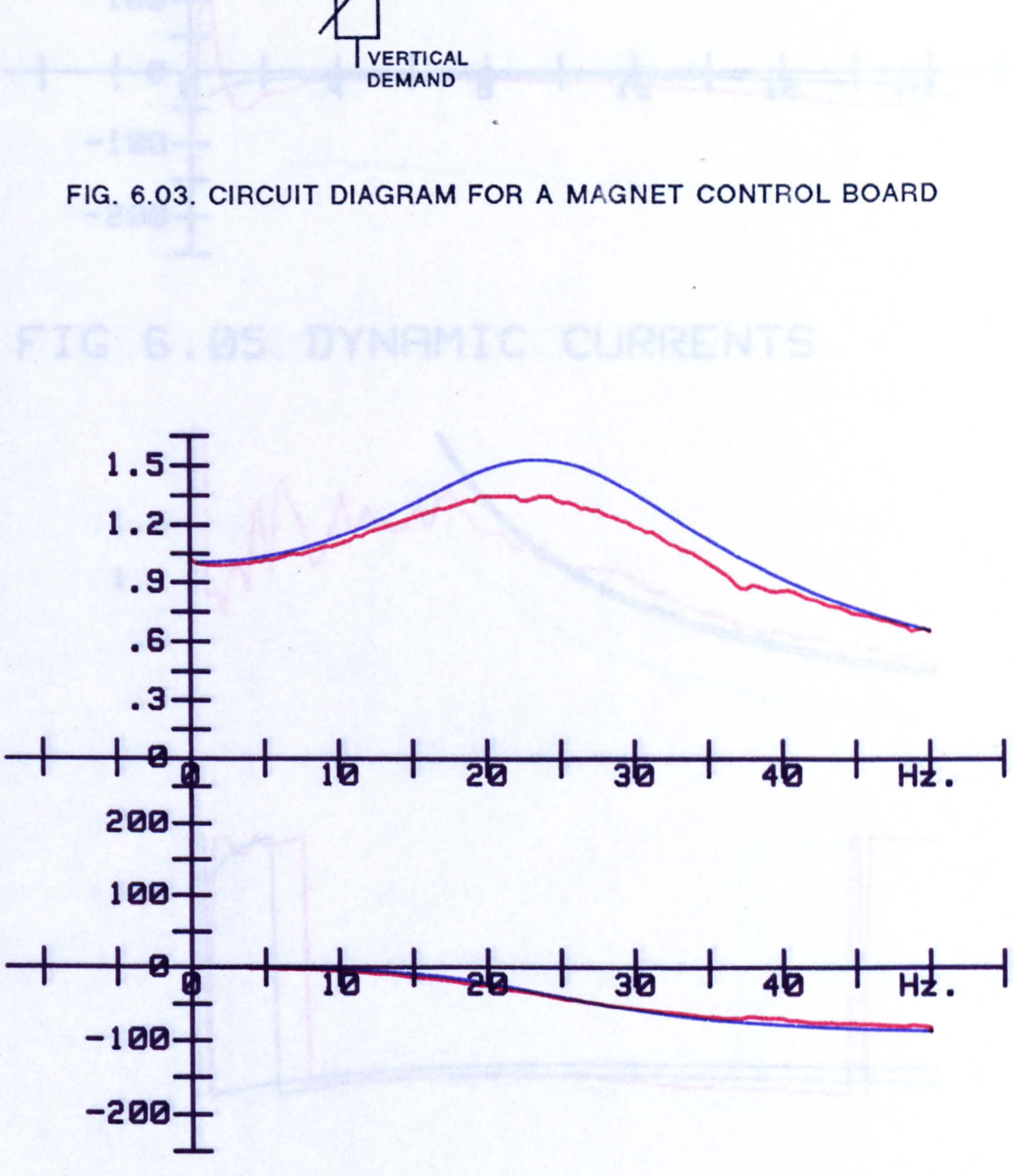

FIG 6.04 STATIC CURRENT

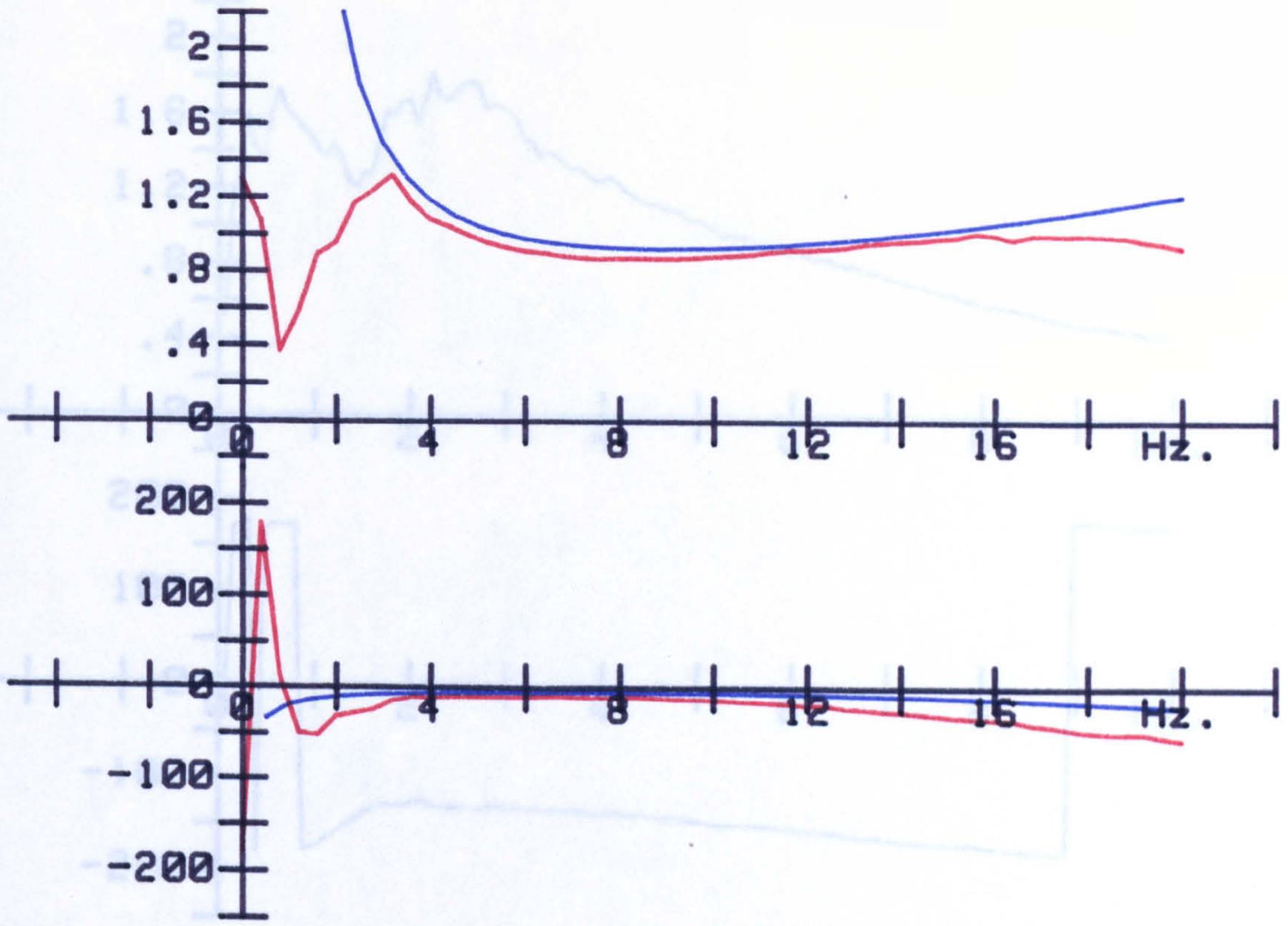

FIG 6.05 DYNAMIC CURRENTS

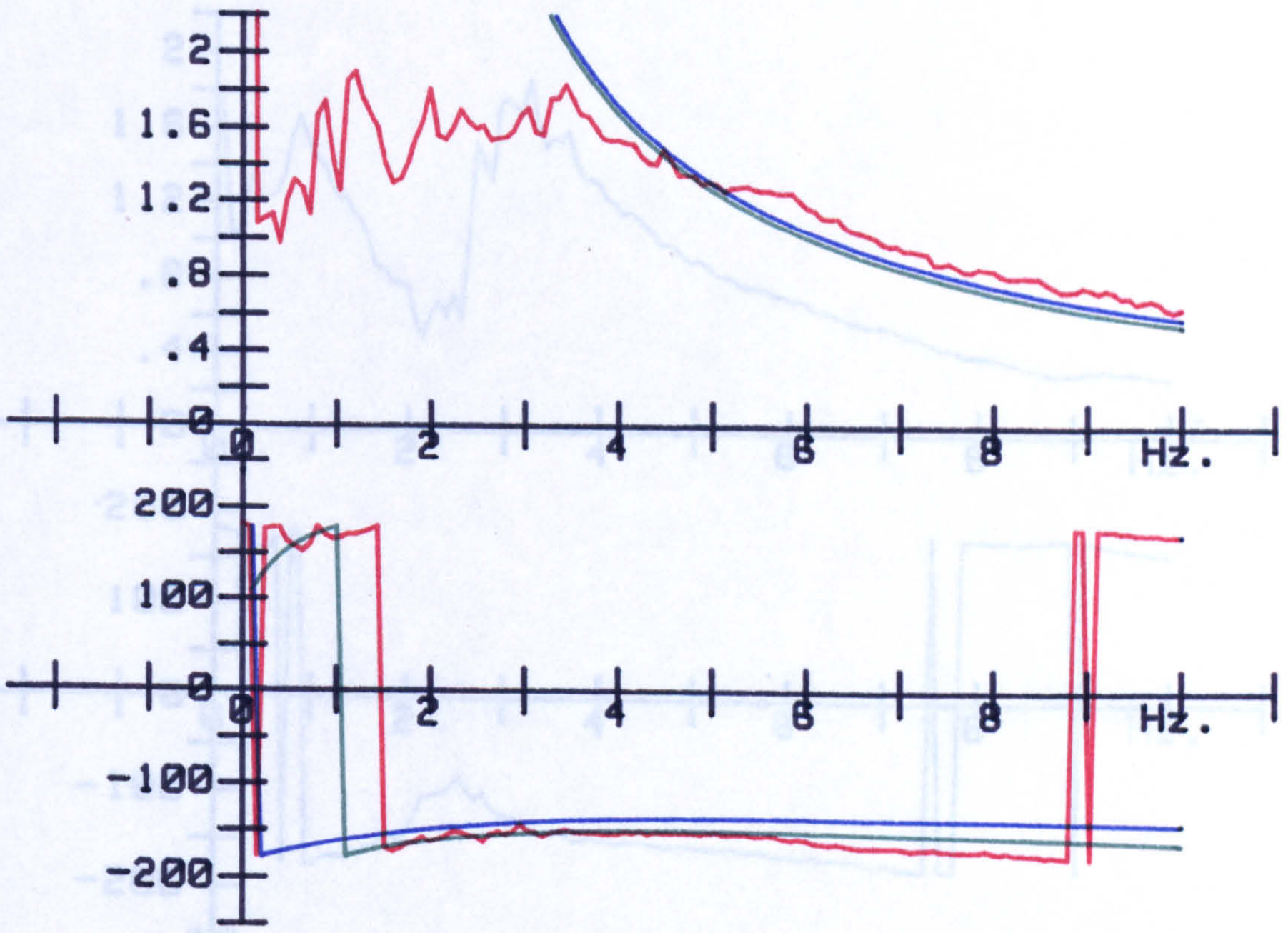

FIG 6.06 BOUNCE OLRs

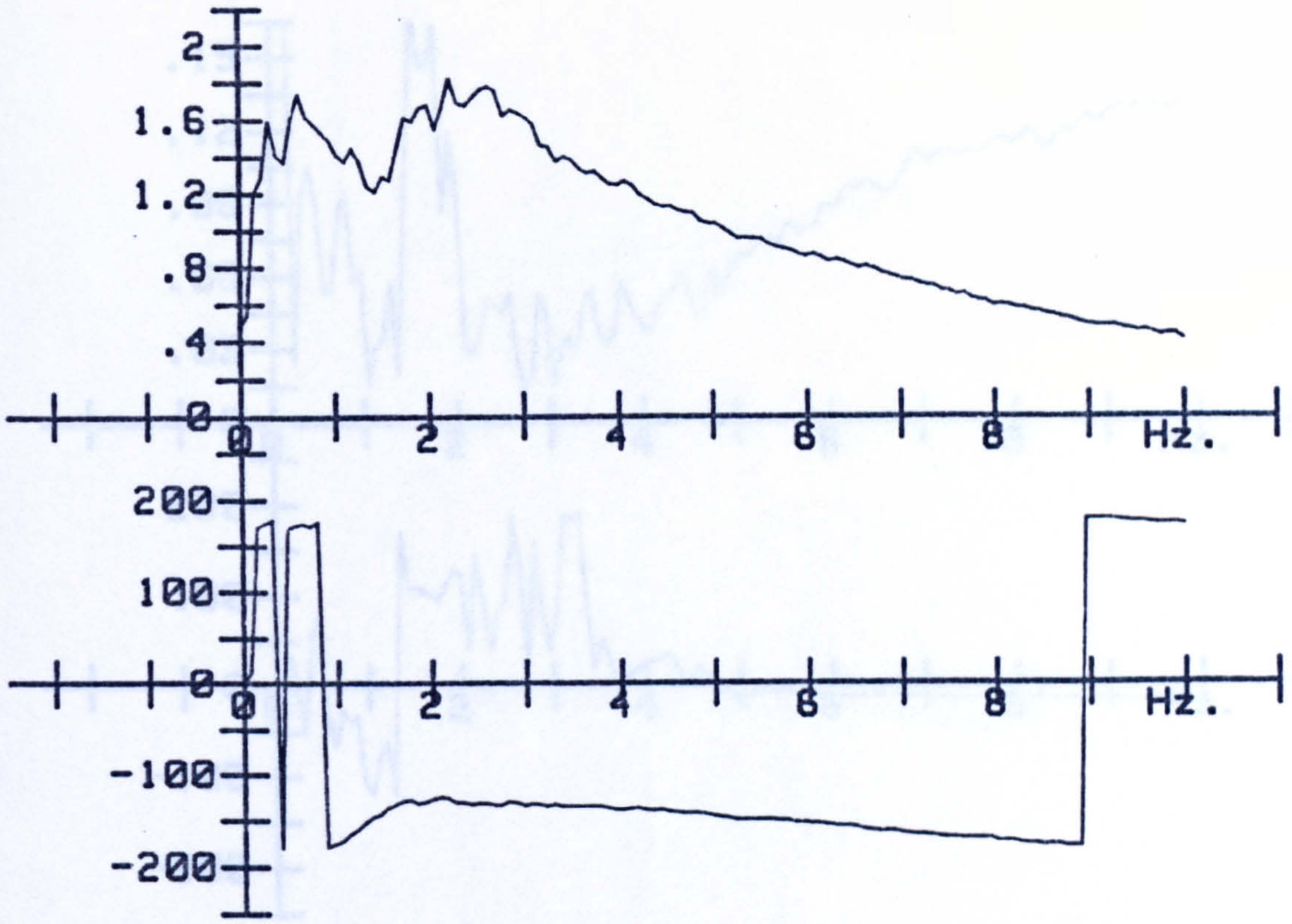

FIG 6.07 PITCH OLR

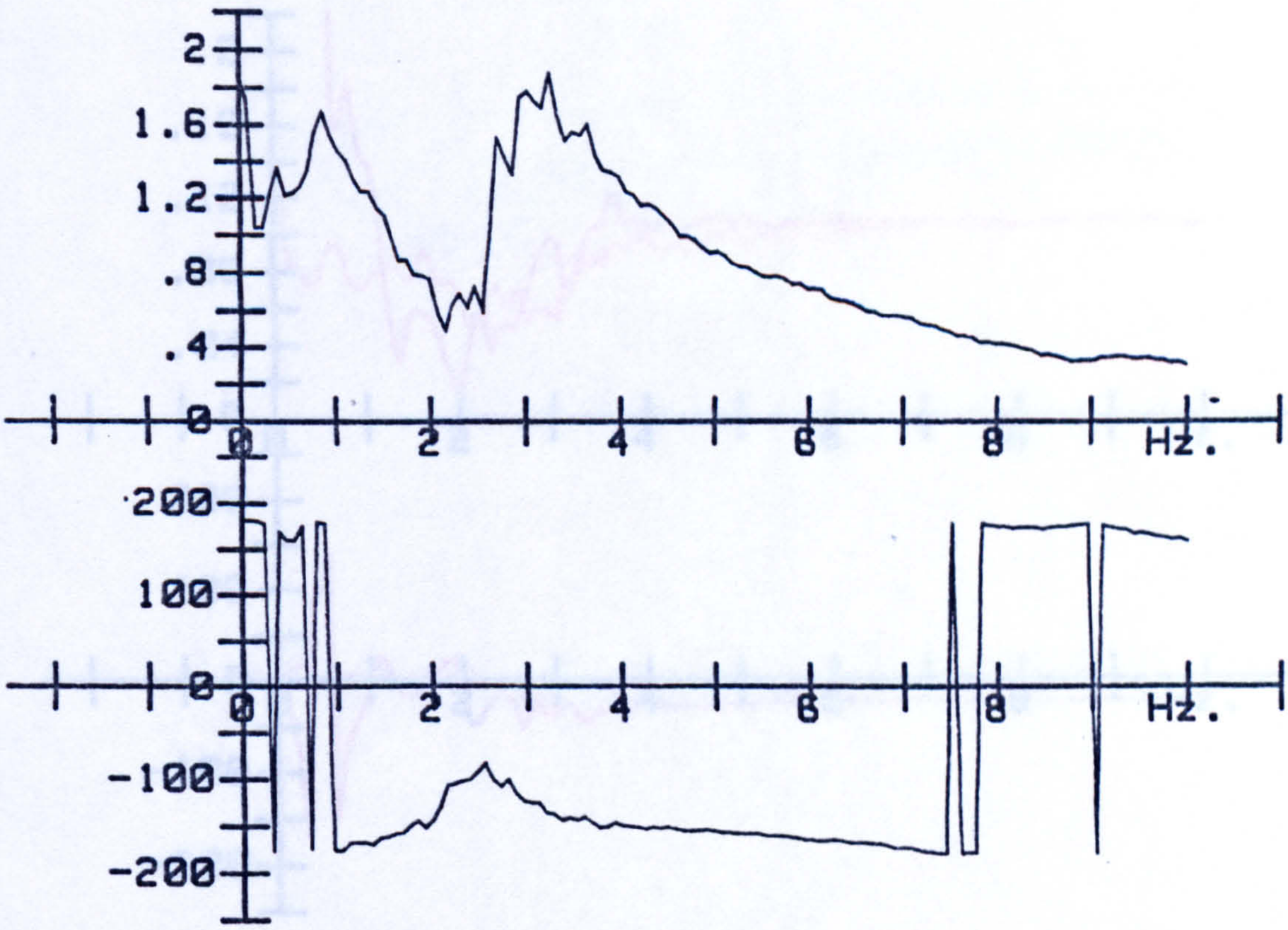

FIG 6.08 ROLL OLR

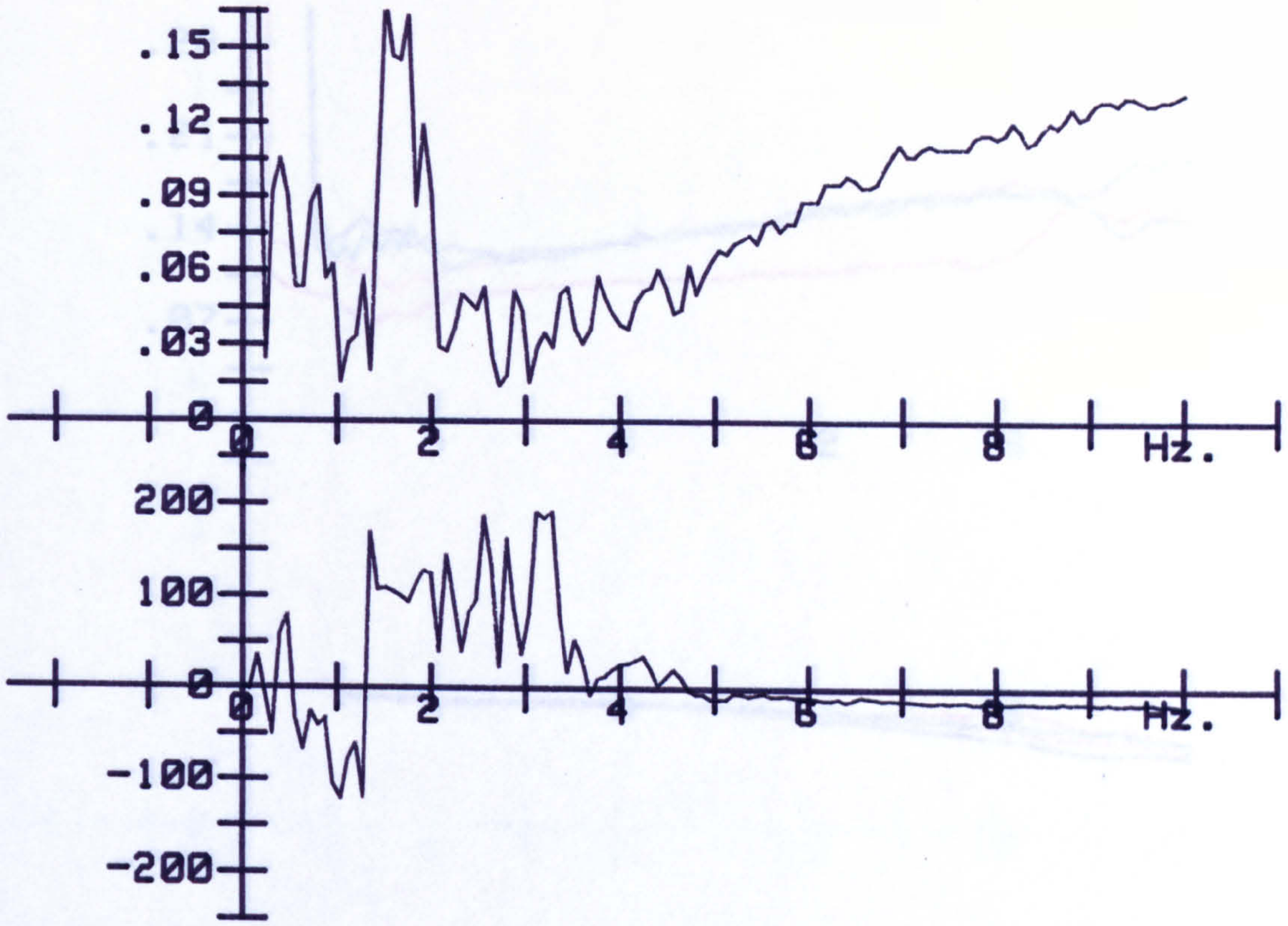

FIG 6.09 FLUX RESPONSE

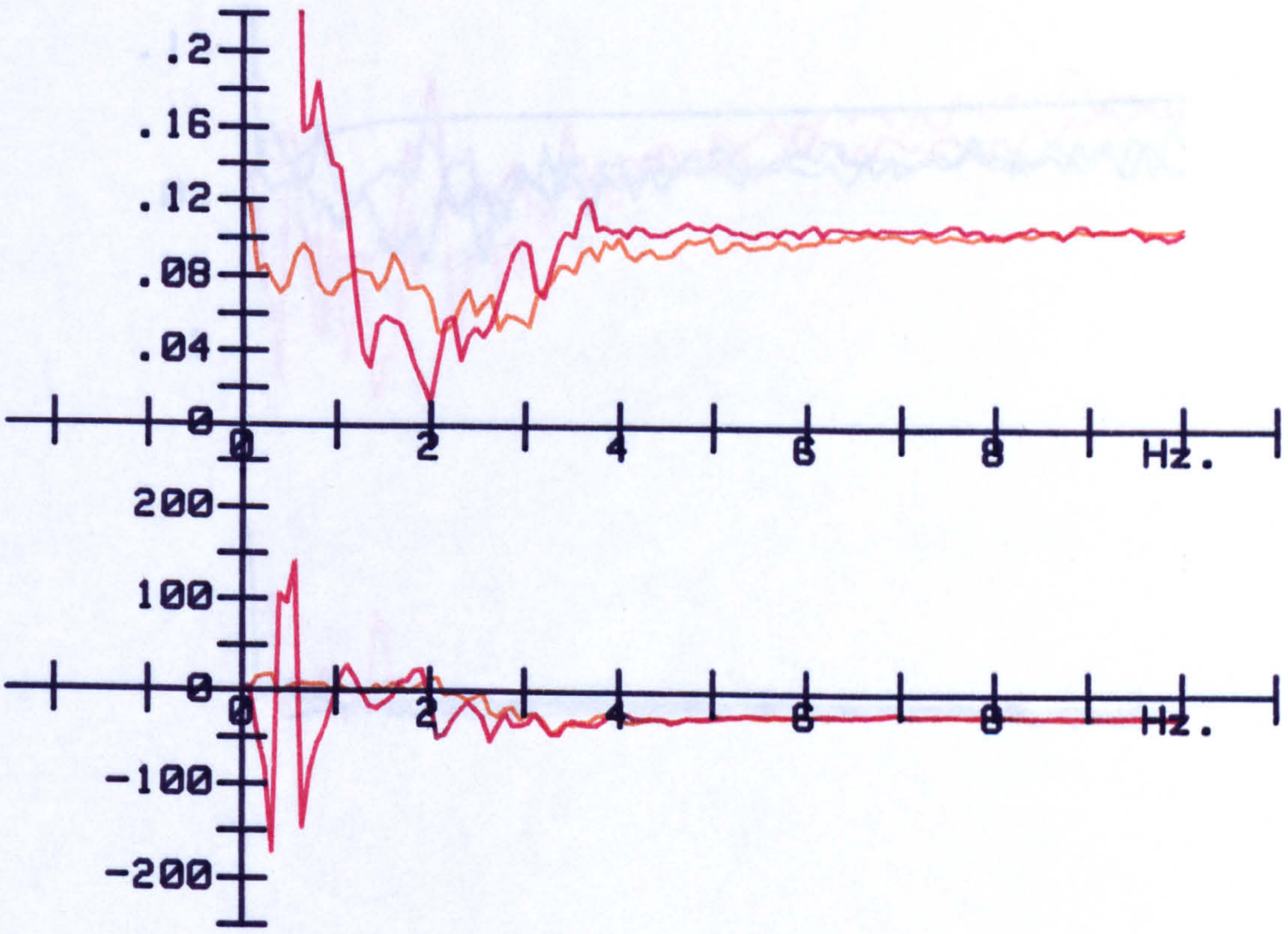

FIG 6.10 FLUX OPTIMISATION

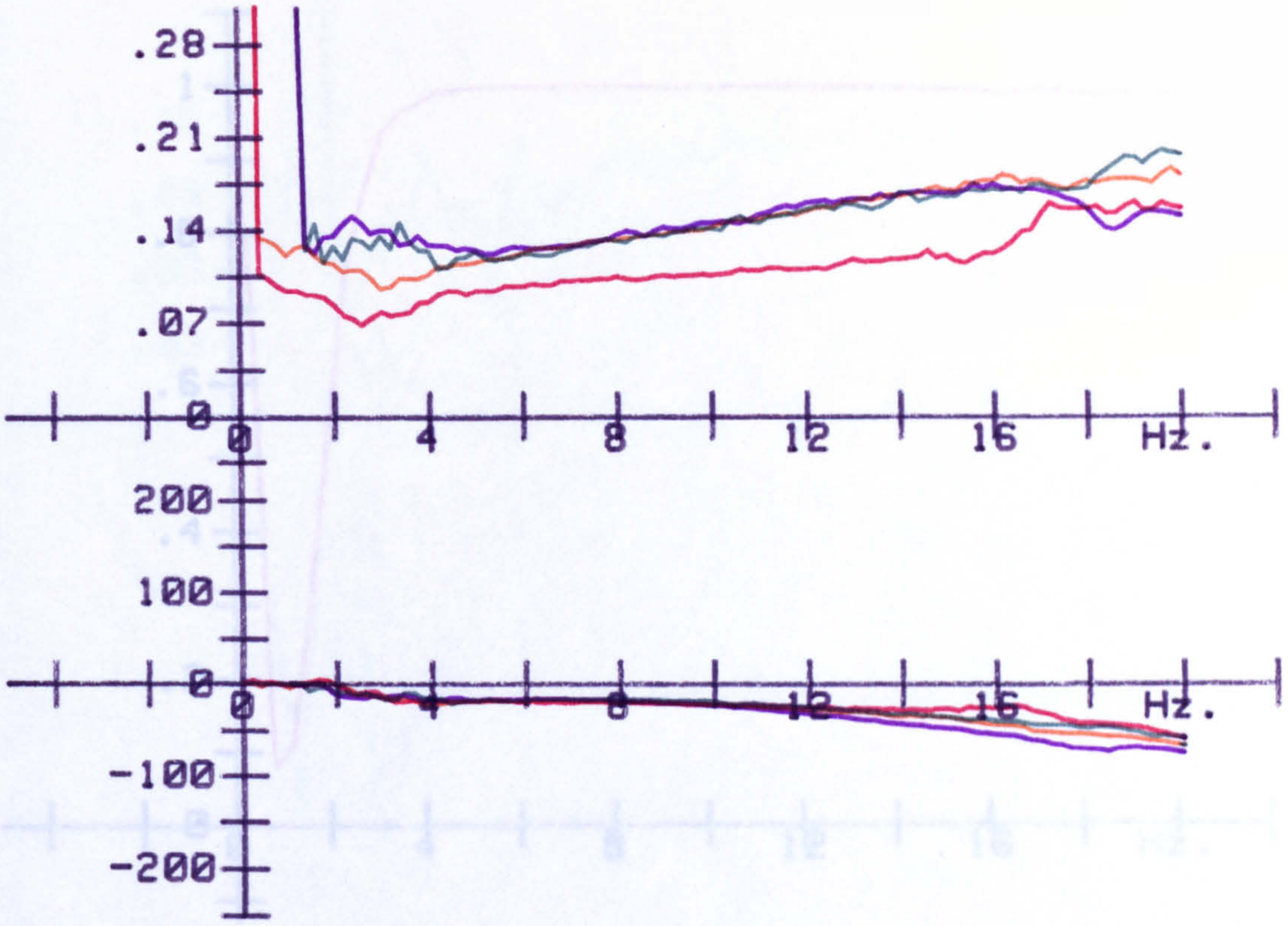

FIG 6.11 MAGNET RESPONSES

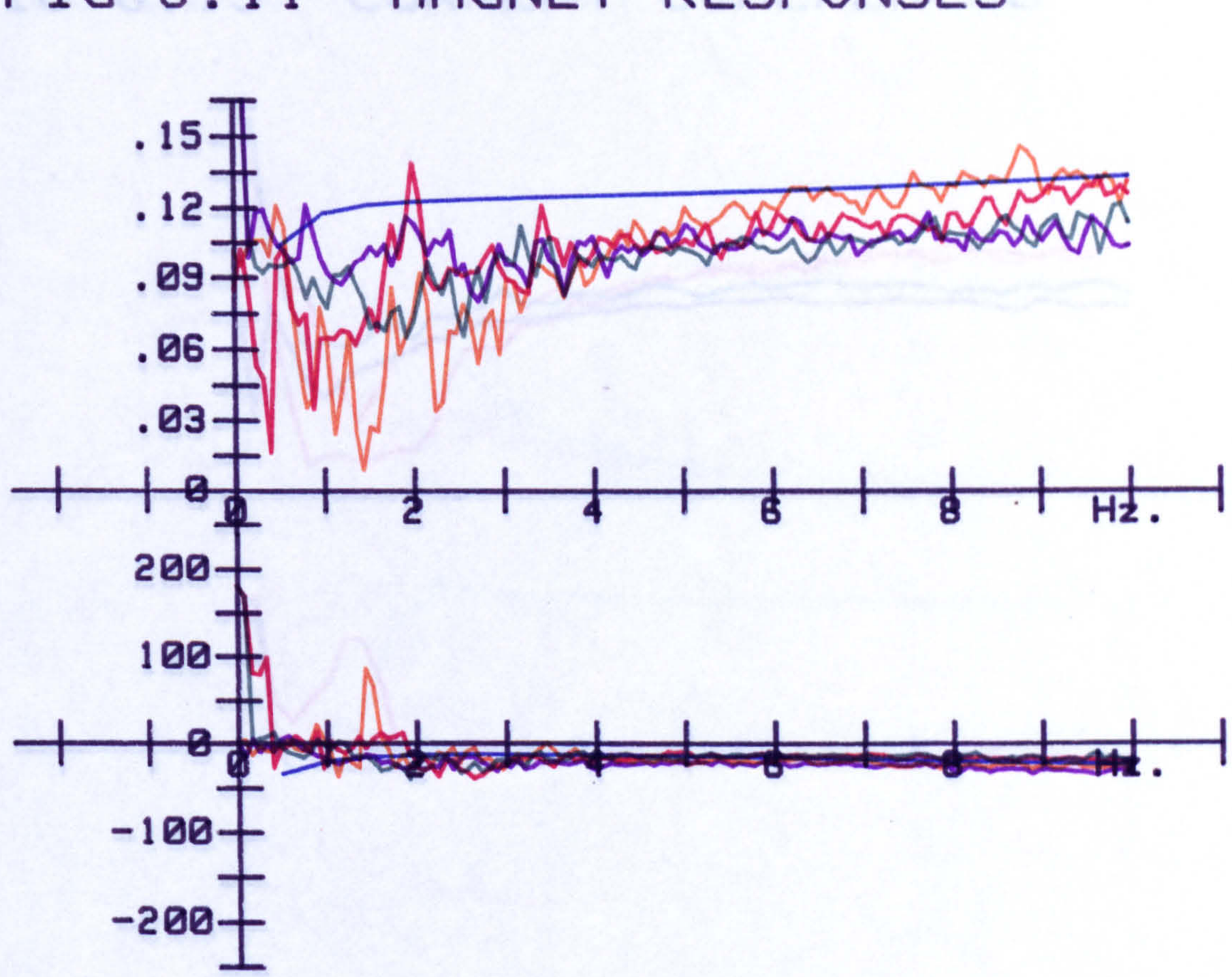

FIG 6.12 MAGNET RESPONSES

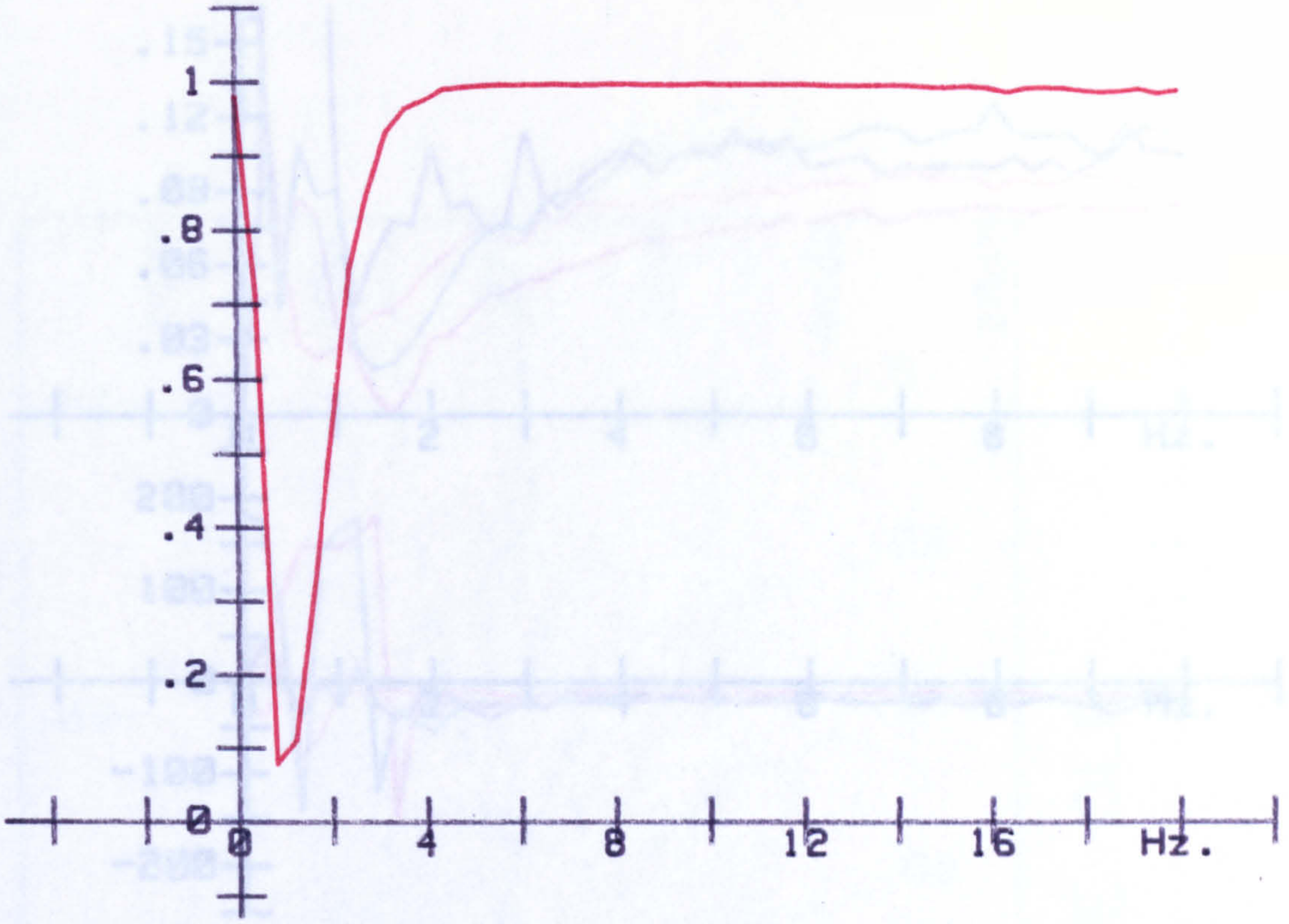

FIG 6.13 CURRENT COHERENCES

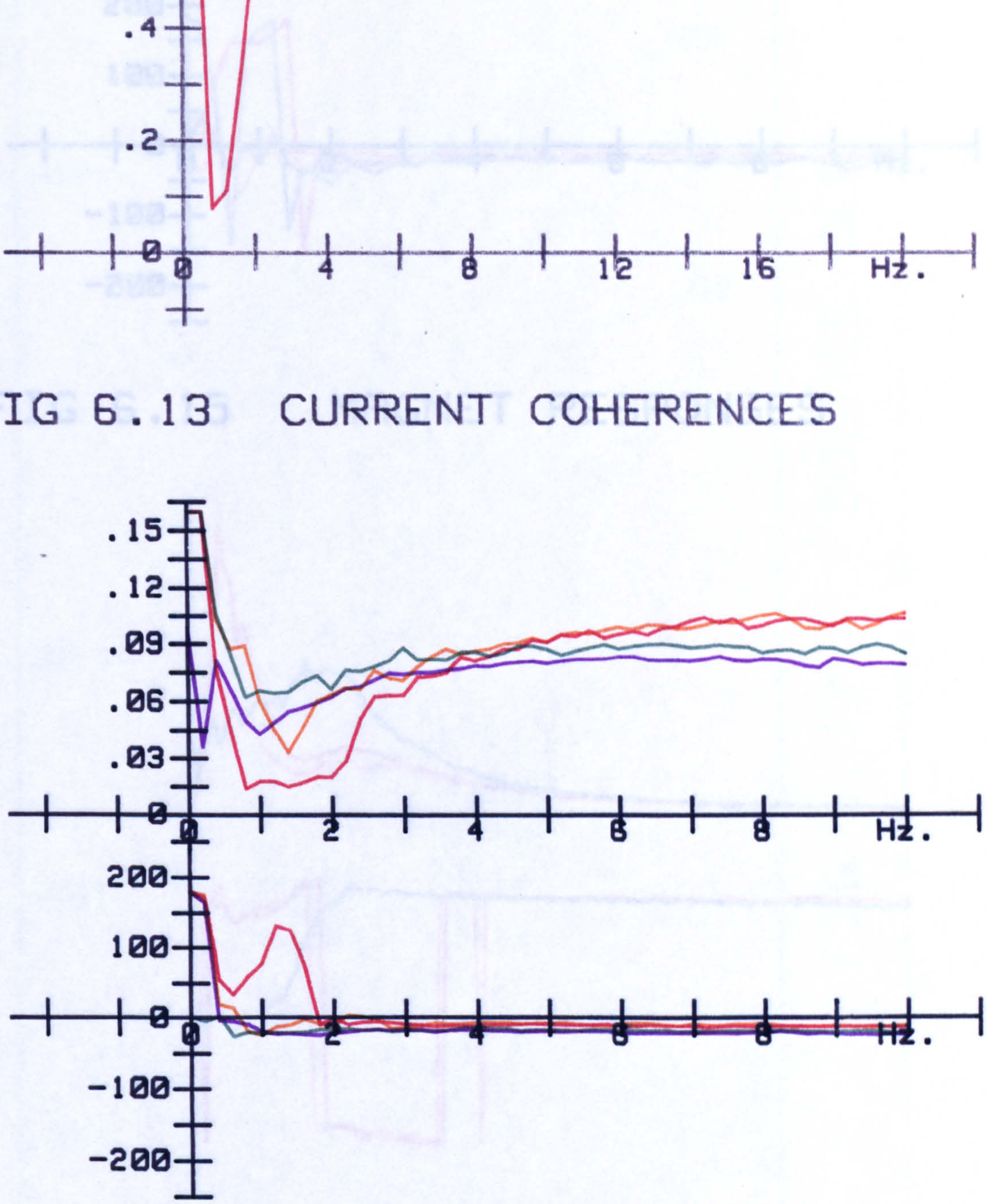

FIG 6.14 MAGNET RESPONSES

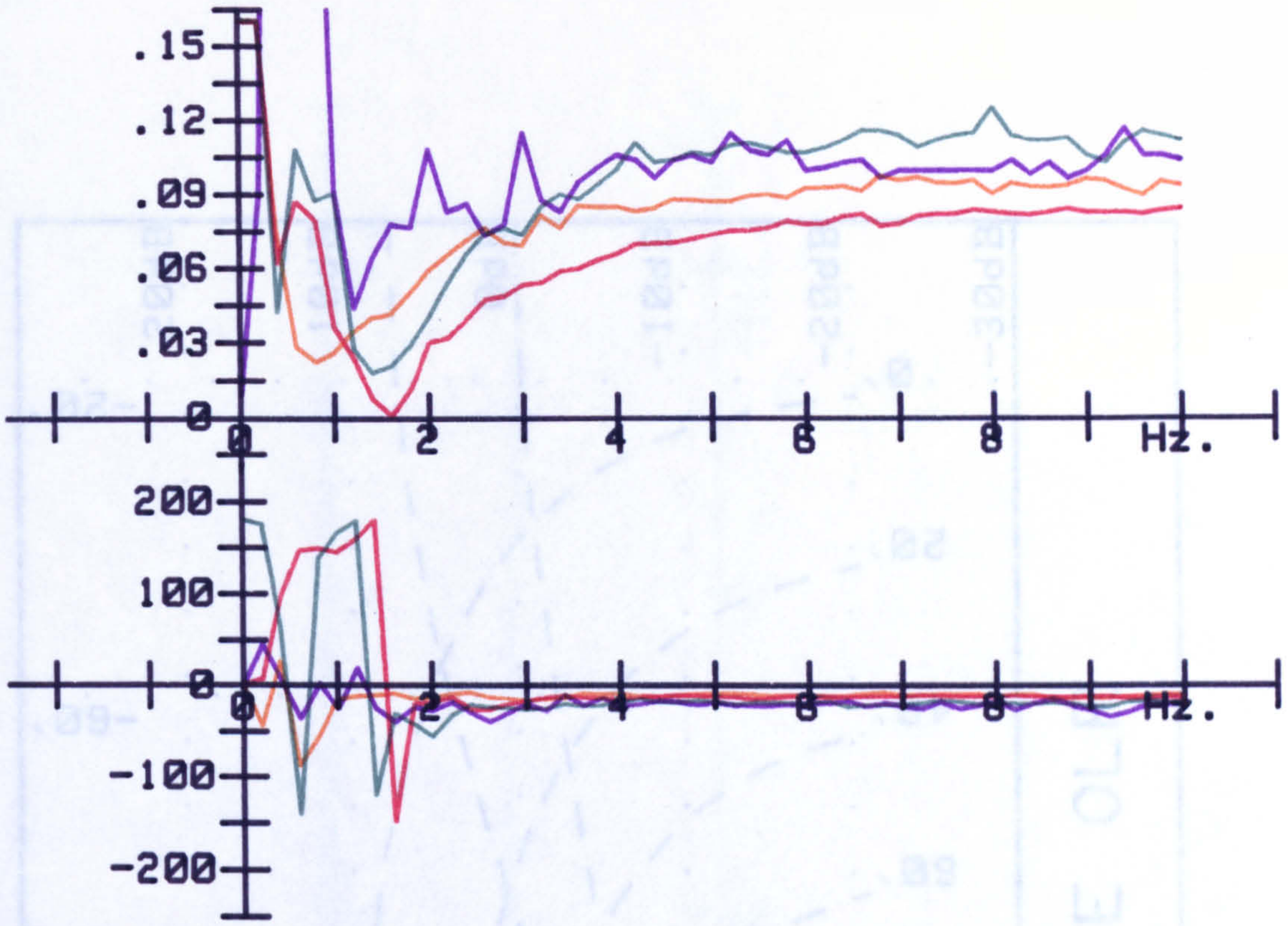

FIG 6.15 MAGNET RESPONSES

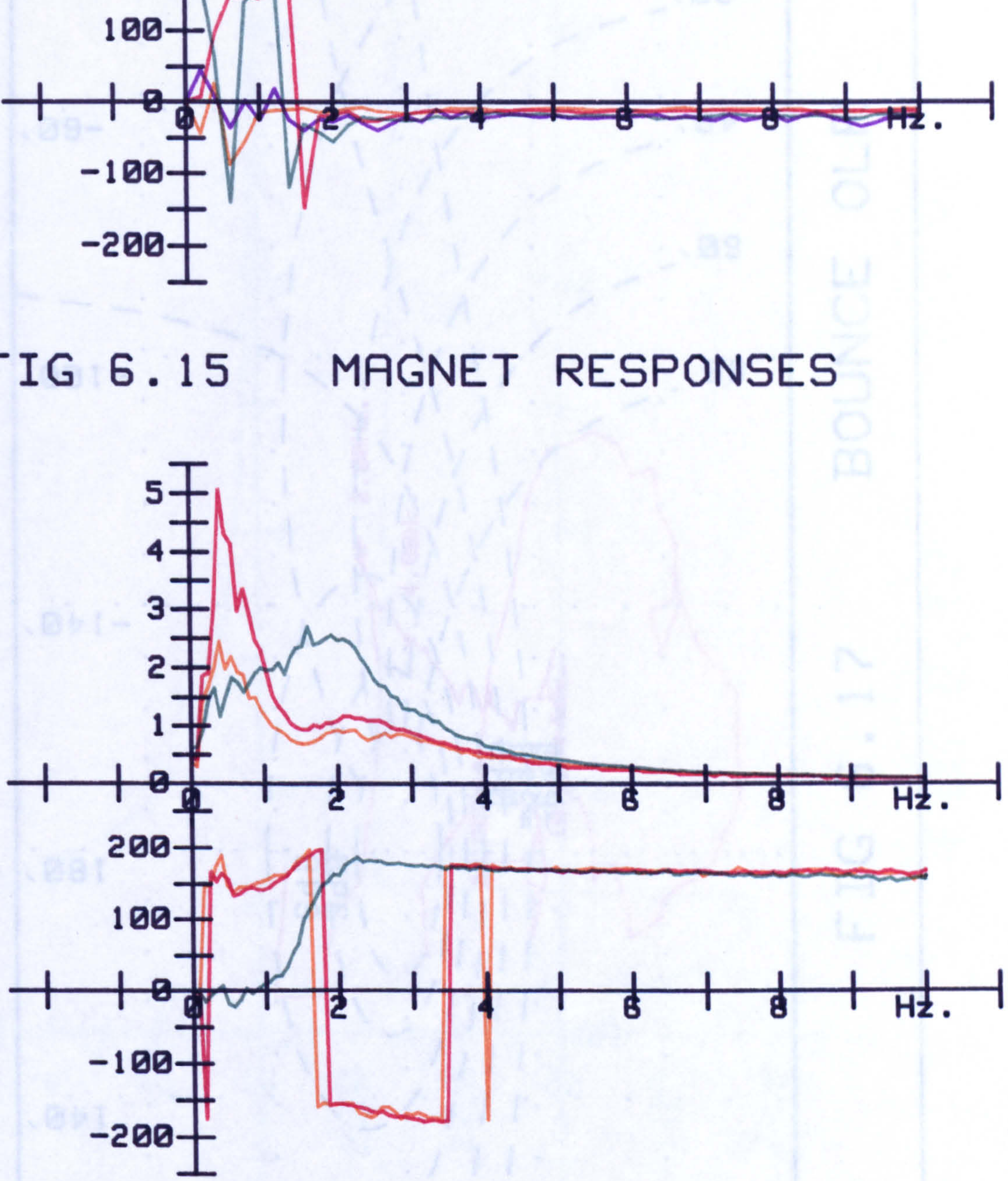

FIG 6.16 QOLRs

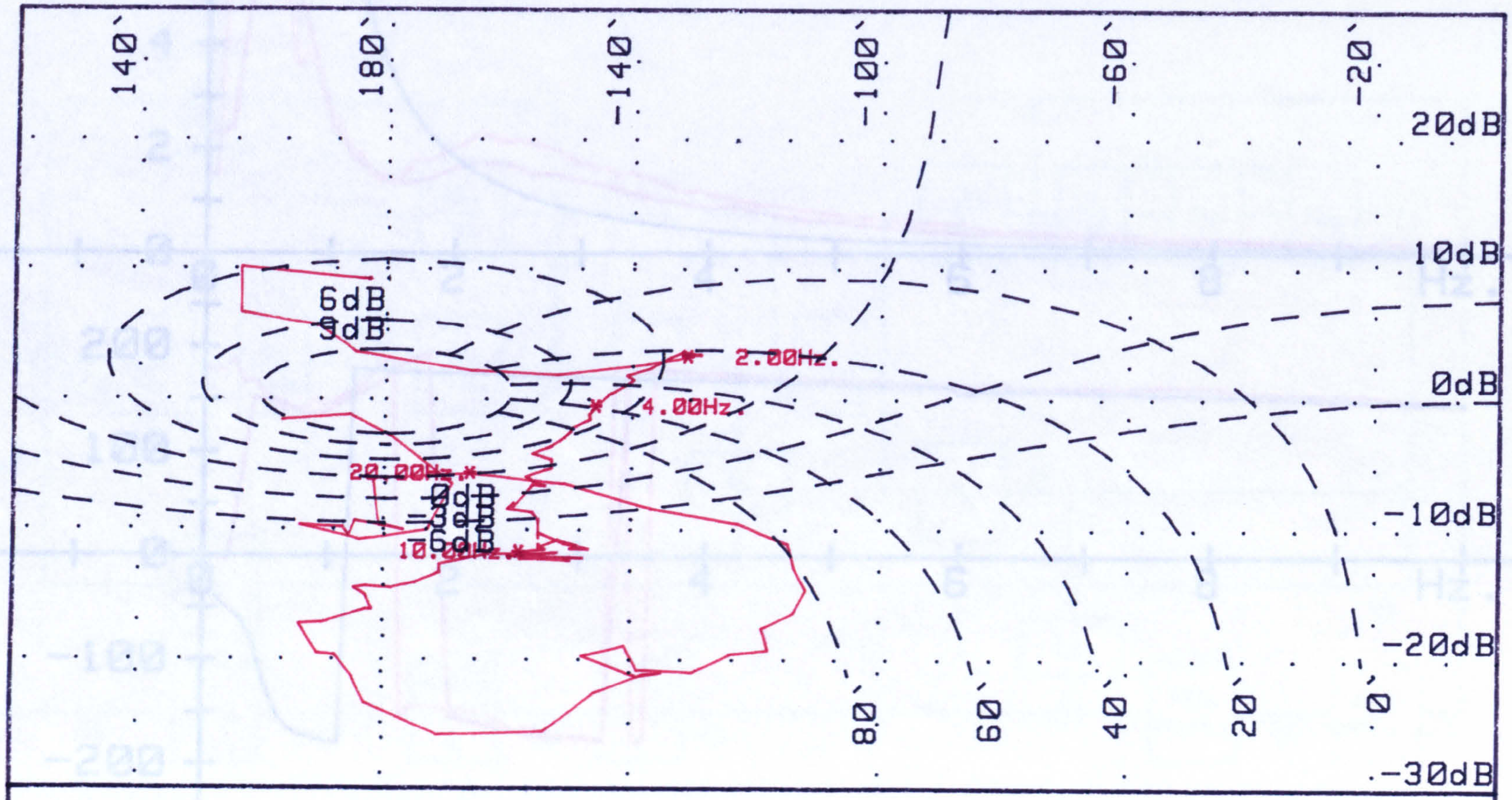

FIG 6.17 BOUNCE OLR

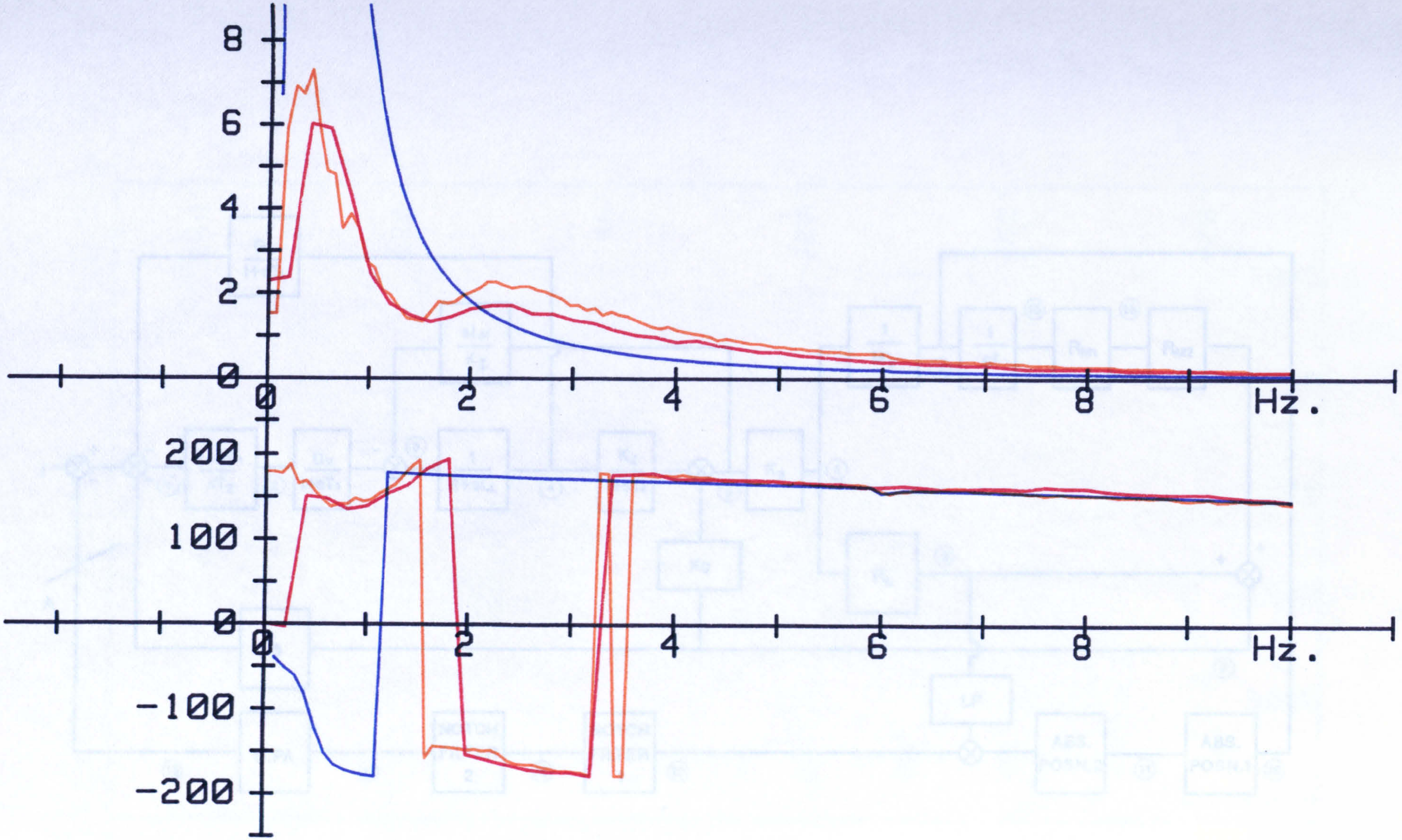

FIG 6.18 QOLRs

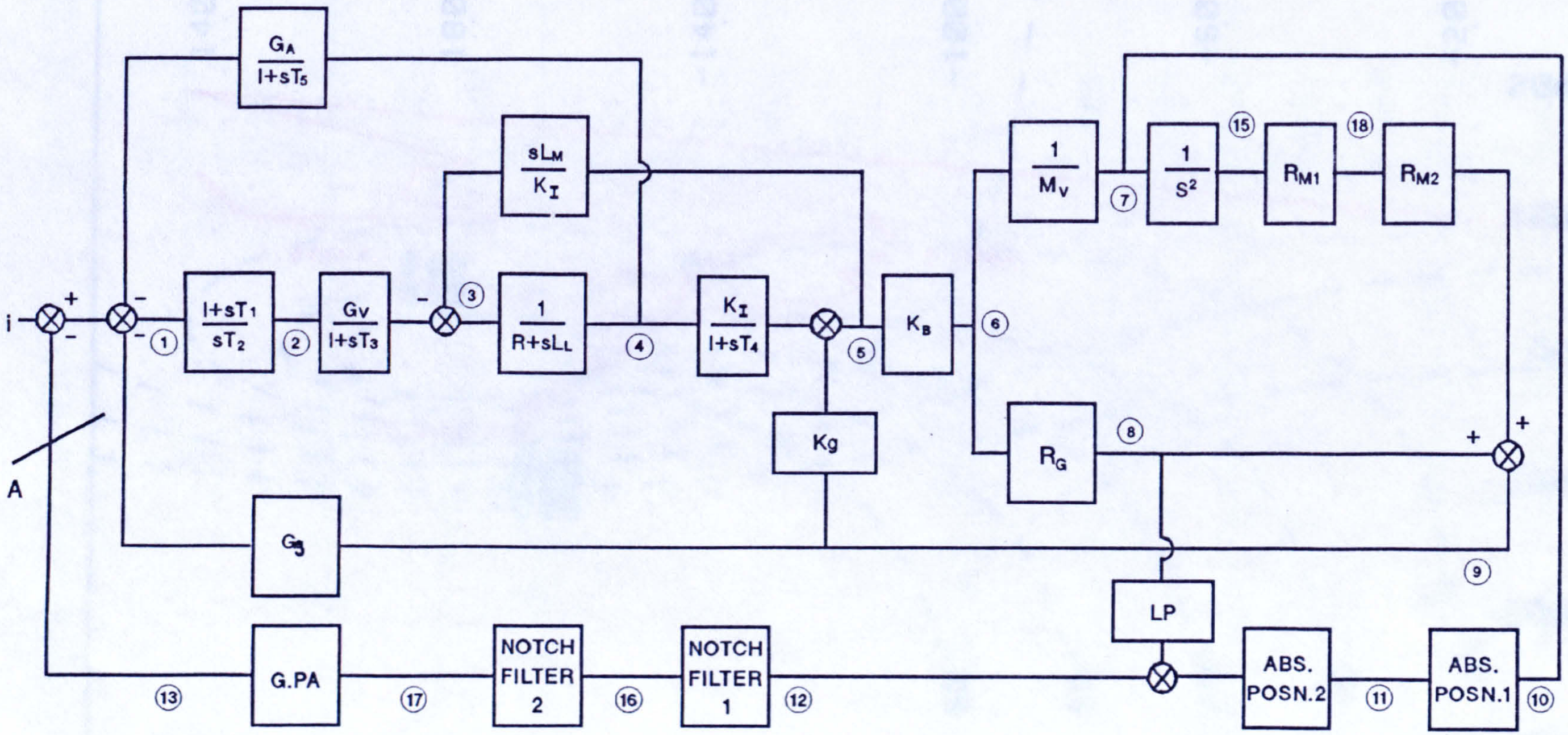

FIG. 6.19. MODEL WITH MAGNET RESONANCES AND NOTCH FILTERS

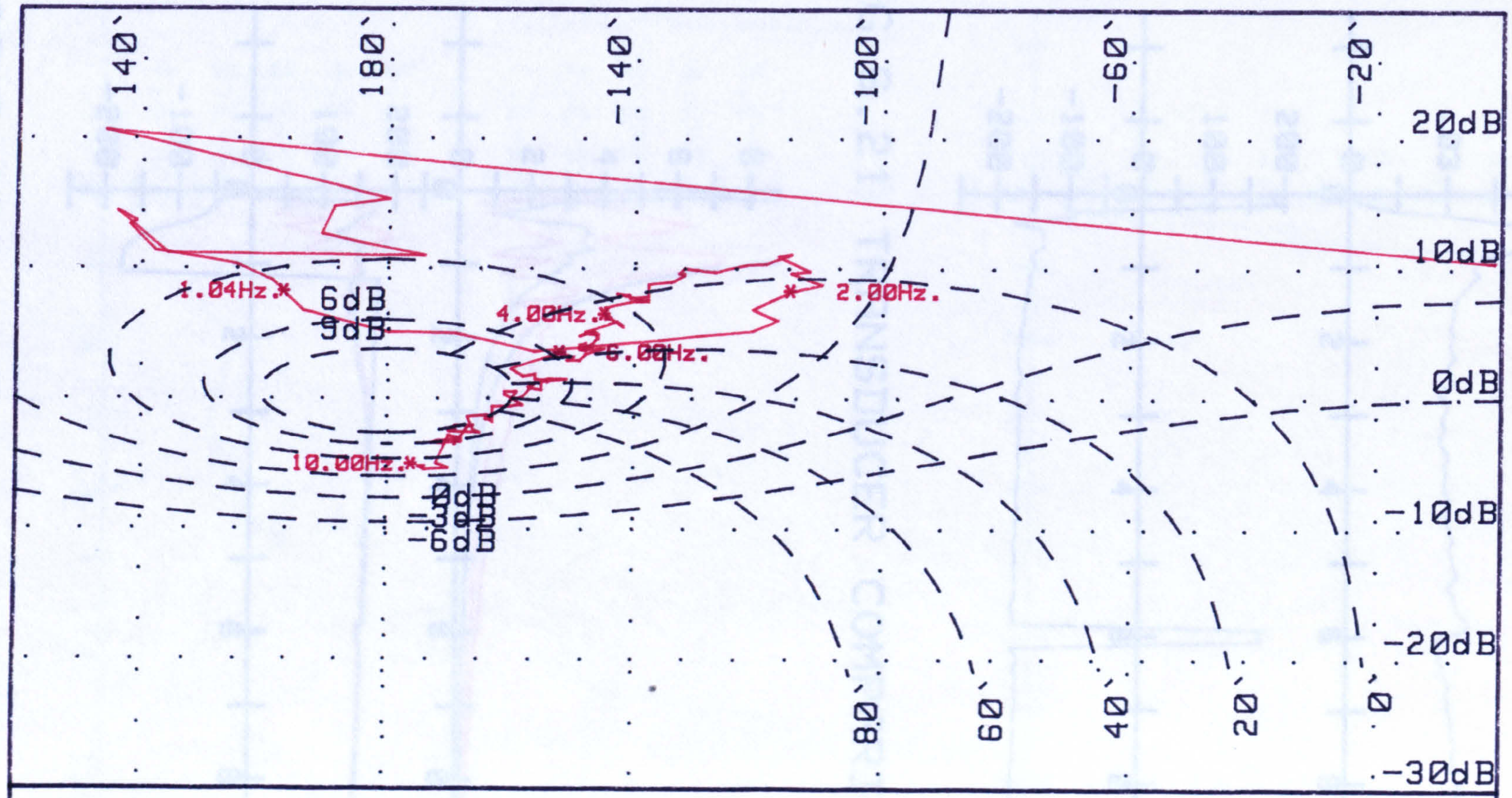

FIG 6.20 FLEXIBLE GUIDEWAY OLR

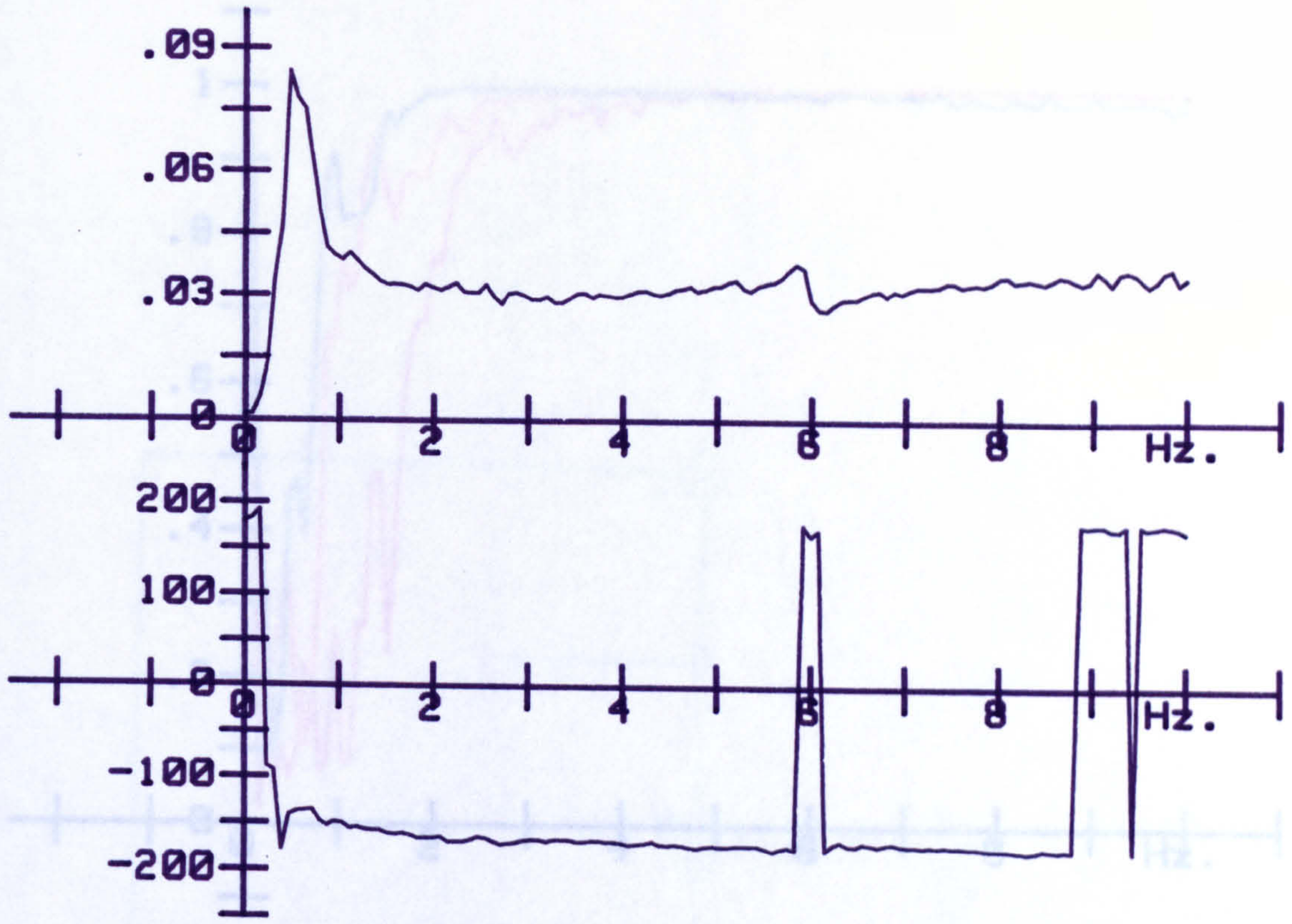

FIG 6.21 TRANSDUCER COMPARISON

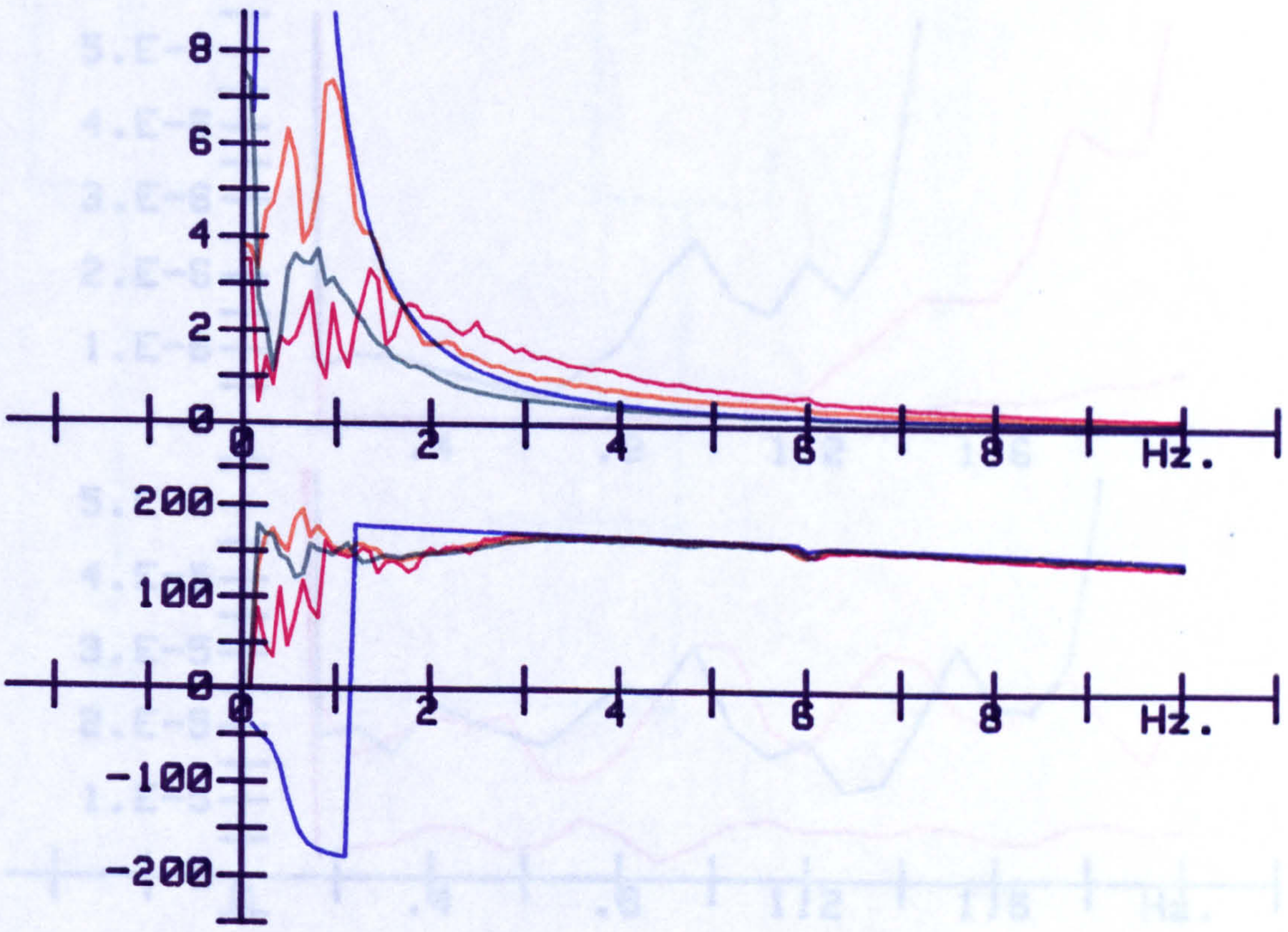

FIG 6.22 QOLR COMPARISON

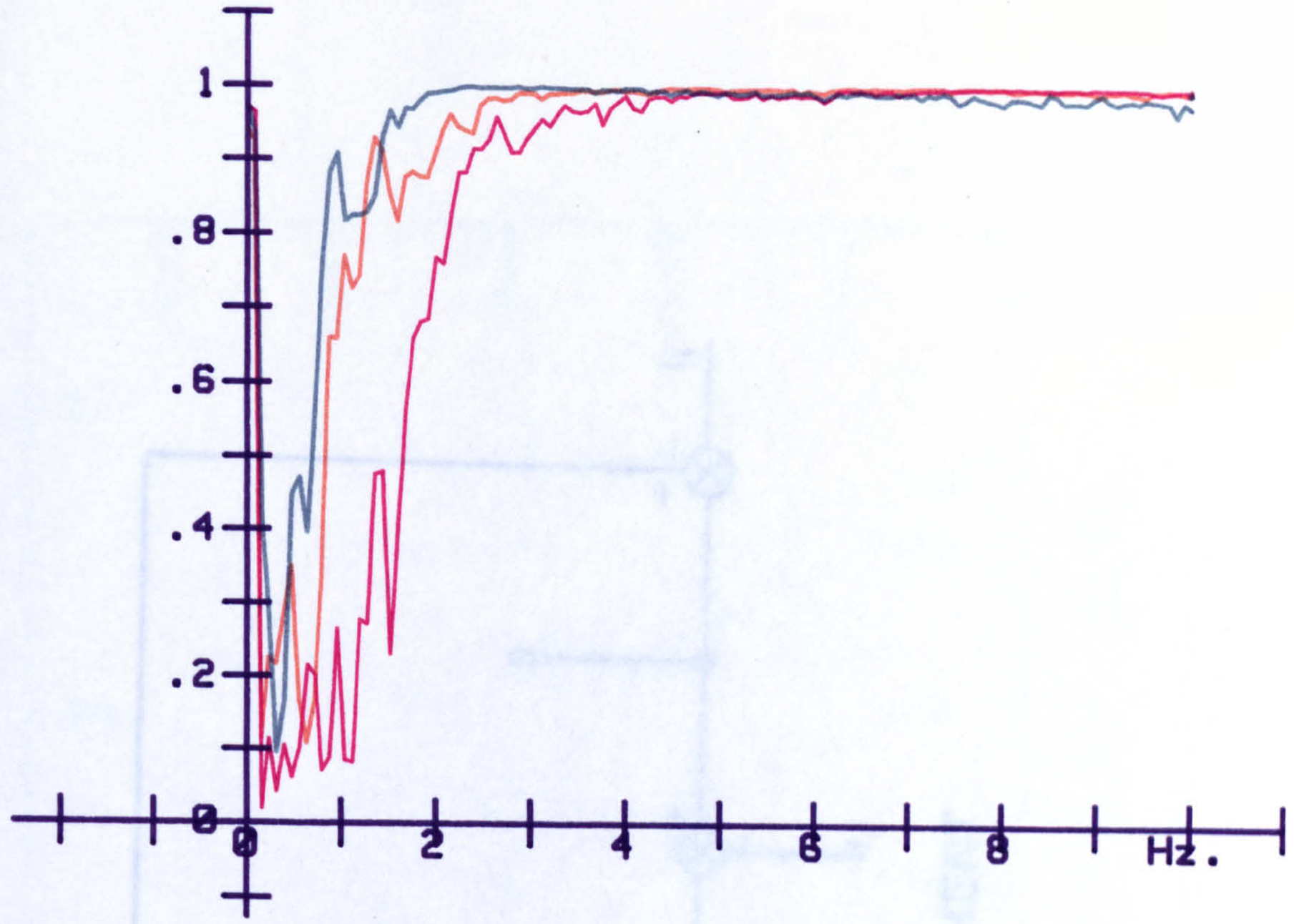

FIG 6.23 COHERENCE COMPARISON

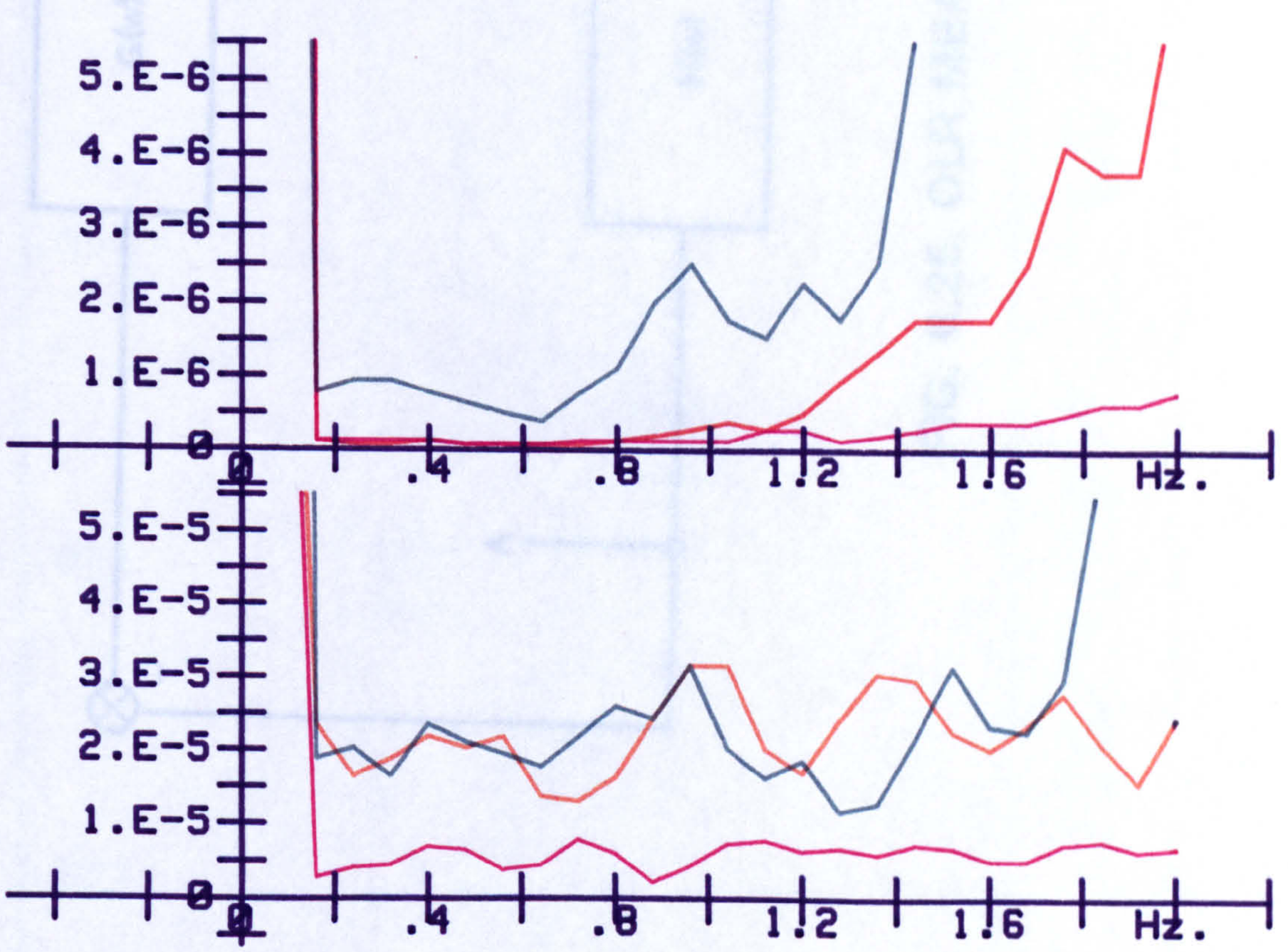

FIG 6.24 PSD COMPARISON

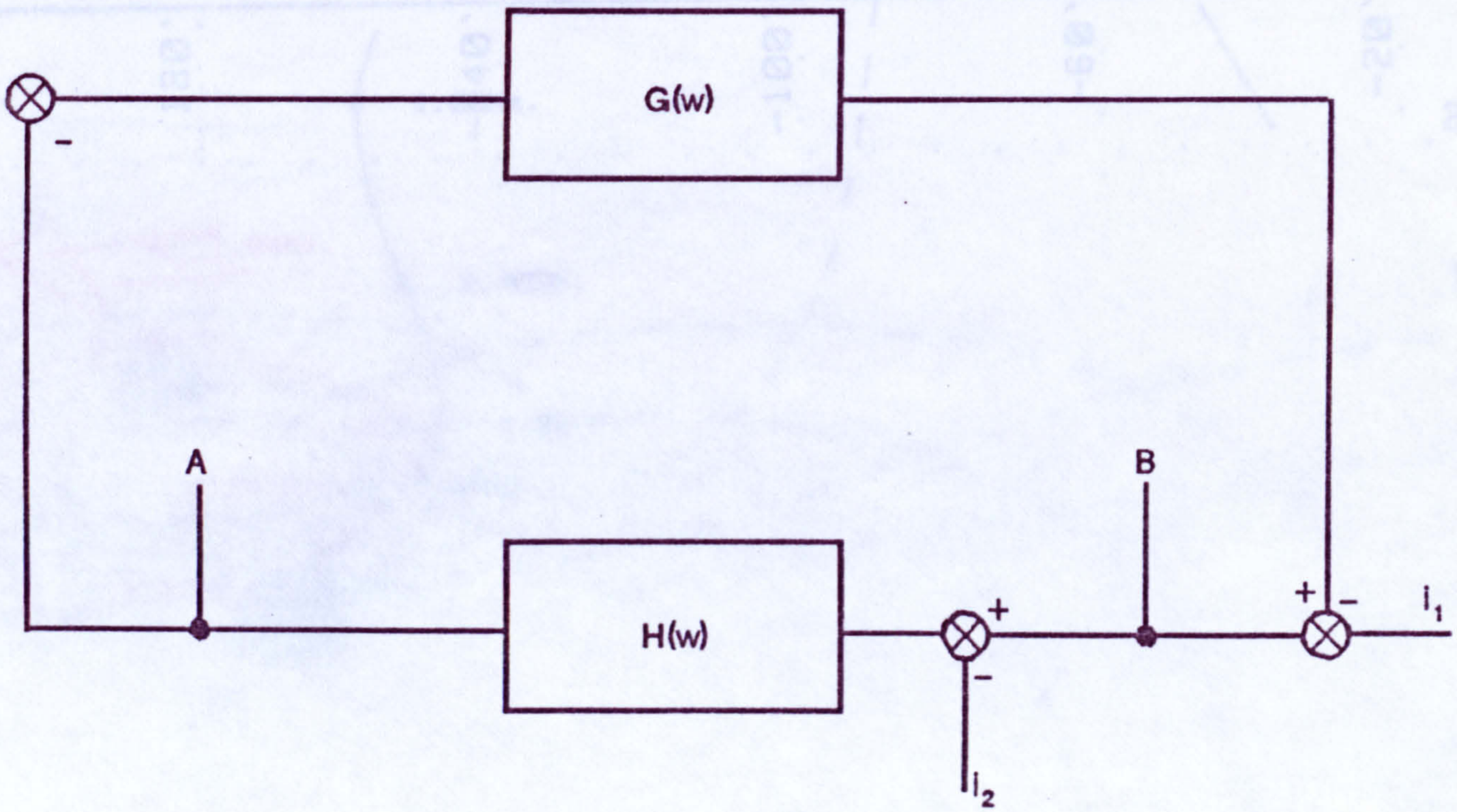

FIG. 6.25. OLR MEASUREMENT

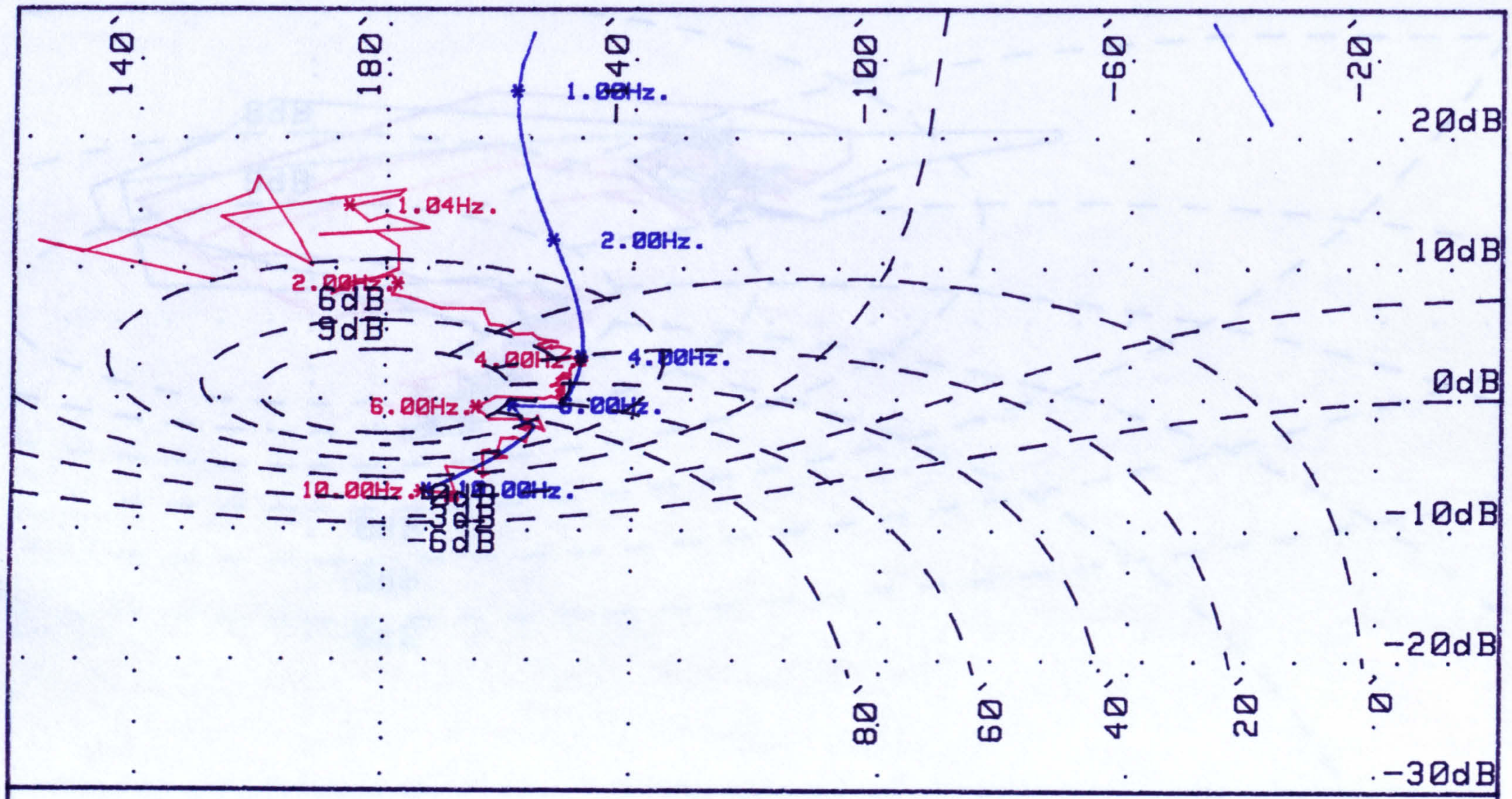

FIG 6.26 FLEXIBLE GUIDEWAY OLR

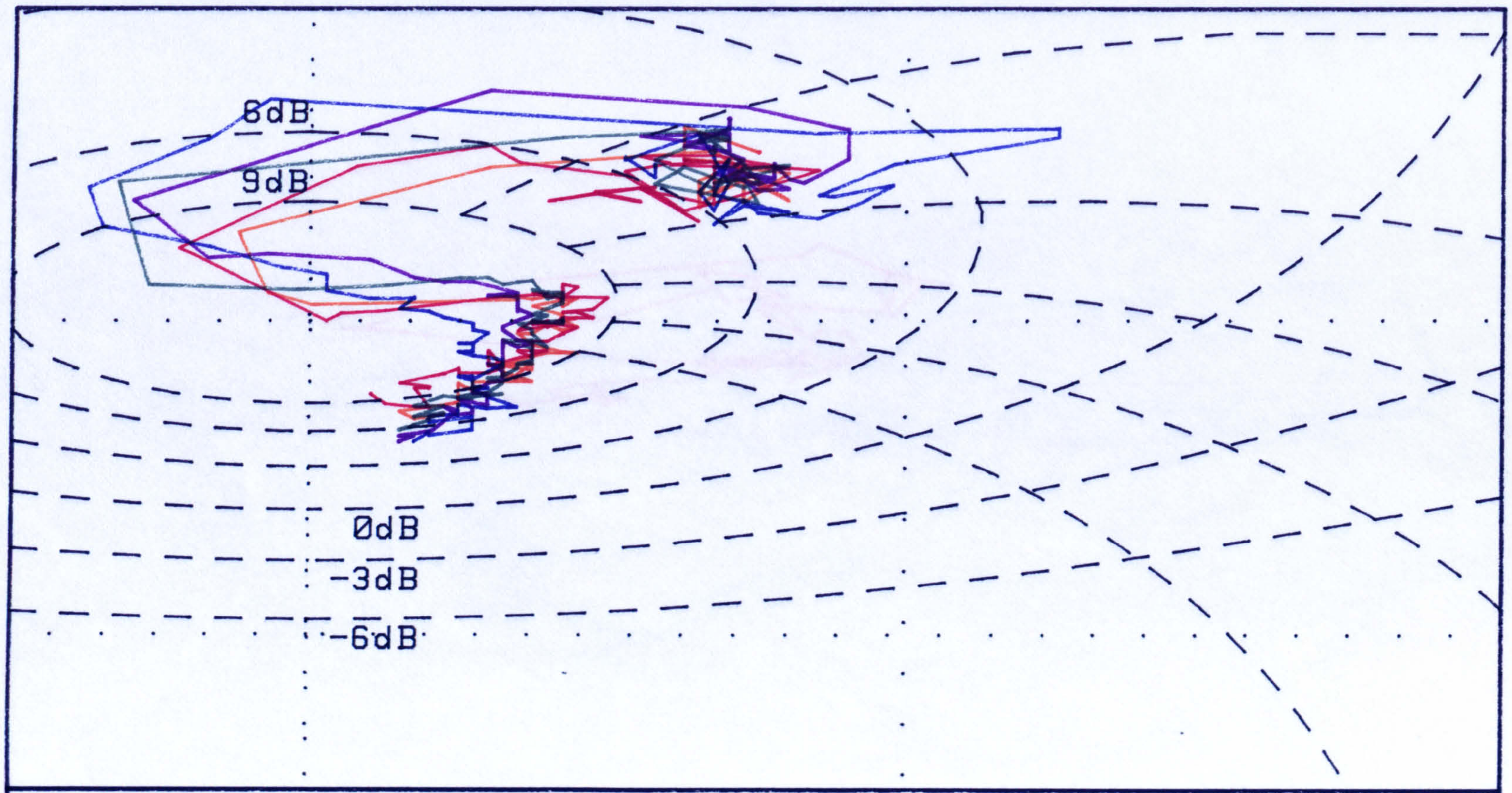

FIG 6.27 NUMERATOR CHANGES

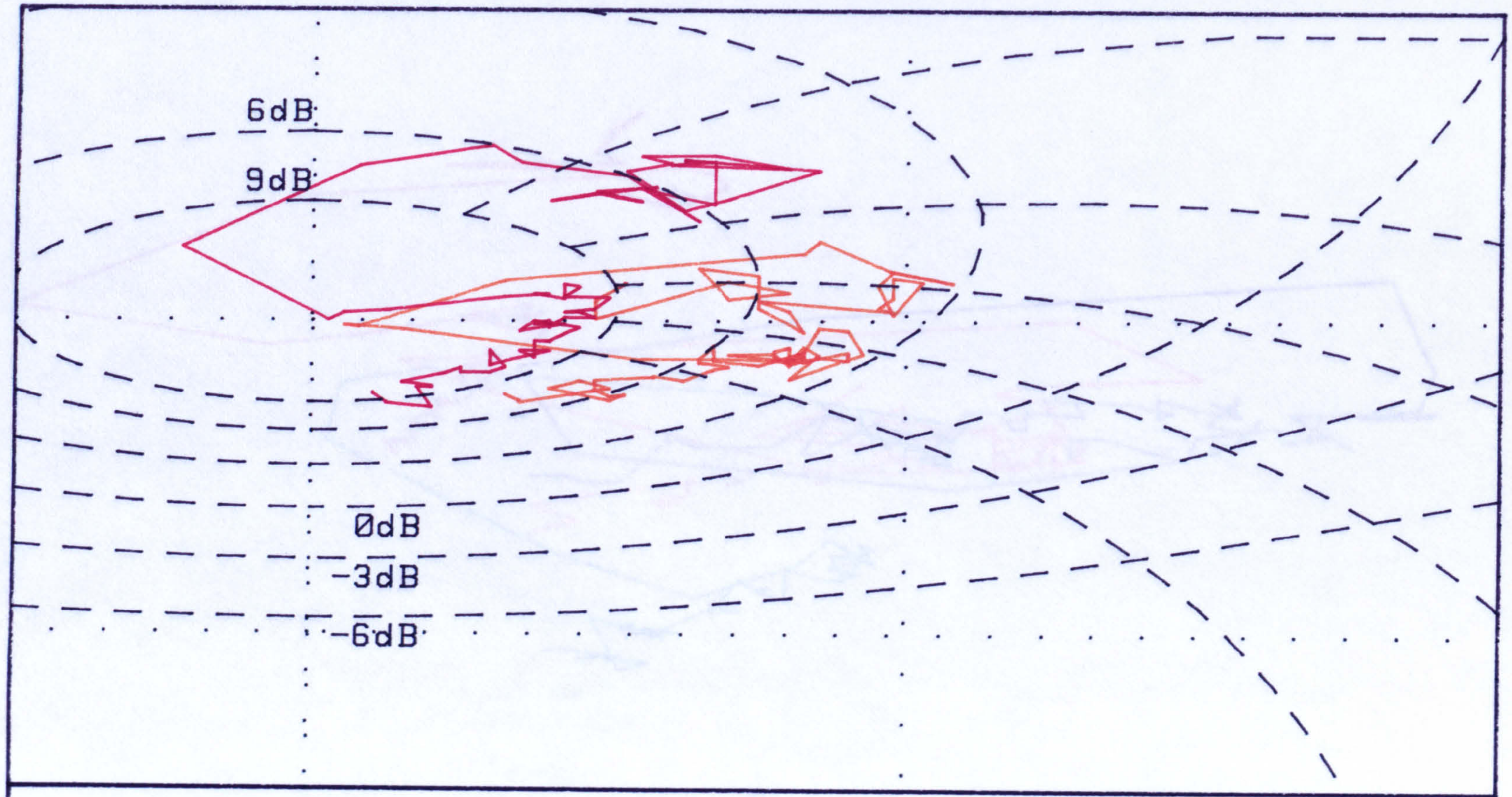

FIG 6.28 PHASE ADVANCE FILTERS

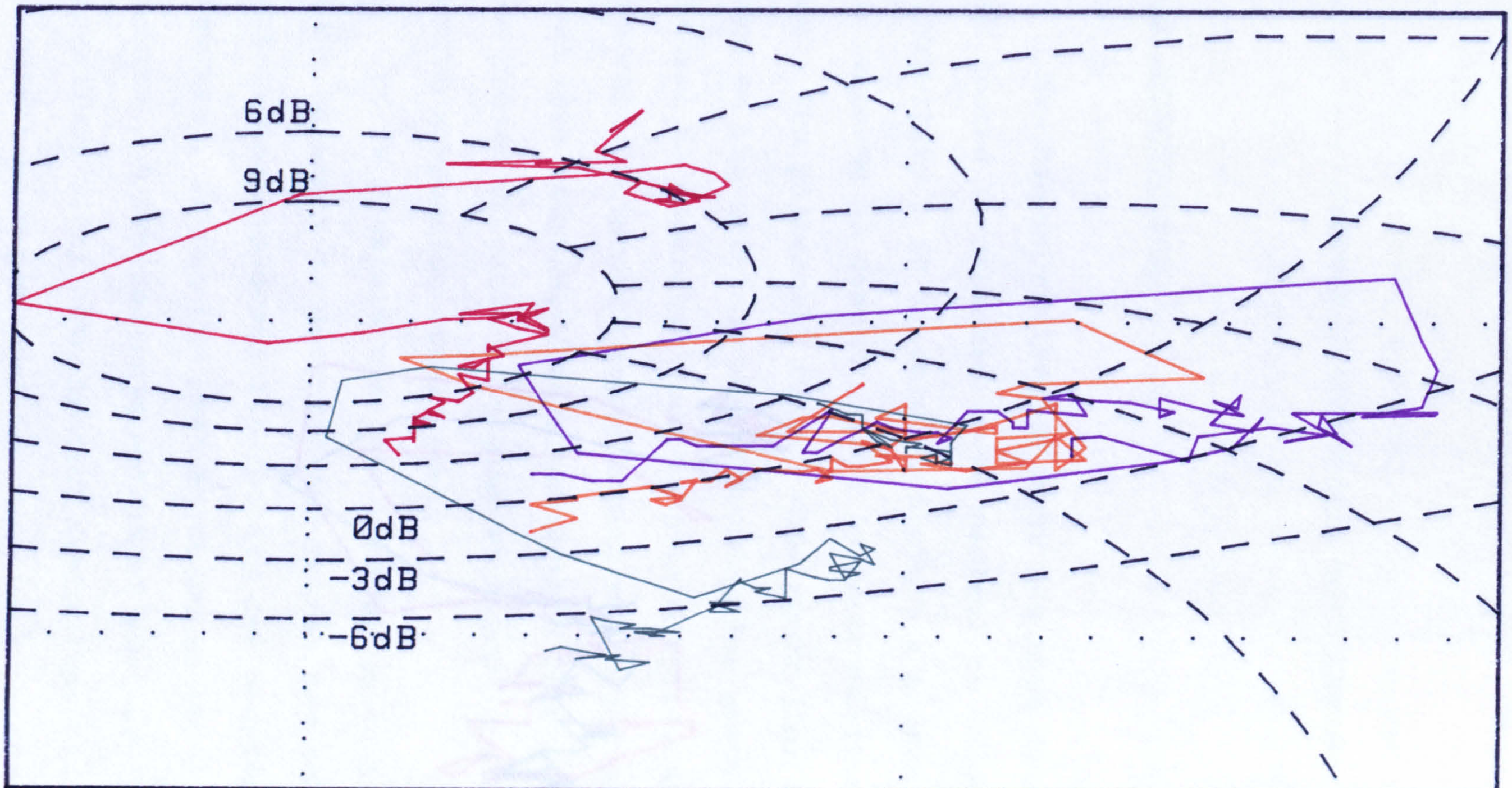

FIG 6.29 QUAD. PHASE ADVANCE

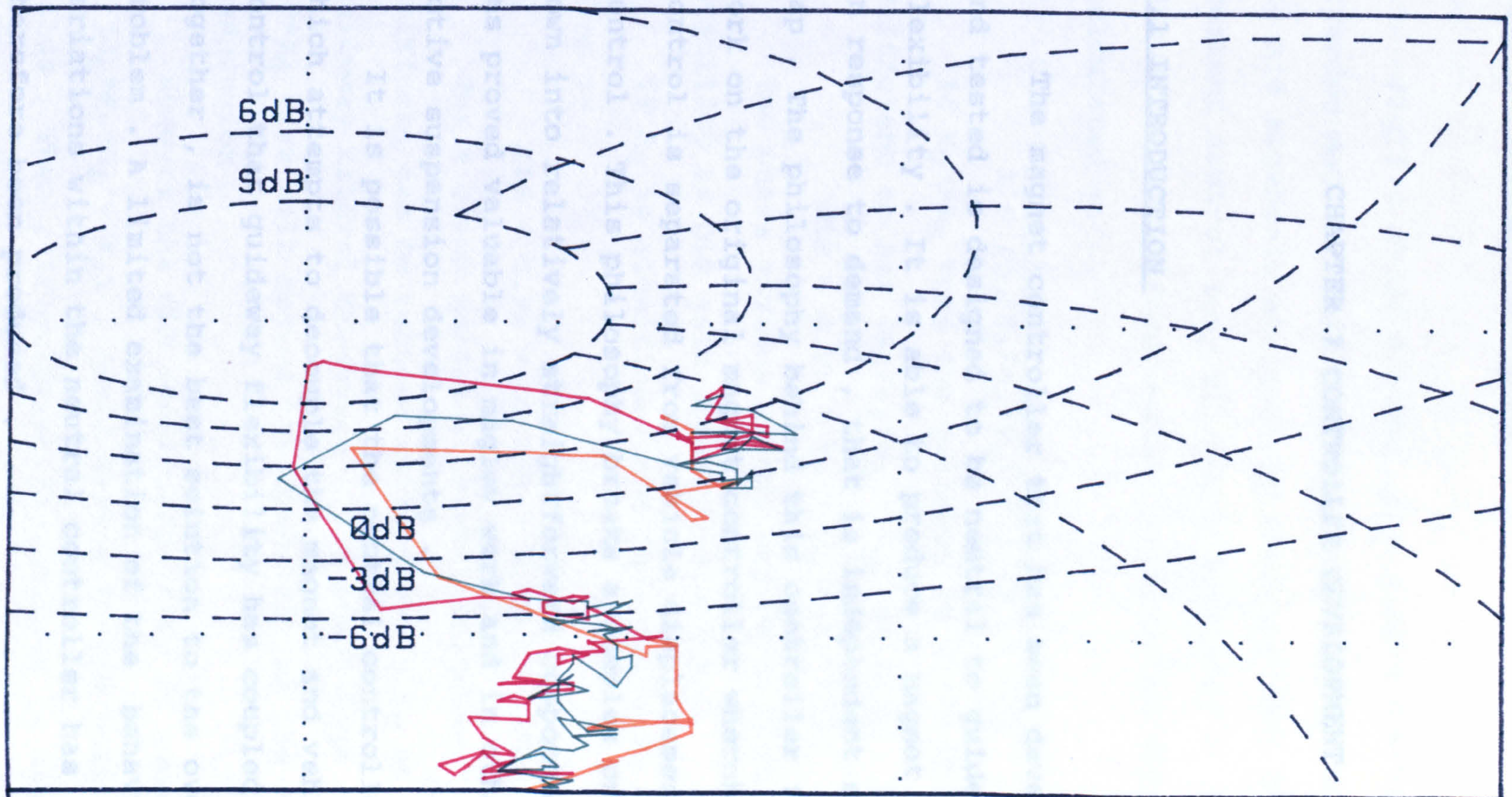

FIG 6.30 SUSPENSION FREQUENCY

CHAPTER 7 CONTROLLER DEVELOPMENT

7.1 INTRODUCTION

The magnet controller that has been developed and tested is designed to be neutral to guideway flexibility . It is able to produce a magnet flux , in response to demand , that is independent of magnet gap . The philosophy behind this controller follows work on the original magnet controller whereby magnet control is separated from vehicle displacement control . This philosophy breaks a complex problem down into relatively straightforward components and has proved valuable in maglev work and in other active suspension developments .

It is possible that the neutral controller , which attempts to decouple the magnet and vehicle control that guideway flexibility has coupled together , is not the best solution to the overall problem . A limited examination of the behaviour of variations within the neutral controller has therefore been produced .

7.2 A MORE ADVANCED CONTROLLER

7.2.1 Controller Analysis

Fig 5.6 shows a model of a single degree of freedom maglev vehicle . This model may be simplified to aid algebraic analysis by assuming that the magnet current control loop will work perfectly . Fig 7.1 shows the simplified system for which an OLR can be calculated :-

$$OLR = \frac{G.PA * K_I * G_A * K_B(R_V + LP\ R_G)}{1 + (G_g*K_I*G_A - K_g) * K_B(R_V + R_G)} \qquad \text{Eq 7.1}$$

If $R_V >> R_G$ then the guideway is rigid and it is sufficient to set $(G_g*K_I*G_A - K_g)$ to zero . Then :-

$$OLR = G.PA * K_I * G_A * K_B * R_V$$

The phase advance filter can be used to retain stability as OLR gain approaches unity .

If R_G is significant and this approach is used then :-

$$OLR = G.PA * G_A * K_I * K_B(R_V + LP*R_G)$$

For a given guideway natural frequency , static stiffness can be reduced until $LP*R_G > R_V$ at the guideway natural frequency , the phase lags of the $LP*R_G$ term will reduce the stability of the vehicle suspension .

However the OLR denominator term in equation 7.1 , $(G_g*K_I*G_A - K_g)$, could have a finite positive value . Then , if guideway flexibility is significant , the phase lag associated with guideway resonance will dominate both numerator and denominator of the

OLR . The net effect on the OLR will therefore be small and this will improve suspension stability .

Fig 7.2 shows the OLR for this novel controller on the Derby vehicle as guideway static stiffness reduces from 30 MN/m to 1.2 MN/m .

Guideway static stiffness (MN/m)	Plot colour
1.2	red
3.0	orange
5.0	green
7.0	purple
10.0	blue
100.0	turquoise

The guideway resonance effects are completely eliminated from the OLR . At 1.2 MN/m (red) the system is on the verge of instability because a new effect is introduced , a control system resonance at a higher frequency than the guideway resonance . This effect is more clearly shown in Fig 7.3 where the OLR data from Fig 7.2 is plotted as magnitude and phase against frequency (identical colours are used) .

Fig 7.2 and 7.3 shows data for a guideway with a 6 Hz natural frequency , guideway stiffnesses between 3 (orange) and 5 MN/m (green) produce dramatic changes in the phase characteristic of the OLR . At 5MN/m , the phase advances 180 degrees and then lags 180 degrees . At 3MN/m , the phase advances 180 degrees and then advances a further 180 degrees . Figs 7.2 and 7.3 show that the vehicle will be close

to instability if there is a 360 degree phase advance , but this novel controller is stable on guideways that are considerably more flexible than the neutral controller could tolerate .

Magnitude and phase values for the numerator and denominator of the OLR in equation 7.1 are shown in Fig 7.4 . At low frequency , the numerator is dominated by R_V with a magnitude peak and a 180 degree phase change when $LP*R_G$ becomes significant at higher frequencies . $R_V$and $LP*R_G$ differ in phase by 180 degrees with $LP*R_G$ a function of w^4 above w_G . Eventually they equate and a numerator minimum is produced .

At low frequency , the denominator is also dominated by R_V until the product of R_V and control gain equals -1 . The denominator is at a minimum and an OLR maximum is produced . At frequencies greater than w_G , R_G is a simple inertia with a 180 degree lag . There is therefore a second denominator minimum , OLR maximum , when the product of control gain and R_G equates to -1 . At high frequencies , the OLR denominator term is unity .

Fig 7.4 shows the two alternatives for OLR denominator phase at this second minimum . The OLR denominator phase will lead or lag at this point , depending upon the imaginary component of the OLR denominator at resonance . The imaginary components of the denominator at typical frequencies come from :-

$$\frac{G_g * K_I * G_A}{C_G s} \qquad 7.2$$

where C_G is the damping value required to model a single mode flexible guideway .

The imaginary component of expression 7.2 is effectively the ratio of phase lags in the current loop and in the guideway damping . This novel controller will therefore be stable on a more flexible guideway if the current loop has a very high bandwidth (with small phase lags) and the guideway is designed for a high level of structural damping .

7.2.2 Controller Optimisation

The optimisation of this controller has been done empirically , relying upon calculation of OLRs . These calculation have been based on a guideway with a 10 MN/m static stiffness , a 6 Hz natural frequency and 1% of critical damping . Fig 7.5 shows how OLR varies with changes in the expression :-

$$G_g * K_I * G_A - K_g \qquad 7.3$$

$(G_g*K_I*G_A-K_g)/K_g$	Plot colour
0%	black
20%	red
40%	orange
60%	green
100%	purple
200%	blue

300% turquoise

This expression was set to zero in the neutral controller . Model changes are produced by increases in the G_g term , similar effects follow changes in G_A although this increases system gain as well .

Substantial phase advances are produced for all the plots in Fig 7.5 but the black . The green line , representing a value for expression 7.3 of 60% of K_g , provides a limited resonant peak and 75 degrees of phase advance . This combination of variables is used in performance calculations for an "optimised" controller .

7.3 PERFORMANCE CALCULATIONS

Eigenvalue calculations were used to determine the minimum guideway stiffness for a stable system with 1% guideway damping and a range of guideway natural frequencies . Fig 7.6 shows the relative performance of the original controller , the neutral controller and this optimised controller . The neutral controller can be stable on guideways that are more flexible than the original controller could tolerate . However , the optimised controller is stable on guideways that are up to an order of magnitude more flexible than the other controllers could tolerate .

Performance prediction for railway (and road) vehicle suspensions is a widely understood science . Such predictions require knowledge of the track (road) roughness and vehicle suspension characteristic . The easiest on-track performance prediction is for the PSD of a particular vehicle variable in response to track input and this requires knowledge of :-

1. The frequency response between vehicle variables and the single input of track roughness .

2. The spatial PSD of track roughness in units of m^2/cycle per m .

3. Vehicle speed .

Design estimates for the performance of the Birmingham maglev vehicle were based around the assumption that maglev track would have similar roughness to mainline railway track . Experience has shown this assumption to be valid and so this track spectrum has been used to predict the response of a single degree of freedom model of the Derby vehicle with the optimised controller at 20 m/s as a conventional PSD . The RMS of a particular variable was then calculated over the 0 to 10 Hz frequency range . Fig 7.7 shows how the RMS of magnet gap , magnet voltage , magnet current and passenger acceleration , weighted to the ISO5 standard , vary with guideway static stiffness . The ISO5 weighting is an attempt by the International Standards Organisation to describe the sensitivity of the human

body to vibration frequency . A 6 Hz guideway with 1% damping is assumed . The calculations are a worst case because it is implicit that guideway stiffness is constant and does not vary with vehicle movement along the guideway .

The optimised controller allows the vehicle to work on guideway stiffnesses that would completely destabilise the original controller and the neutral controller . In the stiffness range chosen , vehicle performance is not dependent upon guideway stiffness .

7.4 PERFORMANCE BENEFITS FOR A PRODUCTION VEHICLE

7.4.1 Measurements at Birmingham

Measurements of bounce and roll OLR for the production vehicles at Birmingham were taken during the afternoon of February 25th 1986 . The measurements were for the vehicle in the centre of the guideway span at the site of the tests described in Chapter 3 , results are shown in red on Figs 7.8 and 7.9 . The measured OLRs show no effect from the flexibility of the guideway .

A model of the Birmingham vehicle is shown in Fig 7.10 . Details of the magnet controllers are not shown but are identical to the magnet controller in

Fig 5.6 . Predicted values of bounce and roll OLR are shown in blue on Figs 7.8 and 7.9 . As with experimental results at Derby there is poor agreement with measurements at low frequencies where coherence was low . Agreement at frequencies above 2 Hz is not as good as was achieved at Derby ; differences in phase are typically 12 degrees for bounce and 4 degrees for roll in the 2 to 6 Hz frequency range . Above 6 Hz the agreement in magnitude and phase is good ; there are differences in phase of less than 3 degrees .

The effects of guideway flexibility are present in the predicted results but not in the measured results . A likely explanation for this difference would be inaccuracies in the modelling of the guideway dynamics , suspension frequency or vehicle inertia .

The Birmingham vehicle is modelled quite accurately , particularly in the frequency range where effects of guideway flexibility might be important . The significant phase effects around 2 Hz are probably due to an inaccurate description of either the suspension filters , the magnet loop filters or the absolute position filters . Unfortunately there was no opportunity to test the suspension components .

7.4.2 Stability in Roll

The model of the Birmingham vehicle was established with similar magnet control parameters to those of the optimised controller for the Derby vehicle , described in 7.2.2 . The value of the expression 7.3 was actually set to 80% of the magnet negative stiffness (K_g) for the Birmingham vehicle .

The model guideway parameters were selected to emulate the guideway at Derby . The first two guideway roll (antiphase bending) modes at 5.0 and 12.4 Hz were modelled with the experimentally determined values for modal damping of 2.1% and 2.0% of critical . The Derby guideway lateral receptance was , regretably , never measured but would have been dominated by rigid body motions on the soft rubber bridge bearings . Prediction and experiment show that lateral guideway dynamics have a strong influence on the stability of the roll mode and the stability of this mode will be impossible with the lateral guideway dynamics as they were at Derby .

The use of chevron rubber bearing pads will provide much higher lateral stiffness so that guideway lateral dynamics may be dominated by guideway flexibility , as happens in the vertical plane . The model has therefore been established using the vertical guideway parameters for the lateral guideway dynamics although only the first mode at 6 Hz is used . Fig 7.11 shows the roll OLR with static stiffnesses of 5 MN/m in both the guideway roll modes and the lateral mode .

Stability is highly dependent upon the lightly damped mode at 6 Hz which is caused by the guideway lateral dynamics . Stability margins may be improved by either increasing the guideway static stiffness or by controlling the lateral vehicle-guideway dynamics in the way that vertical control has been provided . This latter scheme was used during the experimental work at Derby and is described in Chapter 6 .

The guideway at Derby had a measured static stiffness for the first roll mode of 2.7 MN/m (mean of two measurements) . The control system can accommodate this value by increasing G_g and hence increasing expression 7.3 to over 100% of K_g but this produces an unsatisfactory on track performance .

7.4.3 Stability in Bounce

As with the study of roll mode stability , the model guideway parameters sought to emulate the Derby guideway characteristics . The first two guideway bounce (in phase vertical bending) modes at 5.94 and 18.8 Hz were modelled with the experimentally determined values for modal damping of 1.0% and 1.9% of critical . Fig 7.12 shows the bounce OLR for static stiffnesses of 5 MN/m for each mode .

The Derby guideway had minimum stiffnesses in these modes of 3.4 MN/m (the mean of two values) at 5.94 Hz and 31 MN/m at 18.8 Hz . A value of 5 MN/m for the 18.8 Hz mode is much lower than the measured

value for the Derby guideway , stability in this frequency range is no problem . For the mode at 5.94 Hz , the measured value of 3.4 MN/m could be achieved without , apparently , losing too much of the stability indicated in Fig 7.12 . However some of the on track performance criteria become unsatisfactory at stiffnesses below 5 MN/m .

Magnet control parameters are defined by roll stability as this is more difficult to attain than bounce stability . This is because the coupling of lateral dynamics makes the roll system more complex and the effective vehicle roll inertia is 220% of the vehicle mass . Vehicle receptance is therefore smaller in roll than in bounce and guideway receptance is relatively more significant . It would have been desirable to establish the magnet control parameters for expression 7.3 at only 60% of K_g but this would not have given adequate stability margins in the roll mode .

7.4.4 Track Responses

It is easier for a railway or maglev Civil Engineer to maintain a high quality track cross-level than it is to maintain a high quality vertical track profile . The vertical profile is far more difficult to measure than the cross-level and therefore track is produced with less cross-level roughness than vertical roughness . Consequently vehicle roll

effects are far smaller than vehicle bounce effects and so track responses are calculated for vertical inputs only . It is therefore assumed that the two sides of the vehicle will behave in a similar manner . The frequency responses between vehicle bounce displacement , vehicle bounce acceleration , magnet gap , magnet current and the system input , track roughness , appear in Figs 7.13 to 7.16 for the frequency range of 0 to 30 Hz . All of these responses , but for displacement , are significant at higher frequencies .

Fig 7.13 shows the frequency response between vehicle bounce displacement and track roughness , this is the vehicle suspension characteristic . Ideally , this characteristic should match the low pass filter in the vehicle displacement control loop in Fig 7.1 , as discussed in Chapter 1. Fig 7.13 shows that this is not strictly true for the predicted performance of this controller . The resonance effects that were discussed in 7.2.1 produce a peak in the suspension characteristic at 8 Hz and the gain is rather high in the 0 to 2 Hz frequency range .

The PSDs for these variables are calculated with the assumption that maglev track has the same roughness as main line railway track . Fig 7.17 shows the PSD for vehicle body acceleration , weighted according to the ISO5 filter . The RMS value for the 0 to 10 Hz frequency range is 2.0% g with a further

0.6% g in the 10 to 30 Hz frequency range although most of this is within the 10 to 15 Hz range . Passengers of high speed railways are not unaccustomed to have a ride quality of 2.6%g .

Fig 7.18 shows the PSD for magnet gap , the RMS value in the 0 to 10 Hz frequency range is 2.5 mm , available suspension travel is +/- 15 mm . This response has a zero mean and so the RMS value is the Standard Deviation for suspension travel . Therefore suspension travel of six times the Standard Deviation is required before vehicle-guideway contact occurs . It is usual to assume a normal distribution for plain line guideway roughness , therefore vehicle-guideway contact will be an extremely rare event .

Fig 7.19 shows a PSD for magnet current , the RMS value is 1.8 Amps , the magnet current required to levitate a stationary vehicle is around 20 Amps . The dynamic magnet current is only 10% of the static current .

7.5 CONCLUSIONS

This chapter provides a comparison of three different magnet controllers . Clearly the neutral controller has some benefit relative to the original controller but only with guideway natural frequencies above 5 Hz . Fig 7.6 shows that the neutral controller , without magnet strut resonances , notch

filters and magnet hysterisis , would be stable on a significant proportion of the Derby guideway without suspension loop modifications . Fig 7.6 suggests that at low frequency , instability is caused primarily by problems with the suspension control loop . It is only at higher guideway natural frequencies that that improvements in the magnet loop stability become beneficial .

Response predictions for the 6400 kg Birmingham vehicle on a guideway with static stiffnesses of 5 MN/m are highly encouraging . Note that a delevitated vehicle would bounce at only 4.4 Hz at guideway mid-span and roll at 3 Hz . The predicted RMS bounce acceleration of 2.6 %g is perfectly acceptable , particularly for the short journey durations normally associated with urban transport . Predictions for the RMS values of magnet current and gap change are well within the installed capacity . It is also important to realise that these predictions are pessimistic because the vehicle is not on a guideway with constant stiffness .

Only very limited attempts have been made to optimise this suspension controller . The magnet control parameters have not had any great study and no use has been made of manipulations in the form and frequency of the suspension filter nor variations in the phase advance filter .

Changes in the phase advance filter might be succesfully employed in roll where the installed

filter has never seemed to the author a particularly appropriate choice . This would control any stability problems with lateral guideway dynamics and would allow the use of magnet feedback terms that would help bounce stability . This in turn would substantiallly reduce higher frequency bounce acceleration and overall RMS acceleration at the cost of only modest increases in the magnet gap and current .

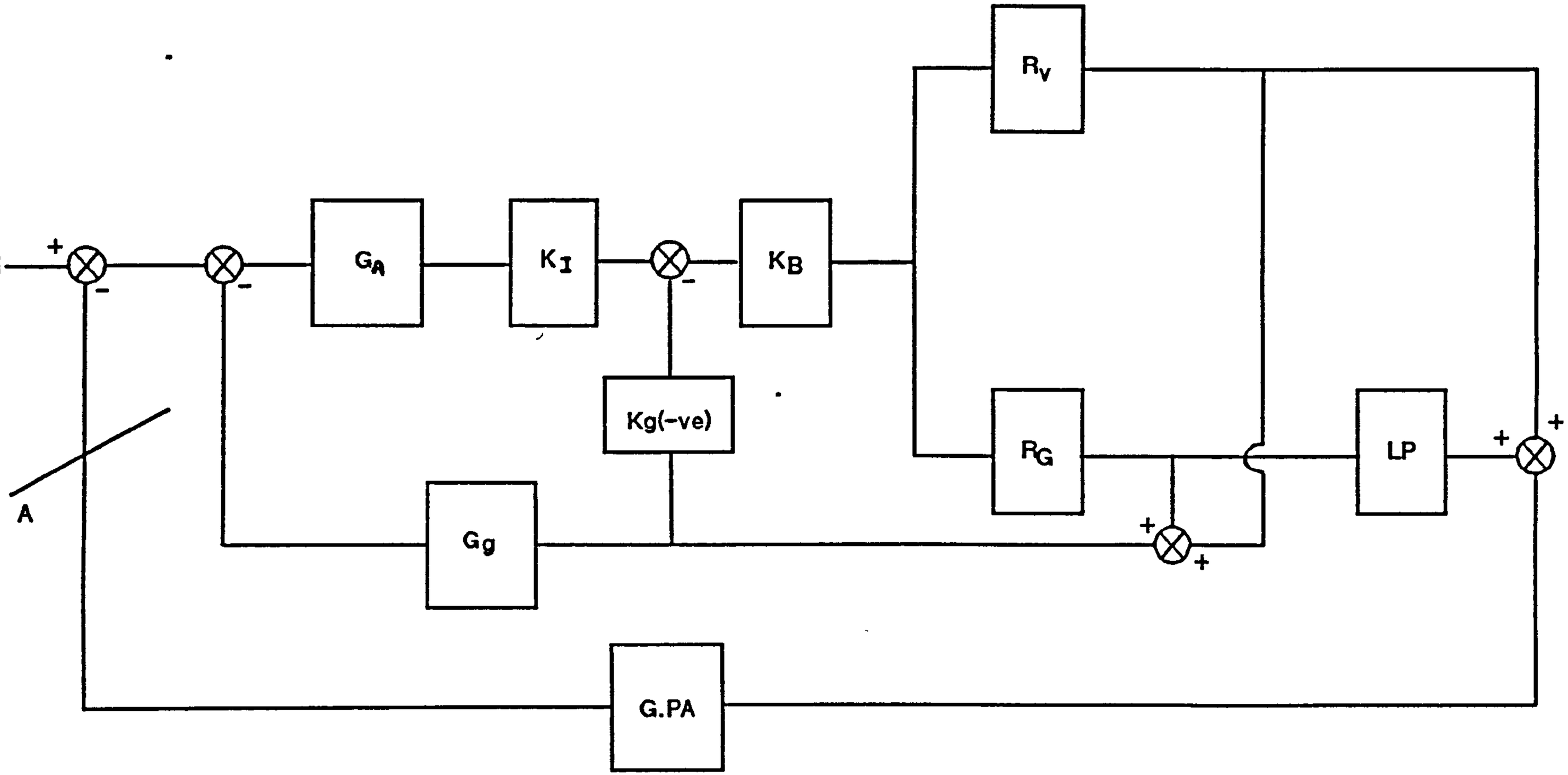

FIG. 7.1. A SIMPLIFIED SINGLE DEGREE OF FREEDOM MODEL

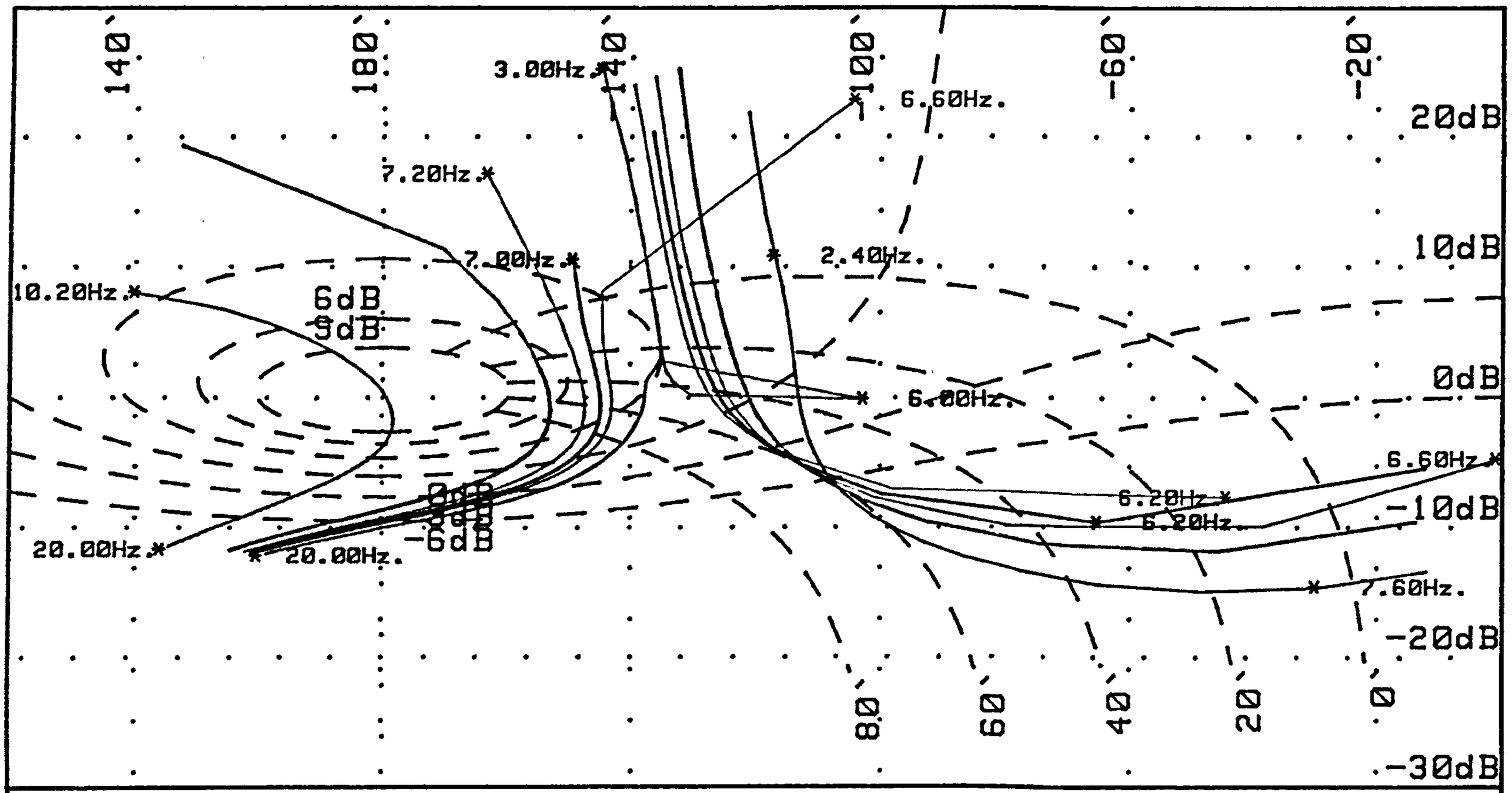

FIG 7.2 OLR VARIATION

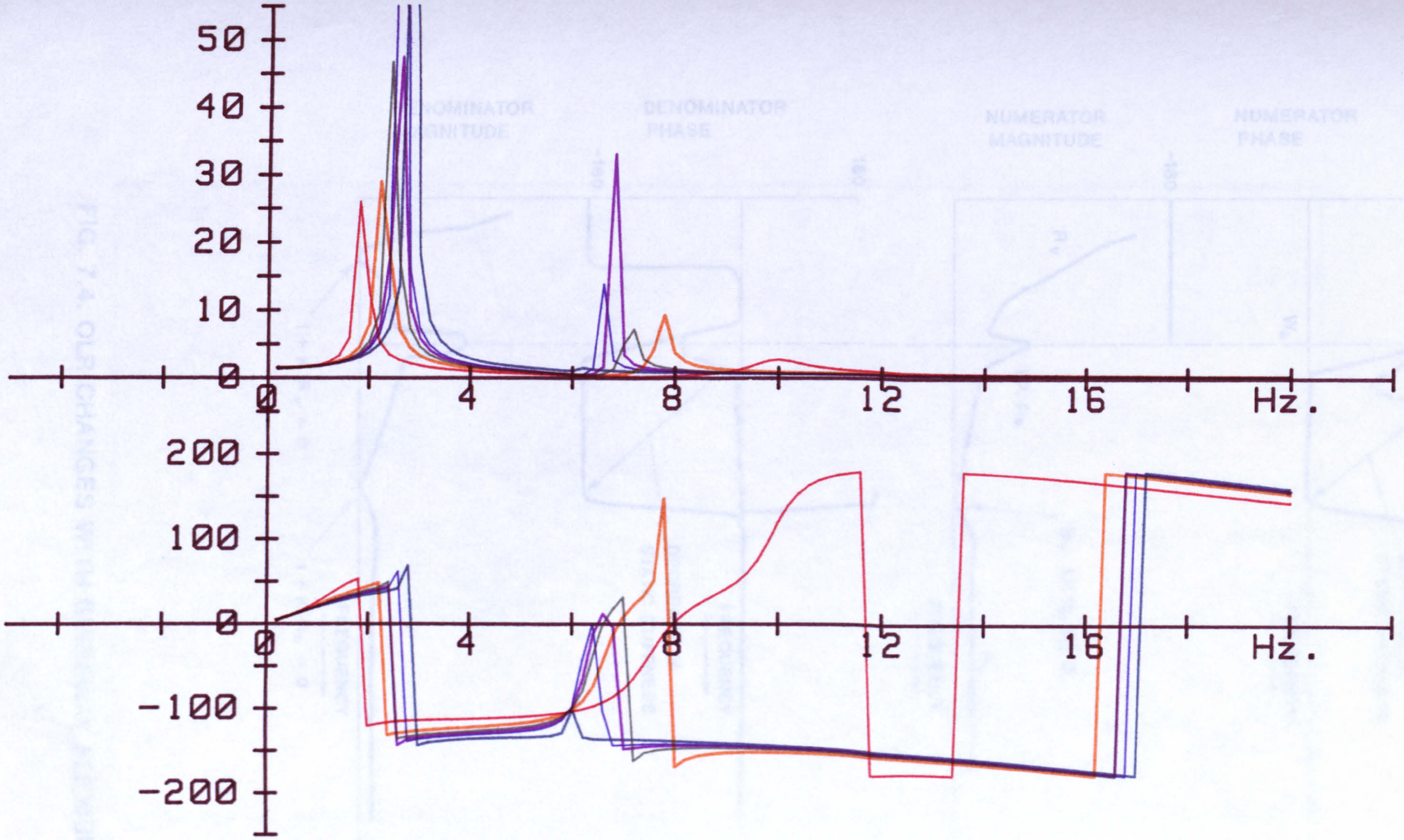

FIG 7.3 OLR VARIATION

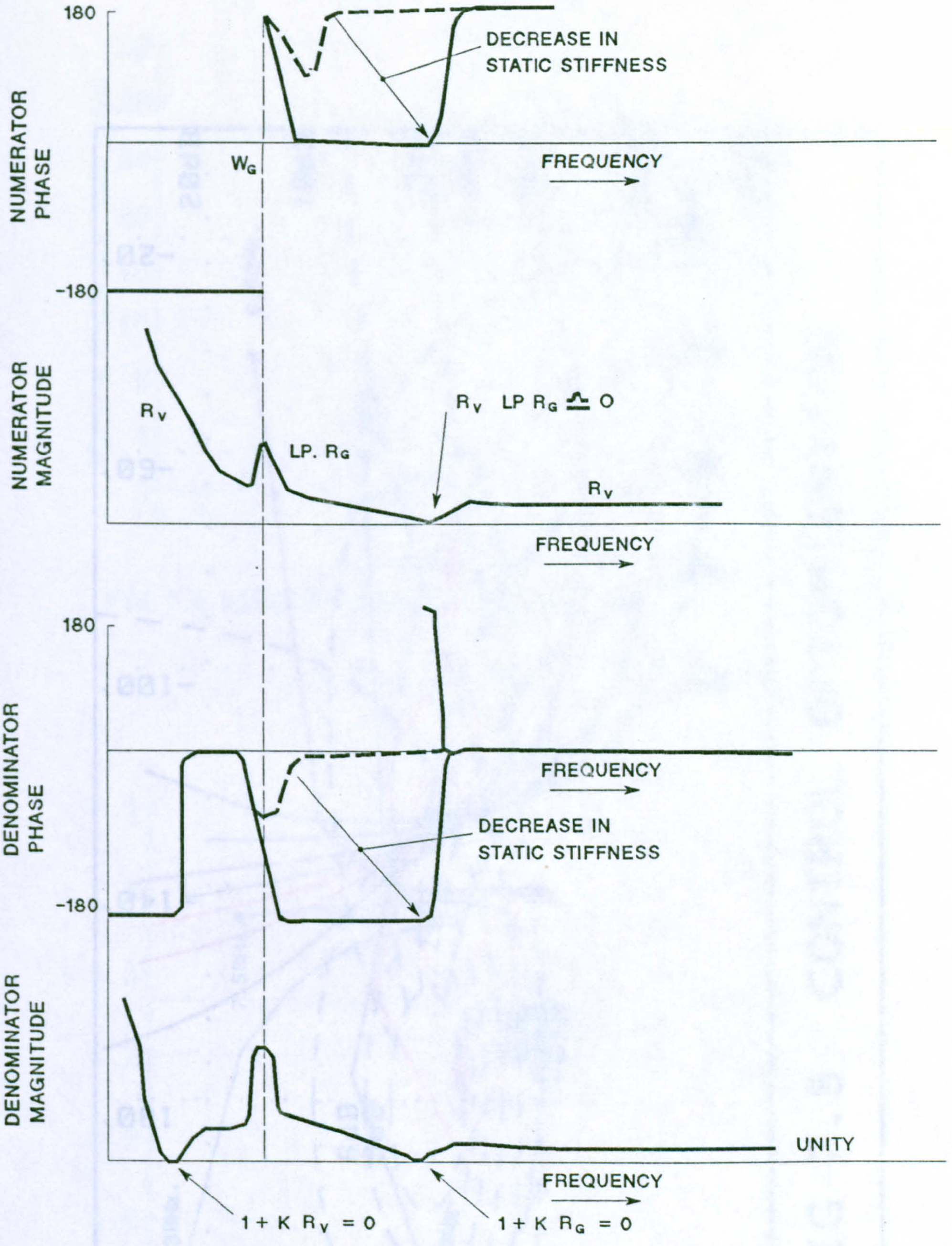

FIG. 7.4. OLR CHANGES WITH GUIDEWAY FLEXIBILITY

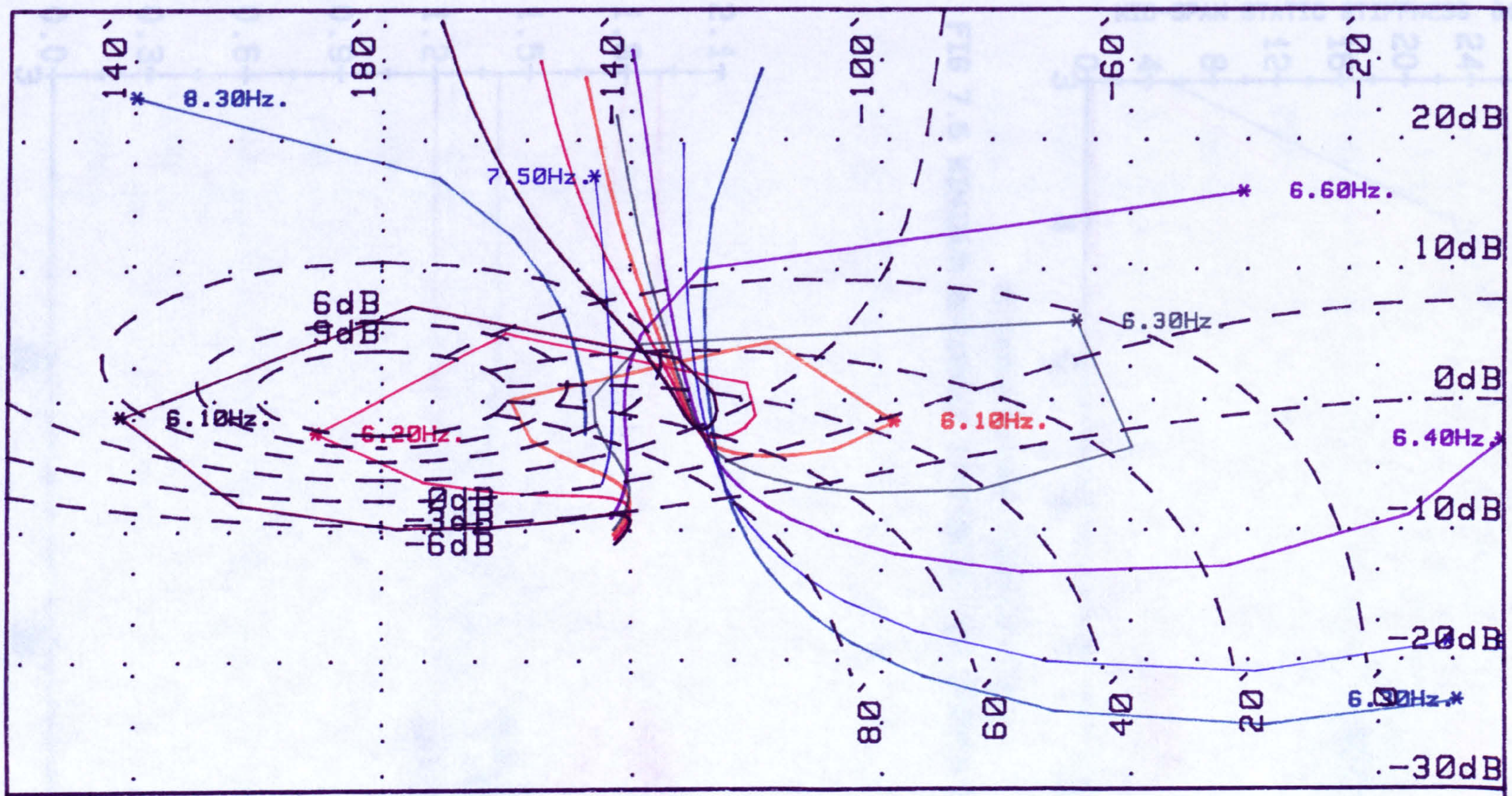

FIG 7.5 CONTROL OPTIMISATION

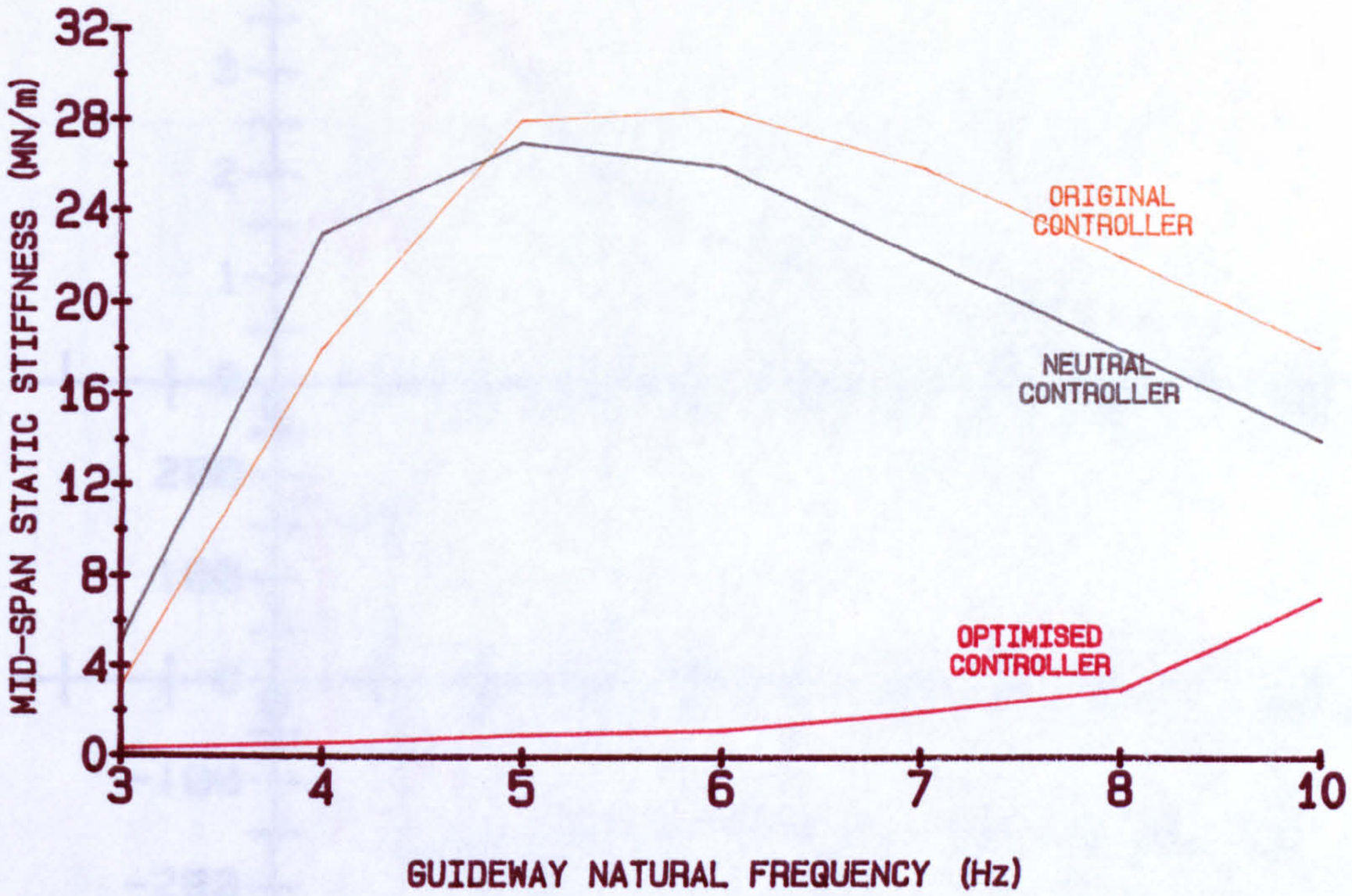

FIG 7.6 MINIMUM GUIDEWAY STIFFNESS FOR SYSTEM STABILITY

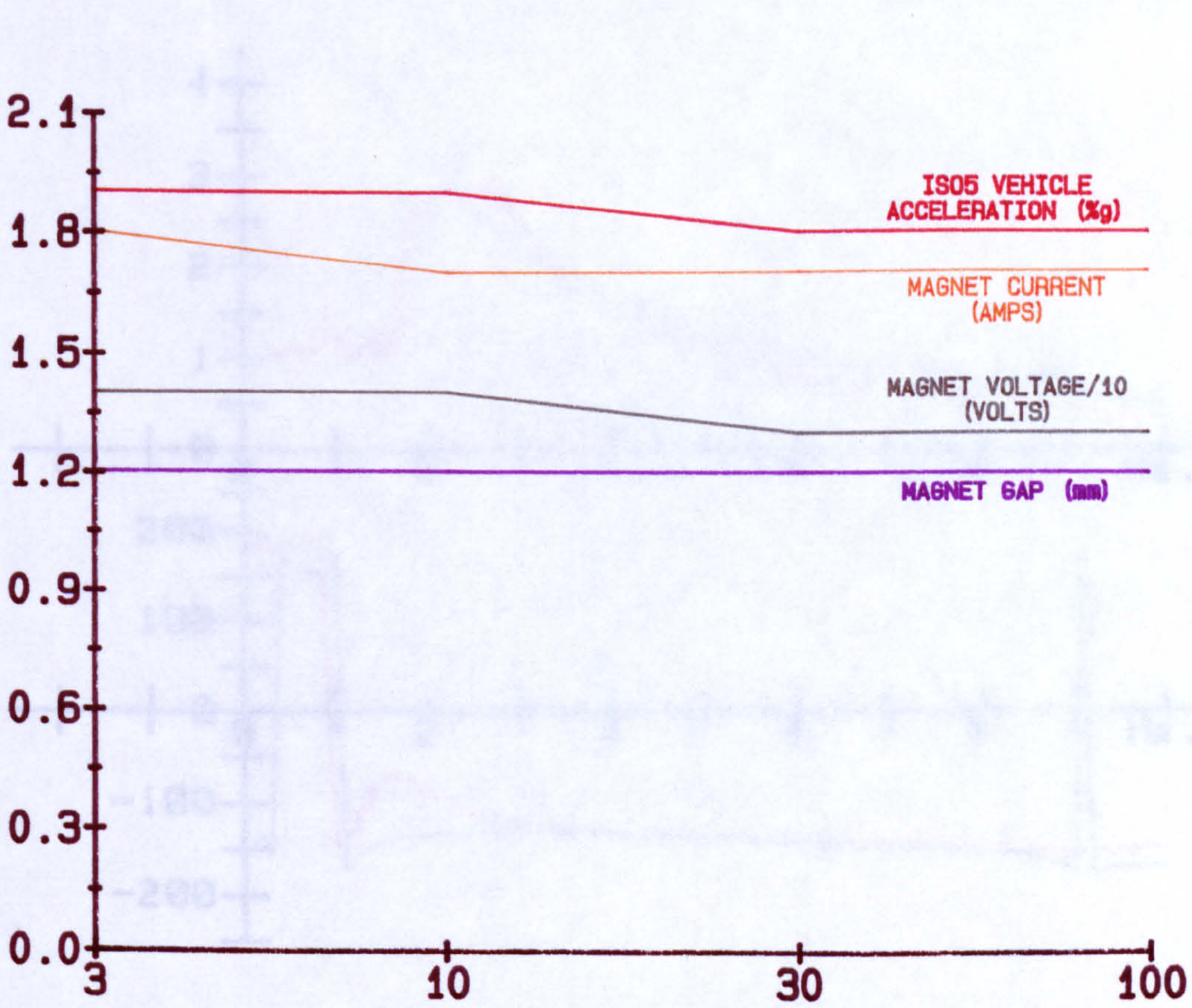

FIG 7.7 RMS VEHICLE RESPONSE TO GUIDEWAY ROUGHNESS

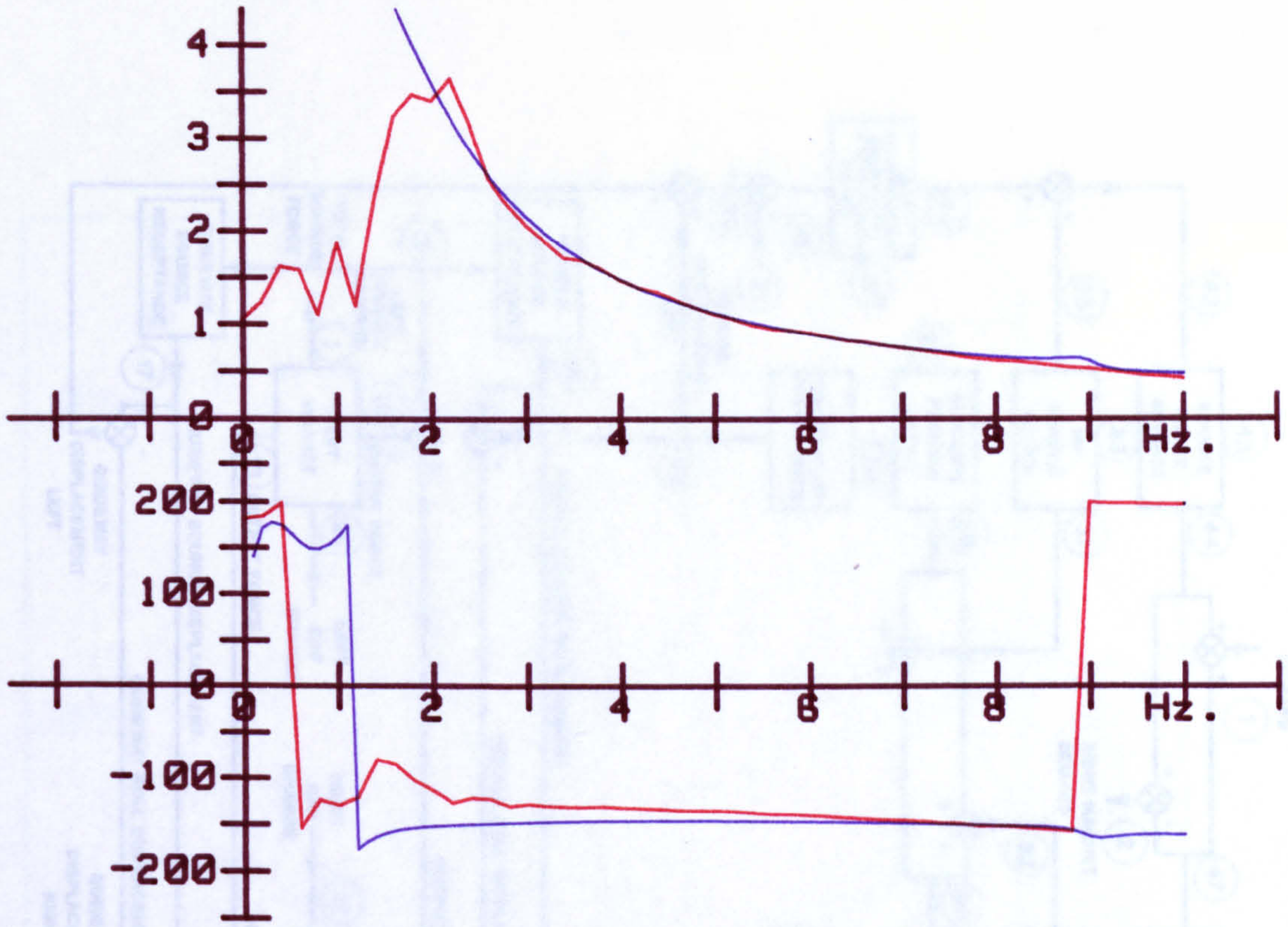

FIG 7.8 BOUNCE OLRs AT B'HAM

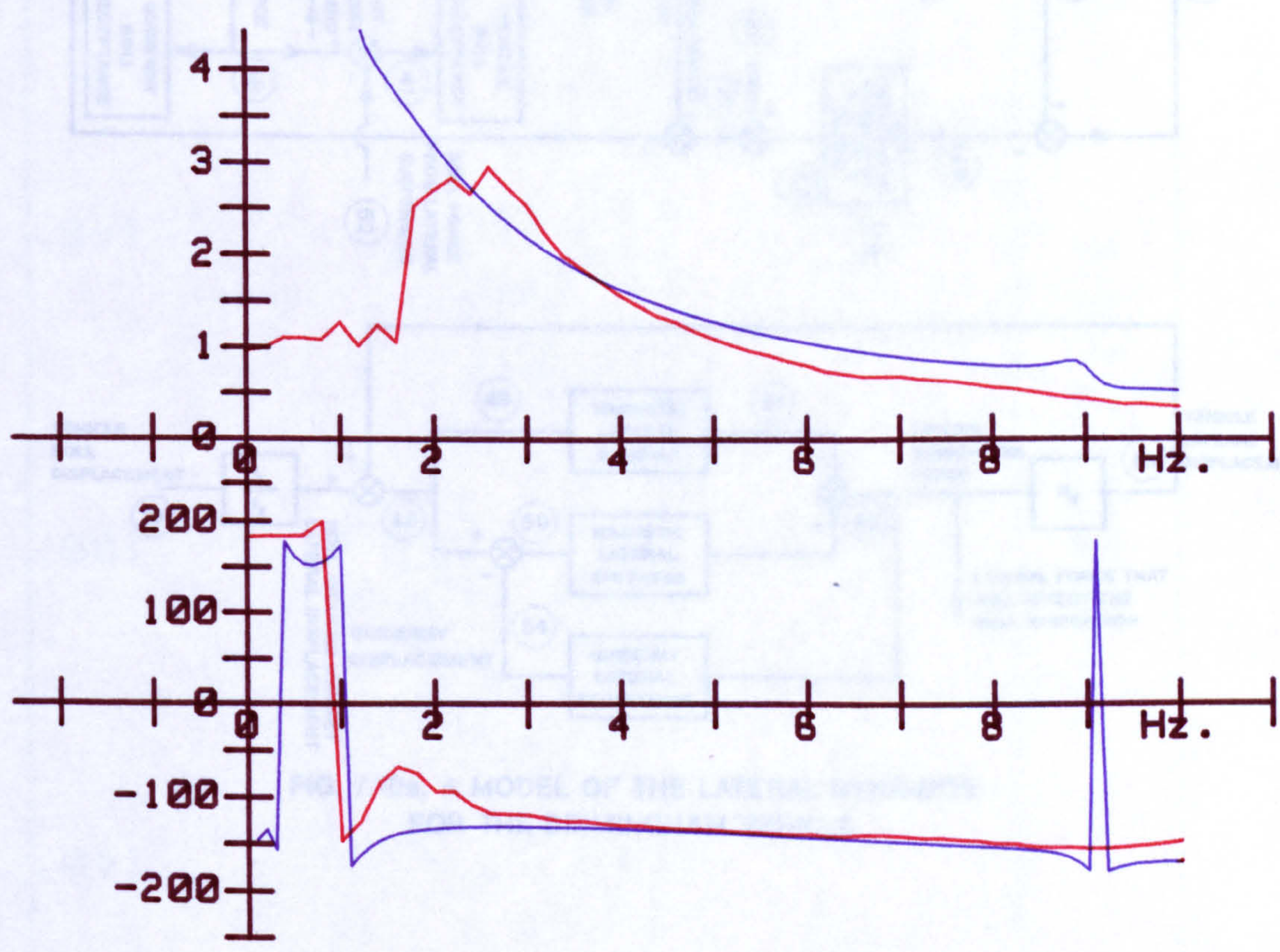

FIG 7.9 ROLL OLRs AT B'HAM

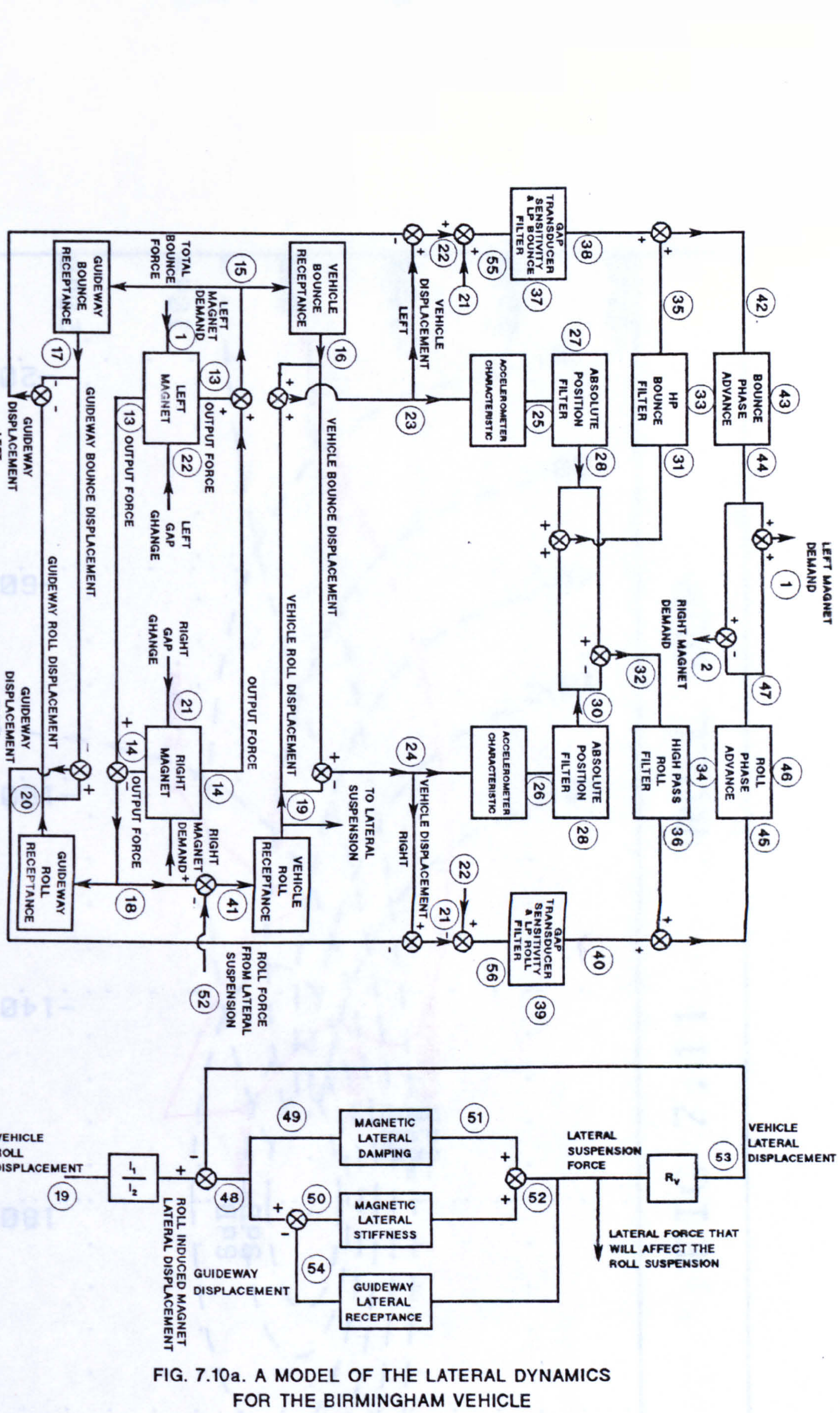

FIG. 7.10. A MODEL OF THE BIRMINGHAM VEHICLE

FIG. 7.10a. A MODEL OF THE LATERAL DYNAMICS FOR THE BIRMINGHAM VEHICLE

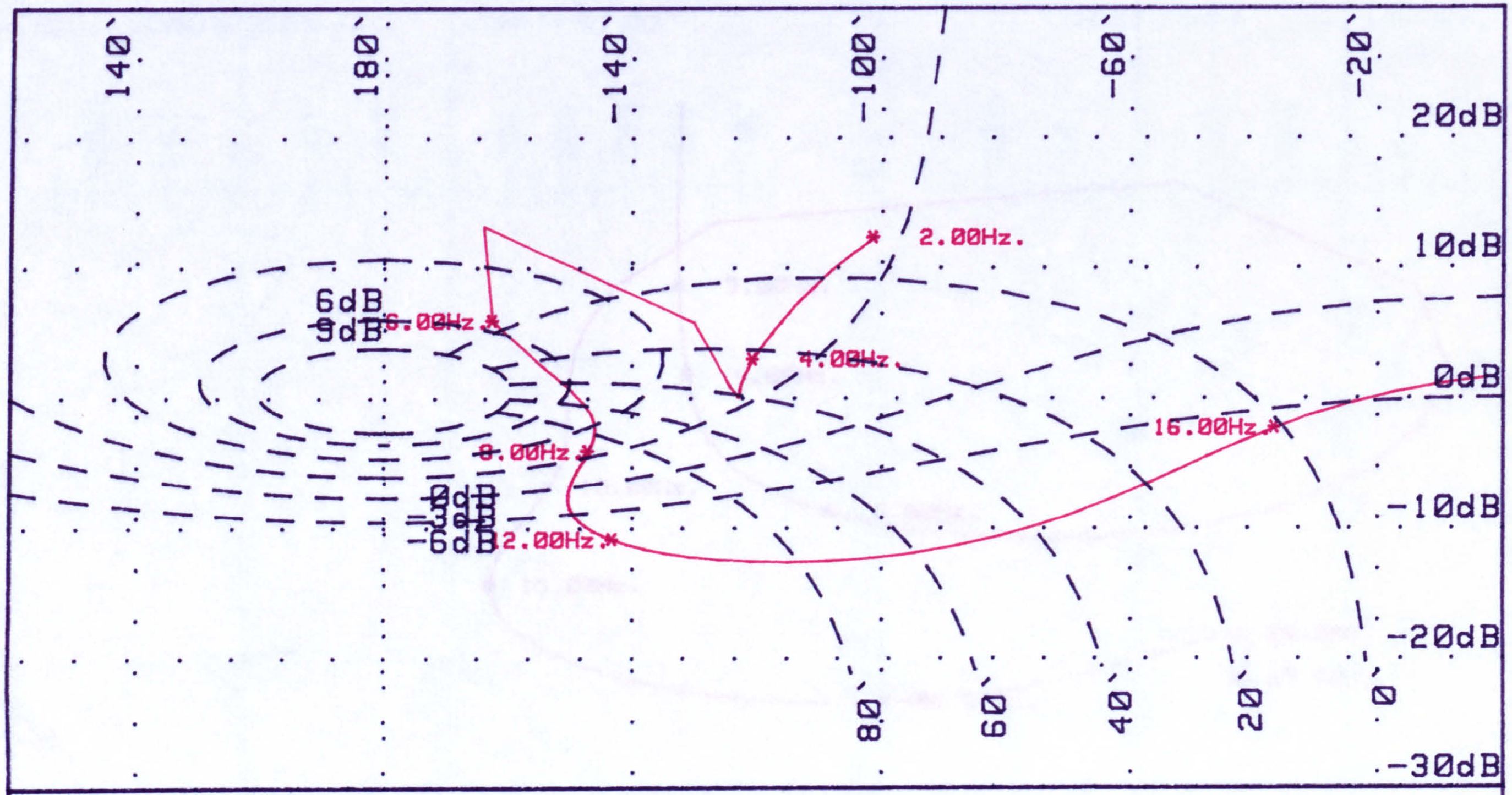

FIG 7.11 ROLL OLR

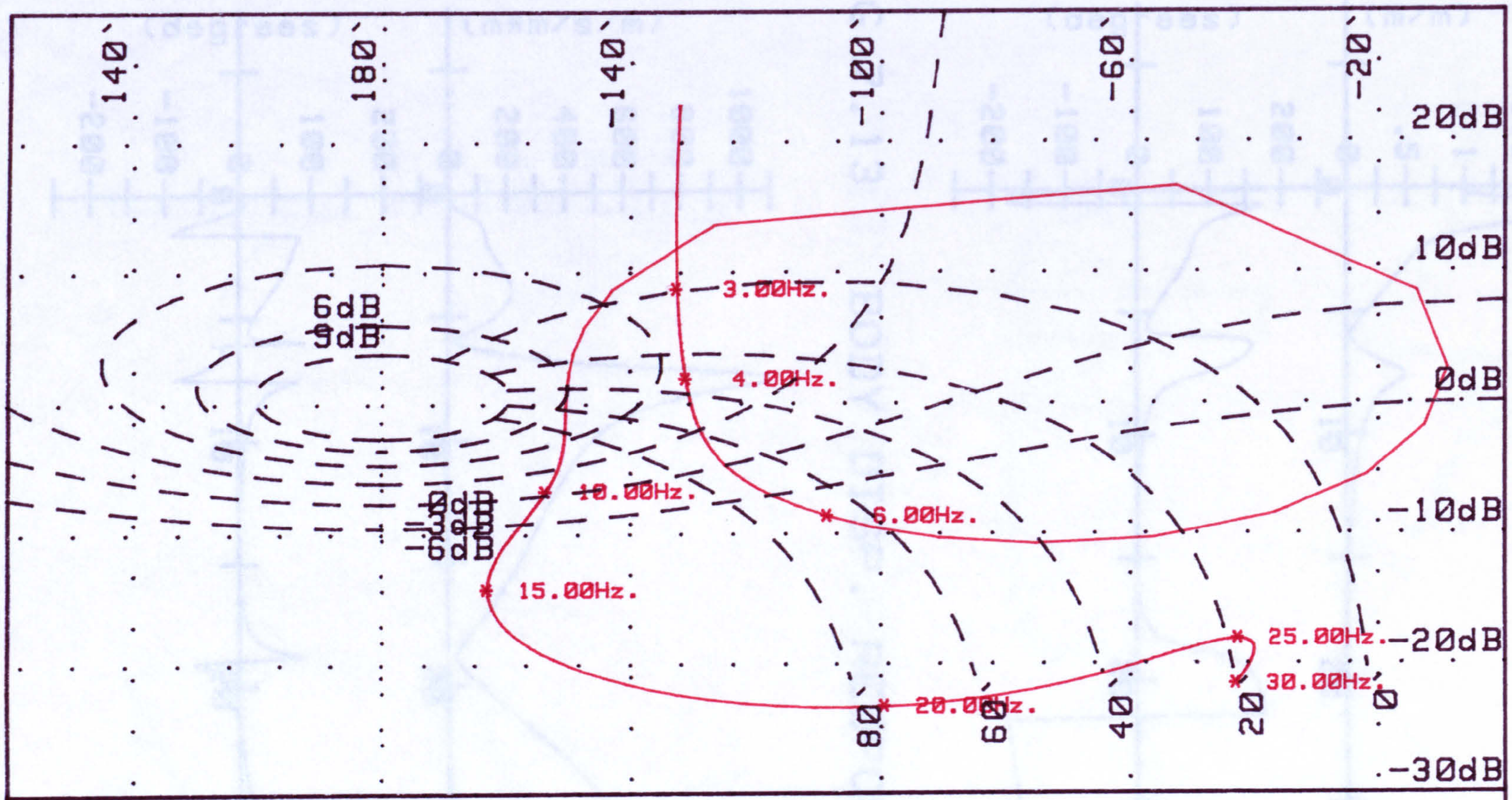

FIG 7.12 BOUNCE OLR

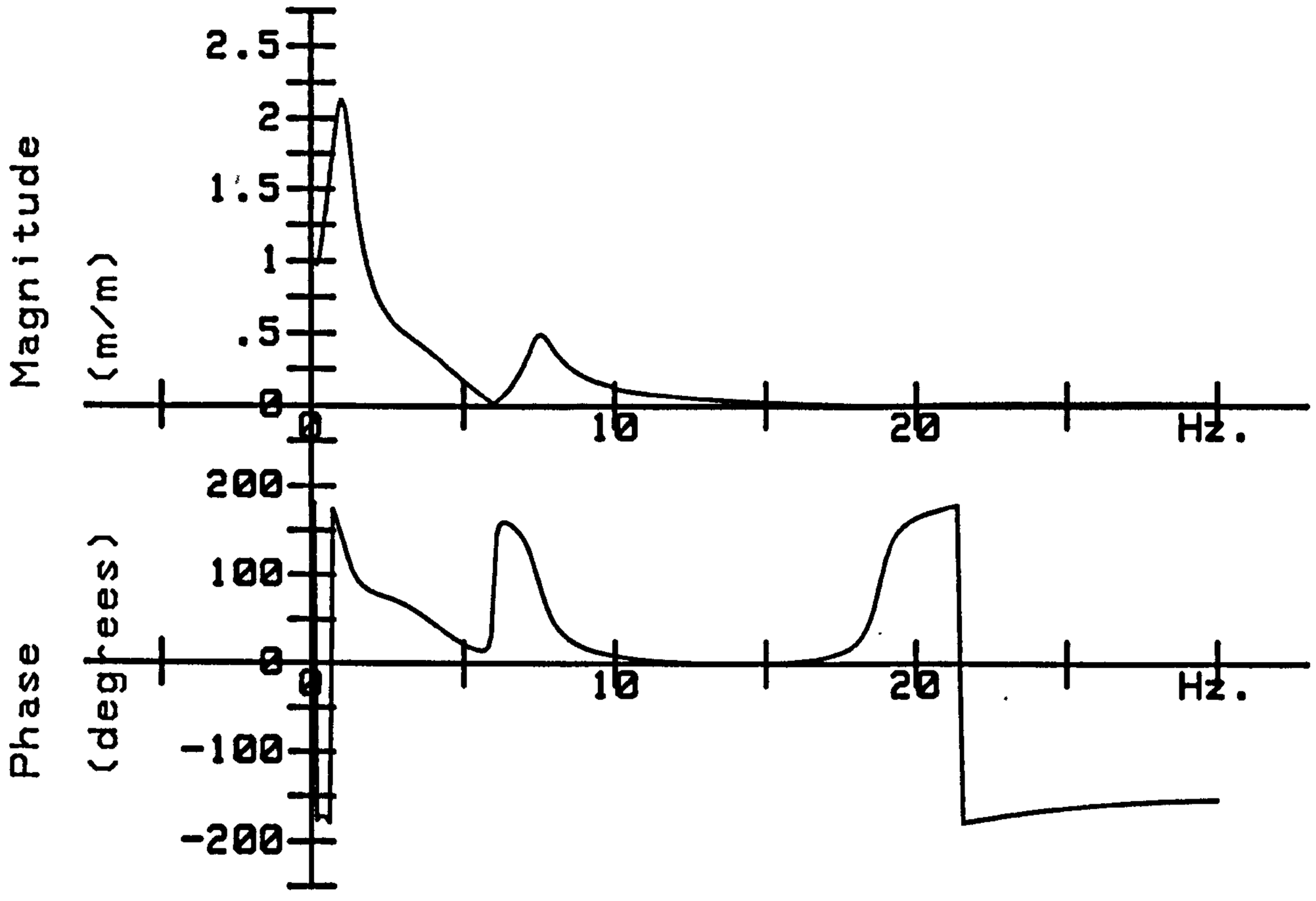

FIG 7.13 BODY DISP. RESPONSE

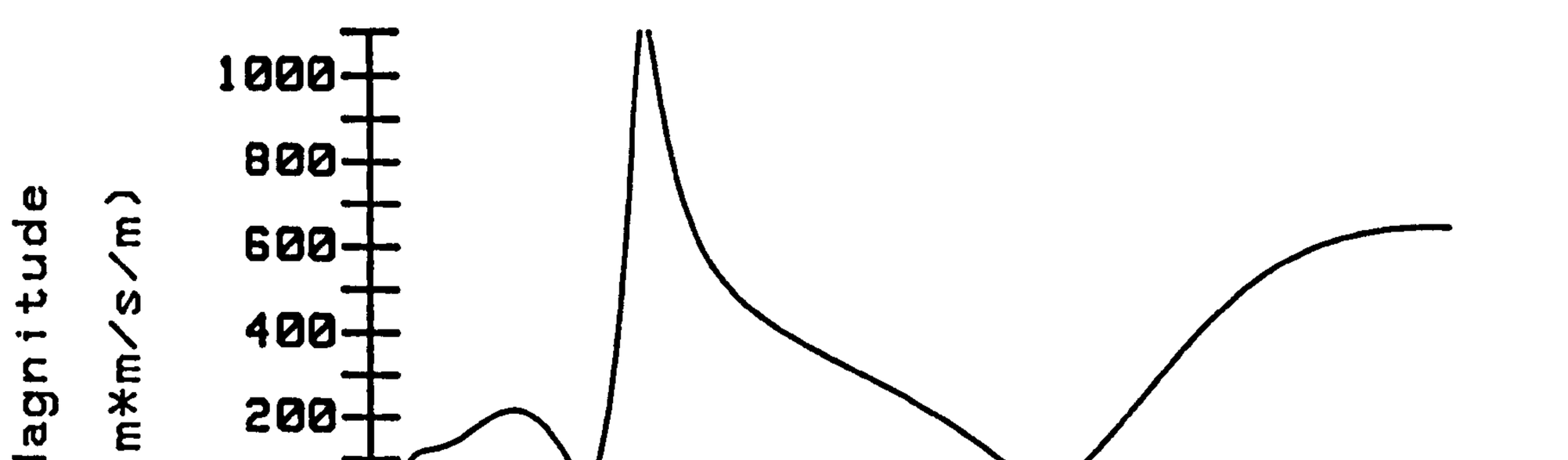

FIG 7.14 BODY ACCN RESPONSE

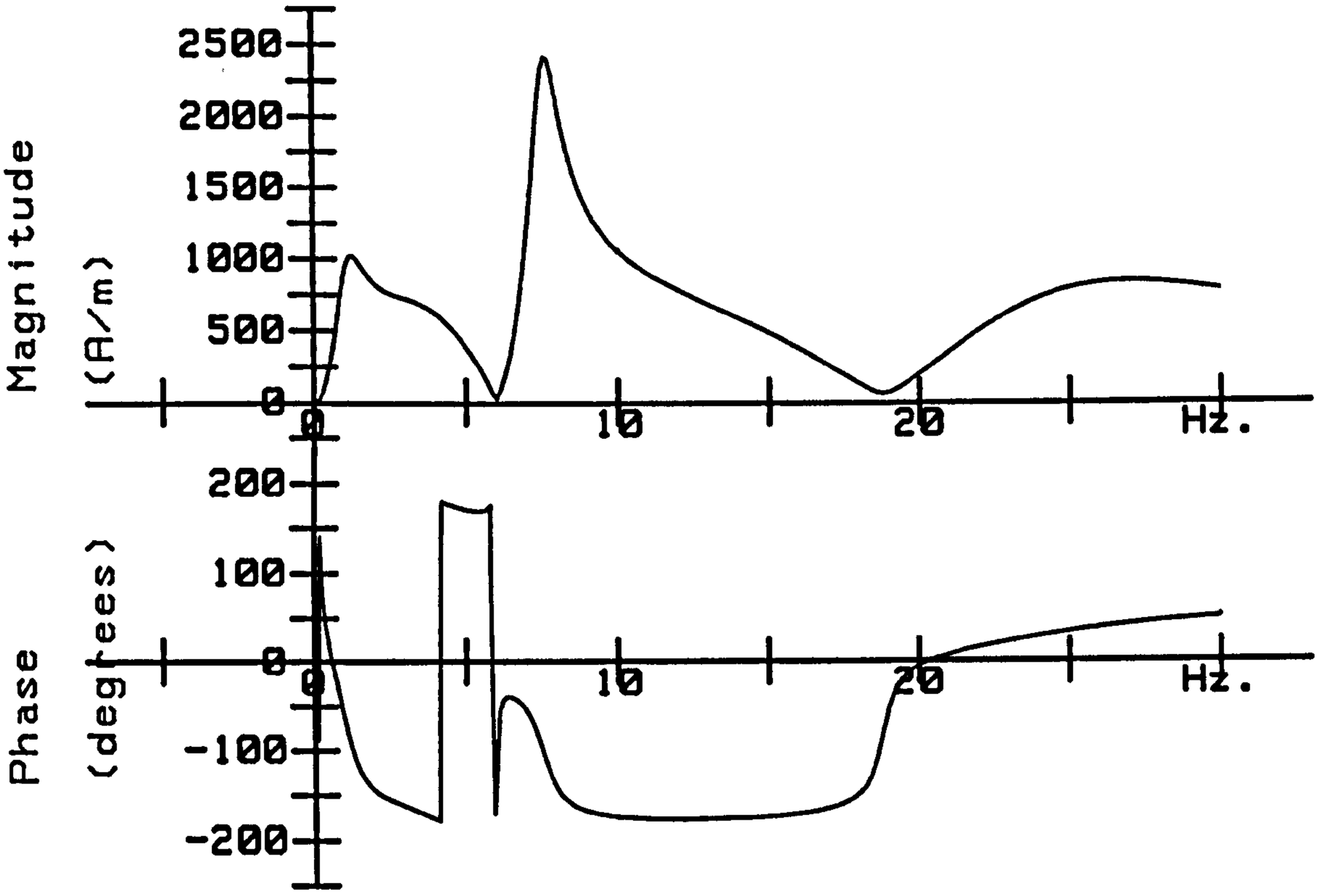

FIG 7.15 CURRENT RESPONSE

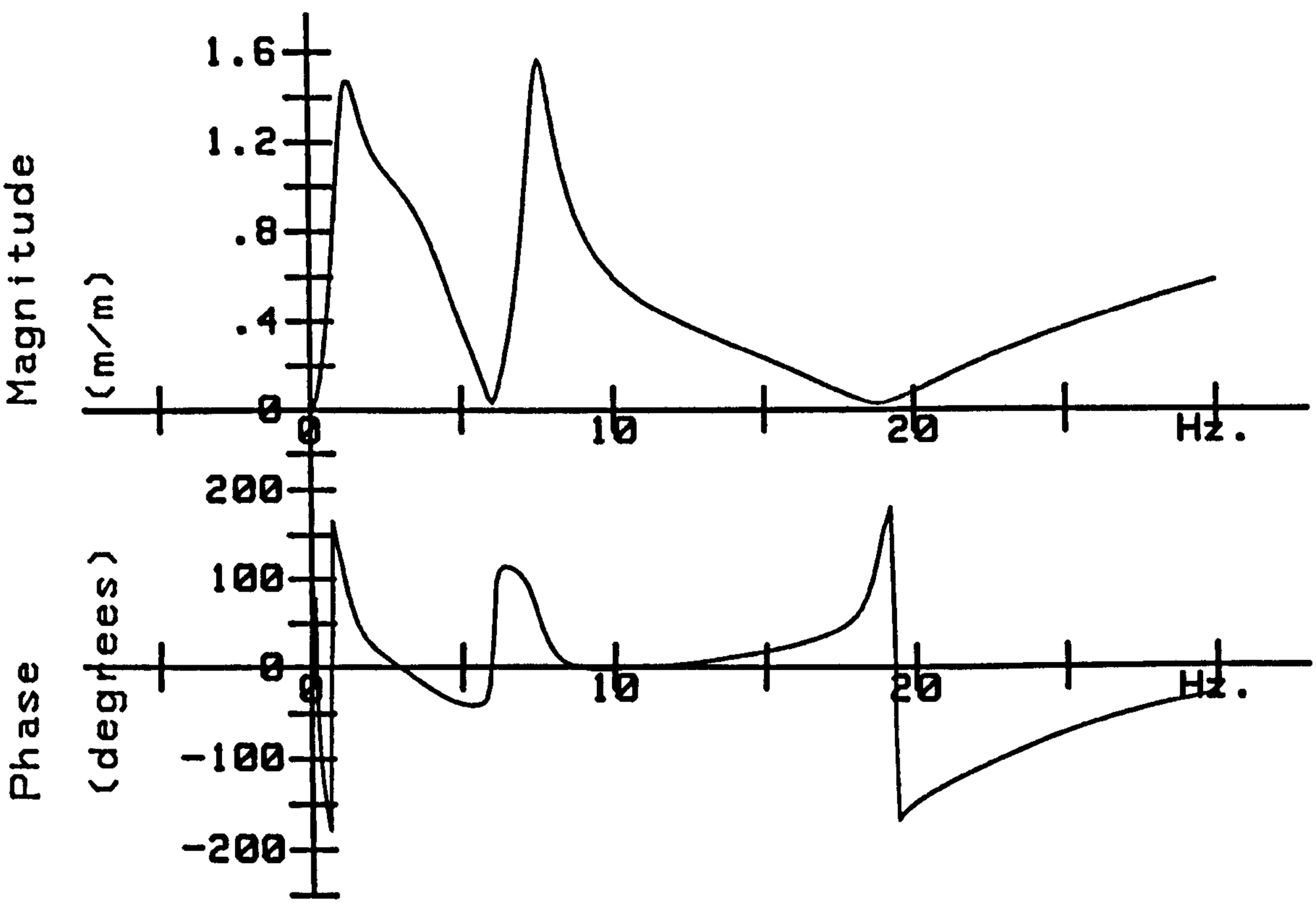

FIG 7.16 MAGNET GAP RESPONSE

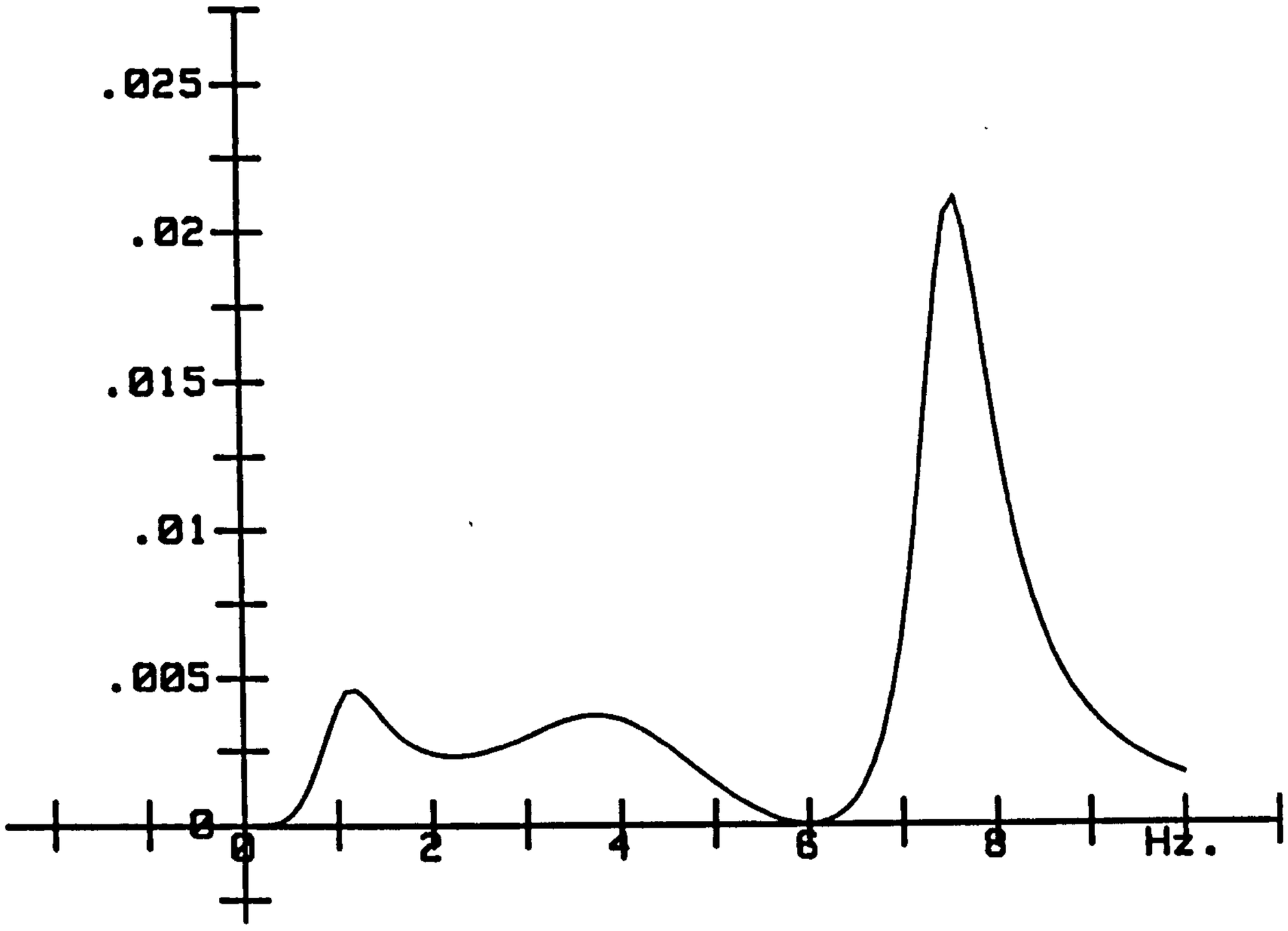

FIG 7.17 ISO5 ACCN PSD (2.0%g)

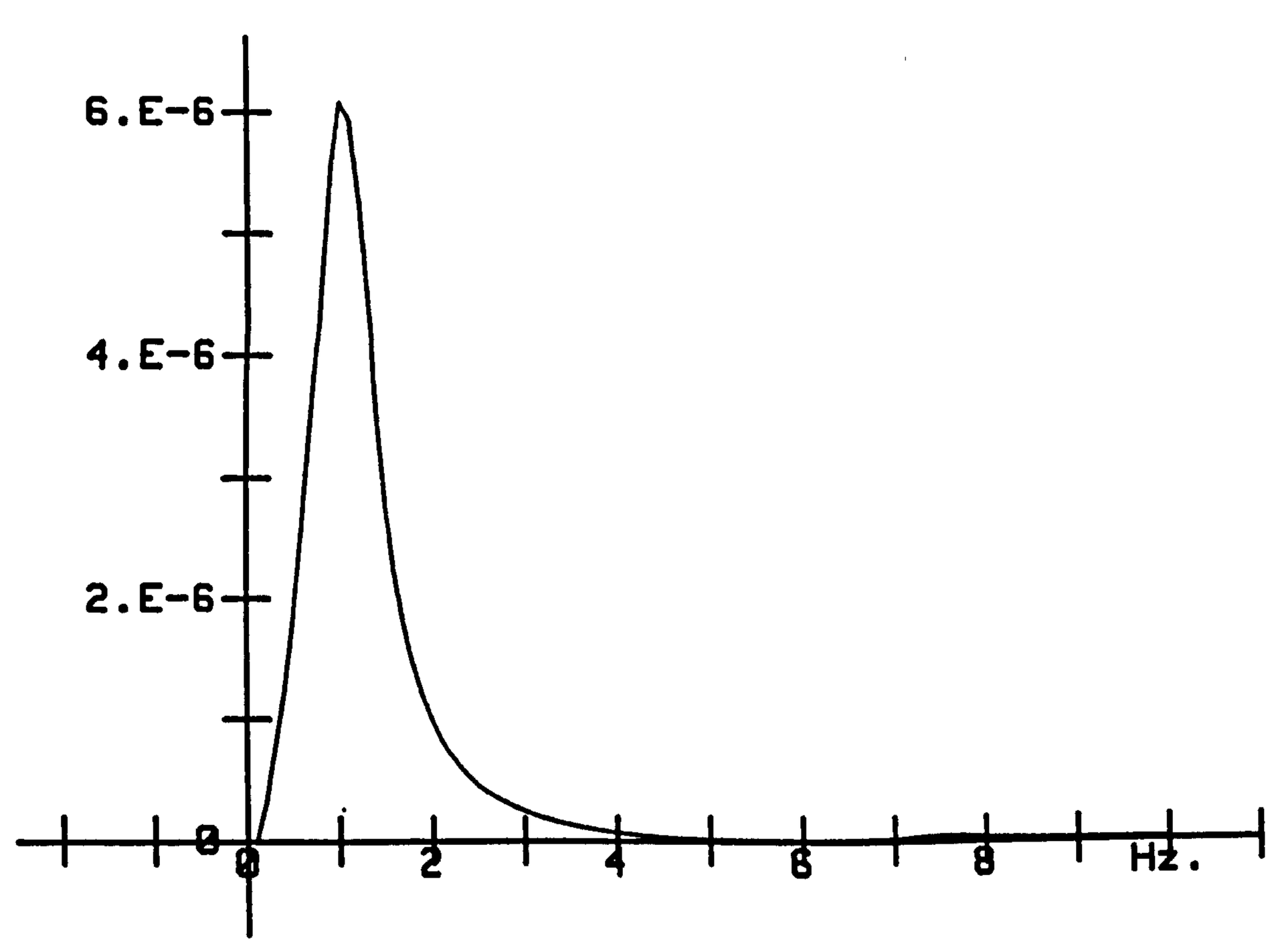

FIG 7.18 PSD OF GAP (2.5mm)

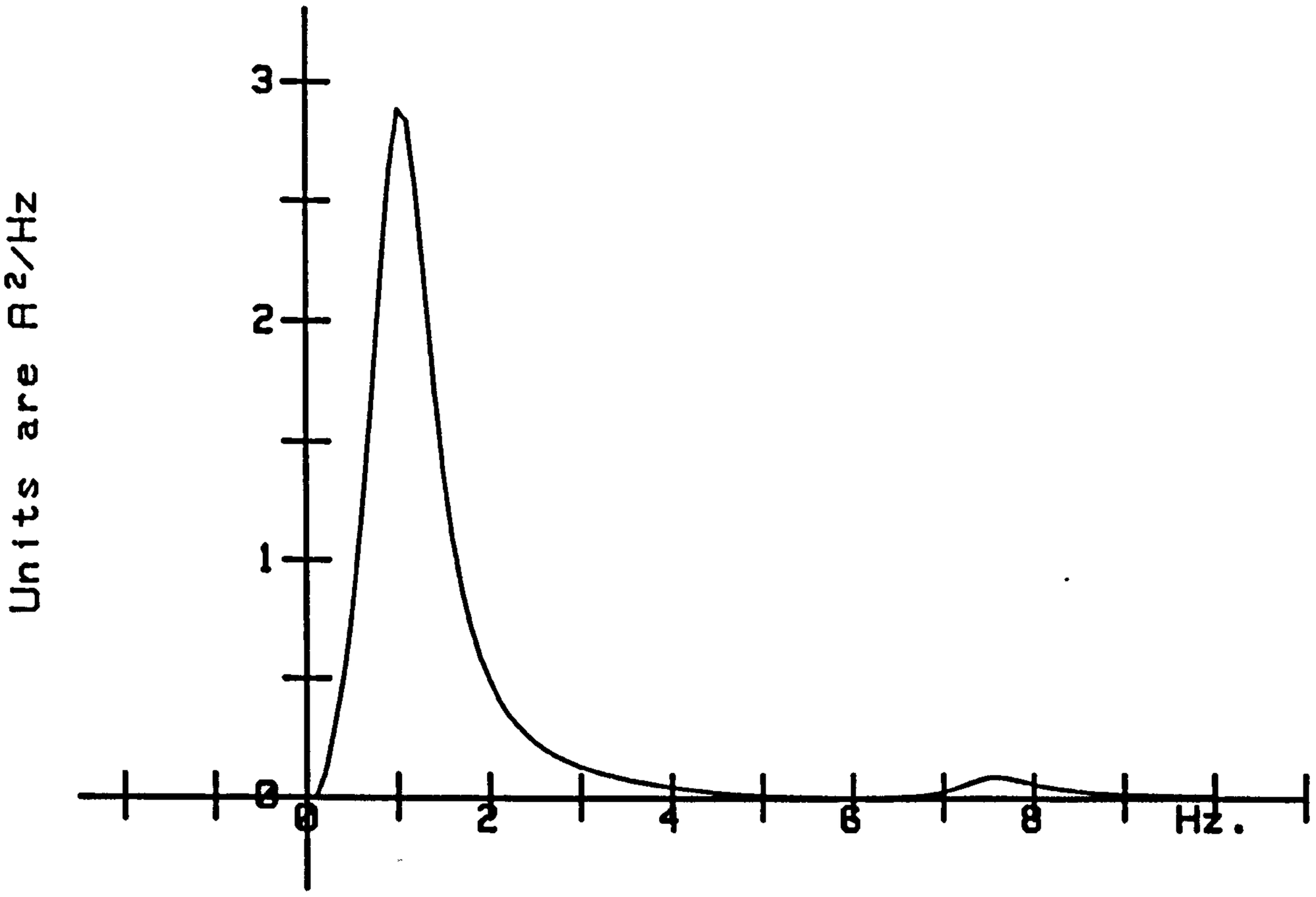

FIG 7.19 CURRENT PSD (1.8A)

CHAPTER 8 •CONCLUSIONS

This work was financed to achieve a direct commercial objective : to make urban maglev transport competitive with the wheeled competition . This objective has not been fully met , but progress has been made . A suspension controller has been devised , through considerable development work , which will support a maglev vehicle on a flexible guideway . A successful guideway design has also been produced , the design is cheap , light and tough enough to have withstood an arduous commissioning period .

Contrasting guideways at Birmingham and Zurich were tested , their dynamic properties varied from the sublime to the ridiculous or perhaps the ridiculous to the sublime . The guideway at Birmingham was built to be rigid , this is why it formed over 70% of the entire system cost . Response tests on the vehicle at Birmingham show that there is not the faintest suspicion of vehicle-guideway interaction and hindsight therefore tells us that the guideway could have been substantially less rigid , massive and expensive . Clearly the Engineers who

specified that system had to be cautious with this ill-understood (at the time) problem , but perhaps any future project might be more relaxed about guideway flexibility , even if the suspension controller were unchanged .

The guideway at Zurich is interesting but it is not easy to envisage a maglev vehicle on an Aerobus guideway in the immediate future . A typical Aerobus guideway span of 300 m could have a mid-span static stiffness of around 1% of the value that the lumped controller in Chapter 7 could manage . It is possible though that the construction of a tensioned guideway with span lengths of 10 m might be economic . The guideway static stiffness would be low (the influence of the catenary would be important in this respect) but the probability of higher natural frequencies might make the problem manageable . Predicted controller performance on the higher frequency guideway modes makes this prospect worthy of further investigation .

Predictions of the performance of the lumped controller in Chapter 7 are encouraging for the economics of a beam guideway . Optimisation of this controller is sure to improve the predicted performance because very little of this work has been done so far . Predictions show that the vehicle will behave admirably on guideway static stiffnesses of 5MN/m , similar to the stiffness of the Derby experimental guideway . Indeed the cost of the Derby

guideway would not change significantly if it were to be stiffened to the minimum level of 5 MN/m . It would be necessary to pack between the sleepers and the main beams to increase the compound second moment of area and also to use a different sleeper section to cope with larger longitudinal bending loads .

The Pie Chart on the next page shows how the system cost at Birmingham is reduced if the flexible Derby guideway were to be used instead of the rigid guideway . Capital cost is reduced by 40% .

However , GEC are not going to read this thesis and begin to quote massively reduced prices for flexible guideway maglev systems . It seems likely that they will adopt a more cautious approach . There are two ways to tackle further work in this area , in the laboratory with a scaled down system or , less conveniently , with a full size vehicle .

Laboratory work would allow the provision of a three (perhaps even one) degree of freedom vehicle and a variable parameter guideway . This would help to restrain costs but would still allow detailed examination and optimisation of the lumped controller .

Real vehicle work is awkward , the vehicles are owned by West Midland County Council (WMCC) and they have passengers to carry . However , WMCC are maglev enthusiasts , or were in 1985 , and might well be prepared to encourage some modest development work .

CAPITAL COSTS FOR DIFFERENT TRANSPORT SYSTEMS

FOR AN AIRPORT LINK

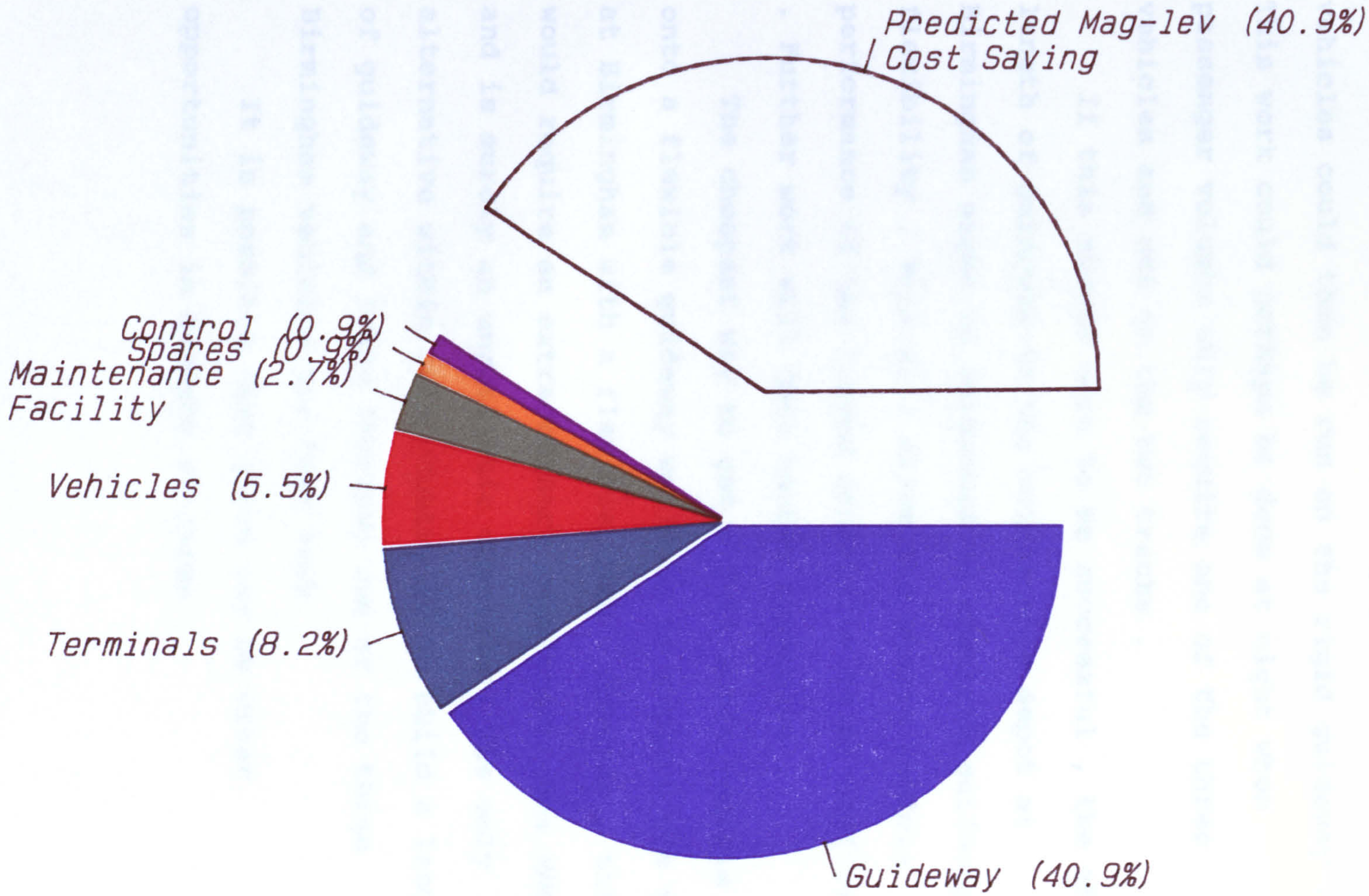

A FLEXIBLE GUIDEWAY MAGLEV VEHICLE

It would be valuable to change the magnet control boards on the Birmingham vehicles for the lumped controller described in Chapter 7 . The vehicles could then be run on the rigid guideway . This work could perhaps be done at night when passenger volumes only require one of the three vehicles and one of the two tracks .

If this change were to be successful , the short length of guideway in the maintenance depot at Birmingham might be suspended to simulate guideway flexibility . This will allow the static vehicle performance of the lumped controller to be confirmed . Further work will then become expensive .

The cheapest way to get a full scale vehicle onto a flexible guideway would be to replace one span at Birmingham with a flexible span . However , this would require an extraordinary commitment from WMCC and is surely an unrealistic scenario . The only alternative within this country is to build a length of guideway and lease (borrow) one of the three Birmingham vehicles for test work .

It is possible that there may be other opportunities in Germany or Japan .